STUDIES

of the

MINERALOGY and GEOCHEMISTRY

of

PROGRESSIVE TOURMALINISATION

at selected localities in southwest England

by

CAROL JANET LISTER, BSc.

July 1981

Thesis submitted for the degree of Doctor of Philosophy
of the University of London.

Department of Mineralogy
British Museum (Natural History)
London SW7

Department of Geology
Royal School of Mines
Imperial College
London SW7

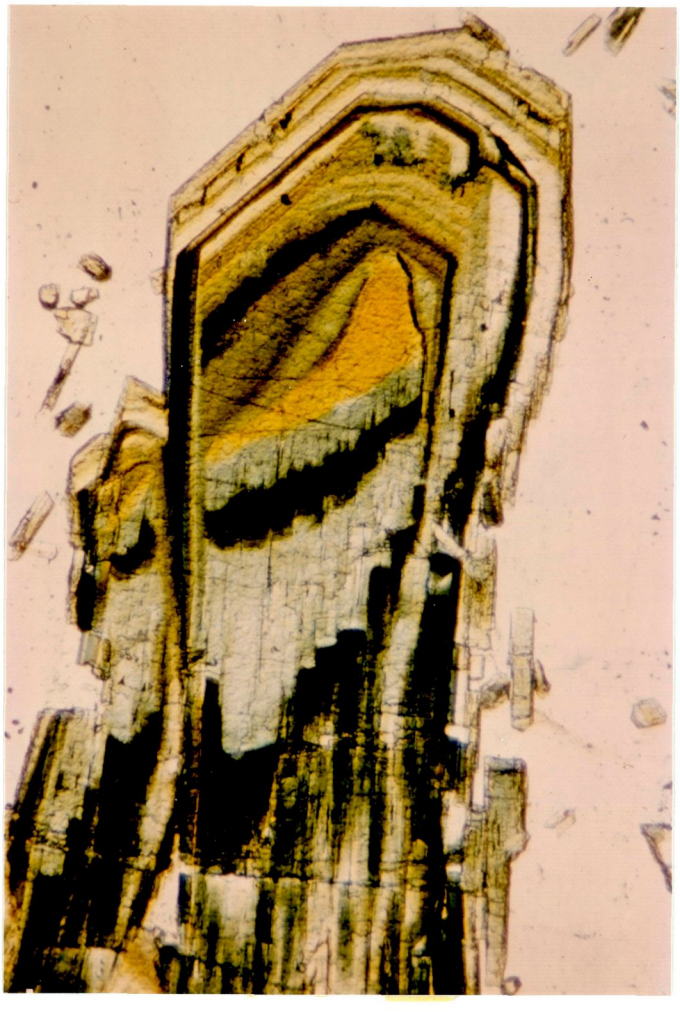

0 0.5mm

Frontispiece: zoned tourmaline from Venford Reservoir Quarry, Dartmoor.

ABSTRACT

Tourmalinisation may be defined as the formation of the complex borosilicate, tourmaline, by allochemical alteration of existing rocks or mineral grains.

Within the Variscan granites of Cornubia, the occurrence of tourmalinised rocks which grade laterally or vertically into untourmalinised granite allows the study of progressive tourmalinisation. Samples collected from such gradational boundaries illustrate the sequence of mineralogical and geochemical changes involved in the tourmalinisation process.

Forty-five rock samples have been described petrographically, and analysed for major and certain trace elements. The analytical work necessitated the development of a routine method for determining boron by neutron activation; this method is non-destructive, and obviates the problems arising from dissolution of tourmaline. A detailed study of the chemical transformations, taking place within individual mineral grains during tourmalinisation, was undertaken using electron probe microanalysis. Geothermometry and salinity data were obtained from fluid inclusions.

The major mineralogical transformations involved are the replacement by tourmaline of biotite (or chloritised biotite) and feldspar, with muscovite or hydromuscovite forming as a by-product. In the replacement of biotite by tourmaline, the original polycrystalline replacement products recrystallise to produce concentrically-zoned, single crystals. Feldspar is replaced by either skeletal or acicular tourmaline, which likewise may recrystallise.

The colour of tourmaline in thin section is not a reflection of its primary or secondary origin. The composition of replacement tourmaline ranges from almost pure schorl to almost pure dravite, and can contain significant calcium and/or titanium; an elbaite component has not been detected.

Tourmalinisation requires the introduction of boron, aluminium, and iron and/or magnesium. At low temperatures, potassium and rubidium increase at the expense of sodium, due to associated K-feldspathisation, and lithium and fluorine are depleted; if the supply of boron is limited, chloritisation accompanies or supplants tourmalinisation. With more intense tourmalinisation, associated with higher temperatures, potassium and rubidium are depleted, while lithium and fluorine may be enriched; tourmalinisation in these conditions may be accompanied by greisening and tin mineralisation.

Fluid inclusions show that in east Dartmoor, tourmalinisation took place at about 400°C in the presence of brines containing around 40 equivalent weight percent sodium chloride, but the possible temperature range would be from about 250°C for tourmaline-chlorite assemblages to about 450°C for the tourmaline-cassiterite association.

Tourmalinisation fluids in Cornubia probably have an ultimate source in the local sediments which, by assimilation, made a major contribution to the composition of the granites, and may also have supplied further material for late-stage metasomatism.

ACKNOWLEDGEMENTS

I acknowledge the financial support of the N.E.R.C., during the tenure of a post-graduate research studentship. It is a pleasure to thank my two supervisors, Dr. Paul Henderson at the British Museum (Natural History) and Dr. Andrew Rankin at Imperial College, London, for their help, advice and forbearance throughout the conduct of the work and the preparation of the manuscript. I am grateful to Dr. A.C. Bishop, Keeper of Mineralogy at the British Museum (Natural History) for the extensive facilities afforded to me during my studentship, and likewise to Professors G.R.Davis and J.L.Knill for facilities at Imperial College; I am also grateful to Dr. M. Kerridge for facilities at the University of London Reactor Centre, Ascot.

For permission to work on material from Venford Reservoir Quarry, I thank the South Western Water Authority. With respect to Tregarden Quarry, Luxulyan, I am grateful to E.C.C. Quarries Ltd. (and particularly to Mr. J. Symons, the quarry manager) for permission and assistance. English Clays, Lovering, Pochin and Company Ltd. kindly allowed me to work on material from Goonbarrow China Clay Pit.

Particular thanks are due to John Easton, Vic Din and Gary Jones, who patiently instructed me in the procedures of analytical geochemistry. Vic Din also kindly determined H_2O and CO_2 in several of the samples in the present work. Bob Symes and Jenny Bevan showed me how to succeed in electron probe microanalysis. Dr. Desmond MacMahon introduced me to radioanalytical techniques at the U.L.R.C. Dr. Nick Walsh kindly allowed me to prepare and analyse samples using the inductively coupled plasma source spectrometer at King's College, London. I owe an especial debt of gratitute to Mike Durkin, who has helped me in innumerable ways, including assistance with fieldwork and criticism of the manuscript.

I am grateful to Dr. David Alderton, Dr. Colin Bray and Dr. Graham Wilson for permission to quote their unpublished data, and to Dr. Colin Bray, Dr. Chris Halls, and Dr. Desmond MacMahon for allowing me to use their unpublished diagrams. I thank Patrick Allman-Ward (*et al.*), Drs. Keith Ball and Ian Basham, Dr. David Manning and Dr. Edwin Roedder for access to manuscripts of their works in the press. I also wish to thank Drs. Jan Hawkes and John Dangerfield for a larger scale copy of their published map showing the Variscan granites of southwest England. I greatly appreciate the generosity of Dr. Bernard Charoy and Dr. Michel Pichavant in giving me copies of their doctoral theses.

I gratefully acknowledge the technical skills of Gordon Burton and Tony Wighton at the BM(NH) and of John Blount and Barry Foster at Imperial College, in the preparation of some particularly difficult polished thin sections and polished grain mounts.

Many aspects of this work have been inspired and encouraged by discussions with friends and colleagues at the BM(NH), Imperial College, King's College, U.L.R.C., I.G.S. and other establishments, as well as with members of the Ussher Society and the Royal Geological Society of Cornwall, and to all these people I extend my thanks.

CONTENTS

		Page
Frontispiece		i
Abstract		ii
Acknowledgements		iv
List of contents		v
List of Tables		xii
List of Figures		xiv
List of Plates		xvii
Chapter 1	Introduction	1
1.1	Tourmaline	2
1.1.1	Structure	3
1.1.2	Nomenclature	6
1.1.3	Chemistry	7
1.2	The role of boron in granitic alteration	13
1.2.1	Boron-bearing minerals	13
1.2.2	Boron geochemistry and geochemical behaviour	15
1.3	The environment of tourmalinisation in southwest England	19
1.3.1	Geology of the province	19
1.3.2	The Variscan granites	21
1.3.3	Post-magmatic processes	27
1.4	Tourmalinisation	29
1.4.1	Distribution of tourmalinised rocks in Cornubia	32
Chapter 2	Field occurrence and petrography of samples	34
2.1	Venford Reservoir Quarry, Dartmoor	35
2.1.1	Field description	35
2.1.2	Petrography	43
2.1.2.1	The parent granite	43

2.1.2.2	The reddened granite	44
2.1.2.3	Tourmalinised vein margin	52
2.1.2.4	Zone of maximum tourmalinisation	59
2.1.2.5	The smaller, cavitous tourmalinised vein	63
2.1.2.6	Thin, monomineralic tourmaline veins	64
2.1.2.7	Mineralogy of tourmalinisation at Venford Reservoir Quarry: a summary	65
2.2	Tregarden Quarry, Luxulyan	68
2.2.1	Field description	68
2.2.2	Petrography	76
2.2.2.1	The parent granite	76
2.2.2.2	Chloritisation with minor tourmalinisation	77
2.2.2.3	Tourmalinisation with minor chloritisation	83
2.2.2.4	Luxullianite	87
2.2.2.5	Pegmatitic joint fill	91
2.2.2.6	Tourmalinisation and chloritisation at Tregarden Quarry: a summary	91
2.3	Goonbarrow China Clay Pit	95
2.3.1	Field description	95
2.3.2	Petrography	97
2.3.3	Tourmaline in the Stockscheider pegmatite	99
2.4	Cape Cornwall	101
2.4.1	Field description	101
2.4.1.1	The Cape Cornwall tourmalinite	103
2.4.1.2	Priest's Cove	107
2.4.2	Petrography	109
2.4.2.1	Cape Cornwall tourmalinite	109
2.4.2.2	Summary of petrographic evidence for tourmalinisation versus magmatic differentiation in the Cape Cornwall tourmalinite	113

2.5	Comparison of tourmalinisation processes at the localities examined	115
2.6	Discussion	117
2.7	Conclusions	120
Chapter 3	Analytical techniques	121
3.1	General analytical procedures	121
3.1.1	X-ray fluorescence spectrometry	121
3.1.2	Atomic absorption spectrometry	122
3.1.3	Pyrohydrolysis for fluorine	123
3.1.4	C,H,N elemental analysis	124
3.1.5	Electron probe microanalysis	124
3.2	Boron determination	126
3.2.1	Conventional chemical techniques	126
3.2.1.1	Spectrophotometry	126
3.2.1.2	Volumetric analysis	128
3.2.1.3	Pyrohydrolysis	128
3.2.1.4	Flame spectrometry	129
3.2.2	Instrumental techniques	129
3.2.2.1	Inductively coupled plasma emission spectrometry (ICP)	129
3.2.2.2	Laser induced plasma emission spectrometry	130
3.2.2.3	Ion microprobe	131
3.2.3	Radiometric techniques	131
3.2.3.1	Nuclear microprobe	131
3.2.3.2	Particle track analysis	131
3.2.3.3	Activation analysis	132
3.3	Neutron capture prompt gamma spectrometry	133
3.3.1	Introduction	133
3.3.2	Previous work	135
3.3.3	Apparatus	136

3.3.4	Method	138
3.3.4.1	Initial experiments	138
3.3.4.1.1	Self-shielding and sample geometry	138
3.3.4.1.2	Sodium interference	140
3.3.4.1.3	Standardisation	141
3.3.4.2	Preparation of standards and samples	142
3.3.4.3	Irradiation and counting	143
3.3.4.4	Data processing	143
3.3.5	Results	146
3.3.6	Comparison of results obtained by neutron capture and those obtained by other methods	146
3.3.7	Conclusions	154
3.3.7.1	Evaluation of the neutron capture method	154
3.3.7.2	Possibilities for improvement	154
Chapter 4	Geochemistry of progressive tourmalinisation	156
4.1	Previous work	156
4.2	Venford Reservoir Quarry, Dartmoor	166
4.2.1	Results	166
4.2.2	Chemical changes during tourmalinisation	166
4.3	Tregarden Quarry, Luxulyan	178
4.3.1	Results	178
4.3.2	Chemical changes during tourmalinisation and chloritisation	182
4.4	Goonbarrow China Clay Pit	193
4.4.1	Results	193
4.4.2	Chemical changes attributable to tourmalinisation	195
4.5	Cape Cornwall	197
4.5.1	Results	197

4.5.2	Chemical changes during progressive tourmalinisation, and the chemical variation within the tourmalinite	197
4.6	Discussion of tourmalinisation geochemistry, and comparison of observations from different localities	204
4.7	Conclusions	216
Chapter 5	Mineral chemistry in progressive tourmalinisation	217
5.1	Previous work	217
5.2	Venford Reservoir Quarry	219
5.2.1	Tourmaline	219
5.2.1.1	Tourmaline after biotite	219
5.2.1.2	Tourmaline after feldspar	223
5.2.1.3	Acicular tourmaline needles	229
5.2.1.4	Outer zones accreted upon existing crystals	230
5.2.1.5	Monomineralic tourmaline veins	240
5.2.1.6	Trace elements in the Venford Reservoir tourmaline	240
5.2.2	Other minerals associated with tourmalinisation at Venford Reservoir Quarry	242
5.3	Tregarden Quarry, Luxulyan	245
5.3.1	Tourmaline	245
5.3.1.1	Yellow-brown, prismatic tourmaline	245
5.3.1.2	Acicular blue-green tourmaline	245
5.3.1.3	Cored tourmalines in pegmatitic joint fill	247
5.3.2	Other minerals associated with tourmalinisation and chloritisation	252
5.4	Goonbarrow China Clay Pit	252
5.4.1	Tourmaline	252

5.4.1.1	Tourmalinised vein	253
5.4.1.2	Cored tourmalines in pegmatite	253
5.4.2	Other minerals associated with tourmalinisation in the tourmalinised vein	253
5.5	Cape Cornwall	255
5.5.1	Tourmaline	255
5.5.1.1	Cape Cornwall tourmalinite	255
5.5.1.2	Cored tourmalines from the pegmatite, Priest's Cove	255
5.6	Discussion	257
5.6.1	Compositional range and distribution	257
5.6.2	Enrichment trends	261
5.6.3	Implications for tourmaline solid solution	262
5.7	Conclusions	264
Chapter 6	Fluid inclusions in progressive tourmalinisation	265
6.1	Previous work	266
6.2	Fluid inclusions in tourmaline	268
6.3	Fluid inclusions in quartz	272
6.3.1	Tregarden Quarry, Luxulyan	272
6.3.2	Goonbarrow China Clay Pit	273
6.3.3	Cape Cornwall	274
6.3.4	Venford Reservoir Quarry	275
6.3.5	Comparison of observations at different localities	277
6.4	Experimental procedures	279
6.4.1	Geothermometry	279
6.4.1.1	Sample preparation	279
6.4.1.2	Apparatus	280
6.4.1.3	Methods	280

6.4.2	Chemical analysis	282
6.5	Results	283
6.5.1	Geothermometry	283
6.5.1.1	Two-phase inclusions	283
6.5.1.2	Halite-bearing inclusions	287
6.5.1.3	Multiphase inclusions	291
6.5.2	Analytical determination of chloride ratios	296
6.5.3	Pressure correction	298
6.6	Discussion	300
6.7	Conclusions	302
Chapter 7	Conclusions and their wider implications	303
7.1	Conclusions	303
7.2	Summary of the tourmalinisation process in Cornubia	307
7.3	Cornubia in the context of global tourmaline distribution	311
7.4	Tourmaline parageneses and their representatives in Cornubia	315
7.5	Future work	317
References cited		319
Appendix 1.	List of samples to which reference is made	334
Appendix 2.	Correction factors for fluid inclusion geothermometry	336
Appendix 3.	Copies of publications submitted with this thesis	337

(i) Luxullianite in situ within the St. Austell granite, Cornwall. Mineralog. Mag. 42, 295-297, 1978.

(ii) Some tourmalinised rocks from Cornwall and Devon. Proc. Ussher Soc. 4, 211-214, 1978.

(iii) Quartz-cored tourmalines from Cape Cornwall and other localities. Proc. Ussher Soc. 4, 402-418, 1979.

(iv) Luxullianite in situ within the St. Austell granite, Cornwall: a reply (to discussion by D.H.M.Alderton). Mineralog. Mag. 43, 442-443, 1979.

LIST OF TABLES

Table		Page
1:1	The tourmaline group: compositional end-members and varieties	8
1:2	Important naturally occurring borosilicate minerals	14
1:3	Classification of granites according to current theories	25
2:1	Comparison of tourmalinisation processes	116
3:1	Methods for boron determination in rocks and minerals	127
3:2	Neutron-capture, gamma-ray energies and maximum sensitivities of important elements in silicate analysis	134
3:3	Counting response for boron in standard glass powder preparations, in neutron-capture prompt-gamma spectrometry	147
4:1	Chemical analyses of unaltered granite and tourmalinite, with an intermediate bleached zone ('granite blanchi') after Chauris (1965)	158
4:2	Unaltered and tourmalinised granites from southwest England, after Hall (1973)	159
4:3	Chemical analyses of granites and tourmalinite from Cape Cornwall, after Charoy (1979a)	161
4:4	Chemical analyses of unaltered granite, tourmalinised vein margins, and luxullianite, from Tregarden Quarry, Luxulyan (from Lister, 1978a)	164
4:5	Chemical analyses of rocks from Venford Reservoir Quarry (major elements)	167
4:6	Chemical analyses of rocks from Venford Reservoir Quarry (trace elements)	168
4:7	Chemical analyses of rocks from the chloritised and tourmalinised sequence at Tregarden Quarry, Luxulyan (major elements)	179
4:8	Chemical analyses of rocks from the chloritised and tourmalinised sequence at Tregarden Quarry, Luxulyan (trace elements)	180
4:9	Chemical analyses of rocks from the tourmalinised and chloritised sequence, Tregarden Quarry, Luxulyan (major and trace elements)	181

4:10	Chemical analyses of rocks from Goonbarrow China Clay Pit and of the Early Lithionite Granite from the St. Austell pluton (the latter after Exley, 1959; Exley and Stone, 1964)	194
4:11	Chemical analyses of rocks from Cape Cornwall (major elements)	198
4:12	Chemical analyses of rocks from Cape Cornwall (trace elements)	199
4:13	Chemical gains and losses associated with different tourmalinisation intensities (B_2O_3%)	211
5:1	Replacement of biotite by tourmaline, Venford Reservoir - the initial progressive replacement sequence	220
5:2	Replacement of biotite by tourmaline, Venford Reservoir - recrystallisation to produce concentric zones	222
5:3	Replacement of feldspar by tourmaline, Venford Reservoir - blue acicular tourmaline replacing K/Na feldspar	225
5:4	Replacement of feldspar by tourmaline, Venford Reservoir - yellow-brown skeletal tourmaline replacing Na-feldspar	226
5:5	Replacement of feldspar by tourmaline, Venford Reservoir - blue and brown skeletal tourmaline replacing K/Na feldspar	228
5:6	Compositional zoning in tourmaline A, from the centre of the main tourmalinised vein, Venford Reservoir	232
5:7	Compositional zoning in tourmaline B, from the centre of the main tourmalinised vein, Venford Reservoir	237
5:8	Tourmaline from the smaller cavitous tourmalinised vein, and from the monomineralic tourmaline veins, Venford Reservoir	241
5:9	Tourmaline from Venford Reservoir and Tregarden Quarry Luxulyan: elements determined in bulk samples of separated tourmaline by methods other than electron microprobe	243
5:10	Hydromuscovite and apatite from the main tourmalinised vein margins, Venford Reservoir Quarry	244
5:11	Tourmalines from Tregarden Quarry, Luxulyan	246
5:12	Compositions of tourmaline crystals with oriented overgrowths, Tregarden Quarry, Luxulyan	249
5:13	Tourmalines from the tourmalinised vein at Goonbarrow China Clay Pit	254

5:14	Tourmalines from the Cape Cornwall tourmalinite	256
6:1	Chloride ratios of fluid inclusions in quartz, Venford Reservoir Quarry	296
7:1	Summary of mineralogy, geochemistry and geothermometry involved in tourmalinisation at Tregarden, Venford Reservoir, Goonbarrow and Cape Cornwall	304
7:2	Paragenesis and age of some major tourmaline occurrences	312
7:3	Classification of tourmaline parageneses	316

LIST OF FIGURES

Fig.		Page
1:1	Structure of tourmaline (after Buerger et al., 1962)	4
1:2	The tourmaline group	10
1:3	The geology of southwest England (simplified after Edmonds et al., 1975)	20
1:4	The Variscan granites of southwest England (after Hawkes and Dangerfield, 1978)	22
2:1	Geology of East Dartmoor and the location of Venford Reservoir Quarry	36
2:2	Sketch map of Venford Reservoir Quarry, showing location of samples	37
2:3	Orientation of joints and veins at Venford Reservoir Quarry	41
2:4	Quartz replacing feldspar in the reddened granite, leaving residual feldspar 'ghost' textures (Venford Reservoir Qy.)	47
2:5	Replacement of biotite by tourmaline in the reddened granite at Venford Reservoir Quarry	48
2:6	Alteration features associated with tourmalinisation at Venford Reservoir Quarry	66
2:7	Igneous facies and hydrothermal alteration in the St. Austell granite (unpublished diagram of C. Halls)	69
2:8	Distribution of facies in the St. Austell granite (simplified after Dangerfield et al., 1980)	70

2:9	Sketch map of Tregarden Quarry, Luxulyan, showing location of samples	71
2:10	Orientation of joints and veins in Tregarden Quarry Luxulyan	75
2:11	Alteration features in chloritised, tourmalinised and luxullianite veins at Tregarden Quarry. Luxulyan	93
2:12	Sketch map of Goonbarrow Pit (after Bray, 1980)	96
2:13	Geology of the Cape Cornwall area (adapted from Hall and Jackson, 1975)	102
2:14	Geology of Porth Ledden (simplified after Charoy, 1979a)	104
2:15	Structure of Porth Ledden (after Charoy, 1979a)	105
2:16	Mineralogy of the Cape Cornwall tourmalinite sequence	114
3:1	Layout of (n,γ) apparatus at U.L.R.C. (unpublished diagram of T.D. MacMahon)	137
3:2	Relationship between sample geometry and count rate	139
3:3	Aluminium sample holder	139
3:4	Prompt gamma spectra for two borosilicate glass standards containing 5.5 and 12.53% B_2O_3	144
3:5	Prompt gamma spectra for three tourmaline-bearing samples and one tourmaline	145
3:6	Calibration curve for borosilicate glass standards	148
3:7	Calibration curve for borosilicate glass standards in the range 0.1 to 1.0% B_2O_3	149
3:8	Comparison of results obtained by neutron-capture prompt gamma spectrometry with those obtained by inductively coupled plasma-emission spectrometry	151
3:9	Calibration curve for boron standards using the ICP at King's College, London	152
3:10	Comparison of results obtained by neutron-capture prompt gamma spectrometry with those obtained by spectrophotometry	153
4:1	a) Geochemical traverse from fresh into altered granite b) Chondrite-normalised REE patterns (both after Alderton et al., 1980)	162
4:2	Behaviour of potassium, sodium and aluminium in progressive tourmalinisation, Venford Reservoir	170
4:3	Chemical changes during progressive tourmalinisation, Venford Reservoir Quarry: variation in Li, F, CaO, MgO, FeO	171

4:4	Relationship between boron, potassium and sodium concentrations in rocks from Venford Reservoir Quarry	174
4:5	Correlation between rubidium and potassium, Venford Reservoir Quarry	177
4:6	Chemical changes in tourmalinisation and chloritisation at Tregarden Quarry, Luxulyan	183
4:7	Alkali changes in tourmalinisation and chloritisation at Tregarden Quarry, Luxulyan	185
4:8	Relationship between boron, potassium and sodium concentrations in rocks from Tregarden Quarry, Luxulyan	186
4:9	Behaviour of fluorine and lithium in tourmalinisation and chloritisation at Tregarden Quarry, Luxulyan	189
4:10	Relationship between K and Rb behaviour in tourmalinisation, Tregarden Quarry, Luxulyan	191
4:11	Relationship between K and Ba behaviour in tourmalinisation, Tregarden Quarry, Luxulyan	192
4:12	Behaviour of boron, potassium and aluminium in progressive tourmalinisation and within the tourmalinite at Cape Cornwall	201
4:13	Chemical variation in progressive tourmalinisation and within the tourmalinite at Cape Cornwall	203
4:14	Relative concentration changes in progressive tourmalinisation at Venford Reservoir Quarry	205
4:15	Relative concentration changes in tourmalinisation and chloritisation at Tregarden Quarry, Luxulyan	206
4:16	Relative concentration changes in tourmalinisation associated with greisening and tin mineralisation at Goonbarrow China Clay Pit	207
4:17	Relative concentration changes in tourmalinisation (and silicification) at Cape Cornwall	208
5:1	Compositions of tourmaline at Venford Reservoir Quarry	258
5:2	Compositions of tourmaline at Tregarden Quarry, Goonbarrow, and Cape Cornwall	259
6:1	Distribution and types of fluid inclusions in tourmaline from Venford Reservoir Quarry	269
6:2	Size and abundance of fluid inclusions in quartz at Venford Reservoir Quarry	276
6:3	Distribution of fluid inclusion types in the progressive tourmalinisation sequence at Venford Reservoir Quarry	278

6:4a	Salinities of fluid inclusions from Venford Reservoir Quarry	285
6:4b	Salinities of fluid inclusions from Venford Reservoir Quarry (contd.)	286
6:5a	Gas-liquid homogenisation temperatures for fluid inclusions from Venford Reservoir Quarry	288
6:5b	Gas-liquid homogenisation temperatures for fluid inclusions from Venford Reservoir Quarry	289
6:6	Densities of fluid inclusions at Venford Reservoir Quarry	292
6:7	Decrease in gas-liquid homogenisation temperatures with increasing tourmalinisation at Venford Reservoir Quarry	293
6:8	Multiphase fluid inclusions from Venford Reservoir Quarry, showing order of dissolution and solution temperatures for solid phases, and T_h for vapour phase	294
6:9	Phase diagram for the system NaCl - KCl - H_2O (after Roedder, 1971; 1979b)	295
6:10	Proportions of KCl and NaCl in fluid inclusions from Venford Reservoir Quarry	297

LIST OF PLATES

Plate		Page
Frontispiece	Zoned tourmaline from Venford Reservoir Quarry, Dartmoor	i
2:1	The northeast corner of Venford Reservoir Quarry	38
2:2	Venford Reservoir Quarry 'luxullianite' from the larger tourmalinised vein	38
2:3	Venford Reservoir Quarry: the smaller, cavitous tourmalinised vein	39
2:4	Biotite replaced at its margins by adjacent feldspar	45
2:5	Granophyric intergrowth between potassium feldspar and quartz	45
2:6	Biotite partially replaced by tourmaline in the reddened granite, Venford Reservoir Quarry	50
2:7	Tourmaline after biotite, in the process of recrystallisation (Venford Reservoir Qy)	50

2:8	Tourmaline after biotite, recrystallised to form a zoned crystal group (Venford Reservoir Qy)	51
2:9	Blue tourmaline and muscovite replacing feldspar in the reddened granite (Venford Reservoir Qy)	53
2:10	An assemblage of acicular tourmaline and hydromuscovite at the margin of a feldspar in the reddened granite (Venford Reservoir Qy)	53
2:11	Skeletal yellow-brown tourmaline replacing feldspar in the tourmalinised vein margin, Venford Reservoir	55
2:12	Skeletal yellow-brown tourmaline after feldspar, with interstices infilled by blue tourmaline, Venford Reservoir	55
2:13	Skeletal blue tourmaline replacing feldspar, growing from a fracture, Venford Reservoir	56
2:14	Radiating blue-green tourmaline aggregates replacing feldspar in the tourmalinised vein margins, Venford Reservoir	58
2:15	Incipient 'tourmaline sun' developing in quartz after feldspar, in the tourmalinised vein margins, Venford Reservoir	58
2:16	'Swarm' of minute, blue tourmaline needles, shot through quartz, in the tourmalinised vein margins, Venford Reservoir Quarry	60
2:17	Extension of minute blue tourmaline needles by accretion of additional outer zones, to form continuous mats in the tourmalinised vein centre, Venford Reservoir	60
2:18	Composite tourmaline crystals, united by outer growth zones, in the tourmalinised vein centre, Venford Reservoir	62
2:19	Euhedral, concentrically zoned tourmaline needles, in the tourmalinised vein centre, Venford Reservoir	62
2:20	Tourmaline-bearing pegmatite pocket at Tregarden Quarry, Luxulyan	73
2:21	Chloritised and tourmalinised vein margin, Tregarden Quarry, Luxulyan	80
2:22	Biotite breaking down to give green biotite, iron oxides and purple fluorite, in the chloritised vein margin, Tregarden Quarry	80
2:23	Yellow-brown tourmaline replacing feldspar by the growth of skeletal networks, chloritised vein margin, Tregarden Quarry	82
2:24	Green-yellow chlorite replacing feldspar, chloritised vein margins, Tregarden Quarry	82

2:25	Yellow-brown tourmaline in contact with biotite; chloritised and tourmalinised vein margin, Tregarden Quarry	85
2:26	Enlargement of part of Plate 2:25	85
2:27	'Castellated' feldspar margin, and pseudomorph of yellow-brown tourmaline after feldspar; tourmalinised and chloritised vein, Tregarden Quarry	86
2:28	Blue and dark brown tourmaline replacing chloritised biotite in the tourmalinised and chloritised vein, Tregarden Quarry	88
2:29	Enlargement of part of Plate 2:28	88
2:30	Fine, acicular tourmaline needles in the maximum tourmalinisation zone, Tregarden Quarry	89
2:31	Yellow-brown tourmaline after feldspar, fringed with fine, acicular tourmaline needles; tourmalinised and chloritised vein, Tregarden Quarry	89
2:23	Oriented overgrowth of blue-green tourmaline upon a smaller yellow tourmaline grain; tourmalinised and chloritised vein, Tregarden Quarry	90
2:33	Blue-green tourmaline directly replacing biotite along cleavages; luxullianite vein margins, Tregarden Qy.	92
2:34	Blue-green tourmaline replacing biotite, and forming an oriented overgrowth upon adjacent yellow tourmaline; luxullianite vein margin, Tregarden Quarry	92
2:35	Tourmalinised and greisened vein traversing kaolinised granite at Goonbarrow Pit	98
2:36	Blue and brown zoned tourmaline with relict feldspar and quartz; tourmalinised and greisened vein, Goonbarrow	98
2:37	The gradational boundary between the Cape Cornwall tourmalinite and the tourmaline granite	106
2:38	The layered structure of the Cape Cornwall tourmalinite, north end of Porthledden beach	106
2:39	The transitional zone between tourmalinite and tourmaline granite, from which samples CC011 to CC015 were taken	108
2:40	Feldspar replaced by skeletal growth of both yellow-brown and pale blue tourmaline; transition zone between tourmalinite and tourmaline granite, Cape Cornwall	111
2:41	Feldspar replaced by skeletal muscovite; transition zone between tourmalinite and tourmaline granite, Cape Cornwall	111

5:1	Zoned tourmaline crystal group (tourmaline A) from the centre of the main tourmalinised vein, Venford Reservoir	231
5:2	X-ray scan photomicrograph of tourmaline A, showing distribution of iron	233
5:3	X-ray scan photomicrograph of tourmaline A, showing distribution of magnesium	233
5:4	X-ray scan photomicrograph of tourmaline A, showing distribution of calcium	234
5:5	X-ray scan photomicrograph of tourmaline A, showing distribution of titanium	234
5:6	Zoned tourmaline crystal group (tourmaline B) from the centre of the main tourmalinised vein, Venford Reservoir	236
5:7	X-ray scan photomicrograph of tourmaline B, showing distribution of iron	238
5:8	X-ray scan photomicrograph of tourmaline B, showing distribution of magnesium	238
5:9	X-ray scan photomicrograph of tourmaline B, showing distribution of calcium	239
5:10	X-ray scan photomicrograph of tourmaline B, showing distribution of titanium	239
5:11	Yellow-brown tourmaline with blue-green acicular overgrowth in optical continuity, Tregarden Quarry	248
5:12	X-ray scan photomicrograph of tourmaline with oriented overgrowth, showing distribution of iron	250
5:12	X-ray scan photomicrograph of tourmaline with oriented overgrowth, showing distribution of magnesium	250
5:13	X-ray scan photomicrograph of tourmaline with oriented overgrowth, showing distribution of calcium	251
5:14	X-ray scan photomicrograph of tourmaline with oriented overgrowth, showing distribution of titanium	251
6:1	Halite-bearing fluid inclusion in quartz from the tourmalinised vein margin, Venford Reservoir Quarry	290

1. Introduction

Tourmaline is a complex borosilicate, which occurs in a wide variety of geological environments, and shows considerable variation in its chemical composition.

In addition to crystallising as an essentially primary mineral, either from a magma, or authigenically in a sediment, tourmaline also has a secondary role in replacing existing rocks and mineral grains. Such replacement constitutes the tourmalinisation process. The term 'tourmalinisation' will, in the following pages, be restricted to the formation of tourmaline by allochemical alteration of rocks or minerals.

Tourmalinisation has, to a greater or lesser extent, affected all the granitic plutons in the Cornubian province of southwest England. Some tourmalinised rocks have also been subject to other post-magmatic processes such as greisening, kaolinisation and metalliferous mineralisation.

Granitic tourmalinisation is generally assumed to result from the post-magmatic introduction of metasomatic fluids, derived either from residua cogenetic with the granites, or from an extraneous source. The common association of elements such as B, Li, F, Sn and W with granitic rocks, rather than with other potential hosts, supports the view that tourmalinisation, greisening and kaolinisation (as well as ore mineralisation) are inherent facets of granite emplacement. Exley (1959) regarded post-magmatic alteration in the St. Austell granite as 'autometasomatism', made possible by the confining pressure of an intact roof; the local release of such confining pressure is evidenced by the recently discovered tourmaline-cemented breccia pipe at Wheal Remfry (described by Halls *et al.*, 1978, and Allman-Ward *et al.*, 1981).

Many of the world's granitic terrains lack extensive post-magmatic alteration and metallisation. In the Caledonian province of Scotland, Plant *et al.* (1980) have shown that metalliferous mineralisation is

associated principally with granites intruded into relatively low-grade metasediments. It seems probable that granitic tourmalinisation may likewise be dependent upon the type of protolith intruded and assimilated by granite, rather than upon magmatic criteria.

Mechanisms responsible for the tourmalinisation of granites may be better understood through a detailed study of the mineralogical and chemical transformations involved in the tourmalinisation process. At certain localities in Cornubia, a progressive tourmalinisation sequence may be observed, through a continuous transition from unaltered granite into its tourmalinised equivalent. Material from these localities forms the basis for the present study, which aims to establish the mineralogical and chemical changes taking place during tourmalinisation, as well as the nature and possible source of metasomatic fluids responsible for this alteration process. By detailed examination of mineralogical features, mechanisms for post-magmatic replacement are evaluated. The geochemistry of tourmaline and tourmalinised rocks in relation to their untourmalinised parent materials allows assessment of the possible origins of metasomatic fluids. The composition and temperatures of such fluids are further elucidated by a fluid inclusion study. Finally, comparison with other reported examples of tourmalinised and tourmaline-bearing rocks in other parts of the world is invoked to help clarify the genetic relationships between granites, intruded sediments, and alteration phenomena.

1.1 Tourmaline

Tourmaline is not a single mineral species, but a group of minerals, having a similar structure. In terms of chemical variation and substitution, the complexity within the tourmaline group is comparable with that in, say, the amphibole group.

Belonging to the rhombohedral class of the trigonal system (space group R3m), members of the tourmaline group have the following generalised

structural formula:

$$(Na,Ca)(Fe^{2+},Fe^{3+},Mn,Mg,Li,Al)_3(Al,Fe^{3+})_6Si_6O_{18}(BO_3)_3(OH,F)_4$$

The crystalline habit and colour adopted by tourmaline is very variable. Crystals may take the form of stout or elongate prisms, or of fine, acicular aggregates or spherulites. The colour in hand specimen is usually black or dark green/brown for the iron-rich varieties, but magnesian tourmalines are generally brown, and lithium tourmalines may be pink, green, blue or colourless. In thin section, iron tourmalines show blue, yellow or brown colouration in plane polarised light (other varieties are very pale coloured or colourless); most tourmalines are strongly pleochroic, with absorption greater for ω than for ε . Where the colour of tourmalines is mentioned in the main part of the present work, this will refer to the colour of maximum absorption in plane polarised light, unless stated otherwise.

Members of the tourmaline group occur in igneous, metamorphic and sedimentary rocks. Tourmalines have been reported from rock types as diverse as eclogites (Smith, 1971), gabbro (Holgate, 1977), mica schists (Ethier and Campbell, 1977) and sandstones (Krynine, 1946); the commonest occurrence, however, is in granites, granite pegmatites, and 'pneumatolytic veins' (Deer et al., 1962). The paragenesis of the different tourmaline varieties will be discussed in the concluding chapter, and is classified in Table 7:3.

1.1.1 Structure

Following the original structural descriptions by Donnay and Buerger (1950), Ito and Sadanaga (1951) and Belov and Belova (1949), the various proposed tourmaline structures were reviewed by Buerger et al. (1962). Structural refinements have since been published for schorl (Fortier and Donnay, 1975), for elbaite (Donnay and Barton, 1972),

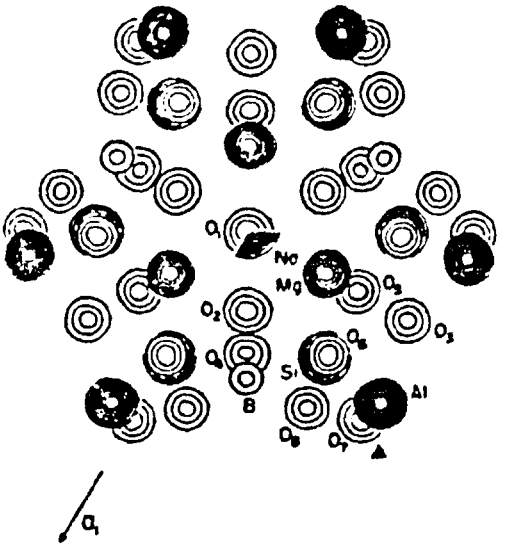

. Projection of the *maxima* of $\rho(xyz)$ on ((10$\bar{1}$0)) of the hexagonal unit cell. (Contour interval 5 e.Å^{-3}.)

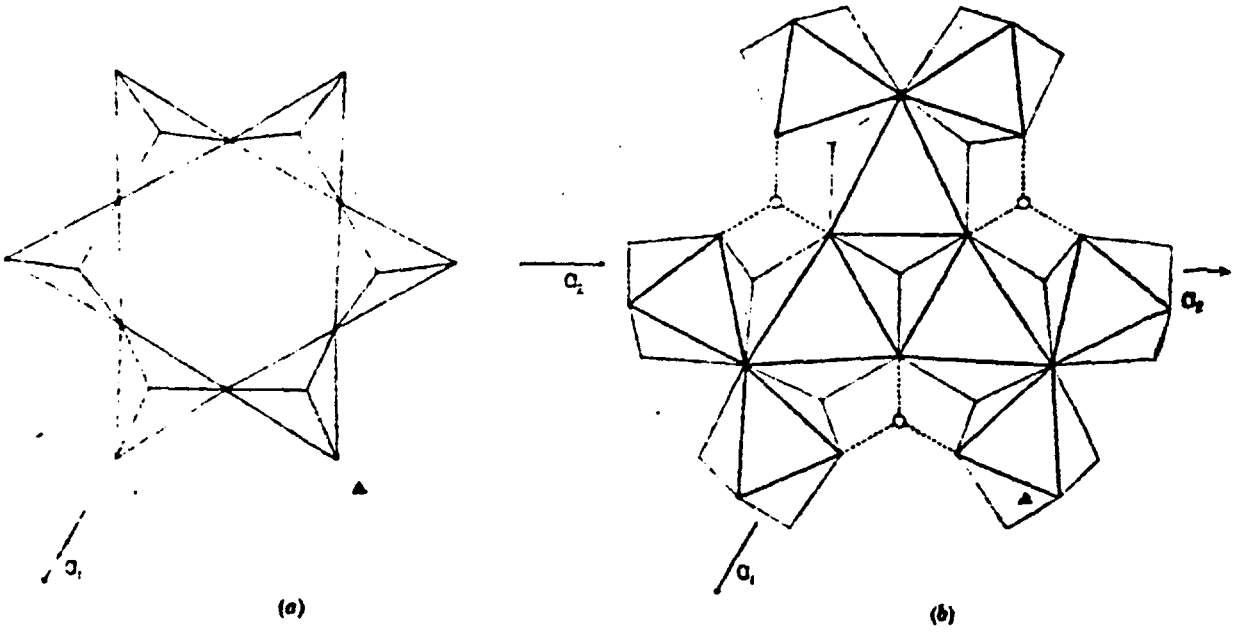

(a) The lower layer of the structure comprising a ring of six rather regular Si tetrahedra.

(b) The upper layer of the structure chiefly consisting of octahedra. The central three larger octahedra contain Mg. The six smaller peripheral octahedra contain Al. The small circles are B atoms bonded along the broken lines to the corners of octahedra. The lower right octahedron is pierced by a 3_1 screw axis to provide correlation with Fig. 2(c).

(c) The manner in which the various octahedral layers of the structure are joined to each other. The specific octahedron mentioned in the legend of Fig. 2(b) is seen here to share an edge with its 3_1 screw equivalent below it. Other features of the structure are omitted to focus attention on the nature of the bonding between these octahedra.

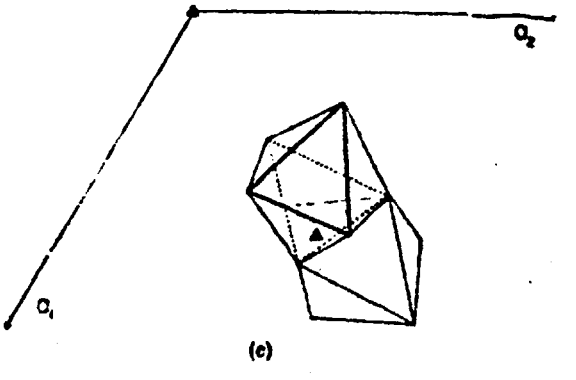

Fig. 1:1 Structure of tourmaline (after Buerger et al., 1962)

and for dravite (Schmetzer et al., 1979). The members of the tourmaline group are essentially isostructural, but there are differences in unit cell parameters, attributable to compositional variation.

According to Buerger et al. (1962), the structure consists of alternating tetrahedral and octahedral layers. In the tetrahedral layers, hexagonal rings of Si tetrahedra surround alkali atoms which occupy the central void. In the octohedral layers, three central positions are occupied by Mg (or Fe, &c.), and three external octahedral pairs by Al; hydroxyls form the centres, and three boron atoms help bind together the octahedral layers. Oxygens are positioned as in Fig. 1:1, which shows the basic structure outlined by Buerger et al. (1962). The SiO_4 tetrahedra point towards the analogous pole (i.e. the negative end of the crystallographic triad axis), at least in schorl and buergerite (Barton and Donnay, 1966; Fortier and Donnay, 1975), and probably in other varieties also.

To simplify discussion in the following pages, the nomenclature of Donnay and Barton (1972) and subsequent writers will be used to denote the structural positions in which the major chemical substitutions occur. The formula

$$(Na,Ca)(Fe^{2+},Fe^{3+},Mn,Mg,Al,Li)_3(Al,Fe^{3+})_6Si_6O_{18}(BO_3)_3(OH,F)_4$$

may thus be rewritten

$$(X^{+})(Y^{2+})_3(Z^{3+})_6Si_6O_{18}(BO_3)_3(OH,F)_4$$

where X = monovalent or divalent alkali cation (3a position of unit cell)

Y = divalent or trivalent cation (or, in the case of Li, monovalent balanced by a further trivalent ion) (9b position)

Z = trivalent cation (18c position)

1.1.2. Nomenclature

The name 'tourmaline' seems to have come to Europe via Holland, from Ceylon (Sri Lanka), whence crystals imported in the early 18th century bore the Cingalese name 'turamali' (Hintze, 1897). The name 'schorl' is, however, much older, printed usage quoted by Dana (1868) dating back to 1562; the etymology of schorl is obscure, but may have been colloquial, since Wilson (1762) states of tourmalines that 'the miners of Germany vulgarly call them schirl'.

Many minerals other than tourmaline have been described as forms of schorl, including axinite (violet schorl of Sowerby, 1811), rutile (schorl rouge of Dana, 1868), pyroxene and leucite (schorl noir and schorl blanc respectively, also of Dana, 1868), phenacite (white schorl of Sowerby, 1811) and topaz (schorlous topaz of Brewster, 1830, and schorlite of a large number of authors; the pycnite variety of topaz still bears the name 'schorlite' in several languages today).

The pyroelectricity of tourmaline was reflected in several early names assigned to the mineral. For example, Garmann's (1707) appellation 'Aschentrecker' refers to the attraction of ash particles by tourmaline; other names used in the 18th and early 19th centuries include 'borax electricus' (Linnaeus, 1768), 'argilla electrica' and 'silex electricus' (both Sowerby, 1811).

The Cornish miners' term 'cockle' (defined by Pryce, 1778, as 'the schorl of the Germans.... in English, schirl') possibly refers to the worthlessness of this mineral by contrast with cassiterite, with which it commonly occurs, since the Cornish 'cok' (Nance, 1955) means empty or worthless.

According to Hintze(1897), schorl and tourmaline were described as separate minerals by several early authors, although similarities were often noted. Bergman (1779) stated that the Cingalese tourmaline belonged to the class of schorls. Haüy (1801) grouped electric schorl and other

tourmaline types under the single heading 'tourmalines', in which the different coloured varieties 'grade imperceptibly one into the other', and all display electrical properties.

Nowadays, the term schorl denotes the ferrous iron end-member of the tourmaline group, in which X = Na, Y = Fe^{2+}, and Z = Al. The other tourmaline varieties and end-members, listed in Table 1:1 and represented diagramatically in Fig. 1:2, were distinguished from one another on chemical grounds, and will be discussed below.

1.1.3 Chemistry

Early attempts at chemical analysis of tourmaline include that of Woulfe (1779), who reported that 'schorl contains nearly as much earth of alum as the Cornish porcellane clay'; this observation has stood the test of time. Most early analyses were incomplete, such as those of Vauquelin and Klaproth, made in the early part of the nineteenth century (and quoted by Brewster in his Edinburgh Encyclopaedia of 1830); these in particular lack boron and sodium. Arfvedson (1818) showed the presence of the newly discovered element lithium, not only in some tourmalines, but also in spodumene and petalite. Probably the earliest reliable chemical analyses of tourmalines are those of Gmelin (1827); although the boron figures are suspect, he recognised three varieties, namely lithium-bearing, lithium-free with only minor magnesium, and high-magnesium tourmalines. A summary of subsequent nineteenth century analytical work on tourmaline is given by Penfield and Foote (1899).

Standardised varietal names for the most common compositional end-members were not adopted until the twentieth century, although the magnesian member had been named 'dravite' by Tschermak in 1883 (after the Drave district in his native Austria), and the ferrous iron variety had long been termed 'schorl'. Thus, at the turn of the century, we still find the tourmaline group classified into lithia, iron and magnesia

Compositional end - members of the tourmaline group

Tourmaline $(Na,Ca)(Fe^{2+},Fe^{3+},Mn,Mg,Li,Al,Ti,Cr,V)_3(Al,Fe^{3+})_6Si_6O_{18}(BO_3)_3(OH.F)_4$

	X (3a)	Y(9b)	Z(18c)		
Schorl	Na	Fe^{2+}	Al	German miners' term (16th century or earlier)	
Dravite	Na	Mg	Al	Tschermak (1883)	Drave, Carinthia (Austria)
Elbaite	Na	(Li,Al)	Al	Vernadsky (1913)	Elba, Italy
Buergerite	Na	Fe^{3+}	Al	Donnay et al. (1966)	after M.J.Buerger
Tsilaisite	Na	Mn	Al	Kunitz (1929)	Tsilaisina, Madagascar
Uvite	Ca	Mg	Al	Kunitz (1929)	Uva, Ceylon
Liddicoatite	Ca	(Li,Al)	Al	Dunn et al. (1977)	after R.T.Liddicoat
Ferridravite	Na	Mg	Fe^{3+}	Walenta & Dunn (1979)	composition
Further compositional variations					
Chromian dravite	Na	(Mg,Cr)	(Al,Cr).	Dunn (1977) ('chrome tourmaline - Cossa & Arzruni, 1883)	
Vanadian dravite	Na	(Mg,V)	(Al,V)	('vanadian tourmaline' - Snetsinger, 1966)	
Titanturmalin	Na	(Ti,Fe,Mg)	(Al,Ti)	Kunitz (1936)	
Nickel tourmaline	Na	(Ni,Fe,Mg)	Al	Taylor & Terrell (1967)	
Cobalt tourmaline	Na	(Co,Fe,Mg)	Al	Taylor & Terrell (1967)	

Table 1:1 The tourmaline group: compositional end-members and varieties

tourmalines (Hintze, 1897; Penfield and Foote, 1899), or, alkali, iron and magnesium tourmalines (Dana, 1892). The lithium varieties had been named according to their colour (rubellite, verdelite, indicolite and achroite), before it was realised that their major element compositions were to all intents and purposes identical; a chemical explanation for their individual colours is still lacking today, despite many detailed investigations (e.g. Bradley and Bradley, 1953). The name 'elbaite', proposed by Vernadsky (1913) was adopted to denote all the lithium tourmalines mentioned above (the name had previously been applied to ilvaite by Giesecke, 1832).

The three major tourmaline end-members, schorl, dravite and elbaite, are represented by the central triangle in Fig. 1:2. Here, X = Na, and Z = Al in each case, and the variation is seen in the Y position. Schorl is by far the commonest naturally occurring variety, but (Fortier and Donnay, 1975) the pure end-member composition has neither been found in nature, nor synthesised artificially; structural work has been based upon the Andreasberg schorl (from the Harz Mountains, Germany), since this is the purest schorl known. A complete solid solution series exists between schorl and elbaite, and between schorl and dravite. According to Donnay and Barton (1972), these solid solutions are made possible by the ability of iron to occupy both Y and Z positions in ferric as well as ferrous oxidation states. The lack of solid solution between elbaite and dravite is due to the absence of such a cation with variable valency.

Additional end-members and varieties result from further substitution in the Y position, while retaining X = Na and Z = Al. Substitution of Fe^{3+} in this position produces buergerite, which was first described from Mexico by Mason *et al.* (1964) and named by Donnay *et al.* (1966). It is likely, in view of the statement by Donnay and Barton (1972) above, that solid solution is possible between schorl and buergerite and between elbaite and buergerite. Kunitz (1929) proposed the hypothetical manganese

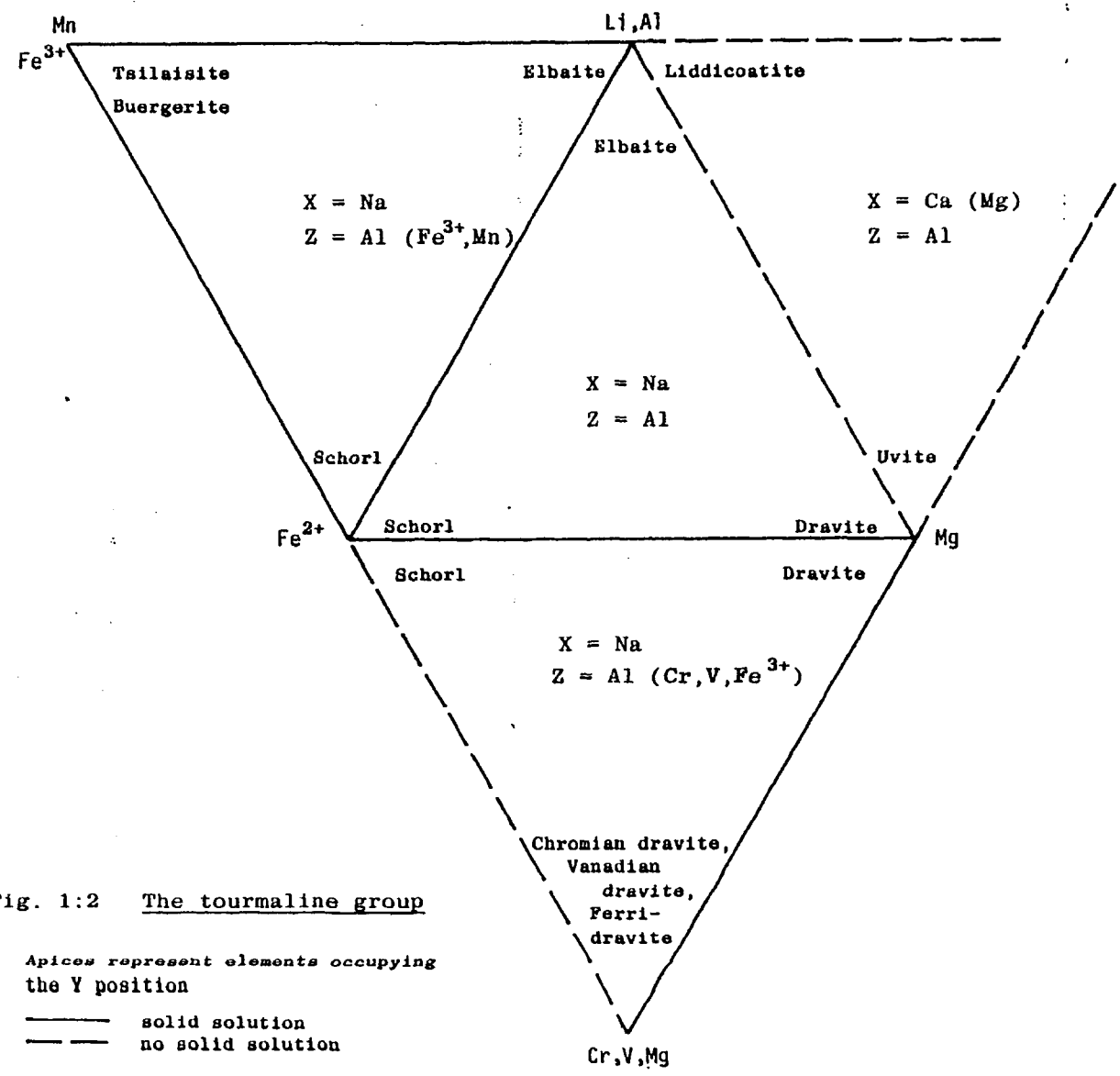

Fig. 1:2 The tourmaline group

Apices represent elements occupying the Y position

——— solid solution
— — no solid solution

end-member tsilaisite, with Mn (valency unstated) in the Y position. Manganese-rich tourmalines had previously been analysed by Prendel (1892) from Siberia, and by Duparc et al. (1910) from Tsilaizina in the Antsirabe district of Madagascar. The pure end-member is not known in nature, although Kunitz cited an example with as much as 8.21% MnO.

It is also possible for substitution, chiefly by calcium, to occur in the X position. Kunitz (1929) also proposed uvite as a hypothetical end-member, with X = Ca, Y = Mg, and Z = Al. Uvite is now known to be quite common in nature, and to show complete solid solution with dravite (Dunn et al., 1977b). Following earlier work on tourmalines from the Antsirabe pegmatites of Madagascar (Lacroix, 1893; Duparc et al., 1910), in which some high calcium levels had been reported, Dunn et al. (1977a) isolated and named the new calcium tourmaline 'liddicoatite'; this is the calcium analogue of elbaite, with X = Ca, Y = Li,Al, and Z = Al. The paragenesis is not certain, since the type material is detrital, but derivation from the said pegmatites is inferred. Substitution of magnesium in the X position is also possible in nature (Wang and Hsu, 1966); Foit and Rosenberg (1977) suggest that this involves coupled substitution, such that alkali-free or alkali-poor tourmalines are only viable when dehydroxylation in favour of oxygen occurs. The X position may also theoretically be occupied by potassium; a high-potassium tourmaline was synthesised by Taylor and Terrell (1967). In natural tourmalines, analyses showing significant potassium are confined to the older literature (e.g. Gmelin, 1827; Prendel, 1892), and the occurrence of such compositions is not confirmed by more recent work.

All the tourmaline varieties discussed above contain aluminium in the Z position. It is now known that Fe^{3+} can substitute for Al to produce the rare, non-aluminous end-member, ferridravite, in which X = Na, Y = Mg, and Z = Fe^{3+}. This was only recently described and named (Walenta and Dunn, 1979), although the possibility of such an end-member was made

clear by Frondel *et al.* (1966), on the basis of their own analysis and that made much earlier by Jannasch and Calb (1889).

Other tourmaline 'varieties' described in the literature are not end-members as such, but represent often significant substitutions, particularly in the Y position. Chrome tourmalines, originally reported from the Urals by Cossa and Arzruni (1883), have also been described from other ultramafic and chromite-bearing terrains by many subsequent authors; the published chrome-tourmaline data are summarised in a recent paper by Nuber and Schmetzer (1979). All the chromian tourmalines reported to date are actually dravites, in which, as Dunn (1977) explains, chromium may be present in both Y and Z positions. It would theoretically be possible to form two separate chromium end-members, namely a chrome-dravite (analogous to ferridravite) with chromium displacing aluminium in the Z position, and conversely, an aluminous chrome-tourmaline (analogous to buergerite) with Cr^{3+} in the Y position. However, since none of the published analyses of chrome tourmalines represent either end-member composition, Dunn's (1977) more appropriate appellation 'chromian dravite' will be used in the following pages.

Dravites containing significant vanadium (plus minor chromium) are known from Tanganyika (Bassett, 1953) and from California (Snetsinger, 1966). The latter locality provided material for Foit and Rosenberg's (1979) structural study of vanadium-bearing tourmaline, which has shown that vanadium substitutes (like chromium) in both y and Z positions, and is accommodated in a structure very similar to that of other tourmalines by a compensating alkali deficiency and dehydroxylation.

Titanium can substitute in the tourmaline structure to a certain extent, presumably also occupying both Y and Z positions. The 'Titanturmalin' of Kunitz (1936) appears to have been accepted as a recognised tourmaline variety (Hey, 1962), despite having been named

without citing actual concentrations. TiO_2 totalling over 2% has since been reported in tourmaline (e.g. by Black, 1971). The possibility of a titanium end-member would probably be limited, since Ti^{4+} would need to be balanced by monovalent ions.

Taylor and Terrell (1967) were unable to grow titanium tourmalines experimentally, but did succeed in synthesising tourmalines rich in either nickel (15.25% NiO), or cobalt (nearly 8% CoO); these authors also report a synthetic sodium-copper tourmaline (no analysis given), and imply that a zinc variety was also sysnthesised.

Tourmalines can contain a wide range of trace elements, which are chiefly divalent and trivalent cations substituting in the Y and Z positions. Power (1968) reported trace concentrations of V, Cr, Ni, Sc, Zr, Co, Ga, Sr and Sn. The distribution of tin in tourmalines was also examined by Nemec (1973).

1.2 The role of boron in granitic alteration

1.2.1 Boron-bearing minerals

Of over 150 known boron-bearing minerals (Erd, 1980), the majority are borates, fluoborates, and complex borate salts, which characterise certain sedimentary evaporite environments. The more important borate hydrate salts include borax and kernite (both Na), ulexite (Na,Ca) and colemanite (Ca); these are mined commercially as a source of boron.

In hot springs associated with contemporary volcanism (notably in Tuscany, Italy), orthoboric acid occurs naturally as the mineral sassolite.

Borosilicates form but a small proportion of the recorded minerals of boron, but are of considerable importance in the context of the present work. Table 1:2 lists some of the major, naturally occurring borosilicate minerals, showing their approximate boron contents (obtained from formulae,

Mineral	Formula	Approx. wt.% B_2O_3
Tourmaline group	$(Na,Ca)(Fe,Mg,Mn,Li,Al)_3(Al,Fe)_6Si_6O_{18}(BO_3)_3(OH,F)_4$	10%
Axinite group	$(Ca,Mn,Fe)_3Al_2BO_3Si_4O_{12}OH$	2-7%
Datolite group	$CaBSiO_4OH$	22%
Searlesite	$NaBSi_2O_5(OH)_2$	17%
Danburite	$Ca\ (BSiO_4)_2$	28%
Grandidierite	$(Mg,Fe)Al_3BO_3(SiO_4)O_2$	11%
Dumortierite	$(Al,Fe)_7O_3BO_3(SiO_4)_3$	6%
Harkerite	$Ca_{48}Mg_{16}Al_3(OH)_6Cl_2(CO_3)_{18}(BO_3)_{15}(SiO_4)_{12}.3H_2O$	9%
Reedmergnerite	$NaBSi_3O_8$	14%
Kornerupine	$Mg_3Al_6O_4(OH)Si_2O_7(Al,Si)_2(Si,B)O_{10}$	up to 2%

Table 1:2. Important naturally occurring borosilicate minerals

or from general texts). Among these minerals, members of the tourmaline group are the most common and widespread.

Boron may enter silicate structures by substitution for tetrahedral silicon or tetrahedral aluminium; the former case in seen in the datolite group, and the latter, more unusual substitution, is presumed to occur in the albite-analogue reedmergnerite (Christ, 1965). Alternatively, boron may occur in threefold co-ordination, as in tourmaline, dumortierite, grandidierite and harkerite (Povarennykh, 1970).

Additionally, minerals in which boron is not an essential element may incorporate up to several percent B_2O_3 in their structures by substitution for silicon; examples are gadolinite and vesuvianite (idocrase), both reported by Oftedahl (1964a,b).

Clay minerals are well known as hosts for boron, which may be either incorporated in their structure or adsorbed onto clay surfaces. Illites generally take up more boron than other clay minerals; Reynolds (1965) reported mean concentrations of over 400ppm B in illites, with some individual values around 700ppm.

Low concentrations of boron are also found in the major constituent minerals of granites. Waskowiak (1969), for example, determined 100ppm in plagioclase, 5ppm in potassium feldspar, 5-15ppm in biotite, 55-100ppm in muscovite, and 1ppm in quartz, in rocks from the Thüringer Wald.

1.2.2 Boron geochemistry and geochemical behaviour

Boron is known to occur in low concentrations throughout the solar system, and it is present in the earth's lithosphere at levels averaging between 10 and 13 ppm (Morgan, 1980). There are two naturally occurring stable isotopes, ^{10}B and ^{11}B. Ratios of ^{11}B to ^{10}B in terrestrial rocks and minerals fall within the range of about 4:1 to about 4.1:1 (Agyei and McMullen, 1968).

The average boron concentration in sediments is higher than that in igneous rocks. Turekian and Wedepohl (1961) quote worldwide averages of 100ppm boron in shales, 35ppm in sandstones, and 20ppm in carbonates. Boron is most strongly enriched in marine clays and shales, in which concentrations between 50 and 200ppm are commonly reported (e.g. Landergren, 1964); this is due to the uptake by illite of boron (especially ^{10}B) from seawater. Since non-marine sediments generally contain less boron, this element is a useful indicator of palaeosalinity, although its reliability in this respect is not universally accepted.

Most igneous rocks contain relatively low boron concentrations. Worldwide averages are quoted variously, including such estimates as 3.1ppm B (0.001% B_2O_3) in all igneous rocks (Goldschmidt and Peters, 1932), and 5ppm in mafic, 30ppm in acidic rocks (Harder, 1959). However, since boron is a highly mobile element, the actual concentrations in igneous rocks cover a wide range. Some granitic and syenitic terrains are highly enriched in boron, which is frequently concentrated, along with other incompatible elements, in late-stage granitic pegmatites.

Boron probably exists in magmas in two configurations, namely the BO_4^{-5} tetrahedron and the BO_3^{-3} triangle (Morgan, 1980). The tetrahedral form is more readily incorporated in magmatic silicates than is the BO_3^{-3} triangle, and this could be a factor in determining the behaviour of boron in magmatic differentiation. Boron-enriched residual melts are capable of producing tourmaline-bearing pegmatites and other differentiation products. The partitioning of boron into the fluid, rather than into crystalline phases at the magmatic stage, may also account for its presence in volcanic and fumarolic gases (e.g. White and Waring, 1963), and its role as a major component of hydrothermal fluids active in post-magmatic alteration processes.

The recent experimental work of Chorlton and Martin (1978) and

Pichavant (1979) indicates that boron in granitic melts may lower the solidus, and therefore the temperature at which magma and hydrothermal fluids can coexist; the latter author has also shown (pers. comm. 1981) that boron may accentuate the partitioning of potassium into crystalline phases (e.g. feldspar) at subsolidus temperatures.

Boron metasomatism (including tourmalinisation) in granites requires the concentration of boron in a fluid phase which is capable of travelling through fissures and other pathways in consolidated rock. Various origins could be proposed for such a fluid phase:

(i) Boron could be introduced from an extraneous source unrelated to the granites (e.g. mantle).

(ii) Boron concentrated in a granitic magma could become partitioned into a residual fluid phase.

(iii) Boron-rich fluids could be derived from illite-bearing clays by one of two mechanisms, a) by total assimilation of clay-grade sediments by granite, and subsequent differentiation of an incompatible fraction, or b) by removal of boron and water from illite on its conversion to muscovite during contact metamorphism within the granitic aureole.

The first suggestion seems unlikely, in view of the very low boron concentrations generally found in mantle-derived materials (average 3ppm in ultrabasic rocks, according to Turekian and Wedepohl, 1961). The second case is theoretically possible, but since not all granites are enriched in boron, a magmatic source cannot be proven. The third possibility is feasible firstly because of the known affinity of boron for clay minerals, secondly because of the considerable capacity of granites to assimilate their sedimentary envelope, and thirdly because the transformation of illite to muscovite involves the release of boron to groundwaters or other coexisting fluids (Landergren and Carvajal, 1969).

The literature contains many examples of tourmaline-bearing metamorphic rocks, in which the boron is thought to have been derived from the original sediments, without the need for metasomatism associated with an igneous body (e.g. Black, 1971; Coleman, 1967; McCurry, 1971; Rickard, 1964). In contact metamorphism, Wodzicki (1971) has described the diffusion of boron, lithium, tin and lead from sources within the intruded sediments, to supply the components of hydrothermal vein systems.

Boron adsorbed onto clay mineral surfaces would be released at temperatures between 200 and 300°C (Landergren and Carvajal, 1969; Morgan, 1980). Tourmaline may form at very low temperatures, simply as a function of sedimentary diagenesis (Krynine, 1946), but it has also been synthesised at temperatures ranging from 250 to 600°C, at fairly low pressures, in weakly acid to weakly alkaline conditions (Frondel and Collette, 1957; Michel-Levy, 1953; Smith, 1949; Tomisaka, 1968). Synthetic tourmalines have been produced in conditions simulating metamorphism or metasomatism, rather than crystallisation of a granitic melt. Pichavant (1979) in his high temperature and pressure experiments, crystallised not tourmaline, but boron-bearing glass. Manning (1981a)was unable to melt tourmalinite rock at 800°C, except in the presence of cryolite as a flux, and considered it therefore unlikely that such rocks could crystallise directly from a magma. Although 'primary' tourmaline certainly occurs (e.g. in pegmatites), the depositing medium should perhaps be regarded as a hydrothermal fluid rather than a magma in the true sense.

Evidence for the geochemical behaviour of boron indicates that intruded clay-grade sediments could be a potential source for the supply of boron to granitic hydrothermal systems. This possibility

will be examined with respect to tourmalinised and tourmaline-bearing rocks in southwest England.

1.3 The environment of tourmalinisation in southwest England

1.3.1 Geology of the province

Fig. 1:3 shows the configuration of the Variscan granites of Cornubia, in relation to the other rock types present.

The Devonian and Carboniferous rocks into which the granite stocks are intruded are locally known as 'killas'. This term encompasses sediments and metasediments of several lithologies (principally pelites, psammites and greywackes) as well as intercalated volcanic horizons, but excludes the Devonian Old Red Sandstone facies of Exmoor. South of Exmoor, the Devonian and Carboniferous sediments differ from those elsewhere in the British Isles, since they are chiefly marine (Edmonds et al., 1975); the Upper Carboniferous rocks contemporaneous with the Coal Measures are here barren, and are known as 'culm'.

Structurally, the region is dominated by a broadly east-west trending synclinorium, in which Devonian rocks form the outermost flanks, and Carboniferous the central trough. Despite intense and multiphase folding within the killas, regional metamorphism does not generally exceed lower greenschist facies (Phillips, 1964). The structural trend is continued in the Variscan fold belt of central and eastern Europe (Krebs, 1977), and probably reflects the orientation of plate collision taking place to the south (Floyd, 1972; Laurent, 1972).

The same plate collision may be responsible for the present position of the older rocks comprising Start Point and the Lizard Peninsula, each bounded to the north by major thrust planes. These older rocks of unknown provenance comprise amphibolites, schists and gneisses, as well as the Lizard complex (Flett, 1946), which is currently interpreted as an

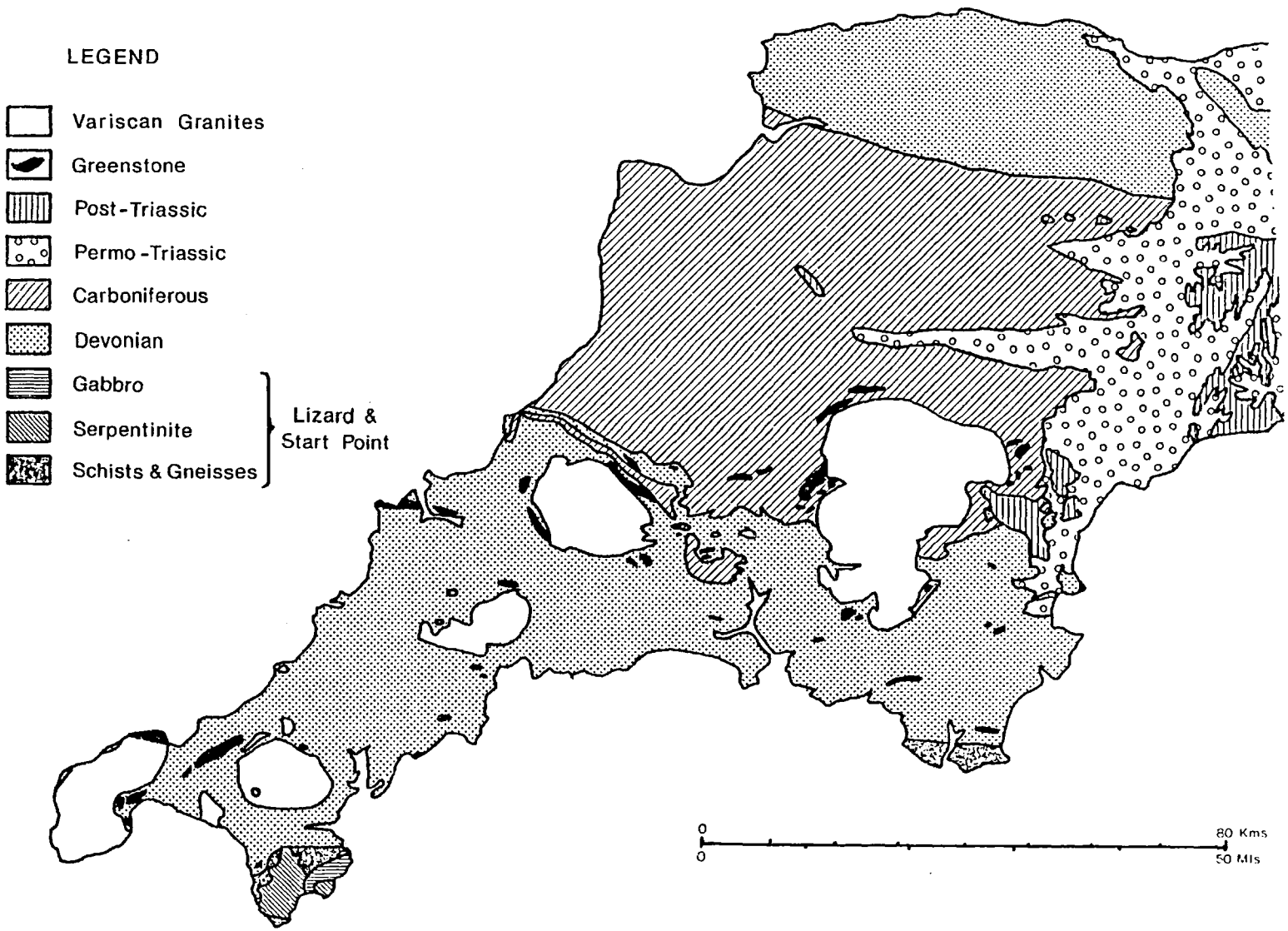

Fig. 1:3. The Geology of southwest England (simplified after Edmonds et al.,1975)

ophiolite (Styles and Kirby, 1980). The age of the Lizard rocks is uncertain; K-Ar dating (Green, 1964) indicates at least 350 m.y. for the last recrystallisation.

The major Variscan tectonism was both preceded and followed by local mafic minor intrusions, chiefly of dolerite, and generally termed 'greenstone' in the literature. These predate granite emplacement, since they are metamorphosed in the contact aureoles.

The period of maximum deformation in Devon is dated close to the Westphalian-Stephanian boundary, about 300 m.y. (Miller and Mohr, 1964), and prior to the emplacement of the granites. The earliest post-orogenic sediments are probably uppermost Carboniferous in age, although generally attributed to the Permian (Edmonds et al., 1968). Potassic, basic volcanism during the early Permian produced lavas and lamprophyre dykes; it is possible that these volcanic rocks acquired excess potassium by interaction with the already intruded granites (Hawkes, in Edmonds et al., 1968), or alternatively, perhaps, that the potassic volcanism was connected with post-magmatic potassium enrichment within the granites.

Permotriassic and Mesozoic sediments are confined to the easternmost part of the southwest peninsula. Tertiary sediments form isolated outliers, notably the Bovey Basin ballclay deposits, east of Dartmoor.

1.3.2 The Variscan granites

The Cornubian granites are generally regarded as post-tectonic, emplacement dates having been determined variously at around 295 m.y. (Fitch and Miller, 1964, K-Ar metamorphic date of Dartmoor aureole), about 285 m.y. (Harding and Hawkes, 1971, Rb-Sr on St. Austell granite), and about 273 m.y. (Miller and Mohr, 1964, K-Ar on Land's End granite). As explained by Hawkes and Dangerfield (1978), there is much uncertainty surrounding the actual date of emplacement, since Sr, Rb, K and Ar isotopes may have been selectively redistributed as a result of post-

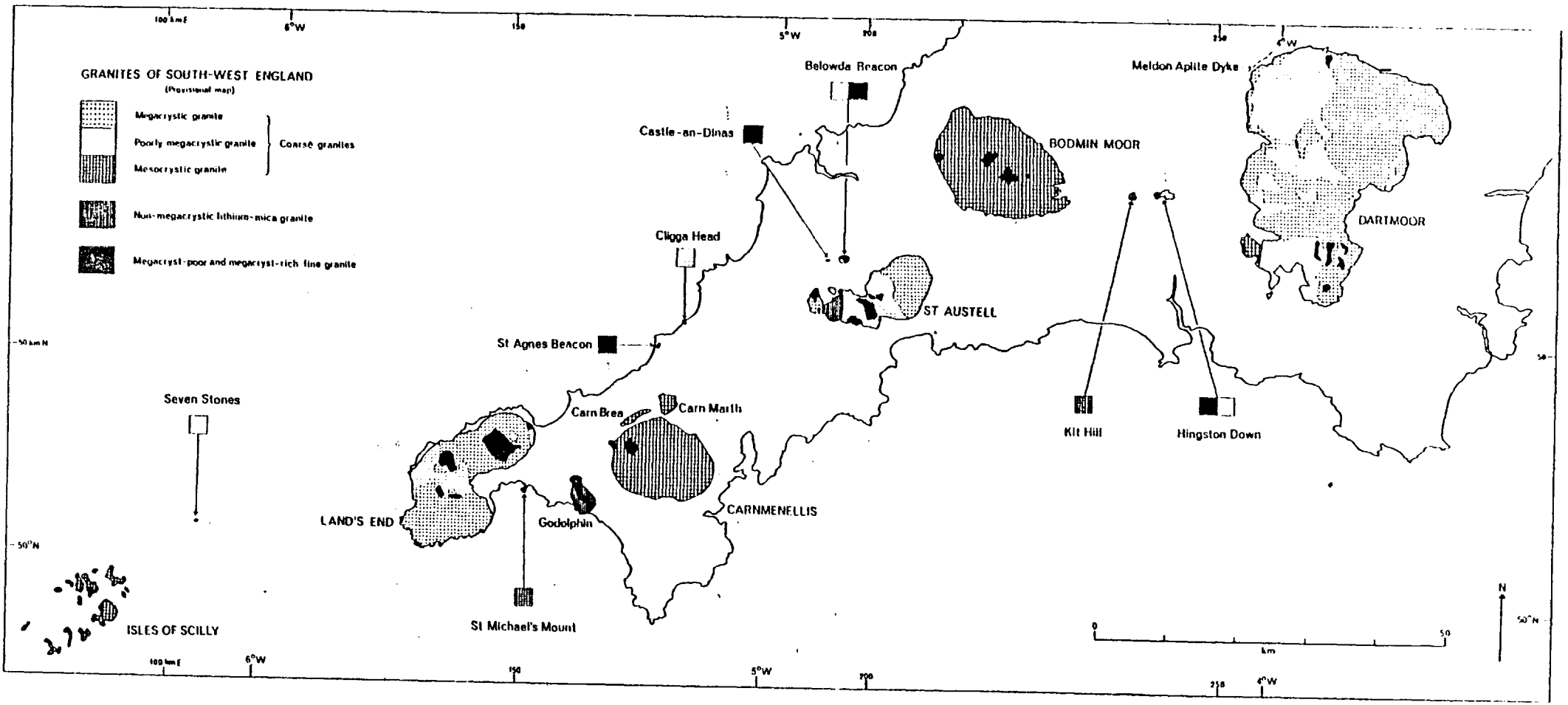

Fig. 1:4. The Variscan Granites of southwest England (after Hawkes and Dangerfield, 1978)

magmatic alteration and volcanism. Further ambiguity, pointed out by Miller and Mohr (1964), results from the fact that biotite yields consistently older K-Ar dates than muscovite (presumed cogenetic) from the same plutons. Taking these factors into account, there is still a spread of ages, which supports the theory of successive diapiric emplacements over a protracted period of time.

The main granite outcrops of Dartmoor, Bodmin Moor, St. Austell (Hensbarrow), Carnmenellis, Tregonning-Godolphin, Land's End and the Scillies, are aligned in an east-north-east - west-south-west trend, which does not coincide with the main structural trend of the surrounding killas. The granites of the mainland (at least) are interconnected at depth to form a continuous batholith, extending the length of Cornubia (Bott et al., 1958, on geophysical evidence).

Early writers (e.g. Ussher, 1888; Reid et al., 1912) suggested that the Dartmoor granite took the form of a laccolith. The gravity survey of Bott et al. (1958) indicated a structure with a cylindrical feeder pipe in the south, supplying magma for a sheet-like body overlying killas in the north; the other Cornubian plutons also yield asymmetric profiles, and may have a similar structure.

Granite emplacement was achieved by the successive intrusion of a series of individual plutons. Brammall and Harwood (1932) noted the composite nature of the Dartmoor granite, and Exley (1959) delineated no less than four separate facies showing a progressive differentiation trend within the St. Austell mass. Fig. 1:4 shows the configuration of the outcrops and and major facies exposed (classified by Hawkes and Dangerfield, 1978, principally on textural grounds), and emphasises that the exposed granite masses consist of several smaller plutons (this is particularly noticeable in Dartmoor, St. Austell and Land's End).

Petrographically, all the granites (except certain lithium-rich varieties) consist of quartz, potassium-feldspar and sodic plagioclase,

with variable quantities of biotite, and accessories such as muscovite, tourmaline, zircon, topaz and apatite (Hawkes and Dangerfield, 1978). The individual granite areas have been the subject of detailed studies as follows: Dartmoor by Brammall and Harwood (1923; 1932), Bodmin by Ghosh (1927), St. Austell by Exley (1959), Carnmenellis by Ghosh (1934), Tregonning-Godolphin by Stone (1975), Land's End by Booth (1966), and the Scillies by Osman (1928).

There is abundant evidence, both textural and chemical, for assimilation of killas by the granites (Brammall and Harwood, 1932; Exley and Stone, 1964). In many areas (e.g. the eastern St. Austell granite), every stage of assimilation may be observed, from biotite-rich schistose fragments to patches of xenolithic material virtually indistinguishable from the surrounding granite. The contribution of pelitic sediment is evidenced by portions of the Dartmoor granite which contain garnet, cordierite, andalusite and corundum (Brammall and Harwood, 1923).

The present chemistry of the Cornubian granites is much complicated by post-magmatic alteration. The porphyritic, biotite-bearing granites which comprise most of the granitic terrains are relatively potassic, while aplites, leucogranites and felsites show more sodic compositions lying close to the ternary minimum of the natural granite system; Exley and Stone (1964) illustrate these trends, and discuss the complex relationships between differentiation, contamination and metasomatism.

The origin of granitic magmas is open to some debate. The classic statement of H.H. Read (1944) that there are 'granites and granites' is proving even more significant in the light of modern geochemical data on granitic terrains, and with greater understanding of tectonic processes. Chappell and White (1974) classified certain Australian granites geochemically into I-types (igneous) and S-types (sedimentary), according to their origin from magmatic sources or from sedimentary remobilisation.

The parallel classification of Ishihara (1977) designates magnetite-series granites of essentially mantle origin, and ilmenite-series granites of crustal origin; the former are associated with porphyry-copper and molybdenum deposits, while the latter are the hosts for greisen-type tin-tungsten deposits. Pitcher (1979) places I-type and S-type granites in the context of their respective Andinotype or Hercynotype orogenic setting; Andinotype orogenies are characteristically associated with subduction, and Hercynotype orogenies (which may include mixed S-type and I-type granites) are generally intracontinental. The main criteria for these various classifications are summarised in Table 1:3.

I-type granites	S-type granites
Tend to be the acid end of a broad compositional spectrum from basic to acid	Tend to occur in restricted ranges of acid compositions
Relatively high Na, low K	Relatively low Na, high K
Low initial $^{87}Sr/^{86}Sr$ (< 0.708)	High initial $^{87}Sr/^{86}Sr$ (> 0.708)
Normal range of $\delta^{18}O$ (6-10‰, SMOW)	High $\delta^{18}O$ ($> \sim$ 10‰, SMOW)
High oxygen fugacity $\Rightarrow$ high $Fe^{3+}:Fe^{2+}$ $\Rightarrow$ magnetite	Low oxygen fugacity $\Rightarrow$ low $Fe^{3+}:Fe^{2+}$ $\Rightarrow$ ilmenite
Accessories: hornblende, sphene, subcrustal restite material	Accessories: muscovite, monazite, cordierite, garnet, crustal xenocryst
Cu-Mo mineralisation	Sn-W mineralisation
Associated with Andinotype orogenies, in subduction regions	Associated with Hercynotype orogenies; intracontinental
Granites mantle-derived	Granites crust-derived

Table 1:3. Classification of granites according to current theories (Chappell and White, 1974; Ishihara, 1977; Beckinsale, 1979; Pitcher, 1979).

Plant et al. (1980) preferred to consider granites as either 'metalliferous' or 'mineralized', in order to distinguish intrusions with a high primary magmatic concentration of metals from those associated with metalliferous mineralisation as a result of water-rock interaction; these authors found that in Scotland, metalliferous granites were predominantly of I-type, and that mineralised granites were principally those intruded into relatively low-grade metasediments.

The granites of Cornubia clearly correspond more closely with the S-type than the I-type, and also show many geochemical similarities to the 'mineralized' granites of Plant et al. (1980), as well as having a low-grade metasedimentary envelope. They are associated with only minor basic intrusions and volcanics, they are largely potassic, and the mineralogical constituents are generally those of S-type granites. $^{18}O/^{16}O$ is enriched (Sheppard, 1977), but $^{87}Sr/^{86}Sr$ data are inconclusive, the only published result being 0.7086 (Harding and Hawkes, 1971; recalculated according to the formula of Brooks et al., 1972 by Hawkes and Dangerfield, 1978). The area is well known as a tin-tungsten province, but copper mineralisation is also widespread (although not on the scale of porphyry copper deposits), and molybdenum minerals are also occasionally present. However, Plant et al. (1980) pointed out that many S-type granites may have been derived from originally I-type granites, by processes of water-rock interaction. A magmatically derived (I-type) granite could also acquire S-type characteristics by assimilation of or contamination by sedimentary material at higher levels of the crust; the possibility that S-type granites at the surface may grade into I-type granites at depth cannot be precluded.

Hence, although the Cornubian granites have S-type affinities, their original S-type genesis is not proven. Their general correlation with S-type and Hercynotype orogenic regimes is, however, consistent with

the theory, long maintained on grounds of low-grade regional metamorphism and post-orogenic plutonism, that the Cornubian province lay at the margins of an orogenic belt in Permo-Carboniferous times. Pitcher's (1979) view of an intracratonic environment for Hercynotype orogens is compatible with Floyd's (1972) model in which Cornubia lies at the very northern extremity of a northward-dipping subduction zone which reaches the surface south of the Massif Central.

1.3.3 Post-magmatic processes

Apart from the more obviously post-magmatic features such as ore mineralisation, there is evidence to suggest that the present fabric of the Cornubian granites has developed by recrystallisation and metasomatism (Stone and Austin, 1961; Exley and Stone, 1964). Assimilation produces many recrystallisation textures, indeed, all the major granitic minerals may be seen replacing xenolithic material, or growing around the margins of xenoliths; the relative importance of assimilation effects and large-scale post-magmatic recrystallisation is not easy to assess.

There is, however, much evidence for post-magmatic potassium-enrichment; Exley and Stone (1964) discuss both the metasomatic growth of potassium feldspars, and the alteration of existing plagioclase to potassium feldspar by alkali transfer. According to Edmonds et al. (1968), the Dartmoor granite, at least, probably originated as a trondhjemite, and this is evidenced by the compositions of plagioclase rims of rapakivi feldspars on Dartmoor (Hawkes, 1967). Potassium enrichment, which has affected sometimes the cores but sometimes the whole feldspar grains, has been interpreted as 'potash-metasomatism'. This process may be a natural consequence of re-equilibration, with temperature and pressure reduction, by interaction of the feldspars with circulating fluids: while at magmatic temperatures and pressures, sodium would preferentially enter

the solid phase (feldspar) in favour of potassium, the reverse is true at lower temperatures and pressures (Orville, 1963).

The effects of other major post-magmatic processes within the granites and associated rocks are more localised, but are nevertheless seen to a greater or lesser extent throughout the province. Metalliferous mineralisation (summarised by Hosking, 1964) took place in several stages, over a considerable period of time, and the higher temperature (Sn, W, Cu) mineralisation is frequently associated with greisening and/or tourmalinisation; low temperature mineralisation may be accompanied by chloritisation. Metalliferous lodes are particularly concentrated in the Godolphin, Carn Brea, Carn Marth and St. Agnes area. Greisening frequently accompanies tin-tungsten mineralisation, as in the example of Cligga Head, described by Hall (1971) and Charoy (1979b). Tourmalinisation is discussed in detail below. The relative ages of these post-magmatic events are not certain, since some examples show greisening post-dating tourmalinisation, while others show the reverse.

Aplites and pegmatites form minor intrusive bodies which generally post-date granitic joint development, but in a few cases, aplites grade laterally into porphyritic granite (Exley and Stone, 1964); their ages with resepct to other post-magmatic events are equivocal. The emplacement of elvans (quartz porphyries) is described by Goode (1973), and, postdating some but not all metalliferous mineralisation and associated alteration, is given a Rb:Sr date of about 269 m.y. by Hawkes et al. (1975).

Kaolinisation evidently began at an early stage, but continued for a longer period than any of the above-mentioned processes. There is good reason to suppose that kaolinisation is still taking place today, since hot groundwaters continue to circulate within the granites. Although it has been suggested (Hickling, 1908) that kaolinisation is simply a weathering process, there is ample evidence for a hydrothermal origin

(Exley, 1959: 1964). It is probable that hydrothermal kaolin has made the rock susceptible to further breakdown by weathering processes (Bristow, 1968).

1.4 Tourmalinisation

De la Beche (1839), writing at length about the occurrence of Cornish schorl and schorl rocks, remarked that 'we seem to have conclusive evidence that this mineral may be decomposed in one place and recomposed in another under given conditions'. The 'recomposition' of which he wrote was the replacement of feldspar by tourmaline, and thus he described the tourmalinisation process.

Tourmalinised rocks were the subject of several subsequent field and petrographic descriptions. Luxullianite, named 'luxulliane' by Pisani in 1864, consists of pink feldspar in a black groundmass of tourmaline and quartz, and was first described petrographically by Bonney (1877). Worth (1887b) examined trowlesworthite, which is essentially luxullianite with purple fluorite, and also (1887a) a rock which he called 'white luxullianite' in which the apparently intact white feldspars are pseudomorphed by quartz. Le Neve Foster (1879) described 'a rock resembling luxullianite' from St. Just. Reid and Flett (1907) described trevalganite from the Land's End coast; this superficially resembles luxullianite. Under the heading of 'tourmalinization', Ussher et al. (1909) discussed luxullianite and the schorl rock (tourmalinite) of Roche Rock, concluding that in the former the metasomatic replacement process had stopped at a half-way stage. The last named authors also mentioned St. Mewan Beacon as a 'quartz-rock with nests of schorl'; this small outcrop actually consists of quartz, schorl and topaz in varying proportions.

Brammall and Harwood (1925) on tourmalinisation in the Dartmoor granite, classified the tourmaline into primary magmatic, and two separate

secondary replacive generations, remarking that the greater part of the tourmaline present is secondary; these authors noted the absence of tourmaline from the earliest-intruded granite facies of Dartmoor, and suggested that tourmaline-rich nodules could arise from early replacement of basic segregations within the magma. Brammall and Harwood (1927) estimated the possible temperature for tourmaline formation in 'geodes' and quartz-tourmaline veins to be below 575°C, on the evidence of coexisting α-quartz.

Agrell (1941) described the only reported occurrence of dravite in southwest England. This is found at Dinas Head within adinoles and spilosites, completely removed from granitic terrain.

The type luxullianite was the subject of a further petrographic study by Wells (1946), who confirmed the view that arrested pneumatolytic alteration of granite was responsible; the material for this study, as hitherto, came from boulders in a field, since the rock had never been found <u>in situ</u>. Blyth (1949) examined a rock superficially very similar to luxullianite, exposed as a vertical vein in a small quarry near Holne, east Dartmoor.

Tourmalinisation in southwest England in discussed in the context of post-magmatic alteration processes by Exley and Stone (1964), who recognised pre-joint, primary tourmaline, and post-joint, secondary tourmaline, and summarised the tourmaline content of the individual granite plutons. They stated that the primary variety is blue, yellow and brown in thin section and is likely to be of schorl composition, while the secondary tourmaline is blue-green in thin section and may possibly be elbaite or at least have a composition in the schorl-elbaite series.

Power (1968) examined trace element concentrations in magmatic and hydrothermal tourmalines from southwest England, in an attempt to

characterise these apparently distinct types. He was able to conclude that hydrothermal tourmaline contained higher magnesium, calcium, strontium, tin, vanadium, chromium and nickel than magmatic tourmalines, and that the strontium:calcium ratio was higher in hydrothermal varieties. A further conclusion of this work was that the tourmalinite of Roche Rock is unlikely, on geochemical grounds, to be a product of hydrothermal tourmalinisation.

Hall (1973) briefly discussed tourmalinisation in southwest England, giving analyses of three different tourmalinised rocks and their untourmalinised equivalents. Jackson (1974) described an example of tourmaline replacing subhorizontal beds of hornfels in association with tin mineralisation at Botallack (Land's End aureole).

The only proven elbaite in southwest England occurs in the Meldon Aplite, northwest Dartmoor; according to Chaudhry and Howie (1976), the early, verdelite generation is more iron-rich than the later, rubellite generation.

Geochemical and fluid inclusion data on tourmalinised rocks from Pendarves Mine, and from the Birch Tor and Vitifer Mines area, were included in Alderton's (1976) work on mineralisation.

A tourmaline-cemented, hydrothermal breccia pipe is exposed in Wheal Remfry China Clay Pit (western St. Austell granite); this was briefly described by Halls et al. (1978), and is interpreted by Allman-Ward et al. (1981) as the result of rapid emplacement due to pressure release. A report by Goode and Taylor (1980) concerns several further examples of such breccias, both tourmaliniferous and tourmaline-free, from Cornubia.

Lister (1978a) described and analysed luxullianite, occurring in situ as a vertical vein at Tregarden Quarry, Luxulyan, close to the type locality. This was compared with the example from Dartmoor (Blyth, 1949) by Lister (1978b). The description of luxullianite exposed for the

first time *in situ* prompted a written discussion by Alderton (1979) and reply by Lister (1979b), concerning the association of tourmalinisation and K-feldspathisation.

The common occurrence of quartz-cored tourmalines in southwest England was examined by Lister (1979a), with the conclusion that the euhedral variety found in pegmatites was formed by direct and rapid crystallisation, and not by replacement.

Charoy (1979a) considered the question of tourmalinisation with particular reference to the Cape Cornwall tourmalinite. On the basis of a detailed study, he presented the arguments in favour of either a magmatic or a hydrothermal origin for this rock; he stated that although there is evidence for both possibilities, an origin by extreme magmatic differentiation seems likely. His work will be discussed further in a later chapter.

Alderton *et al.* (1980), in an examination of rare earth element mobility during granite alteration in southwest England, reported rare earth depletion as a result of tourmalinisation.

1.4.1 Distribution of tourmalinised rocks in Cornubia

Tourmalinised rocks are found predominantly within the Cornubian granites and at their margins, and are particularly prevalent on Dartmoor, the St. Austell granite and the Land's End granite. There are also examples in the other plutons. The occurrence of tourmaline-bearing granite on Lundy Island (Edmonds *et al.*, 1979) should be noted, since this could question the supposed Variscan age of Cornubian tourmalinisation.

On Dartmoor, tourmaline and tourmalinised rocks are particularly abundant in the following areas:

(i) Lee Moor China Clay Pit and vicinity, southwest Dartmoor

(ii) Birch Tor and Vitifer Mines area, northeast Dartmoor

(iii) Holne and Hexworthy area, east Dartmoor

(iv) Okehampton, northwest Dartmoor: contact aureole and Meldon Aplite

(v) Hemerdon Ball (just off southwest Dartmoor); tourmalinite associated with wolframite deposits

In the St. Austell granite, Exley (1959) reported maximum tourmalinisation in the 'early lithionite' facies, with some tourmaline also occurring in the 'biotite-muscovite' facies. Notable examples are:

(i) Roche Rock tourmalinite, isolated at the surface from the main granite outcrop

(ii) Carclaze China Clay Pit (early lithionite granite)

(iii) Wheal Remfry Pit (early lithionite granite, western outcrop)

(iv) Goonbarrow Pit (boundary between biotite-muscovite and early lithionite granites

(v) Luxulyan, Tregarden Quarry (biotite-muscovite granite)

The important Land's End exposures are chiefly around the coast, where the granite-killas contact occurs. These are:

(i) Cape Cornwall tourmalinite and tourmaline veins

(ii) Trevalgan Farm; site of trevalganite

(iii) Porthcurno; tourmaline veining

(iv) Botallack; tourmaline-cassiterite rock

(v) Porthmeor Cove; tourmaline-bearing dykes

Other noteworthy localities include: (i) Hingston Down Quarry, in the Gunnislake microgranite, where feldspar-phyric tourmalinite veins occur, (ii) Megiliggar Rocks on the Tregonning granite coast, where tourmaline is found in pegmatite and aplite sheets, and (iii) Dinas Head, near Trevose Head, where dravite was reported by Agrell (1941).

2. Field Occurrence and Petrography of Samples

In previous work concerning the tourmalinisation process and the distinctions between primary and secondary tourmaline (for references see chapter 1), tourmalinised rocks have generally been considered in isolation rather than with respect to their known parent materials. Those authors who have examined both tourmalinised and untourmalinised rocks (e.g. Hall, 1973; Charoy, 1979a) treated them as separate entities and did not examine transitional material. In many cases, such transitional material is not available, because tourmalinised and untourmalinised rocks are divided by a sharp boundary, or because contacts are not exposed. Transitions between altered and unaltered rocks are, however, crucial to the understanding of metasomatic processes.

The present investigation is designed to provide direct evidence as to the nature of the tourmalinisation process, by examining examples where a continuous transition exists between tourmalinised and untourmalinised rock. At each of the selected localities, a series of samples was collected representing a progressive tourmalinisation sequence, in which the successive stages leading to tourmalinisation could be observed petrographically.

Venford Reservoir Quarry in east Dartmoor, and Tregarden Quarry at Luxulyan in the St. Austell granite, both feature vertical *in situ* replacement veins of tourmalinised rock resembling luxullianite. Goonbarrow China Clay Pit, in the St. Austell granite, contains several vertical and subvertical replacement veins consisting of tourmalinite and greisen. Cape Cornwall is the site of an extensive tourmalinite, overlying subhorizontally a tourmaline granite.

This chapter describes the field occurrence of tourmaline-bearing rocks at the above localities, and investigates the mineralogical transformations observed in the tourmalinisation of the parent granite.

2.1 Venford Reservoir Quarry, Dartmoor

2.1.1 Field description

The quarry is located below the reservoir on the road between Holne and Hexworthy (at SX686714), on land belonging to the South Western Water Authority. Granite was quarried here as building stone for the reservoir dam and works buildings at about the turn of the century, and the quarry is now disused and overgrown.

Fig. 2:1 shows the position of the quarry within the coarse megacrystic granite (of Hawkes and Dangerfield, 1978), southwest of some small areas of fine granite. The coarse megacrystic granite of central Dartmoor grades downwards into coarse-grained, poorly-megacrystic granite, which outcrops in topographic low points (e.g. the nearby Dart Valley). The 'unaltered' biotite granite in Venford Reservoir Quarry just falls within the megacrystic category, since it contains more than 10% megacrysts, and these are mostly about 20 mm long. Black tourmaline pods (a few cm across) occur sporadically within the biotite granite; these were interpreted by Brammall and Harwood (1925) as due to early replacement of basic segregations within the granite, and are probably unrelated to later tourmalinisation events.

Blyth (1949) described the occurrence in this quarry of a near-vertical tourmalinised vein resembling luxullianite, and this was compared with luxullianite veins at Luxulyan by Lister (1978b). The vein is exposed in the north of the quarry (Fig. 2:2; Plate 2:1), and strikes northeast at about 65°. The zone of maximum tourmalinisation, about 1.5 metres wide, grades directly into reddened granite on its western side; on its eastern margin, there is a zone of finely-comminuted tourmalinised rock passing into reddened granite which is traversed by several thin, monomineralic tourmaline veins.

The southeast corner of the quarry affords exposure of a further tourmalinised vein, about 0.5 metre wide, and trending east-southeast at about 100°. This orientation corresponds with the trend of the

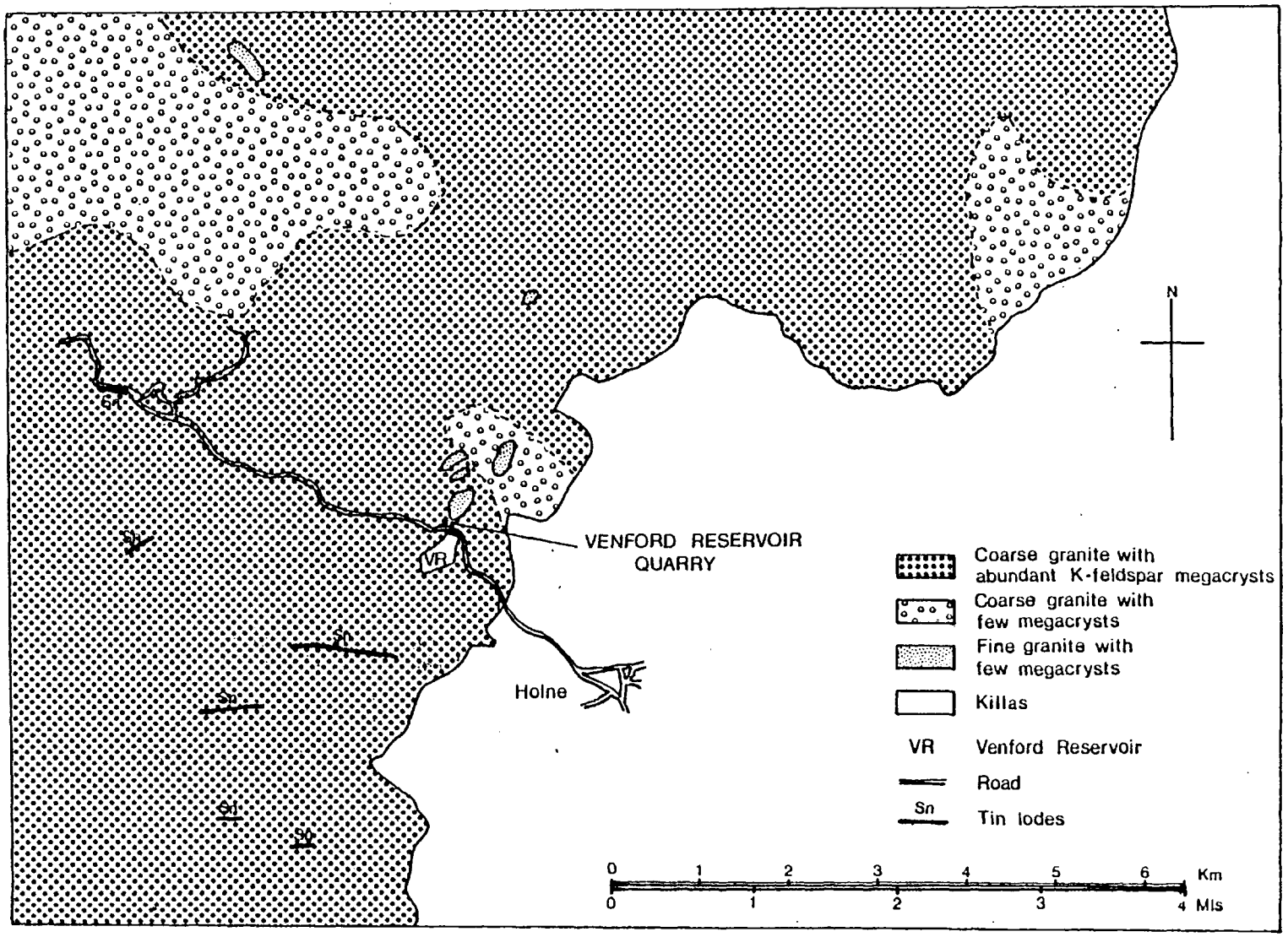

Fig. 2:1 Geology of East Dartmoor and the location of Venford Reservoir Quarry (details from Geol. Survey G.B., 1:50,000 sheet 338; 1977)

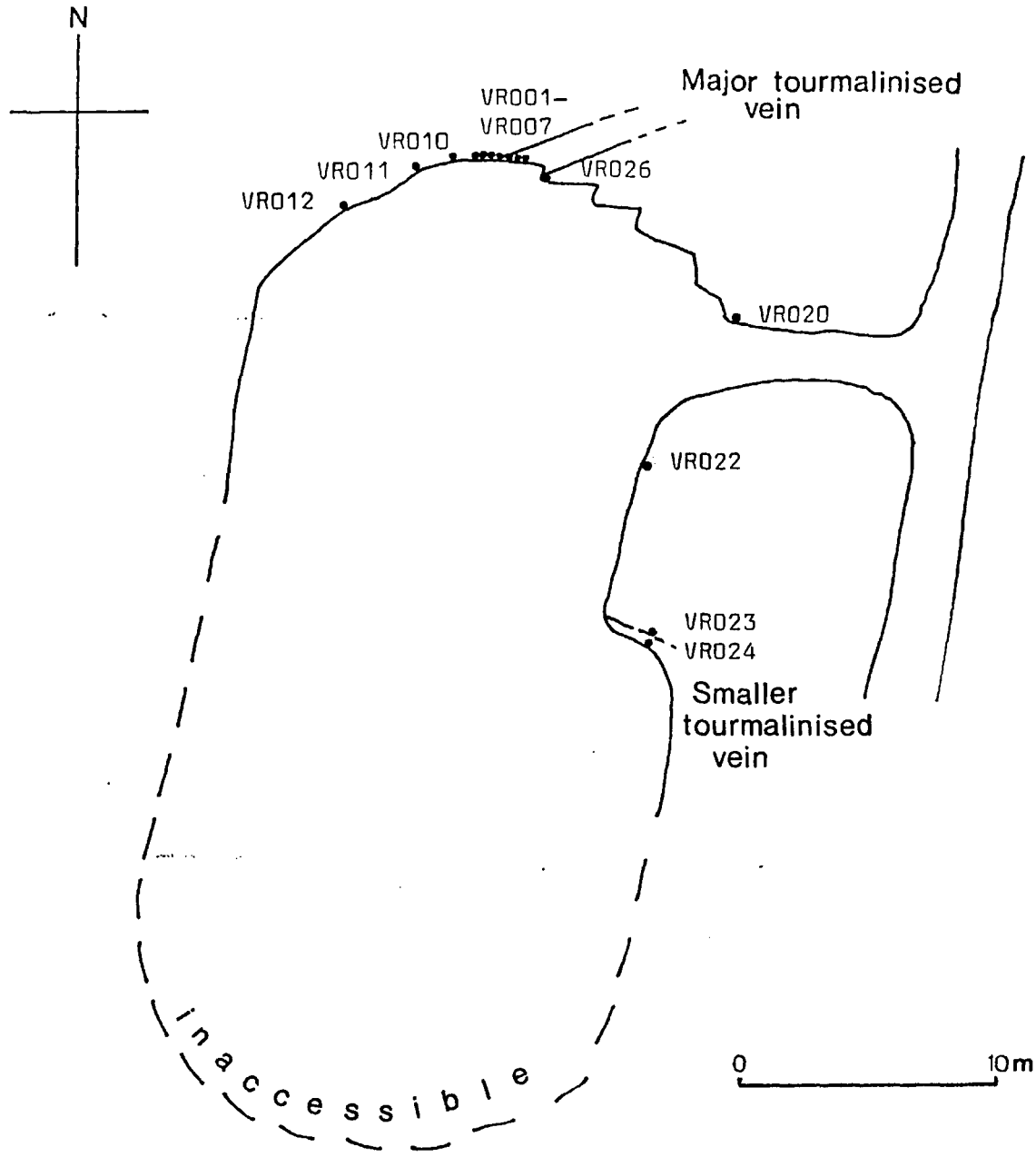

Fig. 2:2 Sketch map of Venford Reservoir Quarry
showing location of samples

Plate 2:1 The northeast corner of Venford Reservoir Quarry. The larger 'luxullianite' vein is exposed in the worked face.

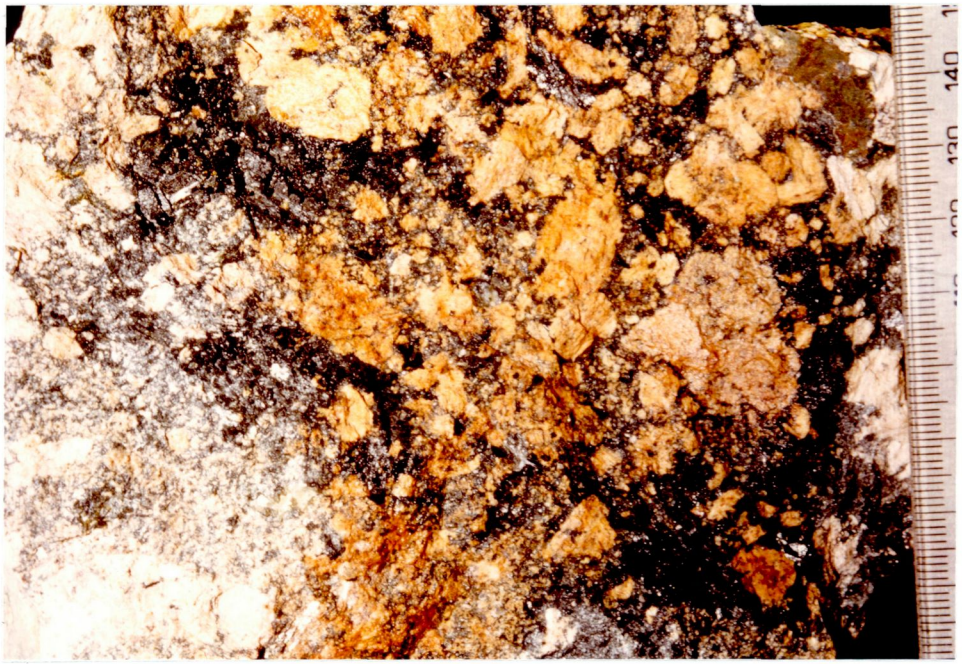

Plate 2:2 Venford Reservoir Quarry 'luxullianite' from the larger tourmalinised vein. (mm scale)

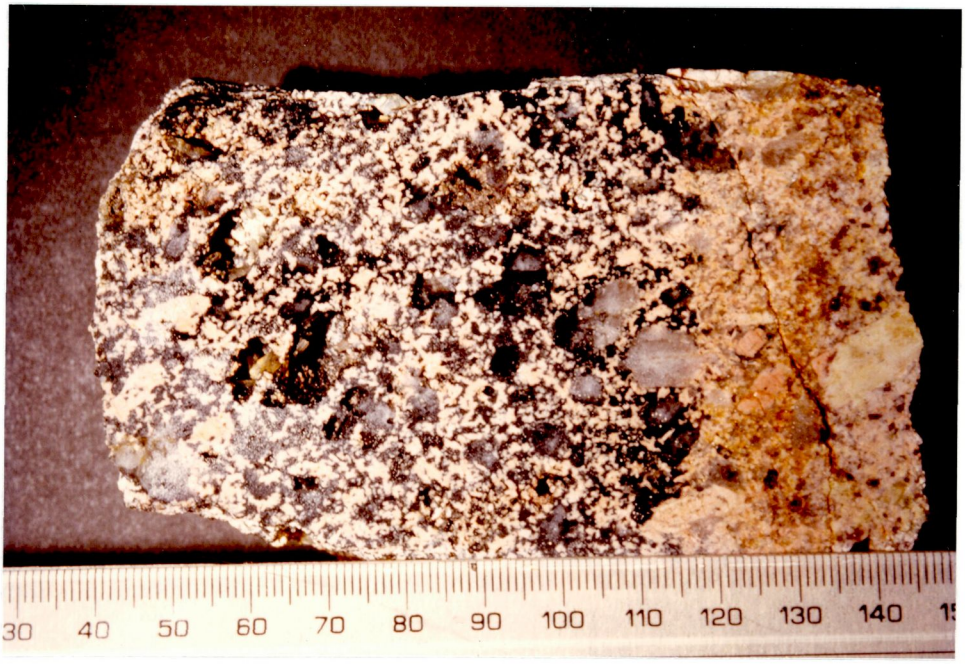

Plate 2:3 Venford Reservoir Quarry: the smaller, cavitous tourmalinised vein material. (mm scale)

thin (up to 1 cm) monomineralic tourmaline veins, which occur throughout the quarry, and traverse the larger tourmalinised vein.

The two tourmalinised veins both consist of partially replaced pink alkali feldspar megacrysts in a dark matrix of quartz and tourmaline, but they exhibit quite different textures. The larger vein (Plate 2:2) is of a massive rock, containing megacrysts larger than those in the 'unaltered' granite, and well cemented by its tourmaline-quartz groundmass. The smaller vein (Plate 2:3) is cavitous, with holes up to 1 cm across, in a matrix which consists of more finely-comminuted pink feldspar, tourmaline and quartz; the few remaining megacrysts are a similar size to those in the 'unaltered' granite. Several thin monomineralic tourmaline veins run through the smaller vein, parallel to it.

The larger vein is bounded by a zone of reddened granite extending about 6 metres from the vein margin; large (up to 3 cm) pink feldspar megacrysts are well developed in this reddened zone. At the margins of the smaller vein, a reddened zone extends only a few centimetres.

Both reddened and unreddened granite contain large (1 cm) rounded quartz blebs. These persist into the tourmalinised vein margins, and since their shape and size are similar to those of the larger cavities in the smaller tourmalinised vein, it is possible that these cavities may represent dissolution of quartz during tourmalinisation.

From the orientations of joints and veins in the quarry, shown in Fig. 2:3, it appears that the larger tourmalinised vein corresponds with what is only a minor joint direction. However, this trend is cited by Blyth (1962) as the dominant orientation of tourmaline veins in the northeastern Dartmoor granite, and by Brammall (1926) as the trend of the nearby Birch Tor and Vitifer tin lodes; according to Blyth (1949), a continuation of the main Venford Reservoir vein eastwards would take in the quartz-schorl (tourmalinite) reef of Leigh Tor. The smaller

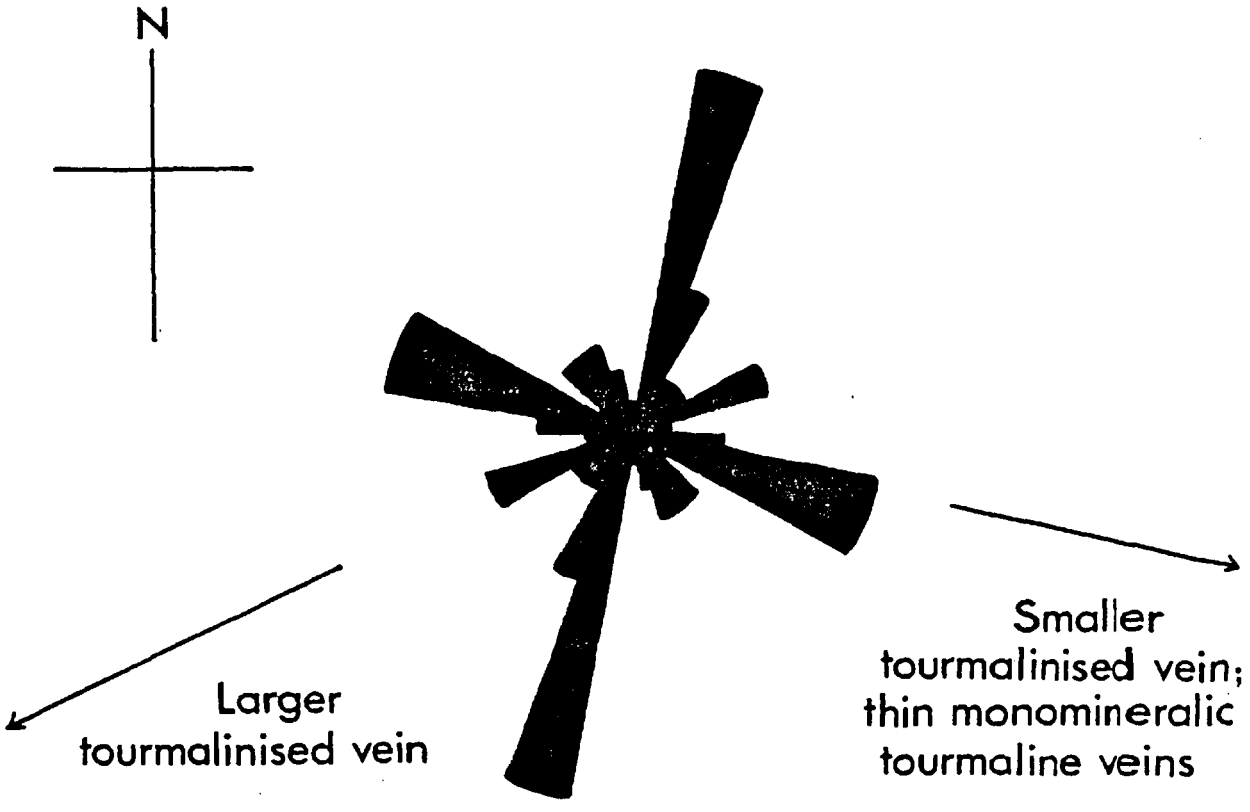

Fig. 2:3 Orientation of joints & veins at Venford Reservoir Quarry

tourmalinised vein and the monomineralic tourmaline veins within the quarry correspond with a major west-northwest - east-southeast joint direction, which shares the orientation of local tin-bearing lodes indicated in Fig. 2:1; according to Grammall (1926) this is also the trend of red-rock veins and tourmalinised joints in the Holne Moor area. The major north-northeast - south-southwest joint direction recorded in the quarry does not appear to coincide with any tourmalinisation features.

Tourmalinisation and related phenomena at this locality may be summarised as follows:

(i) Black tourmaline pods within the biotite granite,

(ii) Two vertical veins of heavily tourmalinised rock similar to luxullianite, trending in different directions,

(iii) Numerous thin, monomineralic tourmaline veins,

(iv) Reddening of the granite, and development of pink alkali feldspar megacrysts, over a wide zone adjacent to the main tourmalinised vein,

(v) Development of rounded quartz blebs in reddened and unreddened granite.

The following samples were collected for petrographic examination and chemical analysis (their locations are shown in Fig. 2:2): VR022 - 'unaltered' biotite granite; VR020 - iron-stained biotite granite 7 m from larger tourmalinised vein margin; VR012 - VR011 - VR010 - reddened granite 5 m, 2 m, and 0.5 m from vein margin; VR001 to VR007 - a continuous sequence across the vein margin in 3 cm increments (VR006 and VR007 represent the zone of maximum tourmalinisation); VR024 - smaller tourmalinised vein centre; VR023 - smaller tourmalinised vein margin; VR026 - monomineralic vein. The sequence from VR022 to VR007 represents progressive tourmalinisation from 'unaltered' granite through reddened granite into the centre of the larger tourmalinised vein.

2.1.2 Petrography

2.1.2.1 The parent granite

A truly unaltered granite would be difficult to find in southwest England, since post-magmatic alkali changes in feldspars, and quartz recrystallisation are almost ubiquitous. The white granite in Venford Reservoir Quarry is, however, unaltered with respect to tourmalinisation, and represents the closest possible approach to a parent rock for the tourmalinised vein material.

The major constituents are white alkali feldspar, biotite and quartz. Tourmaline is mostly confined to isolated pods, and is absent from the general fabric.

In sample VR022, the feldspar megacrysts average 1 cm in length, and often have euhedral form. Several of the larger grains show rapakivi texture, which has been reported elsewhere on Dartmoor by Hawkes (1967). The central portions of such grains appear optically to be orthoclase microperthites, and this identification accords with the results of X-ray studies (Edmonds et al., 1968, p.98); the plagioclase rims have compositions between albite and oligoclase. The rapakivi texture may attributed to preferential potassium attack on the originally more calcic cores. Smaller alkali feldspar grains in the groundmass are often present in granophyric intergrowth with quartz. Although such intergrown textures are often interpreted as features of eutectic crystallisation, the alternative interpretation of recrystallisation (Augustithis, 1973) seems more likely in the present instance. About 7 metres from the main tourmalinised vein (in VR020), the central cores of rapakivi feldspars become sericitised to a greater extent than the plagioclase rims. The rock takes on a slightly iron-stained appearance, and feldspars begin to appear cream-coloured to pale pink. The pink colouration affects sometimes rims and sometimes centres; one megacryst shows oscillatory

reddening, reflecting the original compositional zoning.

Biotite in VR022 forms anhedral to subhedral brown grains and cleavage flakes about 1 mm across. Some grains show incipient exsolution of dark, iron-rich lamellae parallel to the cleavage traces; some minor embayment of the biotite margins may be observed, with replacement by quartz, feldspar (as in Chayes, 1955), or occasionally, finely-divided white mica. Where biotite is particularly abundant (as in part of VR020), it is often very rich in large inclusions of zircon and apatite. The zircons are euhedral, prismatic crystals up to 0.15mm long, optically zoned, and surrounded by black radiogenic haloes; they may remain within feldspar which has replaced biotite (Plate 2:4). The apatites are more acicular, up to 0.4mm long, normally euhedral, and without haloes.

Quartz, as well as forming granophyric intergrowths with feldspar, is also present as large, rounded grains. Fluid inclusions are abundant throughout.

2.1.2.2 The reddened granite

For a distance 6 metres to the west of the main tourmalinised vein, the granite is strongly reddened. It contains pink alkali feldspar megacrysts up to 3 cm long (larger than those in the parent granite), in a matrix of pink feldspar, quartz, biotite, tourmaline, finely-divided white mica, and prominent opaque grains.

Feldspar is rendered almost opaque in thin section, by the concentration of brown iron-oxide flecks; the distribution of reddening in feldspars becomes more uniform as the tourmalinised vein is approached. Rapakivi texture is present in the outer parts of the reddened granite (VR012), but is absent closer to the tourmalinised vein. In the samples taken 2 metres and 0.5 metres from the vein, the larger feldspars are albite antiperthites. Smaller feldspar

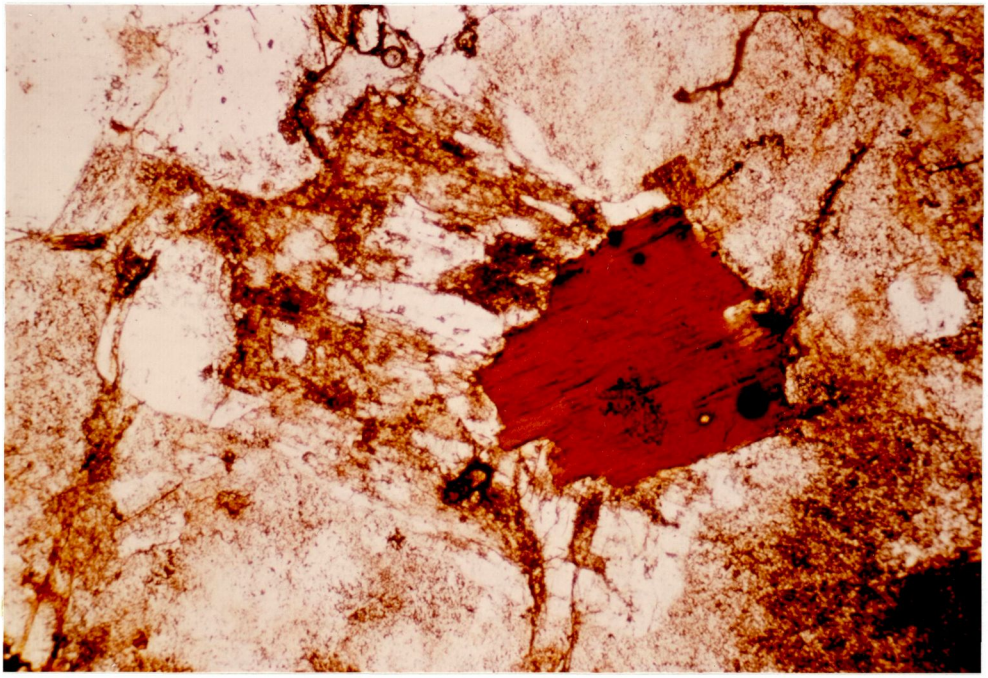

0 0.5mm

Plate 2:4 Biotite replaced at its margins by adjacent feldspar. Note stranded zircon to lower left of biotite. (VR020, p.p.l.) Venford Reservoir Quarry.

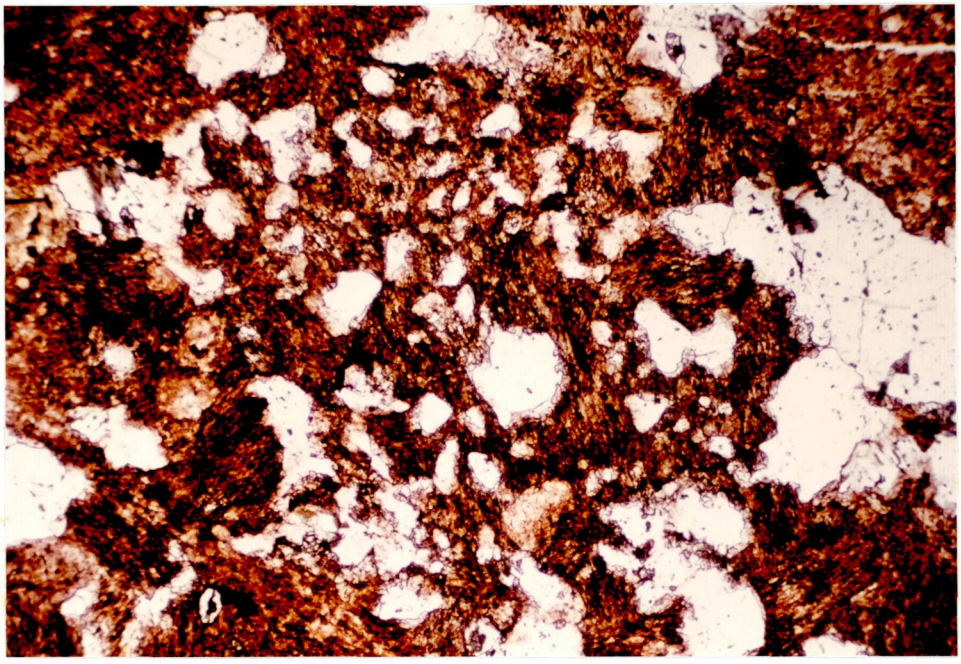

0 0.5mm

Plate 2:5 Granophyric intergrowth between potassium feldspar and quartz. (VR010, p.p.l.) Venford Reservoir Quarry.

grains forming granophyric textures with quartz (Plate 2:5), are chiefly potassium feldspars. The small quartz blebs intergrown with these feldspars become incorporated into larger quartz aggregates as alteration proceeds, so that adjacent to the tourmalinised vein (in VR010), 'ghost' textures (Fig. 2:4) result from remnant stringers of replaced feldspar surrounding quartz.

Biotite in VR012 and VR011 is seen in various stages of degradation and replacement, and is completely absent from VR010. As the biotite structure breaks down, it is replaced either by tourmaline or by white mica, depending presumably upon the availability of ions. The replacement sequence is illustrated in Fig. 2:5, and Plates 2:6 to 2:8, and may be summarised thus:

(i) Brown biotite exsolves dark brown lamellae rich in iron and titanium (confirmed by microprobe) parallel to the cleavage traces. The margins of biotite grains become embayed, and local replacement by quartz and alkali feldspar begins.

(ii) Exsolution proceeds, to give black lamellae, leaving residual green biotite in between. Adjacent quartz and feldspar contain parallel flecks of residual biotite, where marginal replacement has occurred.

(iii) Depending upon the availability of materials, either or both of the following processes may take place. a) Susceptible areas within biotite (e.g. adjacent to cleavages or holes produced by embayment) become replaced by stout prisms of tourmaline, whose crystallographic orientation usually bears no relation to that of the host crystal. b) Similar areas within biotite become replaced by finely-divided white mica, either sericite or hydromuscovite. This stage is illustrated in Fig. 2:5, no. 1.

(iv) Tourmaline replaces large areas of biotite, growing from nuclei both in the centres and at the margins of the host crystals.

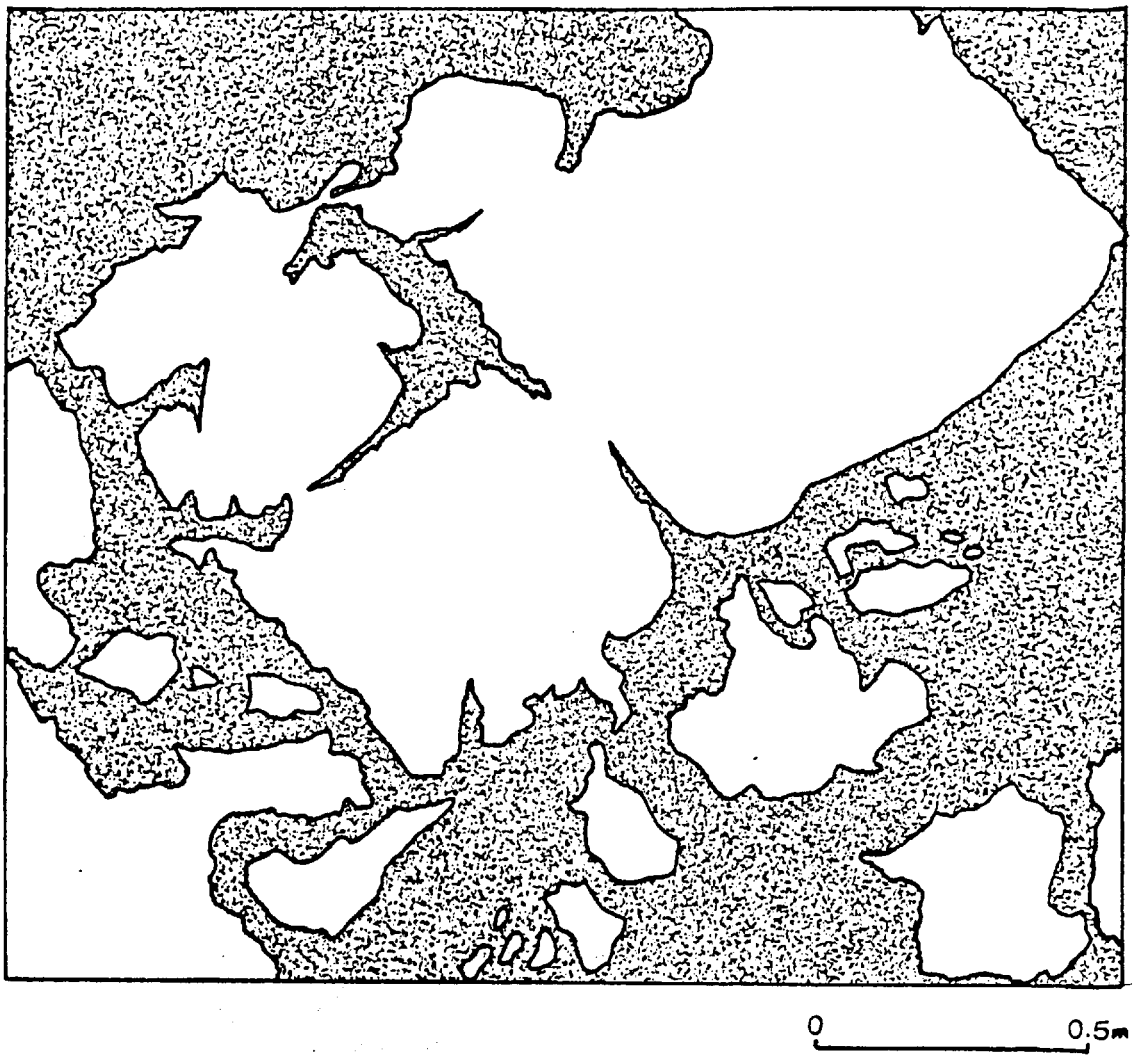

Fig. 2:4 Quartz replacing feldspar in the reddened granite (VR010), leaving residual feldspar 'ghost' textures.

(Feldspar - textured, quartz - no ornament.)

1. Biotite breaking down to give muscovite and dark iron-rich lamellae. Replacement by tourmaline begins.

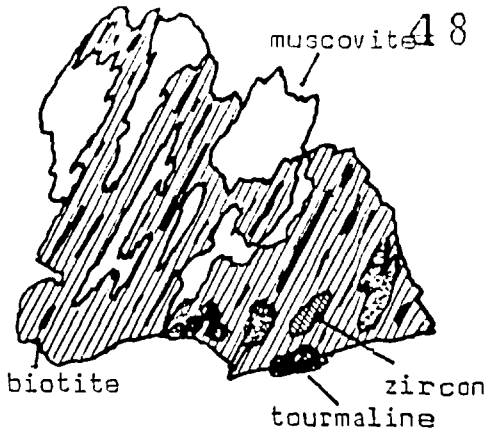

2. Tourmaline after biotite, comprising polycrystalline sheef-like aggregates, and retaining residual biotite cleavage lamellae.

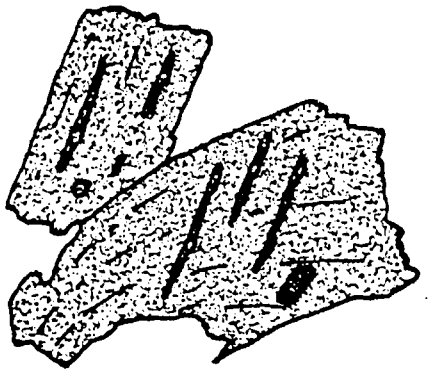

3. Recrystallisation of tourmaline after biotite, evolving a darker coloured component, which migrates outwards.

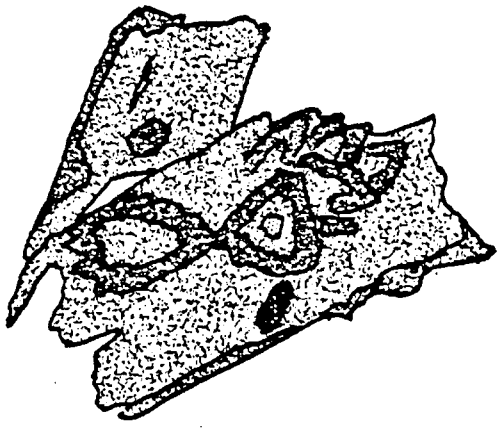

4. Further recrystallisation of tourmaline after biotite, producing composite, zoned crystals. Note retention of zircon.

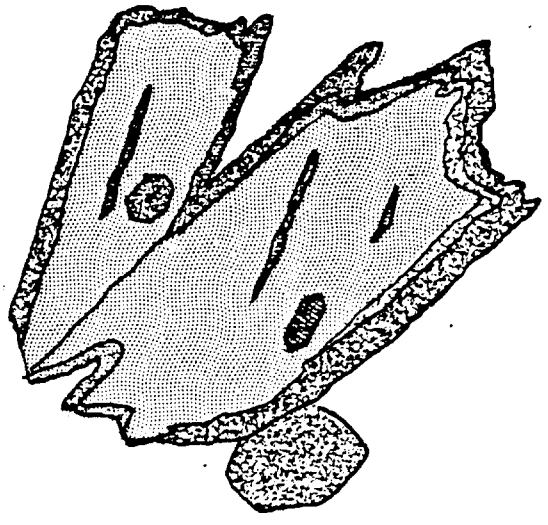

0 0.5mm

Fig. 2:5 Replacement of biotite by tourmaline in the reddened granite (VR012) at Venford Reservoir Quarry.
(All ornaments = tourmaline unless otherwise stated)

Plate 2:6 shows a biotite crystal at this stage of replacement (in VR012). Some areas of the crystal have biotite appearance until the microscope stage is rotated and pleochroism shows them to be tourmaline. Other areas retain biotite pleochroism and structure. Sometimes, successive tourmaline growth zones encroach steadily further into the biotite crystals. Hydromuscovite is sometimes associated.

(v) Biotite is entirely replaced by tourmaline, which is normally blue and brown with a patchy appearance. The resulting material is generally made up not of one but of several individual crystals, sometimes in radiate configuration. The original shape of the biotite, as well as parallel lineations representing biotite cleavages and exsolution lamellae, is often preserved at this stage (Fig. 2:5, no. 2).

(vi) The tourmaline resulting from direct biotite replacement, above, recrystallises to give large, composite tourmaline crystals (Fig. 2:5, nos. 3 and 4). The original, patchy, blue-brown colouring becomes resolved into a pale yellowish centre, which may retain some darker lamellae, with a dark blue component migrating outwards to form the rim (Plate 2:7). This produces zoned crystals such as those in Plate 2:8, with dark blue rims often enclosing several grains. These tourmalines are associated with much apatite and the occasional large zircon.

The reddened granite is thus characterised by a progressive sequence of biotite breakdown and replacement, which culminates in the total elimination of biotite in favour of tourmaline, before the margin of the tourmalinised vein is reached. The tourmaline after biotite is totally unlike the clear, yellow-brown tourmalines of the type luxullianite, for which a post-biotite origin had been suggested (Wells, 1946).

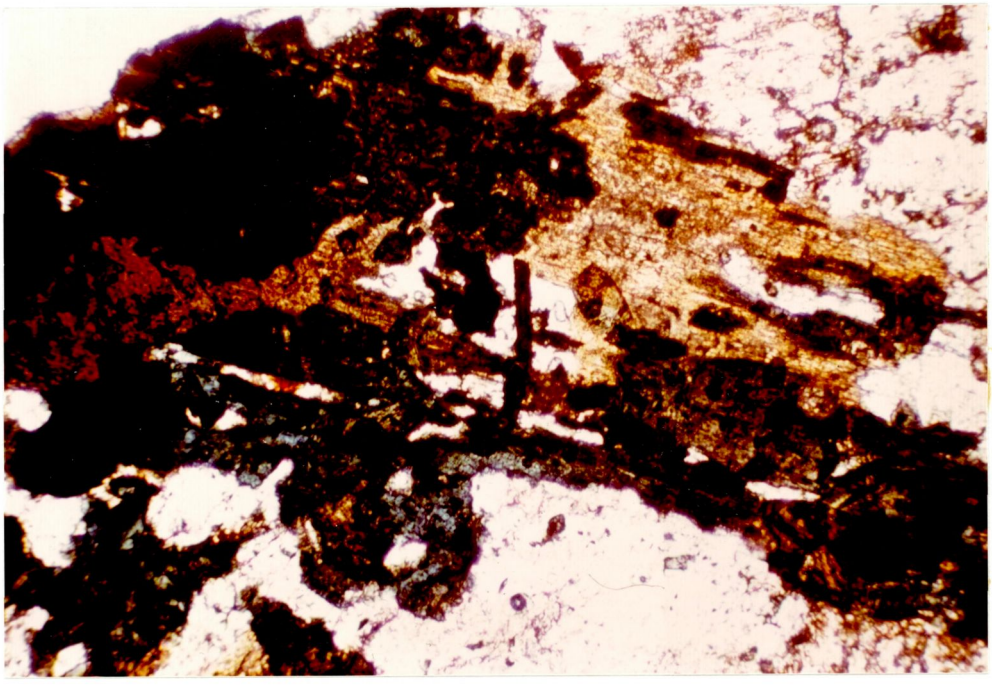

0 0.5mm

Plate 2:6 Biotite partially replaced by tourmaline, in the reddened granite, Venford Reservoir Quarry (VR012, p.p.l.). (biotite pale brown; all other coloured material is tourmaline.

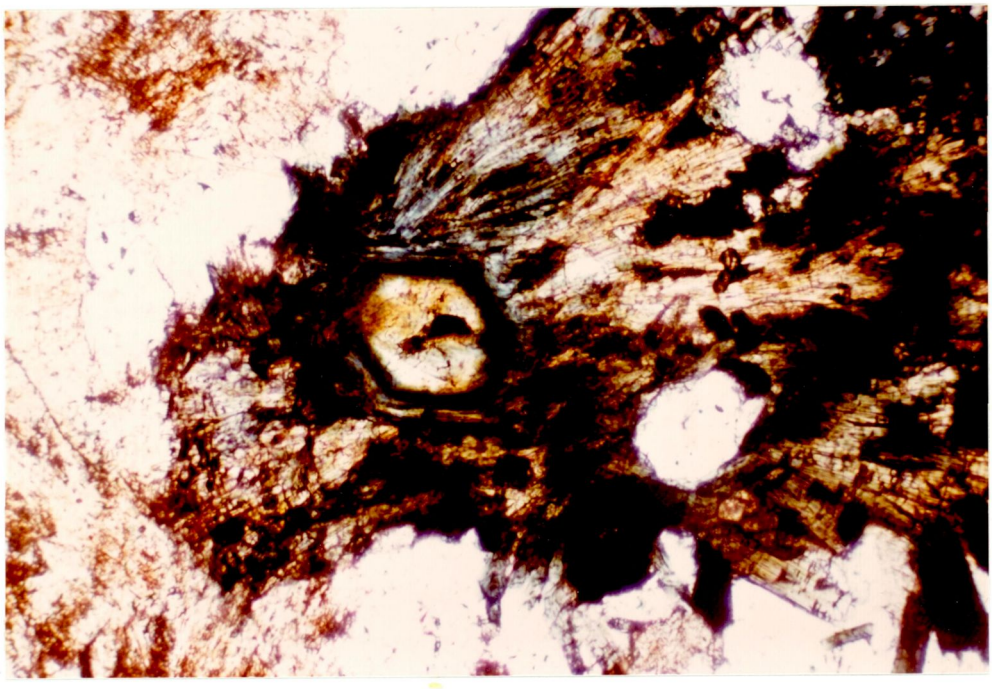

0 0.5mm

Plate 2:7 Tourmaline after biotite, in the process of recrystallisation; Venford Reservoir Quarry. (VR012, p.p.l.)

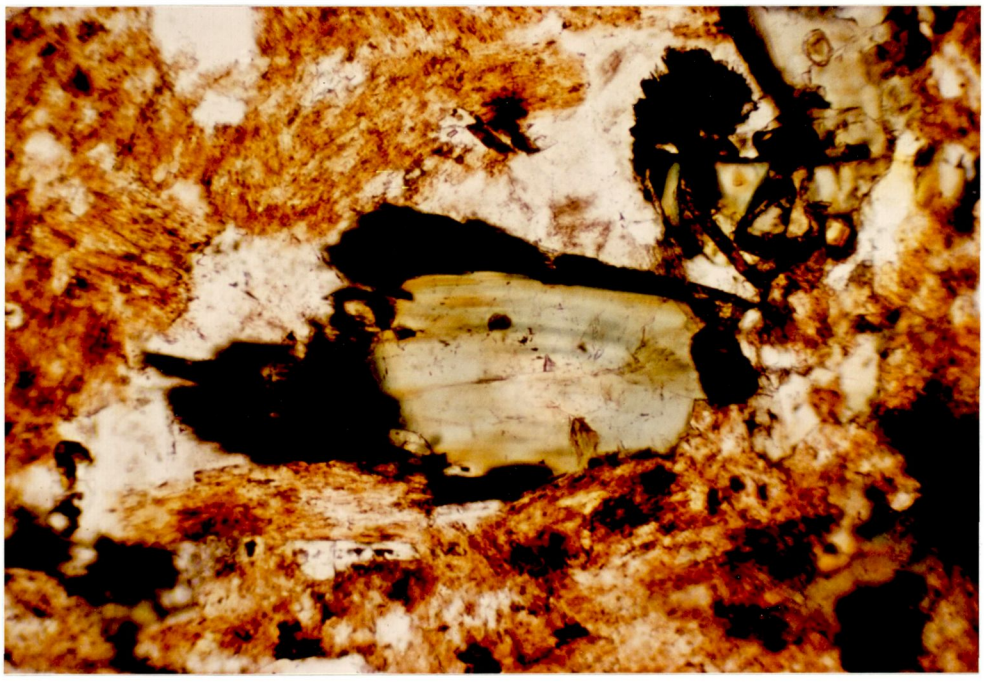

0 0.5mm

Plate 2:8 Tourmaline after biotite, recrystallised to form a zoned crystal group; the dark rim and pale, heterogeneous centre are characteristic. (VR010, p.p.l.) Venford Reservoir Quarry.

The replacement of feldspar by tourmaline begins about 2 metres from the tourmalinised vein, with the sporadic growth of radiating, bluish tourmaline, which is occasionally associated with muscovite (Plate 2:9). Sample VR011 contains one example of a euhedral feldspar megacryst, partially pseudomorphed by blue tourmaline; reddening of the feldspar is more intense adjacent to the tourmaline. In sample VR010, acicular tourmaline is developed at feldspar margins, where it is accompanied by hydromuscovite (Plate 2:10), and sometimes also apatite. Hydromuscovite is common close to the tourmalinised vein margin, and occurs as radiating and sheaf-like aggregates, yellowish in plane polarised light, strongly birefringent, and tending towards pseudohexagonal morphology. It lacks muscovite cleavage, and is biaxial, negative, with a very small 2V.

Apatite recrystallises in the reddened granite to form some quite large, euhedral crystals (up to 0.2 mm diameter, basal section).

Adjacent to the tourmalinised vein (VR010), quartz shows a tendency towards faceted crystal growth instead of rounded bleb development. Feldspar is displaced in the process, and granophyric textures are obliterated. The quartz contains abundant fluid inclusions.

2.1.2.3 *Tourmalinised vein margin*

The boundary between the reddened granite and the 'luxullianite' is diffuse, with the tourmaline content increasing over a distance of about 15 cm, until the zone of maximum tourmalinisation is reached. Although the feldspars become considerably corroded, the megacrystic texture persists across the transition zone. No sharp or chilled margin is visible. The five samples (VR001 to VR005) representing 3 cm increments across the vein margin consist of reddened, megacrystic granite with large quartz areas, becoming increasingly dark in their matrices as the proportion of tourmaline increases.

0 0.5mm

Plate 2:9 Blue tourmaline and muscovite replacing feldspar in the reddened granite, Venford Reservoir. (VR011, p.p.l.)

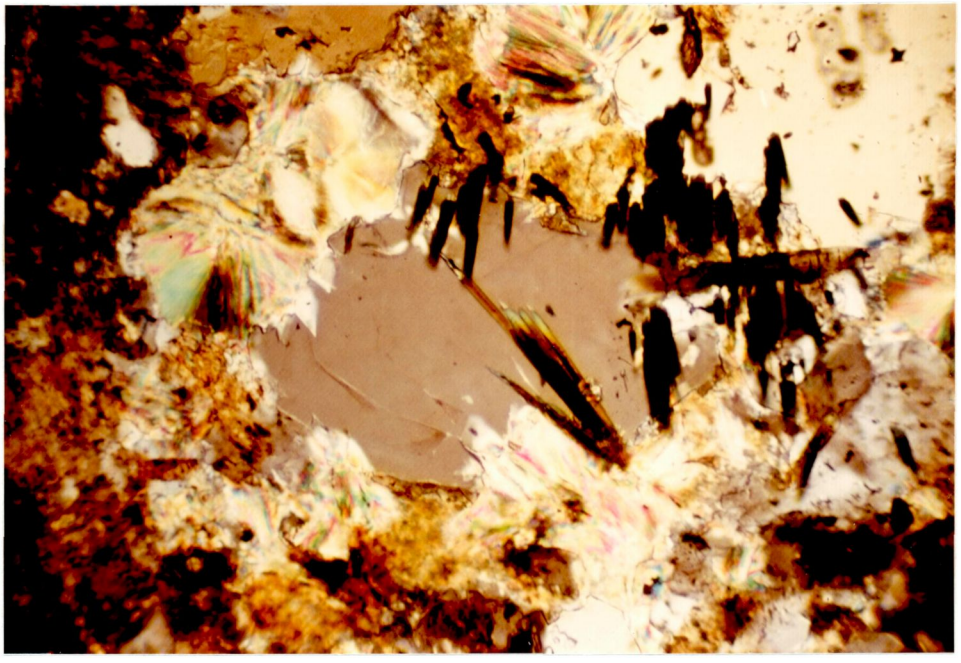

0 0.5mm

Plate 2:10 An assemblage of acicular tourmaline (dark coloured needles) and hydromuscovite (radiating, birefringent) at the margin of a feldspar in the reddened granite, Venford Reservoir. (VR010, x.p.)

Tourmaline grains after biotite undergo recrystallisation and reordering, to produce optically zoned crystals with euhedral terminations. The major replacement process operating at the vein margins is, however, the increasing growth of tourmaline after feldspar, with proximity to the tourmalinised vein.

Feldspar is strongly reddened, and is seen in thin section to be full of brown iron oxide flecks. Albite twinning is common, particularly in feldspar megacrysts, which are up to 2 cm long; all feldspars show extreme heterogeneity of composition (confirmed by microprobe, Chapter 5). Granophyric intergrowths are eliminated in favour of faceted quartz within 'ghost' feldspar networks (Fig. 2:4).

Replacement of feldspar by tourmaline takes several forms, which may be governed by feldspar composition at the time of replacement (this possibility is discussed in the light of microprobe analyses in Chapter 5). The following tourmaline types developing after feldspar may be distinguished optically:

(i) Skeletal mats of yellow, greenish or brown tourmaline invade feldspar, of which residual portions in optical continuity remain (Plate 2:11). The optical orientation of the tourmaline is unrelated to that of the host feldspar. These skeletal mats appear (in VR001 to VR003) to grow from cracks within the feldspar or from its margin, and they become more extensive with proximity to the tourmalinised vein. In VR005, adjacent to the zone of maximum tourmalinisation, the interstices formerly occupied by residual feldspar become replaced by a blue tourmaline, producing large (2 mm), irregularly-shaped crystals with a distinctive, variegated appearance (Plate 2:12).

(ii) Skeletal growth of predominantly bluish tourmaline also occurs within feldspar, nucleating at fractures (Plate 2:13); this is

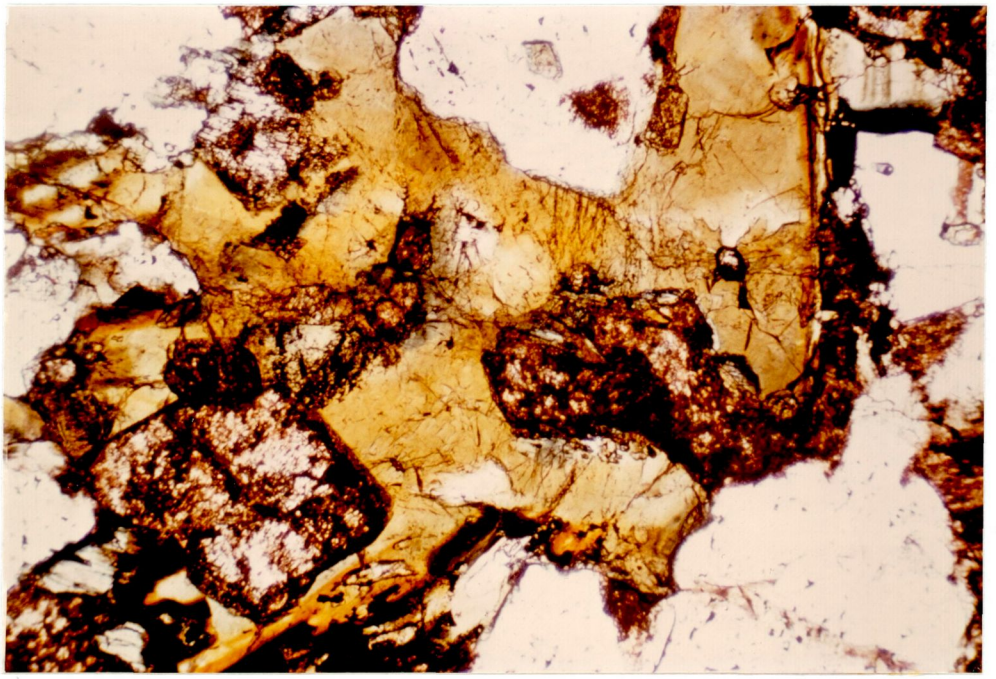

0 0.5mm

Plate 2:11 Skeletal yellow-brown tourmaline replacing feldspar in the tourmalinised vein margin, Venford Reservoir Quarry. (VR004, p.p.l.)

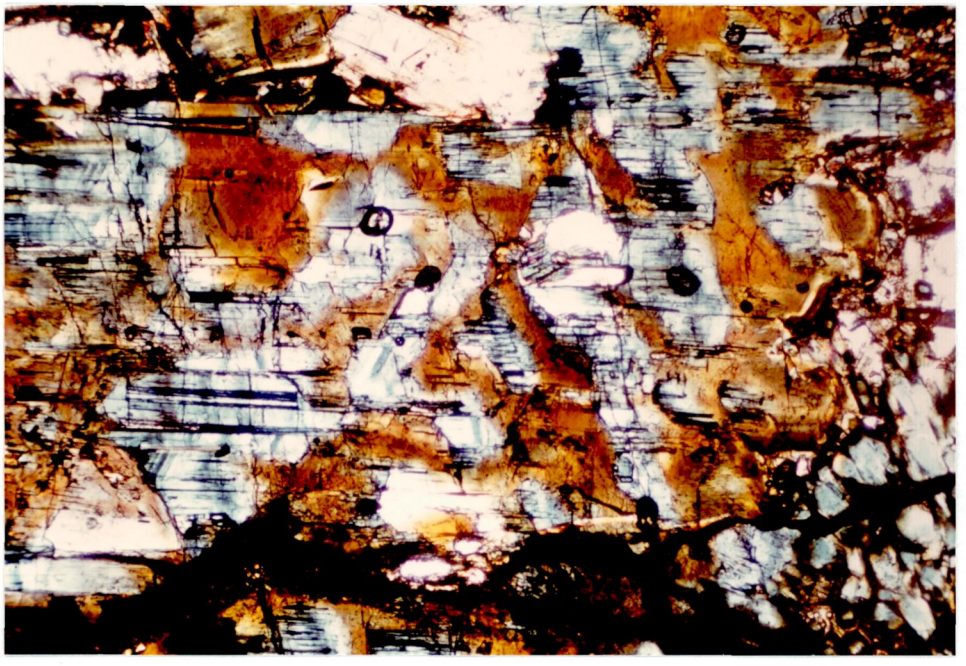

0 0.5mm

Plate 2:12 Skeletal yellow-brown tourmaline after feldspar, with interstices infilled by blue tourmaline, Venford Reservoir Quarry. (VR005, p.p.l.)

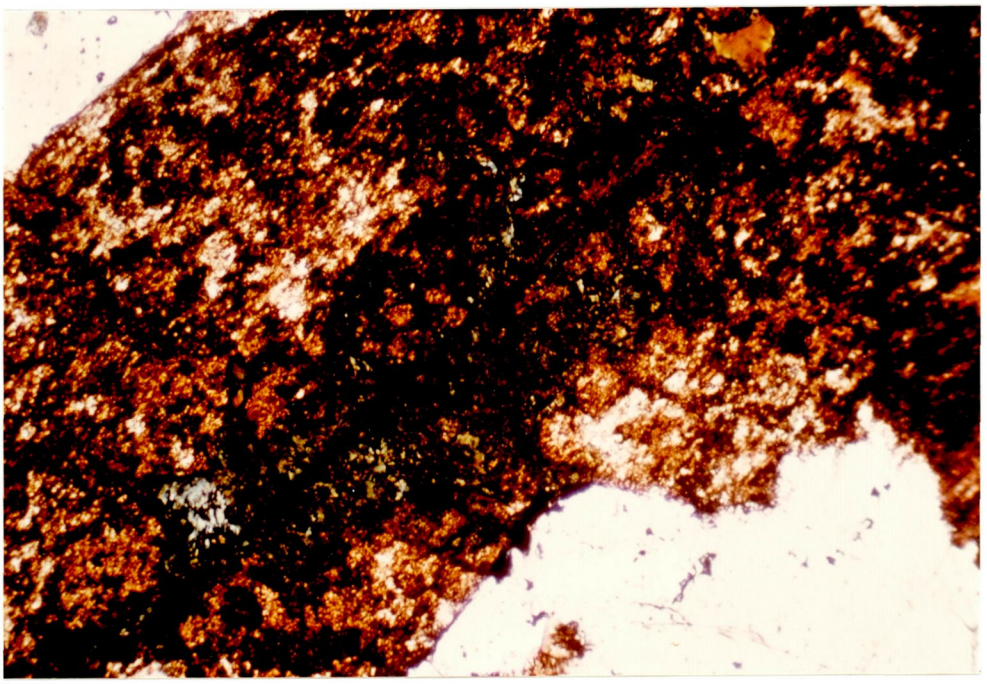

0 0.5mm

Plate 2:13 Skeletal blue tourmaline replacing feldspar, growing from a fracture. A small patch of skeletal yellow-brown tourmaline is also developing in the top right of the picture. Venford Reservoir Quarry. (VR003, p.p.l.)

less common than yellow-brown skeletal development, and becomes incorporated into larger tourmaline mats as alteration proceeds.

(iii) Small, acicular tourmaline prisms of blue-green colour develop within feldspar, from isolated nuclei which are sometimes aligned parallel to the feldspar cleavage traces. Individual tourmaline crystals form asymmetric, radiate or sheaf-like structures, which, with increasing tourmalinisation, amalgamate to produce extensive areas (up to 1 mm) consisting entirely of radiating and randomly oriented tourmaline aggregates (Plate 2:14). Adjacent to the zone of maximum tourmalinisation (in VR005), these aggregates begin to recrystallise into single tourmaline crystals with darker margins.

(iv) In some feldspar crystals, areas roughly aligned to the cleavages are replaced by quartz which appears to be exsolved from the host feldspar; here, a few fine, acicular bluish tourmalines form incipient 'tourmaline suns'. Plate 2:15 shows that where these tourmalines grow within recrystallised quartz, they may adopt a very fine and acicular habit, with crystals no more than 0.01 mm in diameter growing to lengths of up to 0.75 mm. However, where such tourmalines grow in to feldspar (same photograph), they are unable to grow into fine, acicular crystals, and instead form stout prisms. The spherulitic texture characteristic of the type luxullianite is not fully developed at Venford. It appears that the development of very fine, acicular tourmalines and spherulites requires complete recrystallisation of the host mineral (generally quartz), and cannot occur in the solid state within feldspar.

In VR005, adjacent to the maximum tourmalinisation zone, minute blue acicular tourmaline needles begin to appear within the extensively recrystallised quartz. These tourmaline needles are usually less than 30 μm in diameter, so that many lie below the surface of thin sections;

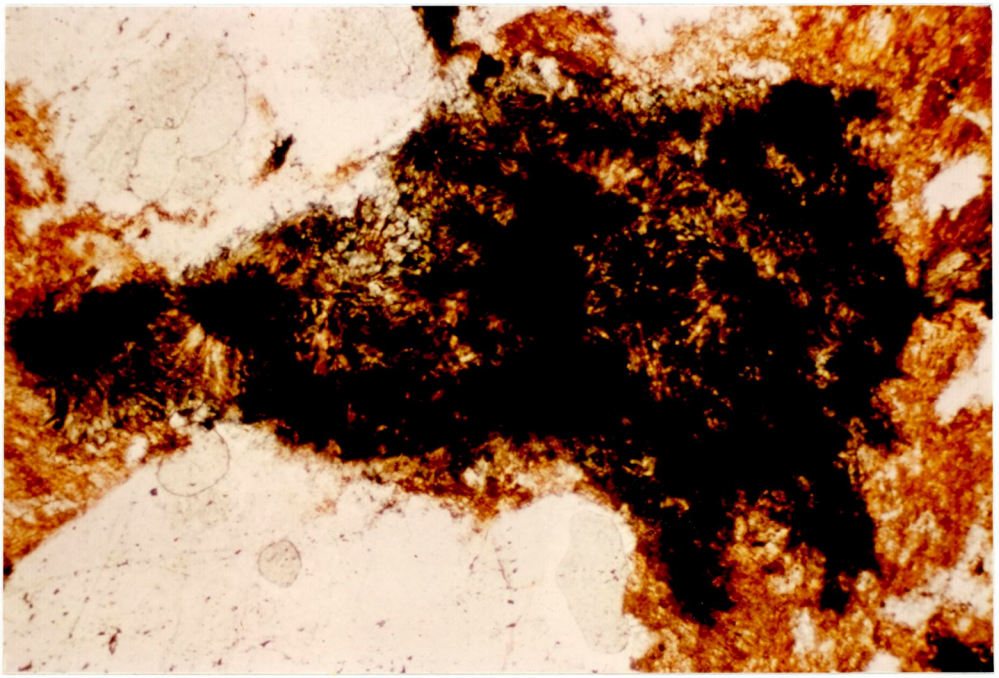

0 0.5mm

Plate 2:14 Radiating blue-green tourmaline aggregates replacing feldspar in the tourmalinised vein margins, Venford Reservoir Quarry. (VR005, p.p.l.)

0 0.5mm

Plate 2:15 Incipient 'tourmaline sun' development in quartz after feldspar, in the tourmalinised vein margins, Venford Reservoir Quarry. (VR005, p.p.l.)

they are either shot through the quartz in random orientation, or nucleated at a point, or in 'swarms' (Plate 2:16). Unlike the tourmaline varieties already described, these fine needles appear to be formed by direct crystallisation from a fluid, rather than by any replacement process.

Hydromuscovite is gradually eliminated, as alteration proceeds across the transition zone. Apatite forms large subhedral crystals, often within feldspar; there are a few examples of apatite skeletally replacing feldspar, in the outer vein margin (VR001 and VR002). Small, deep red, translucent crystals appear in the inner vein margin (VR004 and VR005), and these are probably rutile.

Quartz shows increasing recrystallisation of larger aggregates to produce clear, faceted crystals, and at the inner vein margin (VR005), this recrystallisation results in a reduction in the numbers and size of fluid inclusions.

2.1.2.4 Zone of maximum tourmalinisation

The texture in hand specimen of samples VR006 and VR007 is very similar to that of the type luxullianite, except that the tourmaline component is coarser-grained. The rock consists of largely-corroded pink alkali feldspar megacrysts, in a matrix of tourmaline, quartz, and smaller pink feldspars.

Feldspar retains its megacrystic habit into the centre of the tourmalinised vein, but suffers severe corrosion and replacement by tourmaline and quartz. In some cases, the linear distribution of tourmaline nuclei within quartz marks the former position of a feldspar margin. The remaining feldspar frequently shows albite twinning, but this is obscured by perthitic textures and intense reddening.

Tourmaline is well distributed throughout the rock, of which it

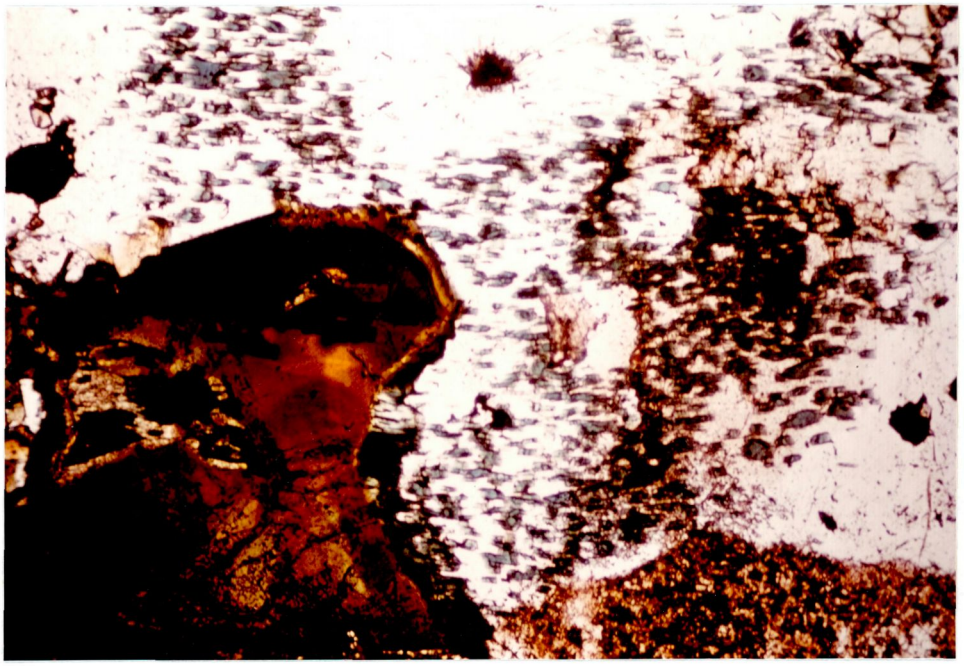

0 0.5mm

Plate 2:16 'Swarm' of minute, blue tourmaline needles, shot through quartz, in the tourmalinised vein margins, Venford Reservoir Quarry. (VR005, p.p.l.)

0 0.5mm

Plate 2:17 Extension of minute blue tourmaline needles by accretion of additional outer zones, to form continuous tourmaline mats. Centre of the tourmalinised vein, Venford Reservoir Quarry. (VR006, p.p.l.)

constitutes about 30% (calculated from boron content, Chapter 4); the proportion of tourmaline appears visually to be greater than this, because the quartz is crowded with fine acicular tourmaline needles.

Tourmaline after biotite is mostly incorporated into larger, composite, zoned crystals after feldspar, and is not easily distinguishable from the latter. Skeletal mats of tourmaline after feldspar are almost completely infilled by replacement of interstices, and subsequent marginal zoning. Radiate and sheaf-like aggregates of blue-green tourmaline after feldspar have also virtually all recrystallised and have become incorporated in the large, composite tourmaline mats.

Existing tourmalines of all types are rimmed by external growth zones with euhedral morphology; these outer zones are dark blue and colourless, and often enclose several adjacent crystals (Plate 2:18). Many fine, acicular needles of tourmaline in quartz are also rimmed by outer zones of blue and colourless material, so that the 'swarms' of individual needles present in VR005 now become amalgamated into continuous, composite tourmaline mats (Plate 2:17). Acicular, oriented overgrowths are rare, and where these have grown, on one end only of existing crystals, they are incorporated into the complex zoning of these crystals by the addition of subsequent zones.

Hydromuscovite is a very minor constituent of the central part of the tourmalinised vein. Apatite forms large, subhedral crystals. Small opaque grains and rutile are fairly abundant, forming about 1% of the rock. Quartz is almost totally recrystallised to optically clear, faceted crystals, shot through with acicular tourmaline needles; many of the tourmaline needles are euhedral and concentrically zoned (Plate 2:19). It is no longer possible to distinguish quartz after feldspar from independently occurring quartz. There is a dramatic reduction in fluid inclusion size and abundance within the recrystallised quartz; large fluid

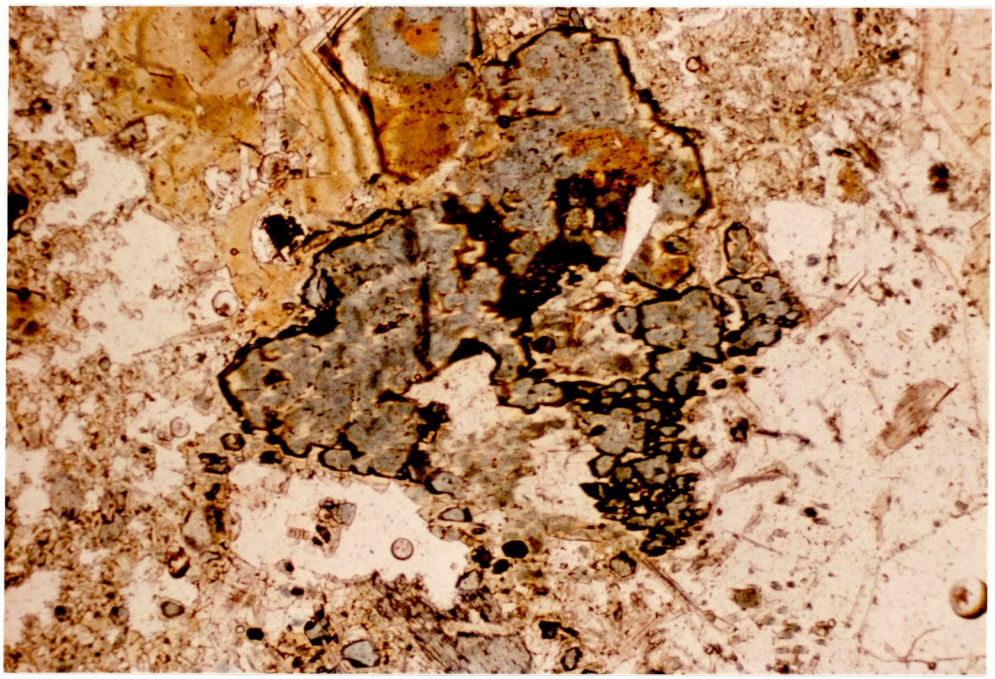

0 0.5mm

Plate 2:18 Composite tourmaline crystals, united by outer growth zones. Tourmalinised vein centre, Venford Reservoir Quarry. (VR007, p.p.l.)

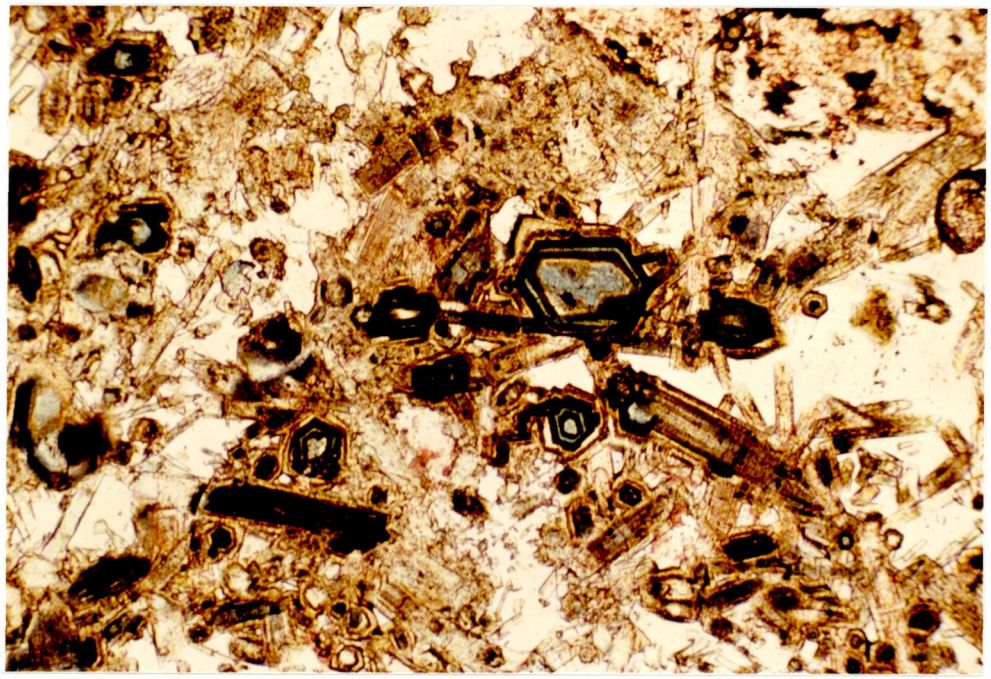

0 0.5mm

Plate 2:19 Euhedral, concentrically zoned tourmaline needles. Tourmalinised vein centre, Venford Reservoir Quarry. (VR007, p.p.l.)

inclusions are almost entirely absent, and are substituted by very small, but equally saline inclusions (see Chapter 6).

2.1.2.5 The smaller, cavitous tourmalinised vein

Samples VR023 and VR024 represent, respectively, the vein margin and the vein centre. The transition zone from 'unaltered' granite to tourmalinised rock, which in the case of the larger vein occupied several metres, is here condensed into a distance of about 3 cm (Plate 2:3), that is, into the length of a single polished thin section.

Two centimetres from the edge of the tourmalinised vein, the rock consists of alkali feldspars with often heavily sericitised centres, anhedral to subhedral quartz, and biotites in various stages of breakdown. One grain of biotite at the edge of slide VR023 is scarcely altered at all, retaining an even brown colouration and unembayed morphology; most grains, however, are broken down into bands of either muscovite or sericite, separated by dark lamellae parallel to the cleavages. Some biotites show marginal replacement by alkali feldspar.

At the vein margin, there is a zone about one centimetre wide, which is reddened but depleted in mafic mineral grains. Any residual biotite is here well altered to feldspar, radiate sheaves of hydromuscovite, or dark, almost opaque brown aggregates (shown by microprobe to be impure iron oxides). A few angular grains of cassiterite are also found in this marginal zone. Euhedral quartzes invade other minerals, particularly feldspar, leaving skeletal networks. Bluish, acicular tourmalines become more prevalent towards the edge of the tourmalinised vein, where they are frequently associated with residual biotite replacement products, and/or with hydromuscovite; there appears to be no direct replacement of biotite by tourmaline.

The tourmalinised vein is characterised by small prismatic and

acicular, blue-brown tourmaline crystals, in random or radiate orientation, surrounded by recrystallised quartz, between areas of pink, perthitic alkali feldspar. Large replacement tourmalines are absent, except for two such grains as the edge of the vein. Hydro-muscovite, iron oxides and cassiterite do not persist into the vein centre. There are a few feldspar megacrysts, 1 to 1.5 cm long, but most of the feldspar is finely comminuted and consists of small, randomly oriented grains. Quartz is both euhedral and interstitial, and like the quartz in the larger tourmalinised vein, lacks large fluid inclusions. A prominent feature of the rock is the presence of large (1 cm) rounded cavities throughout: these may represent quartz dissolution.

2.1.2.6 Thin, monomineralic tourmaline veins

Sample VR026 is taken from the thin, vertical tourmaline vein which traverses the larger 'luxullianite' outcrop parallel to the quarry face. The vein follows a joint surface, and is about three centimetres wide. The margins in contact with the 'luxullianite' are gradational, showing a gradual increase in the proportion of tourmaline, towards a narrow zone uniformly black in hand specimen, and virtually monomineralic. In thin section, the tourmaline is brown, yellow, pale and dark blue, or almost colourless, and forms zoned, composite crystals ranging in size from less than 0.05 mm to 5 mm across; fine acicular crystals are rare. Many crystals are rimmed by dark blue and colourless outer zones similar to those seen in the luxullianite vein. Since monomineralic vein tourmaline from elsewhere in the quarry lacks these outer zones, it would appear that they are produced during formation of the luxullianite vein, which must therefore post-date monomineralic tourmaline vein formation.

2.1.2.7 Mineralogy of tourmalinisation at Venford Reservoir Quarry: a summary of petrographic observations

Fig. 2:6 summarises the distribution of alteration features associated with the formation of the larger, luxullianite-type tourmalinised vein at Venford Reservoir Quarry.

The reddening which affects the granite for a distance some 6 metres beyond the tourmalinised vein margin, is visible in thin section as minute brown flecks of iron oxides within feldspars. The granophyric intergrowth of feldspar and quartz, present in the 'unaltered' granite, is eliminated about 1 to 2 metres from the tourmalinised vein, by the process of continued quartz recrystallisation. The 'unaltered' granite contains feldspars with rapakivi texture, which persists to about 2 metres from the tourmalinised vein, when albite antiperthite becomes the dominant megacrystic feldspar; megacrysts reach 3 cm in length in the reddened granite, but become corroded as tourmaline replaces feldspar in the vein margins.

About 6 to 7 metres from the tourmalinised vein, biotite breaks down to give green biotite, muscovite and iron oxides; biotite margins are replaced by quartz and feldspar. 5 metres from the vein, blue and brown tourmaline replaces remaining biotite. The initial replacement products are polycrystalline tourmaline aggregates, often with radiate configuration; these recrystallise between 5 and 0.5 metres from the vein, to produce single, zoned tourmaline crystals with dark blue margins.

Feldspar replacement by tourmaline begins a few centimetres from the edge of the tourmalinised vein, and takes several forms. Both large skeletal mats of yellow, brown and blue tourmaline, and aggregates of fibrous, radiating blue-green tourmaline, are formed in the outer vein margins; these initial replacement products later become amalgamated

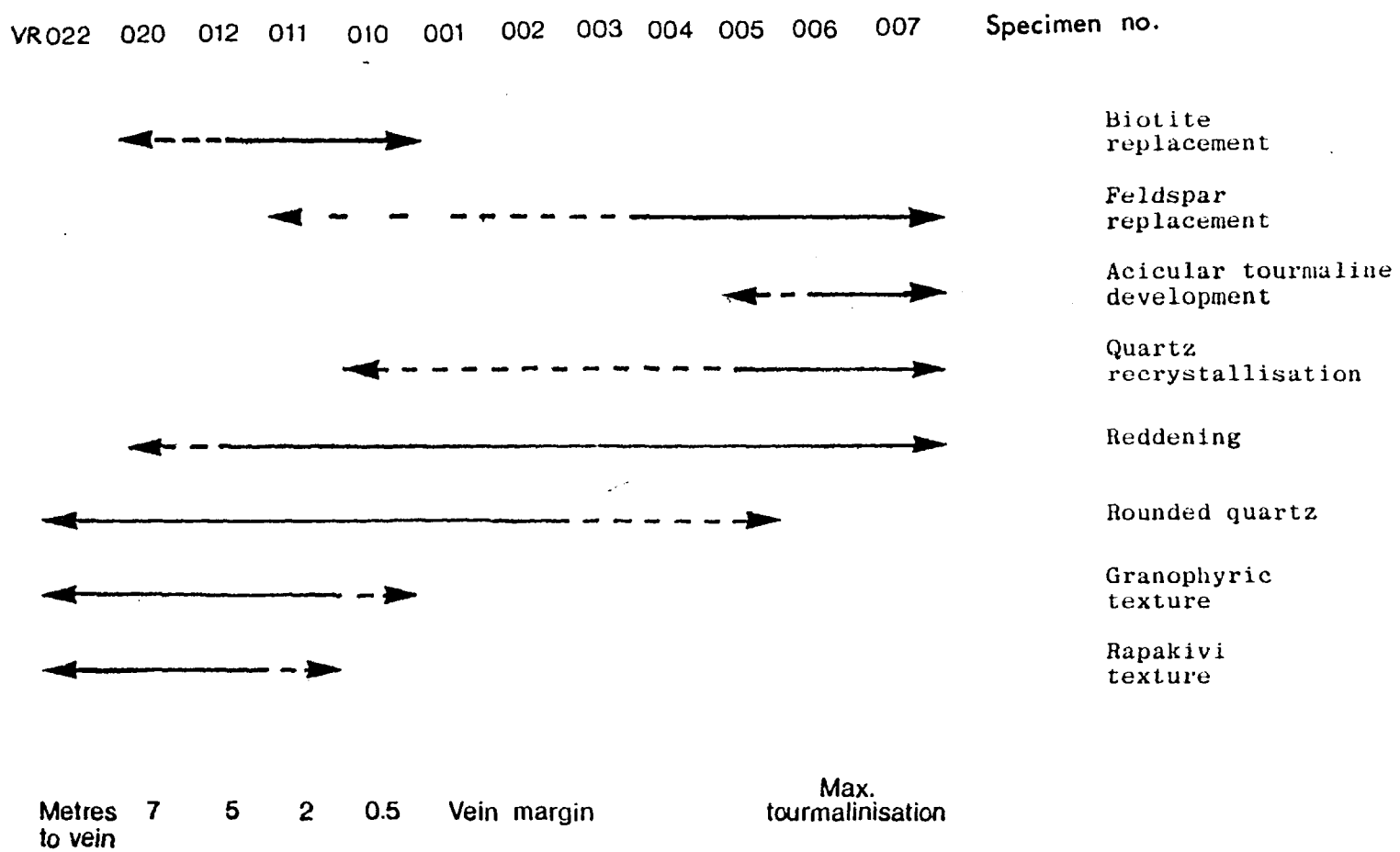

Fig. 2:6 Alteration features associated with tourmalinisation at Venford Reservoir Quarry, Dartmoor.

by recrystallisation and infilling of interstices, to form extensive, composite and zoned tourmaline crystals.

In the vein centre, fine acicular bluish tourmaline needles grow within recrystallised quartz. All tourmaline types become rimmed by dark blue and colourless outer zones in the centre of the tourmalinised vein.

During the tourmalinisation process, iron oxides are released from biotite to form brown flecks within feldspar, and also independent grains of impure iron oxides within the rock. Apatite and zircon are recrystallised but are not lost from the system. Hydromuscovite forms as a by-product of biotite replacement. Feldspar undergoes alkali changes which may not be fully understood by optical observation. Quartz recrystallises to clear, faceted crystals, containing fluid inclusions which are much smaller than those outside the tourmalinised vein, but are equally saline.

In the smaller, cavitous tourmalinised vein at Venford Reservoir Quarry, large replacement tourmalines are virtually absent, most of the tourmaline present being acicular prisms of blue-brown material. The transitional zone marginal to this smaller vein is condensed into a distance of a few centimetres. The margins of the smaller vein contain cassiterite. From field evidence, it seems possible that the smaller, cavitous tourmalinised vein and the many monomineralic tourmaline veins in the quarry may be contemporaneous, and the petrographic evidence indicates that these may pre-date the formation of the larger, luxullianite-type tourmalinised vein.

2.2 Tregarden Quarry, Luxulyan

2.2.1 Field description

This large quarry, currently worked for roadstone by E.C.C. Quarries Ltd., is situated 1 km north of Luxulyan village (at SX 054590). The quarry lies in the eastern lobe of the St. Austell granite (Fig. 2:7), within the granite facies designated 'biotite-muscovite granite' by Exley (1959) and 'megacrystic granite' by Hawkes and Dangerfield (1978).

The individual plutons comprising the St. Austell mass may be classified either on a mineralogical or on a purely textural basis. Exley (1959) recognised four main mineralogical subdivisions, namely (1) biotite-muscovite granite, (2) early lithionite granite, (3) late lithionite granite, and (4) fluorite granite (the numbers in brackets refer to Fig. 2:7). The lithionite granites of this classification are now termed 'lithium mica granites'. It may be seen from Fig. 2:7 that kaolinisation is prevalent in types 2, 3 and 4, and is virtually absent from type 1. Hawkes and Dangerfield (1978) have subdivided the St. Austell granite into textural units, which as shown in Fig. 2:8, roughly coincide with Exley's (1959) subdivisions, except that the fluorite granite is regarded as an alteration facies of the lithium mica granite by these authors.

Fig. 2:9 shows the configuration of Tregarden Quarry, and the distribution of the main alteration features. The 'unaltered' granite contains white alkali feldspar megacrysts up to 6 cm long, and aligned in subhorizontal preferred orientation; biotite inclusions follow concentric growth zones within many megacrysts. The other constituents of the granite are quartz, sodic plagioclase, biotite, muscovite, tourmaline, and accessory apatite and zircon. The lack of kaolinisation is typical of the biotite-muscovite granite facies. Xenoliths in various stages of assimilation are common throughout the quarry; they range in

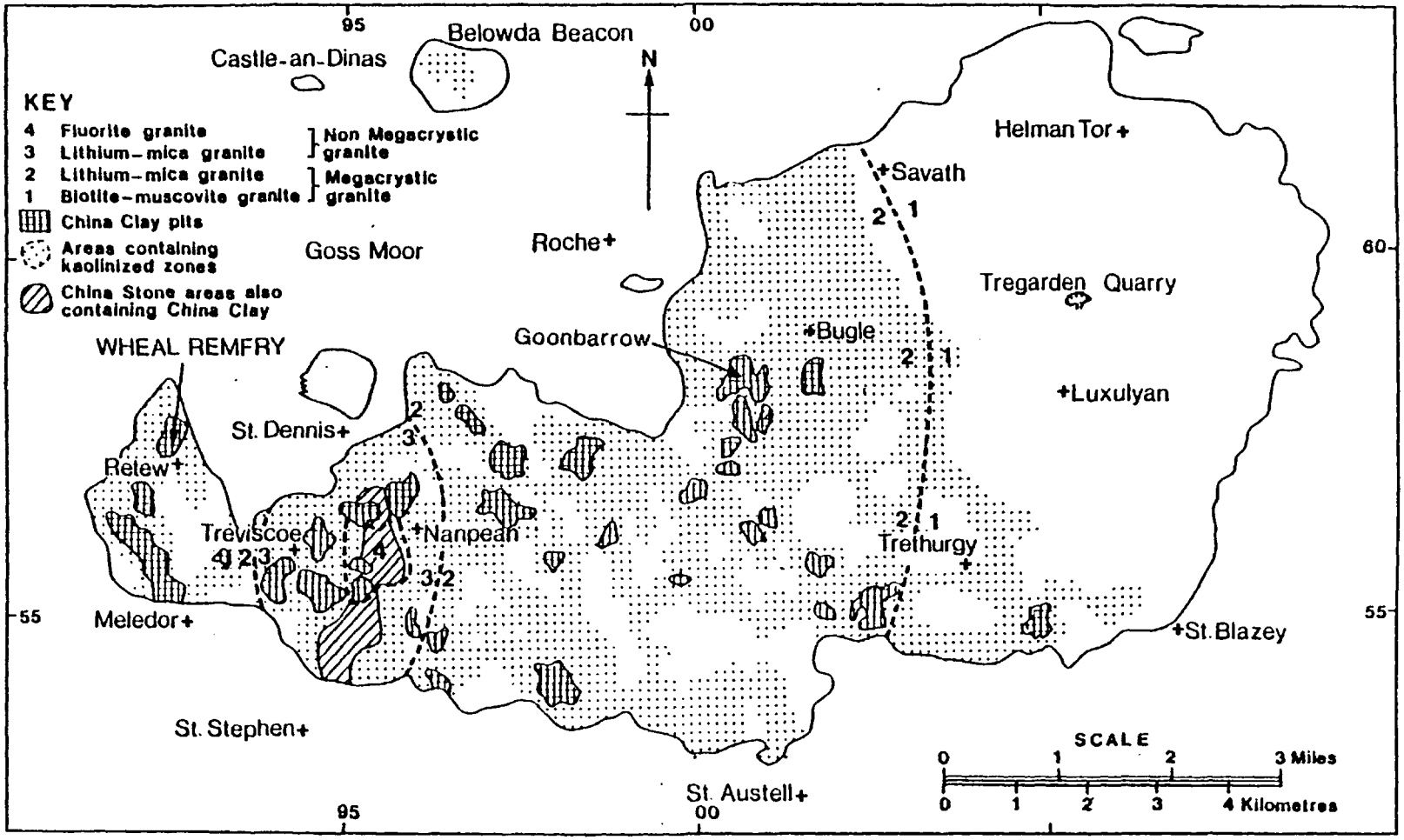

Fig. 2:7 Igneous facies and hydrothermal alteration in the St. Austell granite.
(DETAILS FROM C.S. EXLEY 1959 AND C.M. BRISTOW 1968)

(unpublished diagram drawn by Dr. C. Halls, Imperial College)

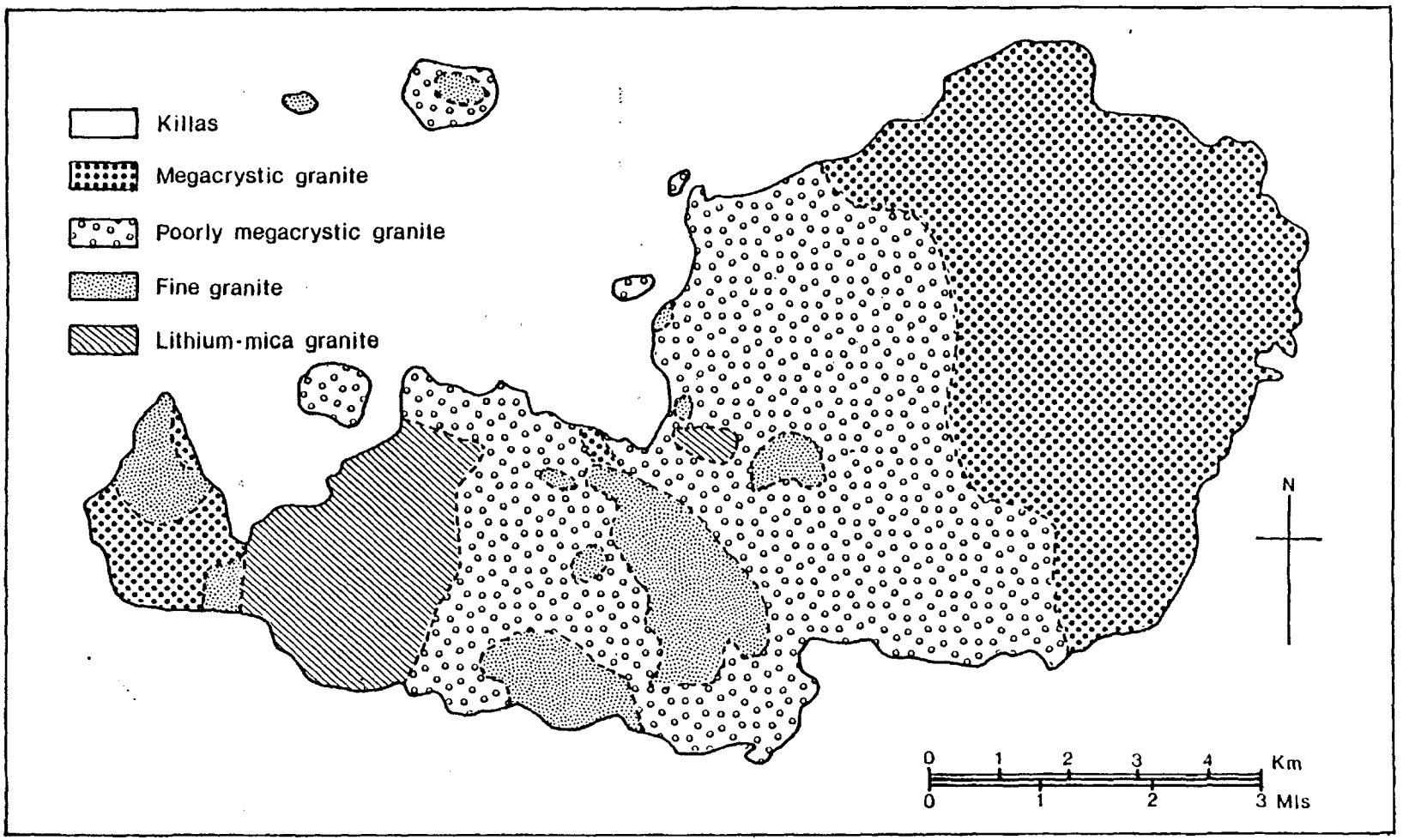

Fig. 2:8 Distribution of facies in the St. Austell Granite (boundaries simplified after Dangerfield et al., 1980)

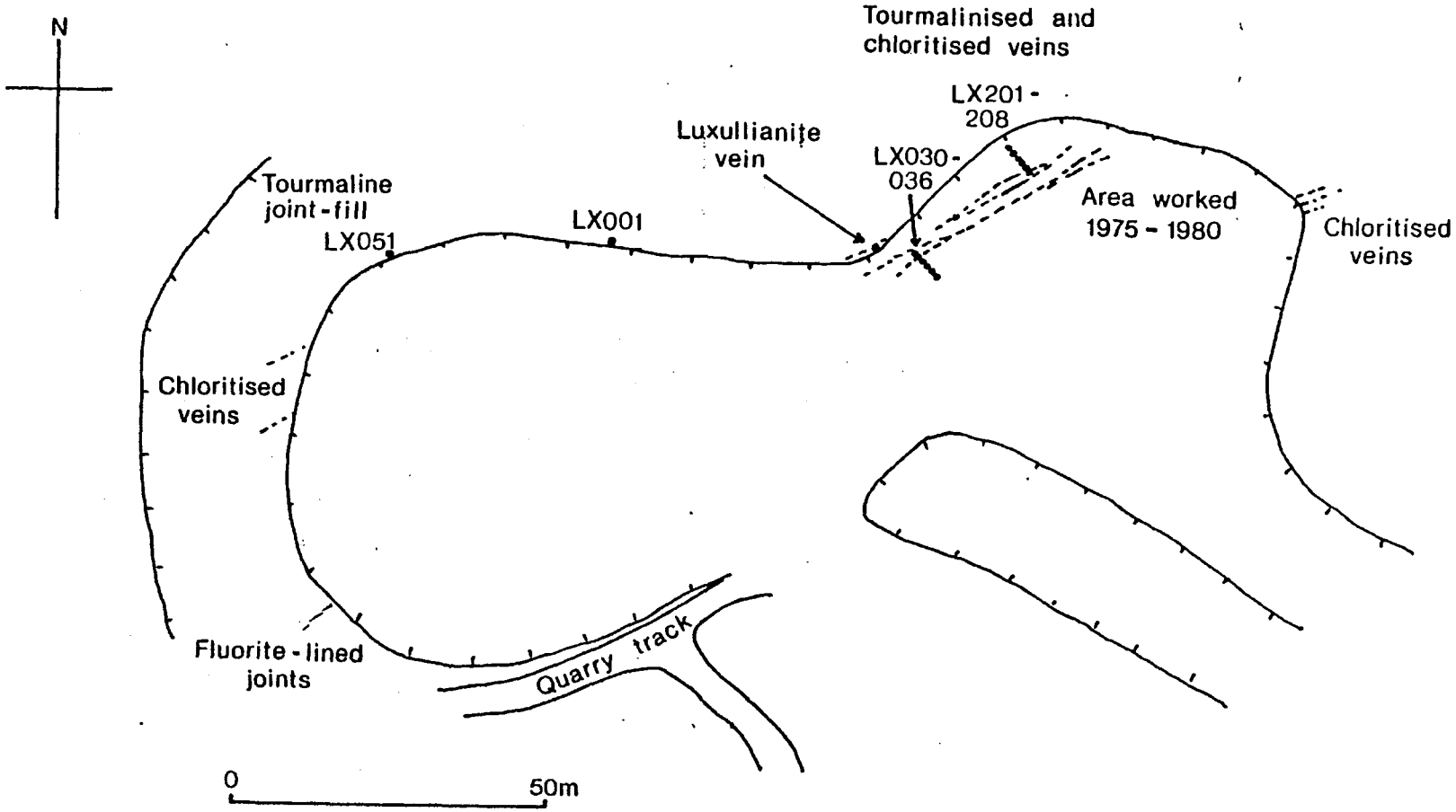

Fig. 2:9 Sketch map of Tregarden Quarry, Luxulyan showing location of samples

size from a few centimetres to about a metre in diameter, and frequently show concentrations of tourmaline (black in hand specimen, yellow in thin section) around their margins. In the more advanced stages of assimilation, xenoliths contain white alkali feldspar megacrysts similar to those in the surrounding granite.

Pegmatitic pockets, up to about 0.5 metre in diameter, occur within the granite, particularly in the northeast and southeast corners of the quarry, and contain quartz, white or pinkish alkali feldspar, muscovite, tourmaline (black or deep green in hand specimen), and sometimes green or blue apatite. An example of an exceptionally large pegmatitic pocket is shown in Plate 2:20. It appears from field evidence that such phenomena are primary segregations produced at the magmatic stage, but a post-magmatic origin cannot be precluded.

Several varieties of vertical replacement veins (up to 2 metres wide), and narrow joint fillings, have been exposed in working faces of this quarry, over a period of some four or five years. Joint surfaces may be lined with tourmaline, fluorite or hematite (not generally in combination); a few centimetres either side of such joint surfaces, feldspars are slightly reddened. Several subhorizontal joints contain a thin pegmatitic fill of feldspar, quartz, and either biotite or tourmaline; the latter type often feature hollow or cored tourmaline crystals (Lister, 1979a).

The larger, vertical replacement vein systems comprise tourmalinised luxullianite (Lister, 1978a), or chloritised material with a superficially similar appearance (Plate 2:21). Every gradation apparently exists between complete tourmalinisation and complete chloritisation, and indeed, several veins have been exposed which represent different combinations of the two alteration facies. Alteration is always accompanied, to a greater or lesser degree, by reddening of the feldspars, which is confined to the

Plate 2:20 Tourmaline-bearing pegmatite pocket at Tregarden Quarry, Luxulyan. (Lens cap diameter 54mm)

lateral extent of the veins (by contrast to the more extensive reddening at Venford). Luxullianite veins contain pink to red potassium feldspar megacrysts, in a matrix of quartz, tourmaline and pink feldspar, plus or minus muscovite and chlorite; two varieties of tourmaline are present, the first anhedral and brown or yellow in plane polarised light, and the second acicular and blue-green, forming spherulites, sheaf-like aggregates and oriented overgrowths upon the yellow variety. Chloritised veins contain pink to red potassium feldspar megacrysts, in a matrix comprising quartz, green chlorite, pink feldspar and muscovite, plus or minus tourmaline and purple fluorite. The margins of both tourmalinised and chloritised veins are gradational, with no sharp or chilled contacts, the megacrystic texture prevailing from granite into the altered rock. The two processes of tourmalinisation and chloritisation seem to have taken place in very similar conditions, the final proportions of the end products depending upon the relative abundance of boron available.

The vertical replacement veins and mineralised joints have north-east - southwest orientations between 60 and 75°; Fig. 2:10 shows that this coincides with a prominent joint direction within the quarry. One of the mean regional joint directions for the St. Austell granite also has a similar trend (Exley, 1959), which is reflected in the stress trajectory nets constucted by Moore (1975) to explain the distribution of vein and dyke systems in southwest England.

Tourmalinisation and associated features exposed in Tregarden Quarry may be summarised as follows:

(i) Pegmatitic pockets contain black or deep green tourmaline, with quartz, alkali feldspar, muscovite, ± apatite

(ii) Vertical luxullianite veins comprise pink potassium feldspar, quartz and tourmaline, ± muscovite and chlorite

(iii) Vertical chloritised veins consist of pink potassium feldspar.

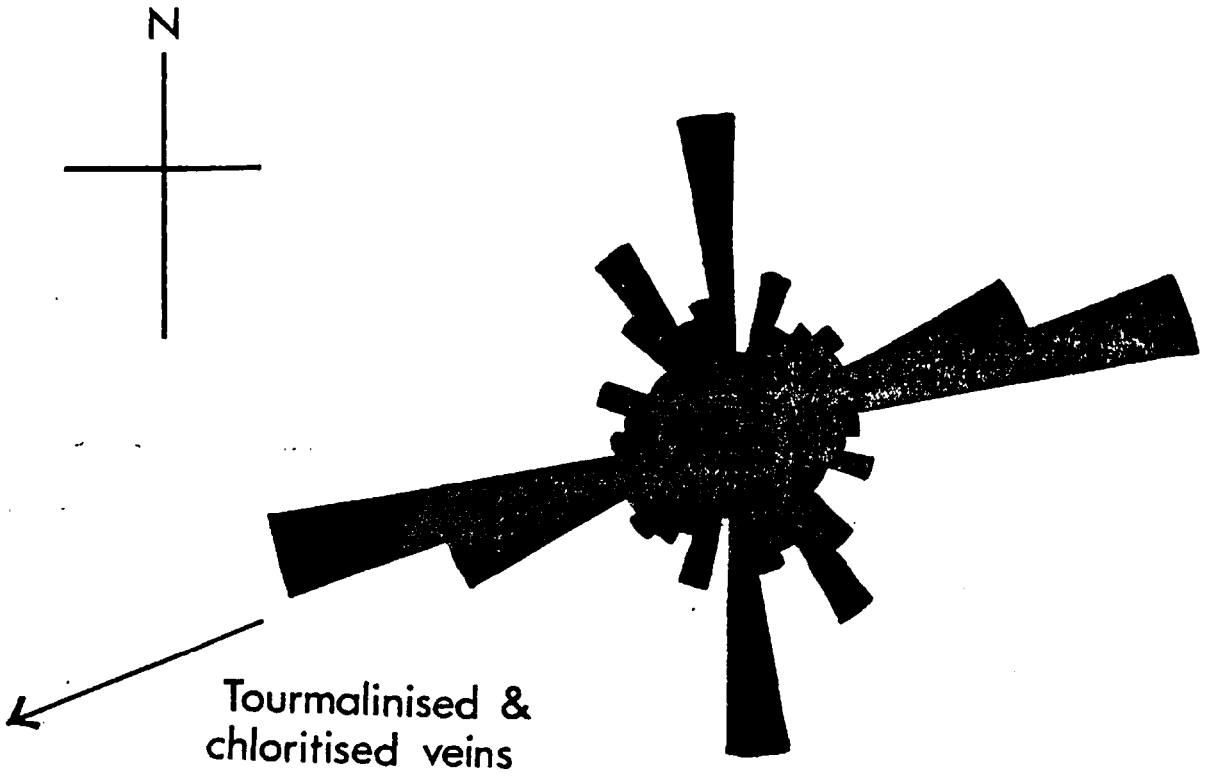

Fig 2:10 Orientation of joints and veins in Tregarden Quarry, Luxulyan

quartz, chlorite and muscovite, ± tourmaline

(iv) Vertical joints may be lined with either tourmaline, purple fluorite, or hematite

(v) Subhorizontal joints containing pegmatitic fill yield cored tourmaline crystals.

Samples for the present study were collected from two replacement veins, one predominantly tourmalinised (LX030 - LX036), and the other predominantly chloritised (LX201 - LX208a, and LX208b from another part of the latter vein). Each continuous sequence represents a transition zone from granite into fully altered rock, sampled in 3 centimetre increments. Sample LX051 was collected from a subhorizontal joint fill containing cored tourmaline crystals. Sample LX001 (from Lister, 1978a) was used to represent the 'unaltered' granite. The locations of these samples within the quarry are shown in Fig. 2:9.

2.2.2 Petrography

2.2.2.1 The parent granite

As at Venford Reservoir Quarry, the parent granite is unaltered with respect to tourmalinisation, but may nevertheless have undergone changes in feldspar composition since its original emplacement. It is also possible at Tregarden that the muscovite may be secondary.

The minerals present in sample LX001 are white, perthitic alkali feldspar megacrysts, sodic plagioclase, biotite, muscovite, tourmaline and accessory apatite and zircon.

Feldspar megacrysts reach up to 6 cm in length, and often have euhedral monoclinic habit, with internal growth zones marked by biotite concentrations. This zonation supports the view that the megacrysts may have grown to their present size in more than one stage. They are orthoclase perthites or microperthites; many crystals show exsolution

lamellae visible in hand specimen. Carlsbad and cruciform twinning both occur. Plagioclase forms smaller crystals; compositions, from symmetrical extinction angles, range from An_8 to An_{12} (Exley, 1959, gives a mean of An_{28} for the biotite-muscovite granite). The centres of plagioclase crystals are all heavily sericitised.

Biotite, even in granite not apparently affected by hydrothermal activity, is often corroded around the edges of grains, and shows partial replacement by muscovite. Many grains have turned pale green, and exsolved dark iron-oxide lamellae; quartz and fine grained muscovite invade these biotites along the cleavage traces. Apatite and zircon inclusions are common, and occasionally, minute (a few micrometres long) acicular needles, possibly of rutile, appear in green biotite.

Muscovite generally appears to be secondary, after either biotite or plagioclase.

Tourmaline forms a few isolated, anhedral and interstitial grains, which are yellow in plane polarised light. Tourmaline is particularly abundant at the margins of pelitic xenoliths.

Quartz is either interstitial, or forms small (2 mm) euhedral grains with hexagonal cross sections, enclosed within alkali feldspar. In interstitial quartz, the grain boundaries between adjacent crystals are very irregular and re-entrant. Fluid inclusions in quartz are small and generally two-phase (gas-liquid).

2.2.2.2 Chloritisation with minor tourmalinisation

The series of samples LX201 to LX207 represents the margin of a 1 metre wide alteration vein, which is predominantly chloritised, with minor tourmalinisation. Sample 208a is from the chloritised centre of this vein, and sample LX208b is from a portion of the vein centre in which tourmaline was more prevalent.

At the outer vein margin (LX201), the feldspars are still essentially white in hand specimen, and comprise both alkali feldspar and plagioclase. With increasing proximity to the vein (LX202 - 204), the feldspar megacrysts retain their perthitic texture, but plagioclase becomes extensively sericitised and converted to alkali feldspar. The megacrysts increase in size, and poikilitically enclose euhedral quartz, micas and former plagioclase grains. About 15 cm from the edge of the vein, all feldspars become very cloudy and flecked with iron oxides, which give a pinkish colouration in hand specimen and an opacity in thin section.

In the vein margins, biotite shows variable degrees of alteration, which could be due to micro-scale differences in the permeability of the rock, allowing hydrothermal fluids greater access to some parts of the rock than others (as suggested by Schwartz, 1958). However, it seems from field evidence that many veins of this kind have a weathered zone parallel to their margins; this may be explained by the outward migration ahead of the tourmalinisation or chloritisation 'front', of fluids which render the rock friable and permeable without subsequently recementing it, as occurs in the vein centres. This condition allows the biotite greater potential for attack both by hydrothermal and later weathering agents. In a zone about 20 cm from the edge of the chloritised vein (LX201 - 202), the rock is rather friable and stained with iron oxides; here the biotite is green coloured, and partially altered to sericite, muscovite, alkali feldspar and a little chlorite. A few centimetres closer to the vein (LX203 - 204), the rock is more coherent and the biotite less altered. The degree of biotite breakdown and replacement then increases steadily with proximity to the vein centre. Biotite is replaced around its margins and along cleavages by sericite and large muscovite flakes, as well as by alkali feldspar (the latter process is

described by Chayes, 1955). Remaining biotite exsolves alternating lamellae, parallel to cleavage traces, of green biotite and dark, iron-rich material. With increasing proximity to the vein, green areas within biotite begin to show the low birefringence and radiate structure of chlorite minerals. A few partially altered biotites contain minute acicular dark needles, possibly of rutile (although Schwartz, 1958, stated that the association of rutile and chlorite is unusual). About 10 cm from the edge of the vein, purple fluorite appears in the cleavage traces of some partially altered biotites (Plate 2:22), and since large (up to 2 mm) fluorite crystals are present in the vein centre, replacement by fluorite introduced from the hydrothermal fluid might have been postulated on petrographic evidence alone. However, it is shown in Chapter 4 that the fluorine content of the whole rock is considerably reduced during alteration, and it therefore appears that fluorine is released from biotite, and forms fluorite as a breakdown product of its host.

In the vein margins, feldspar is replaced by skeletal yellow tourmaline, which leaves residual islands of feldspar in optical continuity. Plate 2:23 shows how tourmaline which has pseudomorphed feldspar in this manner encloses rafts of biotite virtually unaffected. There is a thin band of blue tourmaline, in optical continuity with the yellow, replacing the biotite on one side only. The development of tourmaline and green chlorite increases steadily towards the edge of the vein. Quartz recrystallises to form euhedral, faceted crystals, which displace feldspar.

In sample LX207, which represents the edge of the zone of maximum alteration, the proportion of chlorite and tourmaline increases quite abruptly over a distance of about 2 cm. The megacrystic texture is retained across the vein boundary, but the feldspars become more

Plate 2:21 Chloritised and tourmalinised vein margin, Tregarden Quarry, Luxulyan. (Lens cap 54mm)

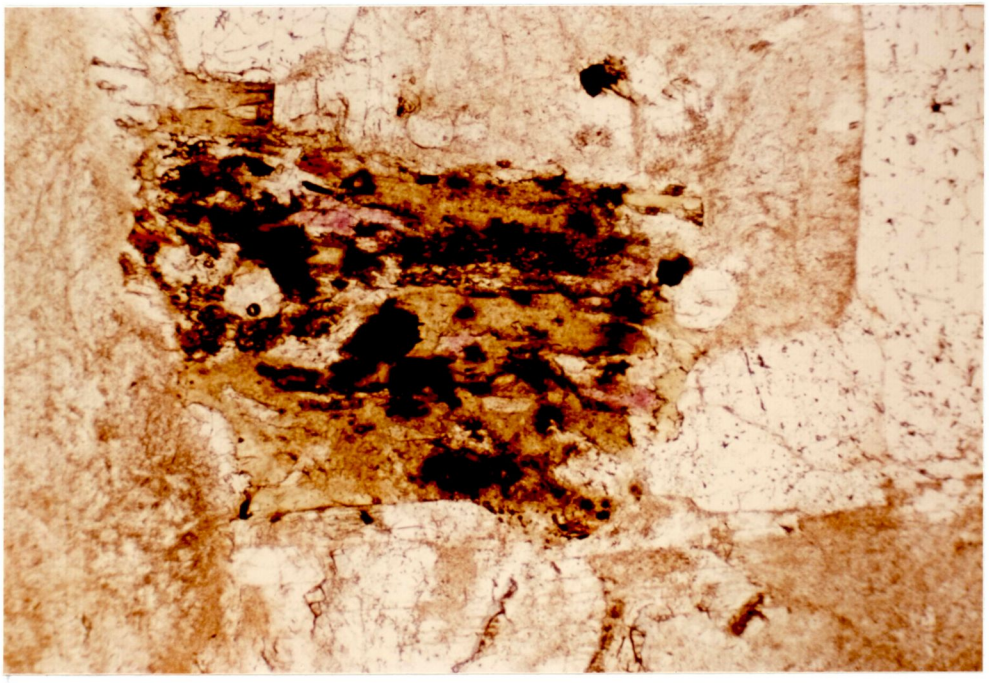

0 0.5mm

Plate 2:22 Biotite breaking down to give green biotite, iron oxides and purple fluorite, in the chloritised vein margin, Tregarden Quarry. (LX202, p.p.l.)

uniformly reddened, and plagioclase is totally eliminated in favour of alkali feldspar. The areas between the megacrysts become greenish-black in hand specimen, with chlorite and tourmaline accounting for about 30% of the rock (tourmaline, from boron concentration, makes up only about 2% of the rock).

Chlorite forms complete pseudomorphs after biotite, in which iron-rich lamellae sometimes mark the original cleavages. The chlorite is vivid green in plane polarised light, and consists of small (0.02 mm) radiate and sheaf-like aggregates. Birefringence is very low; in spite of the masking effect produced by the strong green body colour, the anomalous interference colour of penninite is sometimes apparent. As well as replacing biotite, chlorite also aappears to have replaced large areas of feldspar (Plate 2:24), advancing along grain boundaries, and sometimes pseudomorphing residual feldspar left in between euhedral, recrystallised quartz.

Tourmaline shows several colours and habits. Yellow-brown, anhedral grains after feldspar are now fringed with oriented overgrowths of a finely acicular, blue-green tourmaline (Chapter 5, Plate 5:11). The overgrowths occur at one end only of the original crystals (the antilogous pole), and always grow parallel to the original crystallographic c-axis. The result is very similar to the authigenic overgrowths which develop upon detrital tourmalines during diagenesis (Krynine, 1946), and has been noted in luxullianite from Tregarden (Lister, 1978a). The blue-green tourmalines also form isolated, and radiate groups of, fine, acicular needles within the recrystallised quartz. Spherulitic tourmaline 'suns' are not developed. Where tourmaline is in contact with chlorite, it is either yellow with a blue zone at the contact, or it is totally blue and acicular.

0 0.5mm

Plate 2:23 Yellow-brown tourmaline replacing feldspar by the growth of skeletal networks; biotite (top left) within tourmaline remains unreplaced. Chloritised vein margins, Tregarden Quarry. (LX202, p.p.l.)

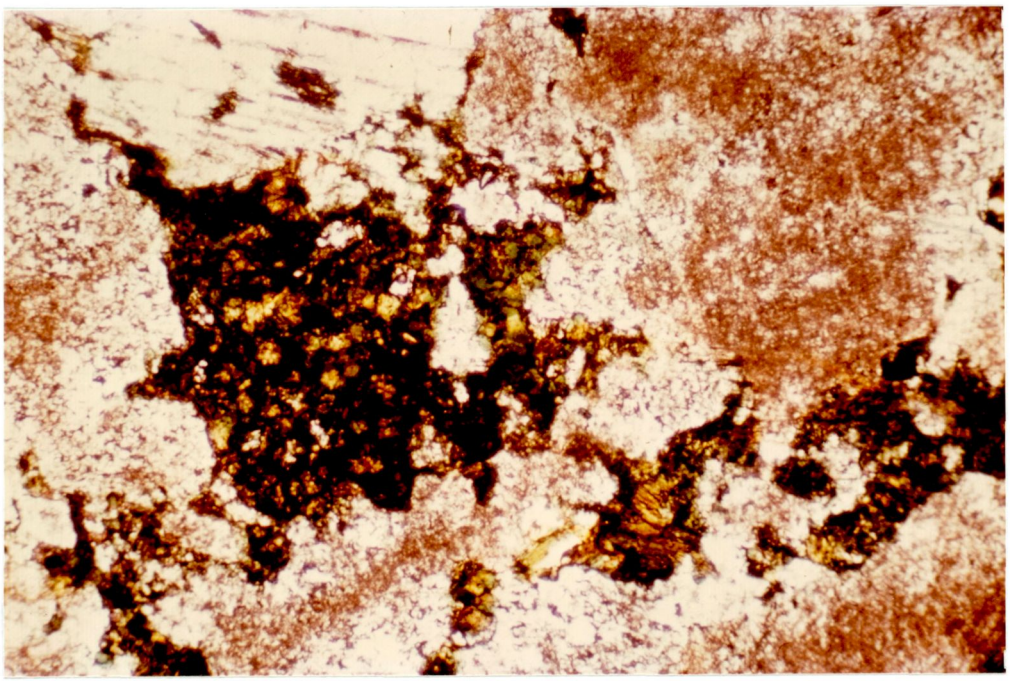

0 0.5mm

Plate 2:24 Green-yellow chlorite replacing feldspar, chloritised vein margin, Tregarden Quarry. Muscovite (top left) is also post-feldspar. (LX206, p.p.l.)

Purple fluorite and apatite are common accessories. Opaque minerals are confirmed by microprobe as ilmenite in the vein margins, and arsenopyrite in LX207. Quartz is largely recrystallised, particularly in areas of high tourmaline concentration, and is characterised by optical clarity and the virtual absence of fluid inclusions.

Samples LX208a and LX208b, from the vein centre, show similar features to LX207. In LX208a, there is very little tourmaline, and the alteration products of biotite and feldspar are green chlorite and large flakes of muscovite. Tourmaline is a more prominent component of LX208b, where it accompanies chlorite, and occurs both as large yellow crystals after feldspar and as blue-green acicular needles.

2.2.2.3 Tourmalinisation with minor chloritisation

Samples LX030 to LX036 represent the transition from granite into the centre of a vertical alteration vein in which tourmalinisation is predominant over chloritisation. The samples were taken in 3 cm increments.

About 10 cm from the edge of the vein (in LX030 to 031), the rock is very friable and iron-stained (more so than in the chloritised vein margin, LX201 to 202).

Megacrysts of microperthitic alkali feldspar show a slight cream to pink colouration. Plagioclase is entirely sericitised, and becomes converted to alkali feldspar in the vein margins. Muscovite also forms skeletal replacement networks in feldspar, developing from sericite.

Biotite is generally pale green, and is seen in various stages of breakdown to give green-yellow chlorite, sericite, muscovite and marginal alkali feldspar. Some grains become completely pseudomorphed by chlorite, while others exsolve an iron-rich fraction into distinct lamellae or sometimes into large opaque grains. Partially chloritised biotite is

replaced by muscovite, feldspar, and occasionally tourmaline.

Yellow tourmaline replaces feldspar by skeletal growth (as in Plate 2:23), and also advances into adjacent quartz by means of stringers following grain boundaries, and thence invading the body of the quartz crystals. Some tourmaline crystals become extended in more than one direction simultaneously, by replacing sericitised feldspar at one end and biotite (or chloritised biotite) at the other. The direct biotite replacement product is a bluish tourmaline, and this often forms the boundary between biotite and yellow tourmaline; blue and yellow tourmaline are in optical continuity, and the junction between them is a sharp, straight line (Plates 2:25 and 2:26).

Towards the vein margins, quartz begins to recrystallise into euhedral grains, which displace feldspar, and produce 'castellated' feldspar-quartz boundaries. Feldspar replaces biotite and chlorite, and is itself replaced by yellow tourmaline.

As the edge of the vein is approached, the rock becomes much less friable, and the feldspar megacrysts acquire a distinct pink colouration in hand specimen. The groundmass begins to appear dark greenish black.

In the maximum alteration zone (LX034 to 036), all feldspars are pink, potassium-rich microperthites. Microprobe analyses (Chapter 5) indicate extreme heterogeneity, although the microperthitic texture is masked in thin section by the very cloudy and iron-flecked appearance. There is extensive replacement of feldspar by muscovite and yellow tourmaline. Plate 2:27 shows how yellow tourmaline pseudomorphs feldspars with the castellated form derived during the growth of adjacent euhedral quartz.

All biotite is eliminated, either by incorporation into surrounding feldspar and white mica, or by chloritisation. The chloritised biotite is extensively replaced by tourmaline. Blue fibres of tourmaline

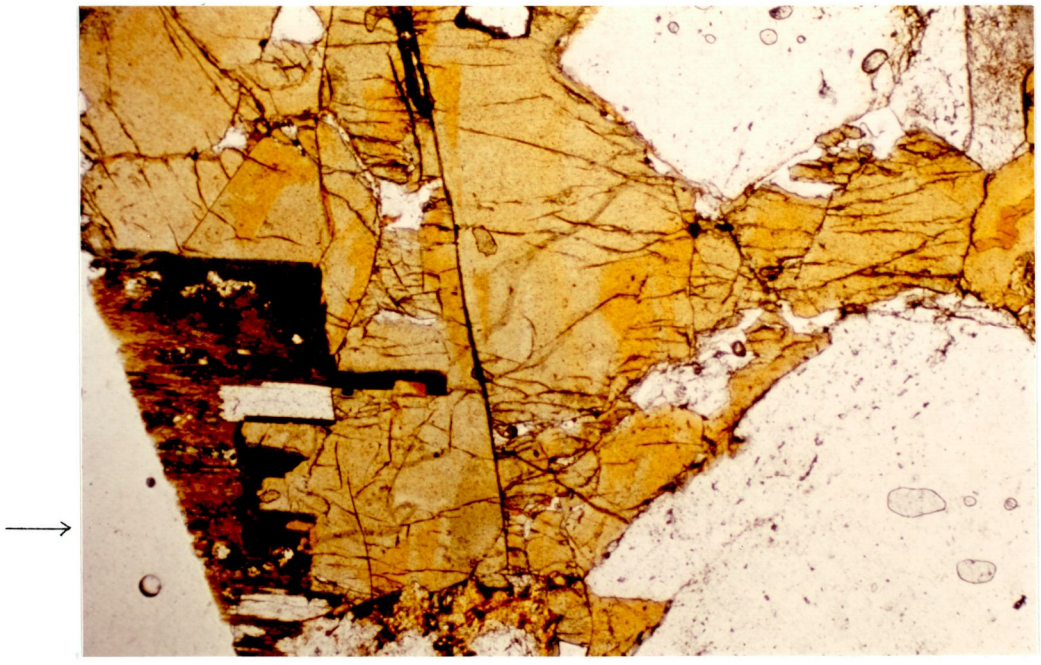

0 0.5mm

Plate 2:25 Yellow-brown tourmaline in contact with brown biotite (left); blue tourmaline, in optical continuity with the yellow, replaces biotite at the line of contact. Margin of the tourmalinised and chloritised vein, Tregarden Quarry. (LX031, p.p.l.)

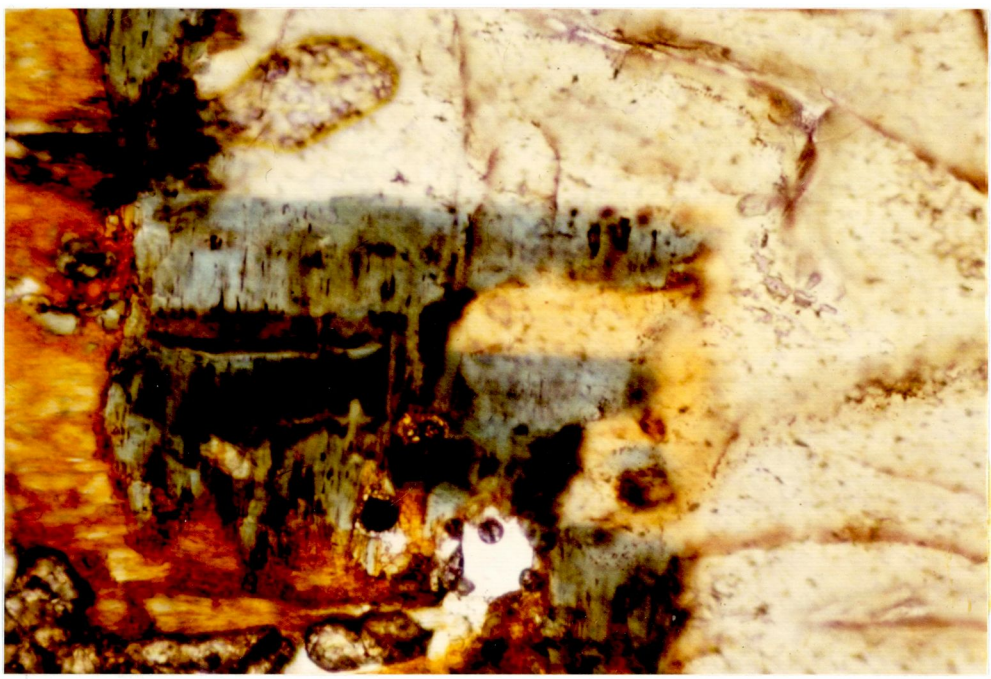

0 0.1mm

plate 2:26 Enlargement of part of the above contact, showing replacement of biotite by blue tourmaline. (LX031, p.p.l.)

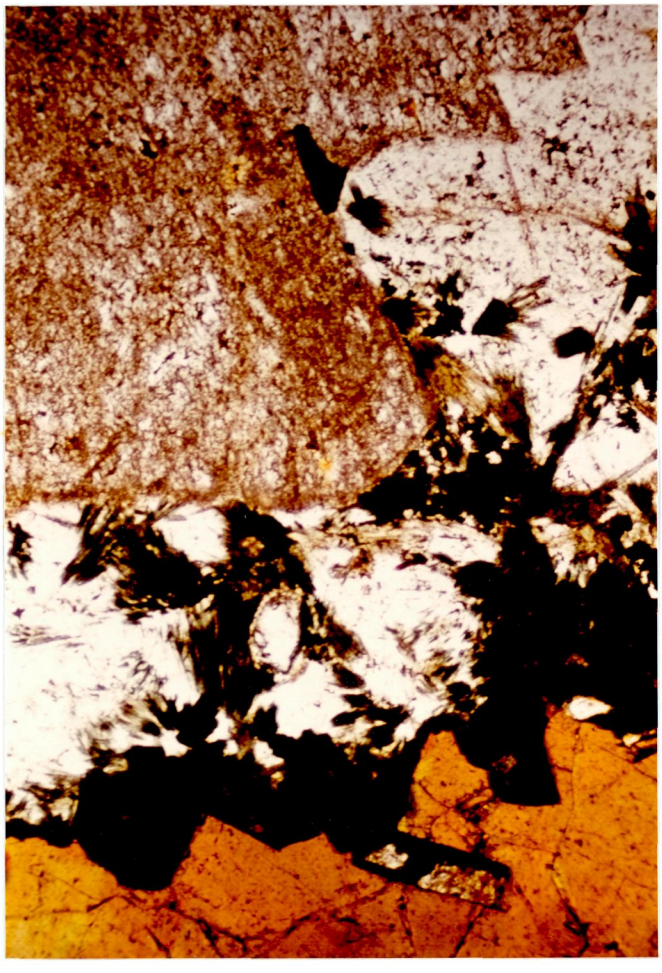

0 0.5mm

Plate 2:27 'Castellated' feldspar margin (top), and pseudomorph of yellow-brown tourmaline after feldspar (bottom); the dark, fibrous mineral is also tourmaline. Tourmalinised and chloritised vein, Tregarden Quarry. (LX033, p.p.l.)

penetrate the chloritised biotite both at its margins and centrally along lineations marking the former cleavages; some such replacements consist of brown cores with blue rims (Plates 2:28 and 2:29).

Tourmaline shows a marked increase both in abundance and in diversity of habit, and now accounts for nearly 20% of the rock, according to the boron concentration; visually, the amount of tourmaline appears greater than this, since much of it is fine and acicular. In addition to the replacive tourmalines described above, recrystallised quartz now becomes crowded with very narrow blue-brown and blue-green acicular tourmaline needles (Plate 2:30). These are present either as isolated needles, or as radiating clusters within quartz, sometimes approaching the spherulitic tourmaline 'sun' configuration. The radiate, acicular tourmalines sometimes nucleate upon the margins of feldspar, or upon the margins of yellow tourmaline after feldspar (Plate 2:31). In other cases, they form oriented overgrowths upon yellow tourmaline, as in LX207 and LX208b, and the overgrowths may be larger than the original crystals (Plate 2:32).

Muscovite forms large (1 - 2 mm) flakes, accompanying tourmaline as a replacement product of biotite and feldspar. A few pyrite grains were confirmed by microprobe. Quartz is extensively recrystallised to euhedral crystals, almost free from fluid inclusions, but shot through with minute tourmaline needles.

2.2.2.4 Luxullianite

The occurrence of luxullianite veins at Tregarden Quarry has been described by Lister (1978a). The mode of occurrence of the veins, and the petrography of alteration, are similar to those of the chloritised and tourmalinised veins described above. The final tourmaline concentration may be calculated, from boron content, to be nearly 40%. A small

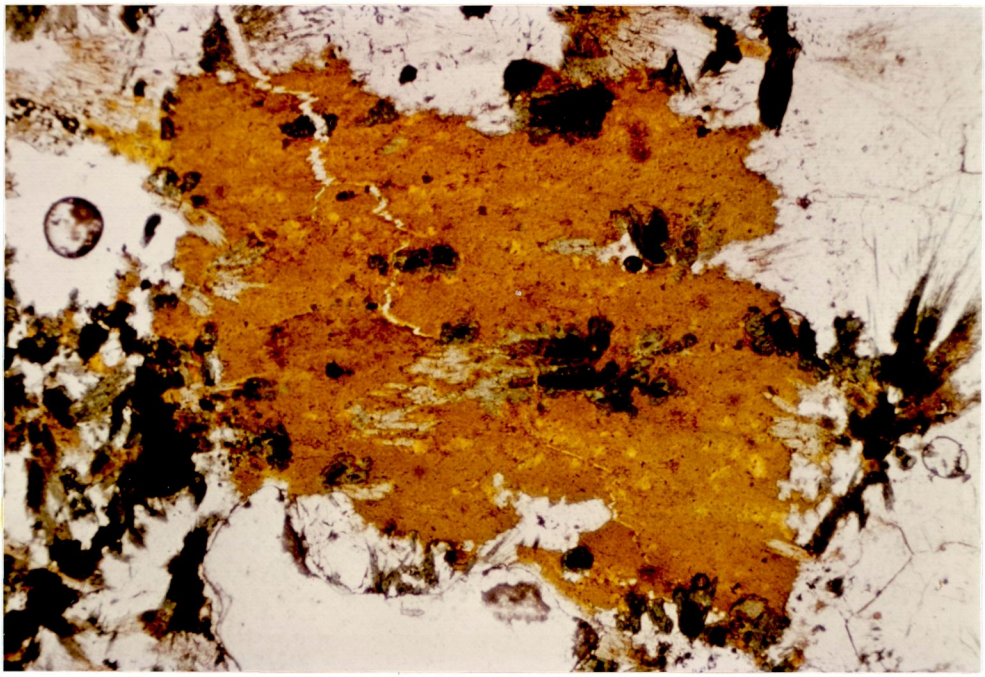

0 0.5mm

Plate 2:28 Blue and dark brown tourmaline replacing yellow chloritised biotite; tourmalinised and chloritised vein, Tregarden Quarry. (LX033, p.p.l.)

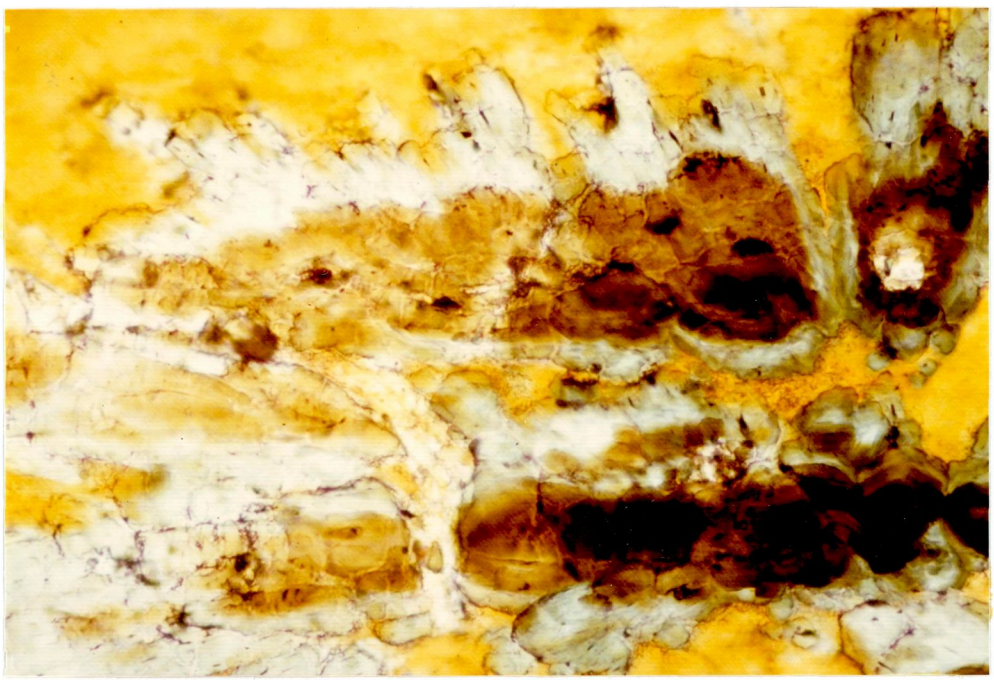

0 0.05mm

Plate 2:29 Enlargement of central area in the above grain, showing replacement of chloritised biotite by tourmaline with blue rim and brown centre. (LX033, p.p.l.)

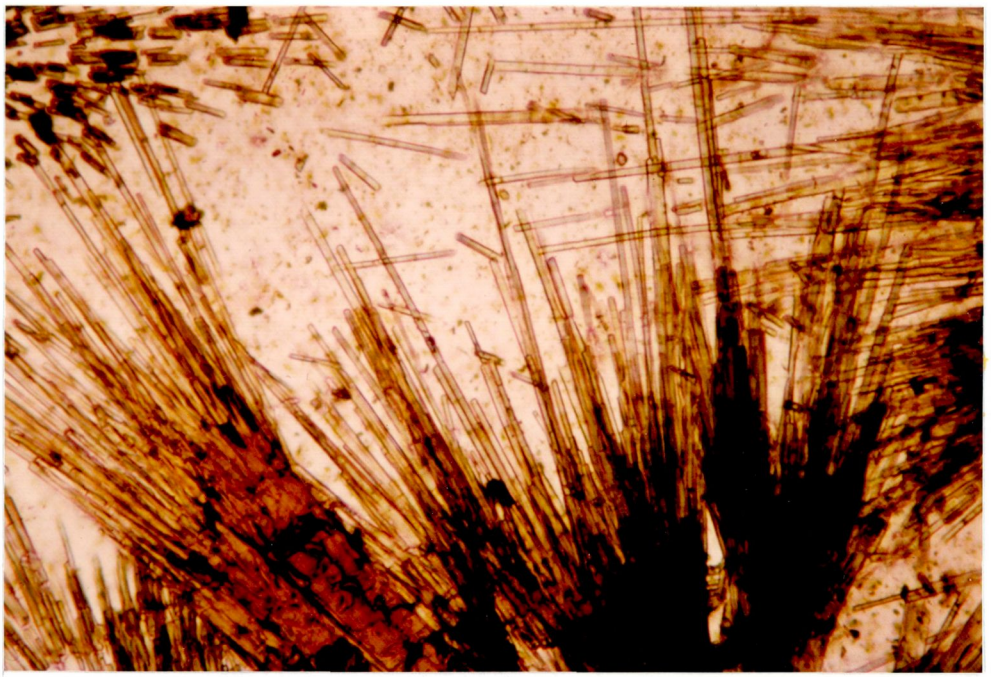

0 0.05mm

Plate 2:30 Fine, acicular tourmaline needles in the maximum tourmalinisation zone of the tourmalinised and chloritised vein, Tregarden Quarry. (LX036, p.p.l.)

0 0.5mm

Plate 2:31 Yellow-brown tourmaline after feldspar, fringed with fine, acicular tourmaline needles. Tourmalinised and chloritised vein, Tregarden Quarry. (LX036, p.p.l.)

0 0.5mm

Plate 2:32 Oriented overgrowth of blue-green tourmaline upon a smaller yellow tourmaline grain. Tourmalinised and chloritised vein, Tregarden Quarry. (LX036, p.p.l.)

amount of chlorite is present, but tourmalinisation is by far the dominant process.

Plate 2:33 shows the direct replacement of biotite by blue-green, acicular tourmaline, following the cleavage planes. Where biotite is adjacent to yellow tourmaline, it is replaced by blue tourmaline which thereby forms an oriented overgrowth in optical continuity with the yellow tourmaline grain (Plate 2:34). Spherulitic tourmaline 'sun' development within quartz is fairly common, although it is not present throughout the rock.

2.2.2.5 Pegmatitic joint fill

Sample LX051 was taken from a subhorizontal pegmatitic joint fill. It contains tourmaline which is brown in thin section, and forms hollow trigonal prisms up to 5 mm in diameter, with cores consisting of quartz, alkali feldspar, and occasionally muscovite. Unlike the skeletal tourmalines which may be seen to result from replacement, these show euhedral to subhedral morphology, and there is no optical continuity between quartz and feldspar within the tourmaline core and that outside. Comparison with other examples of cored tourmalines from southwest England has shown (Lister, 1979a) that they could be derived by direct crystallisation rather than by replacement.

2.2.2.6 Tourmalinisation and chloritisation at Tregarden Quarry: a summary

Tourmalinised and chloritised replacement veins at Tregarden have many features in common. They both represent <u>in situ</u> alteration, and are oriented in the same direction within the granite. Reddening of feldspars, and the conversion of plagioclase to alkali feldspar, occurs in all veins. In all the examples examined, biotite is replaced by

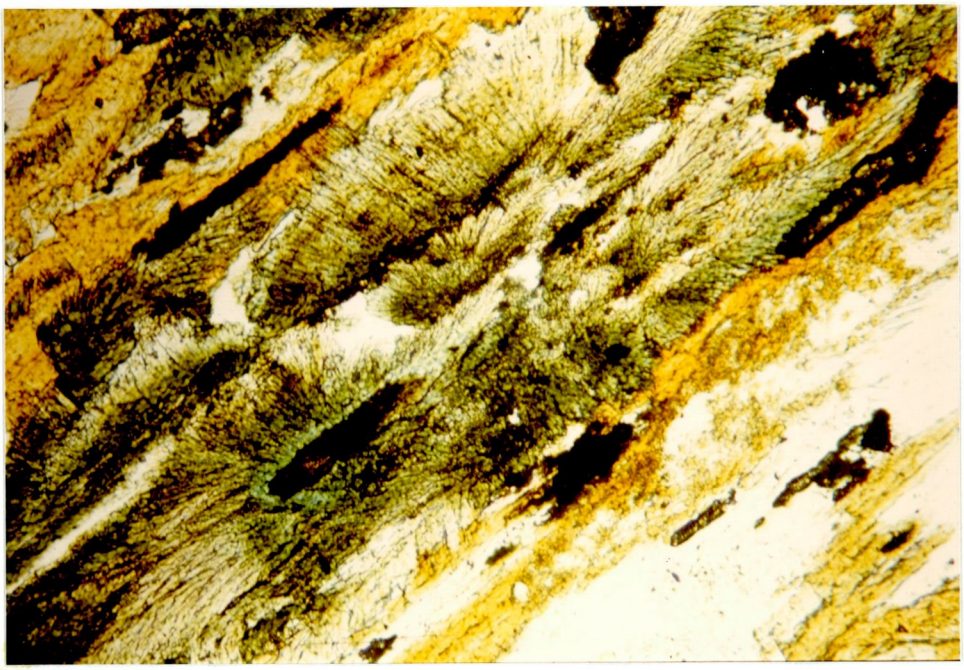

0 0.1mm

Plate 2:33 Blue-green tourmaline directly replacing biotite along the cleavages. Luxullianite vein margins, Tregarden Quarry. (LX B-2, p.p.l.)

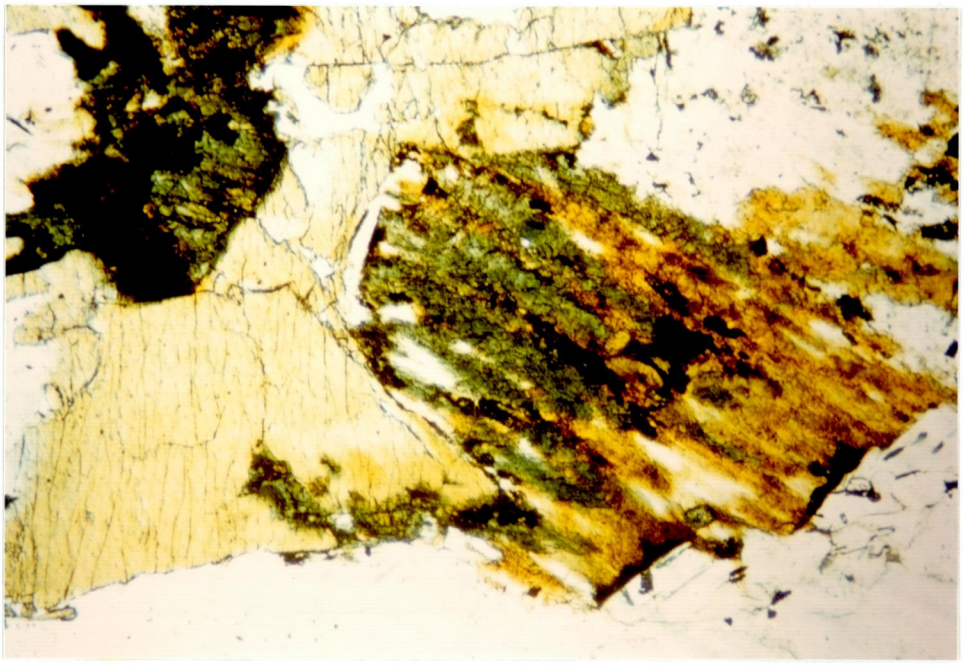

0 0.5mm

Plate 2:34 Blue-green tourmaline replacing biotite, and forming an oriented overgrowth upon adjacent yellow tourmaline. Luxullianite vein margins, Tregarden Quarry. (LX B-2, p.p.l.)

	Chloritisation with minor tourmalinisation	Tourmalinisation with minor chloritisation	Tourmalinisation to form luxullianite
	LX201 - 207	LX030 - 036	LX 81-3 - LX008*
Max. B_2O_3 wt.%	0.18%	1.73%	3.6%
Max. tourmaline content	2%	17%	35%

Yellow-green chlorite replacing feldspar

Yellow-green chlorite replacing biotite

Yellow tourmaline replacing feldspar

Blue-green tourmaline replacing biotite

Blue-brown tourmaline replacing chloritised biotite

Acicular tourmaline in quartz

Acicular tourmaline overgrowths

Feldspar reddening

Muscovite replacing feldspar

Potassium enrichment in feldspar

Quartz recryst-allisation

Purple fluorite fm.

Arsenopyrite fm.

Fig. 2:11 Alteration features in chloritised, tourmalinised and luxullianite veins at Tregarden Quarry, Luxulyan.

* Samples from Lister (1978a).

fibrous blue tourmaline, and feldspar (and possibly also some biotite) is replaced by yellow tourmaline; however, green-yellow chlorite can adopt the same replacement roles as tourmaline. Chloritisation is generally regarded as a lower temperature phenomenon than tourmalinisation, and it may be that what is essentially the same alteration process, the supply of materials for complete tourmalinisation (in particular, boron) is limited by a temperature constraint. It seems that any combination of tourmalinisation and chloritisation can occur.

In both types of vein, tourmalinisation of feldspar occurs in the outer vein margins, and continues into the vein centre, producing yellow tourmaline. In view of this observation, it seems possible that the yellow tourmaline in luxullianite could also arise by skeletal replacement of feldspar. The so-called 'primary' tourmaline in the untourmalinised granite, which has a very similar appearance,(Lister, 1978a), could likewise be a product of feldspar replacement either at the granitic emplacement stage, or post-consolidation.

Biotite is only replaced directly by tourmaline in conditions of intense tourmalinisation. Chlorite frequently replaces biotite, and is then itself replaced by tourmaline. During chloritisation, biotite releases fluorine to form purple fluorite.

The main alteration features observed in chloritised, tourmalinised and luxullianite veins are summarised in Fig. 2:11.

2.3 Goonbarrow China Clay Pit

2.3.1 Field description

Goonbarrow Pit is situated (Fig. 2:7) in the northern St. Austell granite, at about SX 007583, within the main outcrop of the heavily kaolinised, poorly-megacrystic granite. The pit, which is currently worked by English Clays, Lovering, Pochin and Company Ltd., encompasses several older china clay workings, as well as the Old Beam tin mine. The geology of mineralisation and alteration at Goonbarrow has been described by Bray (1980).

Although the major boundary between poorly megacrystic and megacrystic granites lies about 1.5 km to the east, a contact between these two facies is exposed in unkaolinised material in the floor of the pit. The contact is marked by a 'Stockscheider' pegmatite, with crystals oriented downwards towards the later, poorly megacrystic granite. This pegmatite, which traverses the pit from northwest to southeast (Fig. 2:12), had previously been described by Badham et al.(1976) as a dyke-like body, but has now been shown (Charoy, 1979a; Bray, 1980) to be a Stockscheider formed during the emplacement of the second intrusion. A northeast - southwest trending elvan dyke cuts across the southeast corner of the pit.

Several different types of mineralised veins are exposed. Bray (1980) has described these under the following headings: (1) quartz/tourmaline veins, (2) cassiterite/wolframite veins, (3) multimineral veins, and (4) barren quartz veins, and has also commented upon the close spatial association between mineralisation and kaolinisation. Types (1), (2) and (3) contain tourmaline, and strike northeast - southwest.

The vein examined in the present study is a tourmaline-quartz-topaz rock, with cassiterite at the centre. Plate 2:35 shows that this vein consists of a very narrow channelway (maximum of 1 mm wide), bordered by a few centimetres of alteration similar to greisening. The outer margins

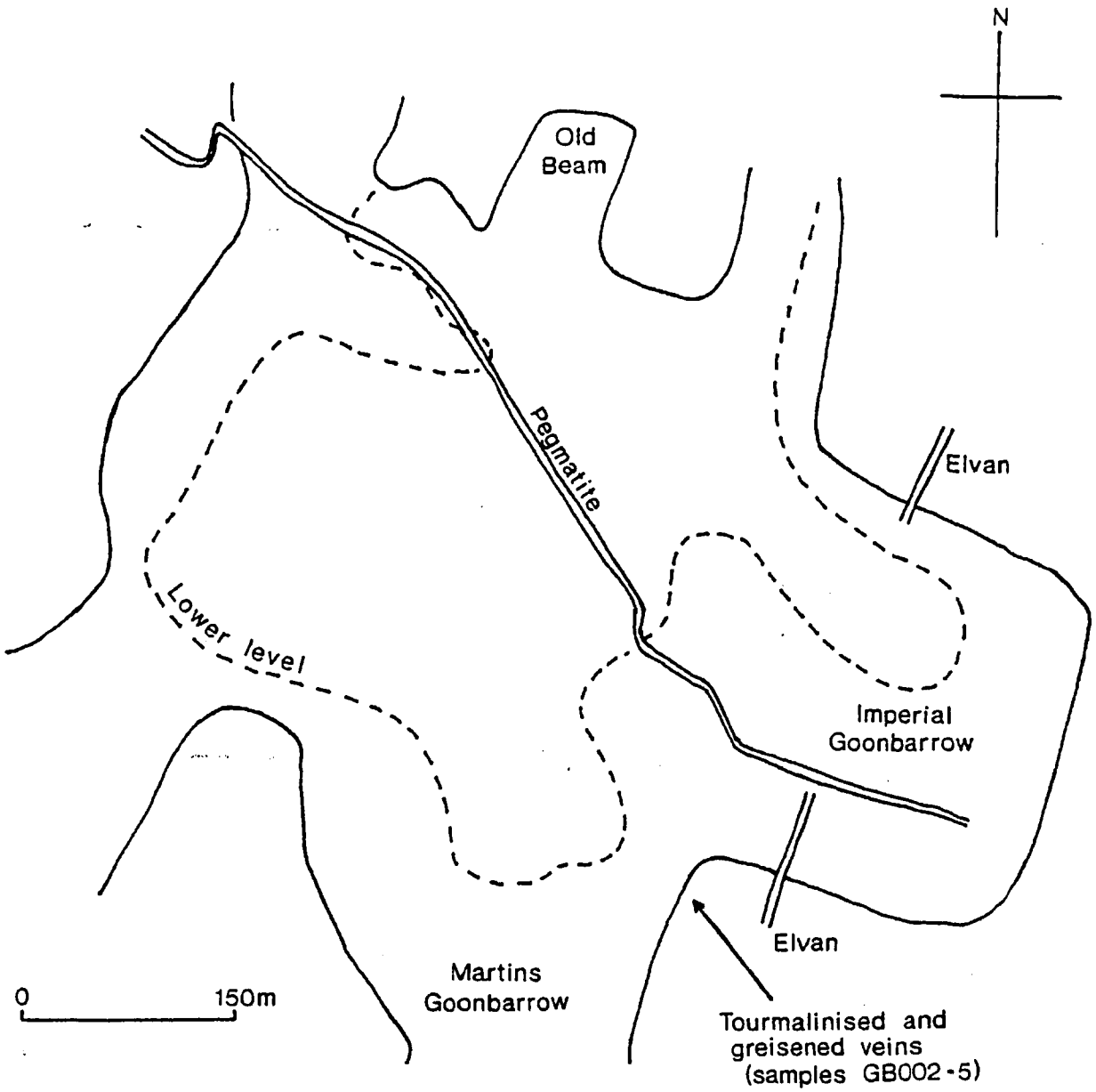

Fig. 2:12 Sketch map of Goonbarrow Pit
(details from Bray, 1980)

of the altered zone are diffuse and irregular. The vein was exposed in the southeast corner of the pit in the area between Imperial Goonbarrow and Martins Goonbarrow (Fig. 2:12), and was almost vertical, striking northeast at about 40°; it should probably be regarded as one of Bray's (1980) cassiterite/wolframite veins, but also shows similarities to the quartz/tourmaline and multimineral veins.

2.3.2 Petrography

Samples G8002 to G8005 represent the transition from kaolinised granite into the centre of the tourmalinised vein, taken continuously over a distance of a few centimetres. As noted by Bray (1980), kaolinisation is most intense in the areas of the pit which are cut by mineralised veins: it is hence difficult to identify the unaltered parent granite. However, in view of the textural characteristics of the kaolinised granite adjacent to the vein, it seems likely that the parent rock would have been the poorly-megacrystic, coarse-grained lithium-mica granite (corresponding with the early lithionite granite of Exley, 1959, and the poorly-megacrystic granite of Hawkes and Dangerfield, 1978). This contention is supported by the position of the vein to the south of the Stockscheider pegmatite. Bray (1980) described this granite facies as the 'small feldspar granite', consisting of quartz, perthitic potassium feldspar megacrysts up to 1 cm long, plagioclase (An_8), lithionite mica (probably zinnwaldite), primary and secondary muscovite, and interstitial, zoned tourmaline.

At the vein margins, feldspars retain their euhedral to subhedral morphology, and many show albite twinning, but they are intensely kaolinised and sericitised. Some large feldspar grains are completely pseudomorphed by aggregates of white mica, kaolinite and quartz; further into the vein centre, the original feldspar shape is lost, as the

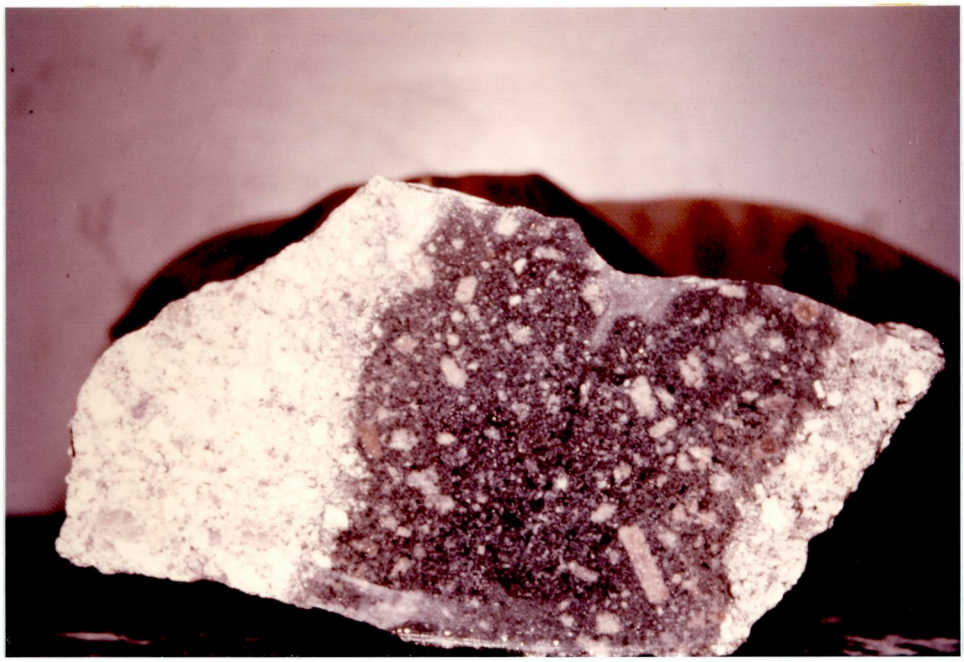

0 20mm

Plate 2:35 Tourmalinised and greisened vein traversing kaolinised granite at Goonbarrow Pit. This specimen furnished samples GB002 to GB005.

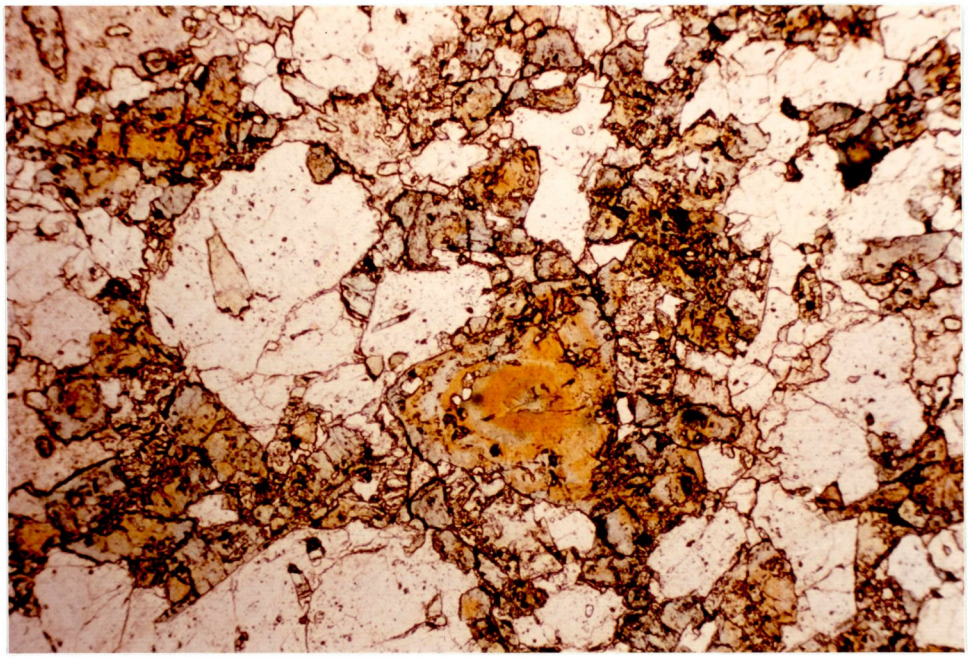

0 0.5mm

Plate 2:36 Brown and blue zoned tourmaline, with relict feldspar (cloudy) and quartz, from the tourmalinised and greisened vein at Goonbarrow. (GB005, p.p.l.)

replacement products are displaced by the growth of larger quartz and topaz crystals. There is no coloured lithium mica, even in the outer vein margins, but there are large (up to 1 mm) muscovite flakes which could have replaced the original lithium mica in the granite. Tourmaline forms irregular and skeletal grains intergrown with the recrystallised quartz, muscovite and topaz. Tourmalines do not selectively replace any particular mineral, but accrete from many nuclei between recrystallising grain boundaries.

In the vein centre, feldspar is virtually eliminated, and white mica and kaolinite are much reduced in quantity, The maximum alteration zone contains about 64% tourmaline, 15% topaz and 15% quartz, the remainder of the rock consisting of residual fine-grained white mica, kaolinite, and a few zoned brown grains of cassiterite. Plate 2:36 shows a typical tourmaline crystal from sample GB005 (vein centre); all tourmalines are yellow-brown and pale blue, often with brown cores and alternating yellow-brown and blue outer zones. Fibrous and acicular tourmaline is absent. Topaz is difficult to distinguish from quartz in thin section, particularly since the two minerals adopt similar habits, and appear as both euhedral and rounded grains; topaz is, however, biaxial, and has cleavage. The presence of topaz in the vein was indicated by the high fluorine concentrations in whole rock analyses, and was confirmed by microprobe.

2.3.3 Tourmaline in the Stockscheider pegmatite

The pegmatite contains curved and branching crystals of twinned alkali feldspar, which appear to have grown towards the lithium-mica granite below. In places, the pegmatite consists of several successive curved-crystal layers parallel to the upper and lower boundaries, and has a total thickness of over 1 metre; the texture has been likened to

comb-layering by Badham et al. (1976).

Tourmaline, where present, has an elongate and curved habit similar to that of the feldspar, and forms 'hollow' crystals, with multiple quartz cores. It is black in hand specimen and yellow-brown in plane polarised light, with concentric zoning, and blue radiogenic haloes surrounding minute inclusions. By comparison with cored tourmaline crystals elsewhere in southwest England, it appears that an origin by direct crystallisation rather than replacement is possible (Lister, 1979a), and this is consistent with the supposed mode of emplacement of the Stockscheider pegmatite. However, the texture of these tourmalines, particularly the multiple quartz cores and embayed outlines, suggests a replacive origin. This latter hypothesis would require that the pegmatite be formed by replacement of an existing granite in the solid state, in which case the dendritic habit of feldspars and tourmalines would be difficult to explain. It must be concluded that the origin of the tourmalines is not yet certain.

2.4 Cape Cornwall

2.4.1 Field description

Cape Cornwall is located on the Atlantic coast of the Land's End granite, at the westernmost point 2 km from the village of St. Just. Along this coast, the contact between granite and killas approximately coincides with the cliff-line, so that contact phenomena are well exposed in beach sections. Like the Dartmoor and St. Austell granites, the Land's End mass consists of several individual plutons; inland from Cape Cornwall, the granite is non-megacrystic, while a few kilometers further south, megacrystic granite becomes the predominant type.

The geology of the Cape Cornwall area is outlined in Fig. 2:13. Quartz-veined hornfels forms the headland of Cape Cornwall, and is visible at low tide along the seaward side of Porthledden Cove; Kenidjack Cliff to the north consists of hornfels and metabasites. A non - megacrystic granite outcrops on the southern side of Priest's Cove (SW 352317) and in isolated exposures on the beach in Porthledden Cove (SW 354321), where it underlies a tourmaline granite, a tourmalinite (quartz-schorl rock), and a coarse, megacrystic granite. The area is cut by numerous tourmaline-bearing veins and pegmatites, as well as northwest - southeast trending tin lodes; one such lode was formerly worked in Boswedden Mine immediately north of Porthledden Cove.

The particular interest of Cape Cornwall in the present study is centred around the controversial origin of the Cape Cornwall tourmalinite. Charoy (1979a) discussed evidence supporting its genesis by extreme magmatic differentiation, as suggested by Power (1968) for the tourmalinite of Roche Rock. The former author's geochemical and fluid inclusion data indicate that a magmatic origin is possible, but that a hydrothermal origin cannot be precluded. In the following pages, the possibility of such a hydrothermal origin will be reconsidered.

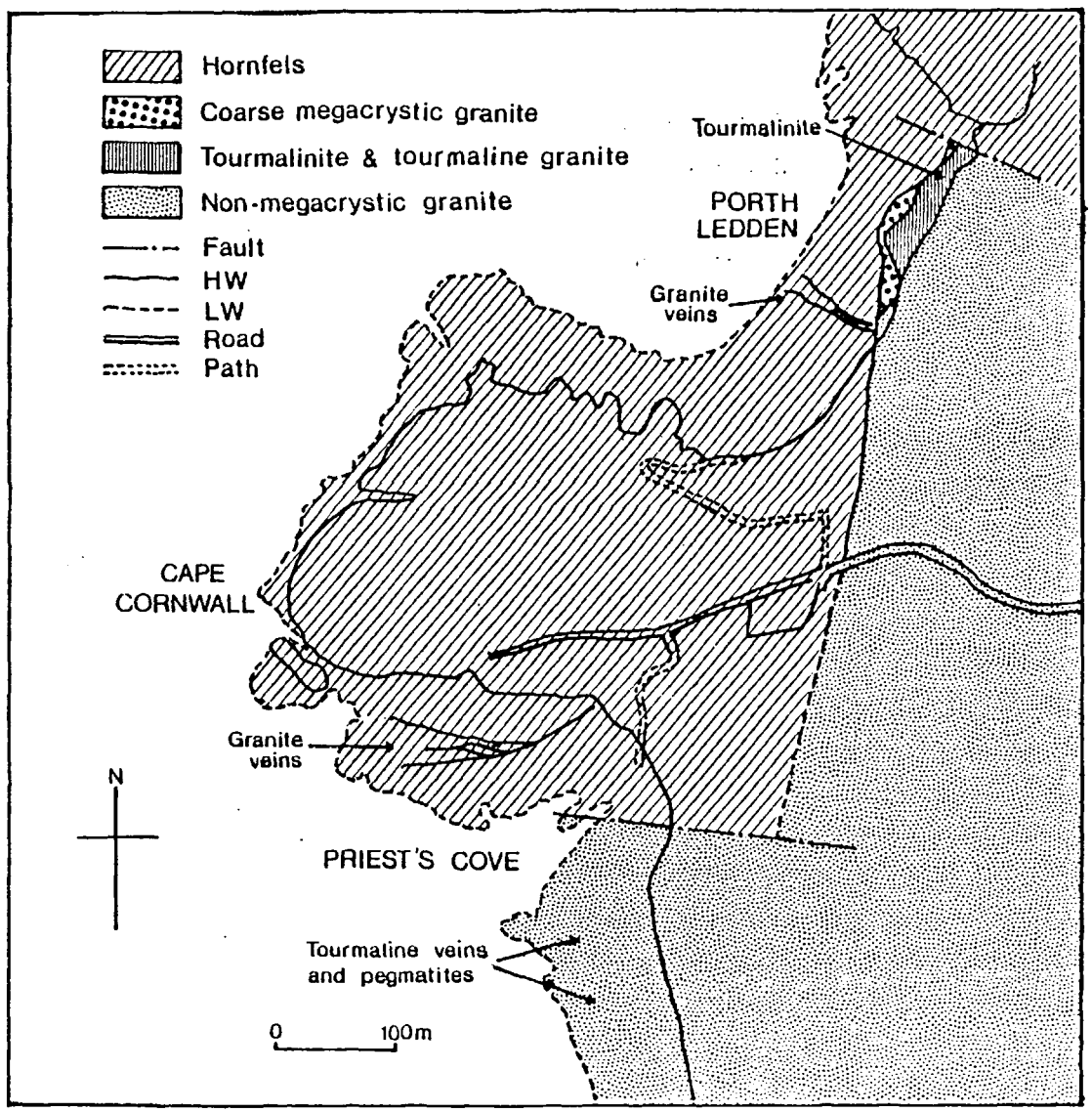

Fig. 2:13 Geology of the Cape Cornwall area (adapted from Hall and Jackson, 1975)

2.4.1.1 The Cape Cornwall tourmalinite

The tourmalinite forms a sub-horizontal sheet about 6 metres thick, dipping at a shallow angle towards the sea, and extending about 0.2 km from north to south along Porthledden Cove. The sketch map and diagrams of Charoy (1979a), reproduced as Figs. 2:14 and 2:15, show that the tourmalinite is overlain by megacrystic granite and underlain by tourmaline granite. The granites and tourmalinite are terminated to the north by a major, near-vertical fault, striking northwest - southeast.

The megacrystic granite is a discontinuous intrusion interposed between tourmalinite and killas; in the south part of Porthledden Cove, the megacrystic granite lenses out, so that the tourmalinite is directly overlain by metasediments. There is a strong preferred orientation of alkali feldspar megacrysts within the granite, which, according to Charoy (1979a), contains comb-layered structures in its apical zone adjacent to its contact with the killas. The boundary between megacrystic granite and tourmalinite is a sharp one, and is marked by a silicified zone.

The tourmaline granite is only exposed in topographic low points on the beach, and is itself underlain by a biotite granite described by Charoy (1979a) as the Priest's Cove microgranite. The tourmalinite, tourmaline granite and Priest's Cove microgranite are all very similar texturally (grain size 2 to 3 mm; fairly equigranular, with no megacrysts), and although Charoy (1979a) drew sharp boundaries between these units, the boundaries are actually gradational, as shown in Plate 2:37 . Occasional stringers of tourmalinite (up to 10 cm across) extend downwards into the tourmaline granite, and their boundaries with the granite are also gradational. Conversely, rafts of tourmaline granite are also found within the tourmalinite.

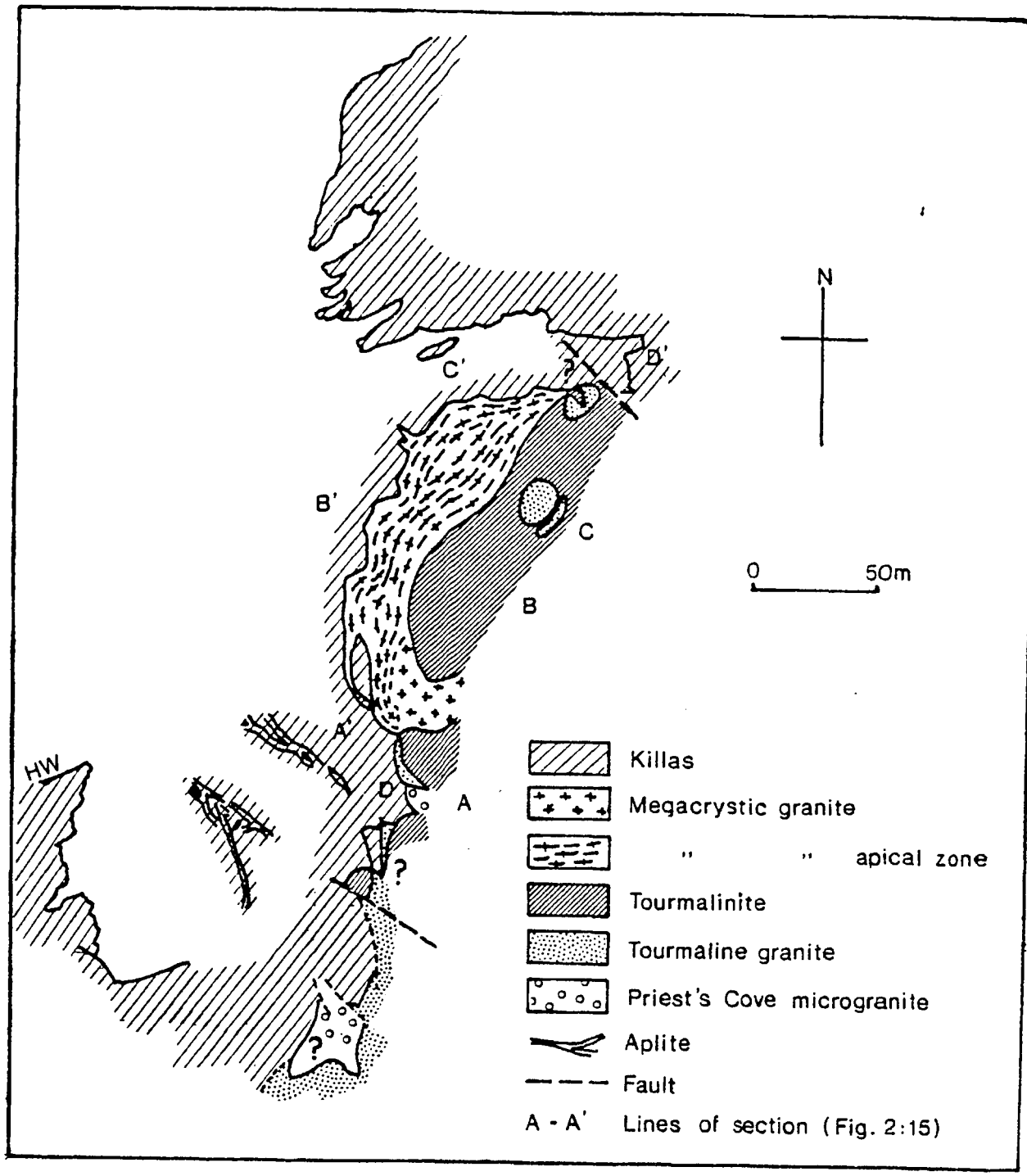

Fig. 2:14 Geology of Porth Ledden
(simplified after Charoy, 1979a)

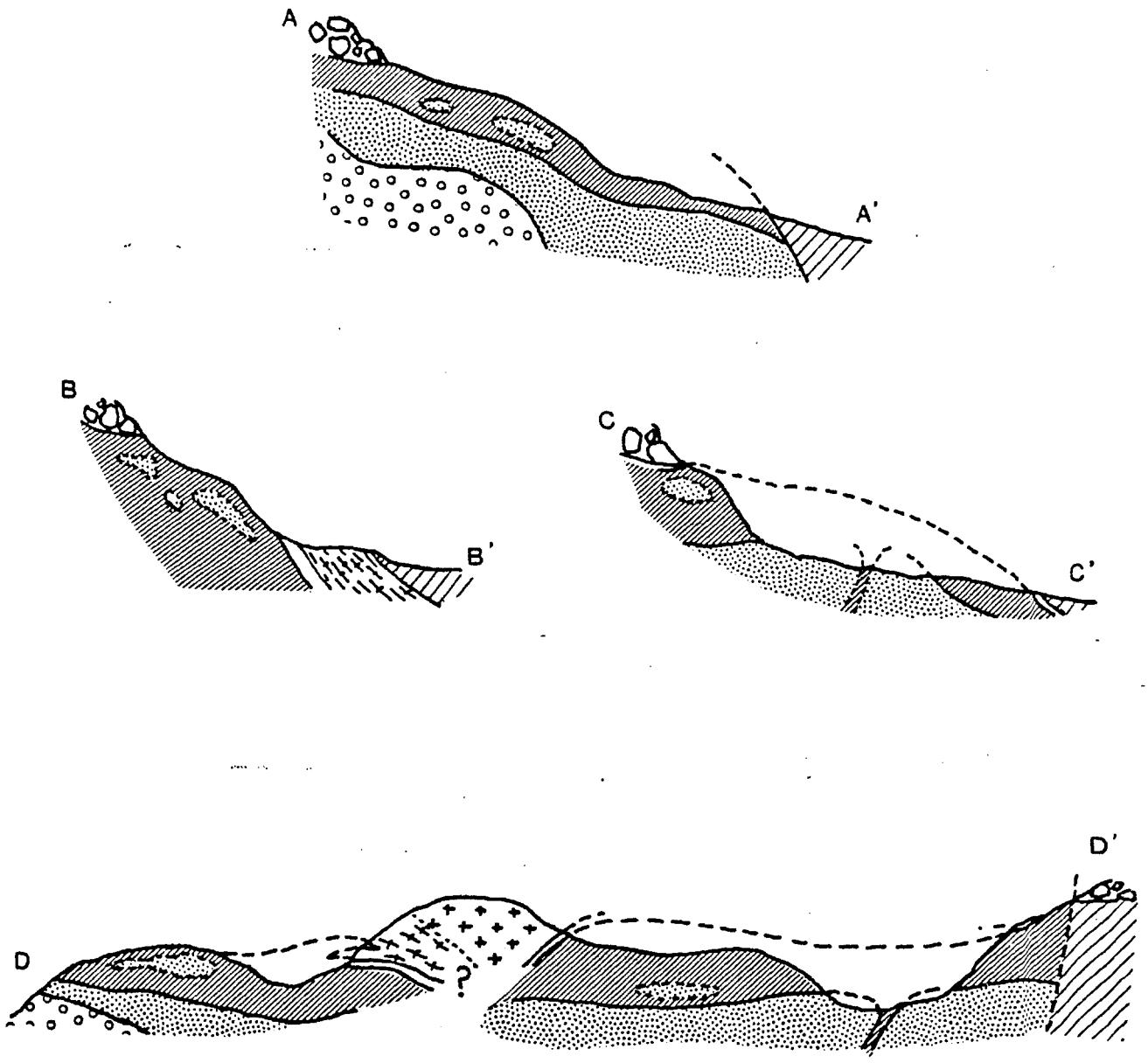

Fig. 2:15 Structure of Porth Ledden
(after Charoy, 1979a) not to scale

For legend and lines of section (A - A' &c.), see Fig. 2:14.

= silicified zone

Plate 2:37 The gradational boundary between the Cape Cornwall tourmalinite (above) and tourmaline granite (below). (Hammer shaft 0.65m)

Plate 2:38 The layered structure of the Cape Cornwall tourmalinite, north end of Porthledden beach, looking north towards Kenidjack.

The tourmalinite has a layered structure (Plate 2:38), comprising successive horizons which are quartz-rich at the base, and become steadily more tourmaline-rich upwards over a distance of 10 to 20 centimetres. This structure is reminiscent of rhythmic layering in some mafic and ultramafic rocks (as described by Wager and Brown, 1966). The layering dips at a shallow angle towards the sea, and is approximately parallel to the upper and lower boundaries of the tourmalinite body. Within the tourmalinite, there are several pockets of almost pure tourmaline (up to about 20 cm in diameter), as well as some later, discordant veins (2 or 3 cm across) of quartz and tourmaline.

The field evidence indicates that the succession from biotite granite through tourmaline granite into tourmalinite could represent a vertical, progressive tourmalinisation sequence. Since the deepest levels of this succession are not exposed, it is not possible to sample the untourmalinised parent granite. However, sample CC010 was taken from the tourmaline granite one metre below the tourmalinite, and the transition zone from tourmaline granite into tourmalinite (Plate 2:39) was sampled continuously in 3 cm increments (CC011 to CC015). Samples CC001 to CC005 are from a tourmalinite layer, showing increasing tourmaline content, and illustrate the range of mineralogical and chamical variation within the tourmalinite.

2.4.1.2 Priest's Cove

The Priest's Cove granite is mostly non-megacrystic and equigranular, and outcrops south of a major east-west trending fault (Fig. 2:13). Charoy's (1979a) term 'microgranite' was presumably intended simply to distinguish this granite from the megacrystic granite of Porthledden. The grain size is about 2 to 3 mm, except where tourmalinised lenticles and narrow veinlets

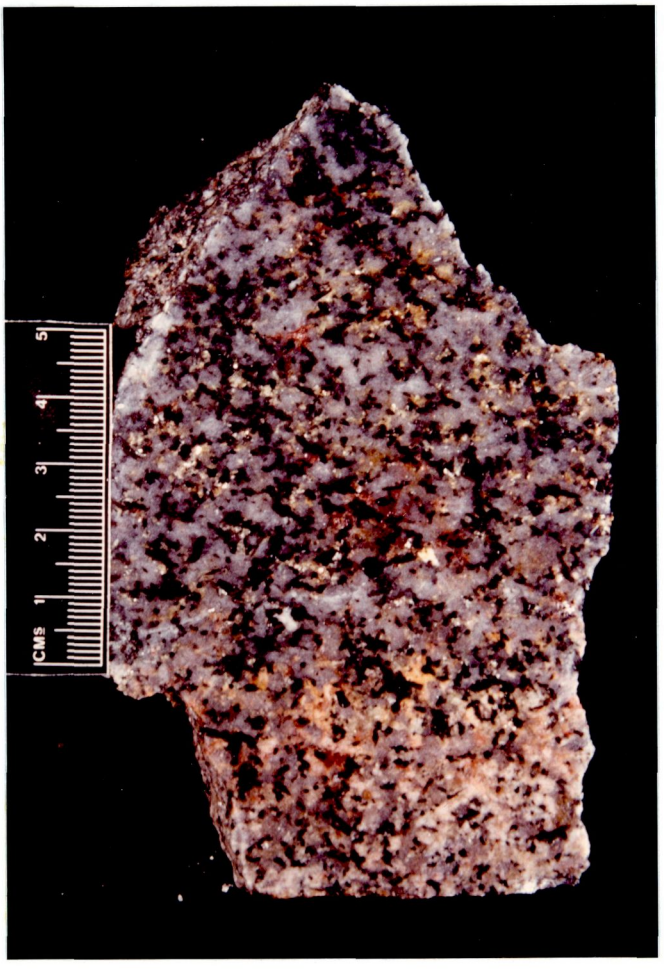

Plate 2:39 The transitional zone between tourmalinite and tourmaline granite, from which samples CC011 to CC015 were taken.

are associated with the development of pink alkali feldspar megacrysts. Radiate tourmaline, black in hand specimen, is common, and has grown both on joint surfaces and from isolated nuclei within the granite. Areas of tourmaline concentration within the granite are strongly reddened.

There are several vertical, discordant pegmatite veins cutting the granite. These contain quartz, pink or cream coloured alkali feldspar, muscovite and tourmaline. The tourmaline is black in hand specimen, and forms elongate, trigonal prisms up to 10 mm in diameter (basal section) and up to 10 cm long; they are euhedral to subhedral, and have polycrystalline quartz cores. These quartz-cored tourmalines are described in the appended paper (Lister, 1979a).

2.4.2 Petrography

2.4.2.1 Cape Cornwall tourmalinite

The reader is referred to the work of Charoy (1979a) for detailed petrographic descriptions of the tourmalinite and associated rock types. The present study is aimed specifically at establishing the petrographic evidence for tourmalinisation, as opposed to magmatic differentiation.

According to Charoy (1979a), the Priest's Cove microgranite contains quartz, at least two generations of plagioclase (the earlier An_{18} to An_{12}, and the later averaging An_6 to An_8), coloured mica, muscovite, and secondary potassium feldspar megacrysts; accessories are tourmaline, cordierite, apatite, topaz, zircon and fluorite. He described the tourmaline as brown, sometimes zoned with light blue, invading both coloured mica and potassium feldspar.

Examination of sample CC010 from the tourmaline granite confirmed Charoy's (1979a) mineral constituents as quartz, potassium feldspar, very minor albite, muscovite, and blue and brown zoned tourmaline.

In sample CC010, collected 1 metre below the tourmalinite, the tourmalines are clearly replacive in nature. In plane polarised light, the tourmaline is yellow-brown and pale blue. The yellow-brown tourmaline forms the centres of zoned crystals, and appears to have pseudomorphed large areas of feldspar; there are some dark and patchy coloured areas within such tourmaline, which could be post-biotite. Pale blue tourmaline forms outer zones accreting in optical continuity upon brown crystals. Both yellow-brown and pale blue tourmaline shows intricate skeletal networks invading feldspar (Plate 2:40). Plagioclase is virtually eliminated in favour of alkali feldspar, which contains irregular, granophyric intergrowths with quartz. Feldspars are flecked with brown iron oxides, and show heavy sericitisation, as well as replacement by skeletal muscovite (Plate 2:41) and skeletal tourmaline. There are a few larger (0.5 mm) flakes of muscovite away from feldspar; these could be post-biotite.

The tourmaline granite adjacent to a tourmalinite vein was also sampled (CC021 and CC022), and this shows similar replacement features to those in sample CC010. Many of the tourmalines contain blue-green haloes around minute included particles and grains, as well as similar blue-green discolouration bordering irregular fractures, which presumably must once have contained radiogenic material. Sulphides, principally chalcopyrite, are present as discrete grains within and at the margins of tourmalines, but also within rounded globules enclosed by tourmaline; the globules are surrounded by radiogenic haloes.

The boundary between tourmaline granite and tourmalinite is seen in samples CC011 to CC015, in which the equigranular texture prevails across the transition zone. Charoy (1979a) treated the tourmaline granite and tourmalinite as discrete petrographic units, and did not consider the transitional zone between them; the petrography of this zone is, however, considered to be of crucial importance in establishing the mode of origin

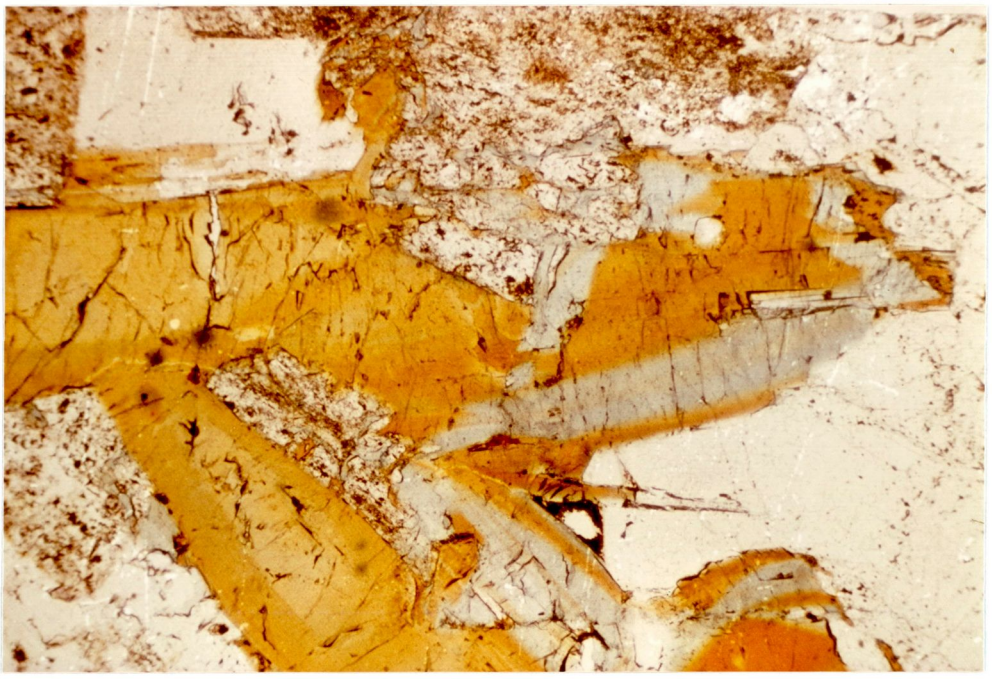

0 0.5mm

Plate 2:40 Feldspar (cloudy) replaced by skeletal growth of both yellow-brown and pale blue tourmaline, in the transition zone between tourmalinite and tourmaline granite, Cape Cornwall. (CC012, p.p.l.)

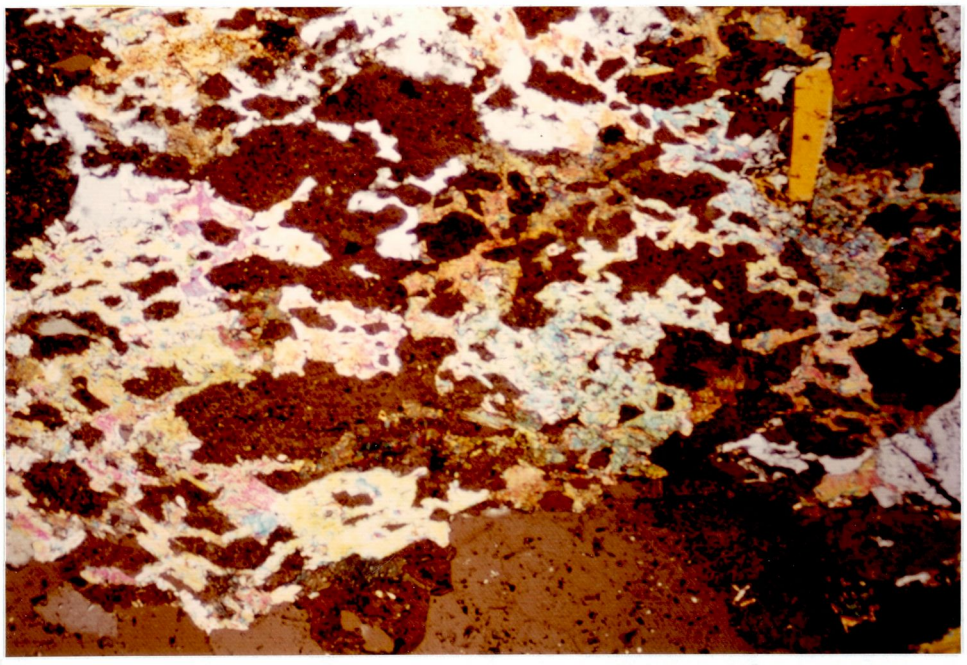

0 0.5mm

Plate 2:41 Feldspar replaced by skeletal muscovite (birefringent), in the transition zone between tourmalinite and tourmaline granite, Cape Cornwall. (CC012, x.p.)

of the tourmalinite.

In the lower part of the transition zone (CC011 to CC013), feldspar, which is now entirely iron-flecked alkali feldspar, becomes progressively replaced. In CC012, all feldspars are either strongly veined with skeletal intergrowths of tourmaline, muscovite and/or quartz, or are pseudomorphed by intense sericitisation. In CC013, the interstices between skeletal replacement products are infilled (Plate 2:40) so that hardly any feldspar remains. Tourmaline most commonly shows a zonation scheme of yellow-brown cores with pale blue rims, although the outer zones may alternate between pale blue and yellow-brown; occasionally, dark blue tourmaline forms outer rims or fills skeletal interstices. Muscovite likewise develops skeletal networks after feldspar, which infill to produce larger crystals. The lower transition zone contains sufficient muscovite to warrant the term 'tourmaline greisen'. Occasional sulphides and apatite grains are present.

In CC014 to CC015, feldspar is almost completely obliterated, and muscovite becomes less common as it is engulfed and incorporated into large tourmalines. The tourmaline shows similar zonation schemes to that in CC011 to CC013, but with an increase in the proportion of pale blue material; some grains now approach euhedral morphology. The tourmalinite of CC015 contains approximately equal proportions of quartz and tourmaline, with small amounts of muscovite, residual feldspar, apatite (fluorapatite, according to Charoy, 1979a), and isolated sulphides.

The sequence CC001 to CC005 is taken from within the tourmalinite body, and represents a unit which becomes more tourmaline-rich upwards. Grains of muscovite and reddened and sericitised residual feldspar are found in the lower portions of this unit (CC001 to CC003), but these are virtually absent from CC004 and CC005. Tourmaline is brown and blue zoned as in CC015, and frequently approaches euhedral morphology; although the

margins are often irregular, intricate skeletal networks are absent. Sample CC001 at the base of the unit contains about 16% tourmaline, 3% muscovite, 0.5% sericitised and reddened feldspar, 0.5% apatite, and 80% quartz, while sample CC005 at the top of the unit contains over 40% tourmaline, more than 1% apatite and nearly 60% quartz. Chalcopyrite grains are occasionally present, as is a deep red mineral which is possibly rutile.

2.4.2.2 Summary of petrographic evidence for tourmalinisation versus magmatic differentiation in the Cape Cornwall tourmalinite

The cogenetic origin of the biotite granite, tourmaline granite, tourmaline greisen and tourmalinite, is supported by the homogeneity of the equigranular texture which prevails throughout the sequence, and also by the transitional nature of the boundaries between these rock types. The existence of such a cogenetic sequence could imply either differentiation of a magma into successive horizontal layers, or progressive tourmalinisation.

However, throughout the tourmaline granite and the transitional zone into the tourmalinite, tourmaline shows unequivocal replacement features. Similar skeletal invasion of feldspar has been observed in tourmalinised veins at other localities described in this chapter. The development of tourmaline greisen grading into a quartz-tourmaline rock is known from vertical alteration veins elsewhere (e.g. at Goonbarrow). Most of the muscovite present in the tourmaline greisen also shows clear evidence for a secondary origin after feldspar.

The sequence from biotite granite through tourmaline granite then tourmaline greisen into tourmalinite (Fig. 2:16) has also recently been reported from the Bosworgey borehole, north of the Tregonning granite (Ball and Basham,

1981). The Cape Cornwall sequence shows many similarities with the borehole material, including the association with sulphides, as well as sulphide-bearing globules generating radiogenic haloes within surrounding tourmaline (some of the globules described by Ball and Basham, 1981, contain uraninite and uraniferous hydrocarbon). The tourmaline greisen of the Bosworgey borehole yields cassiterite, and Charoy (1979a) also reported occasional cassiterite from the Cape Cornwall tourmaline granite and tourmalinite (although none was observed in samples collected for the present study). The presence of sulphides, cassiterite and possibly also uraniferous materials (the latter enclosed in tourmaline) in both sequences militates against a primary magmatic origin, and tends to support the formation of such tourmalinites by late-stage hydrothermal alteration.

It is suggested, therefore, on petrographic evidence, that both the Cape Cornwall and Bosworgey successions represent vertical, ascending sequences of progressive tourmalinisation. Other lines of evidence relating to this contention will be discussed in later chapters. The Cape Cornwall sequence is summarised in Fig. 2:16.

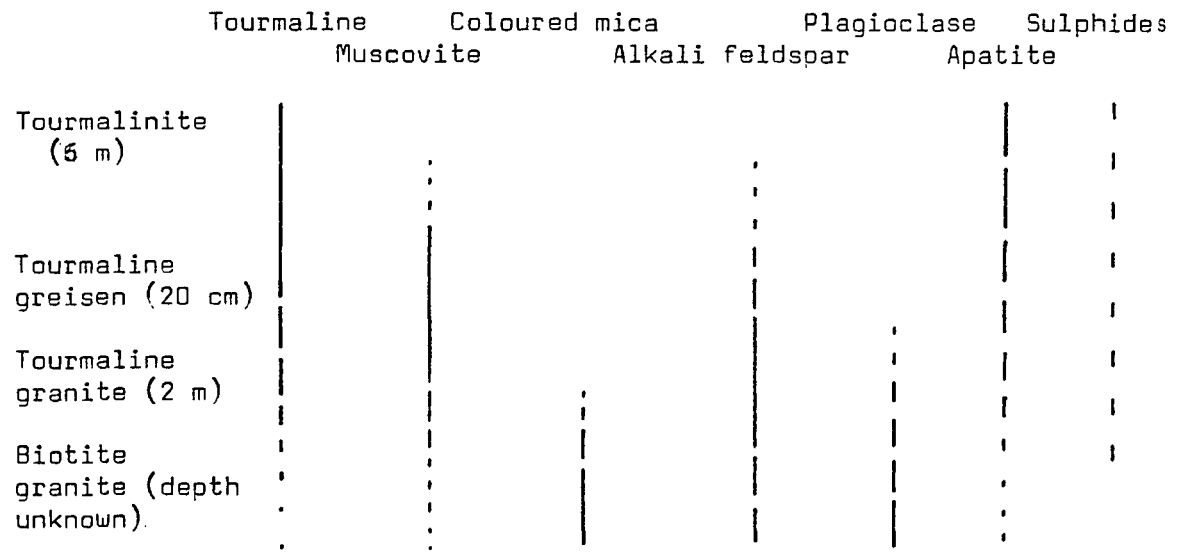

Fig. 2:16. Mineralogy of the Cape Cornwall tourmalinite sequence

2.5 Comparison of tourmalinisation processes at the localities examined

Table 2:1 summarises the field occurrence of the tourmalinised rocks described, and the mineralogical changes associated with the tourmalinisation process.

The Tregarden, Venford and Goonbarrow tourmalinised rocks all occur in the form of vertical, in situ replacement veins, while the Cape Cornwall tourmalinite has a horizontal, sheet-like form. All contacts with the host granites are gradational.

The Venford 'luxullianite' is the only example associated with an extensive reddened zone, but reddening of feldspars accompanies tourmalinisation at all localities except Goonbarrow, where kaolinisation has obliterated any such effect.

In all the examples investigated, dark mica and plagioclase are totally replaced during tourmalinisation; at Goonbarrow and Cape Cornwall, alkali feldspar is also almost completely eliminated, while at Tregarden and Venford, alkali feldspar is both generated and replaced.

Greisening is associated with tourmalinisation at Goonbarrow and Cape Cornwall, and muscovite (or hydromuscovite) is an important by-product of tourmalinisation at all localities.

Chlorite occurs along with tourmaline at Tregarden, and the heavily chloritised vein at this locality also contains fluorite and sulphide (arsenopyrite). Cassiterite is prominent in the Goonbarrow vein, and is present in smaller quantities at Cape Cornwall and in one of the Venford veins. Chalcopyrite also occurs in the Cape Cornwall tourmalinite. The Goonbarrow vein is the only one examined which contains topaz. Apatite is an almost ubiquitous accessory in granites and altered rocks alike, but it is particularly prominent at Venford and Cape Cornwall.

	Tourmalinisation product(s)	Configuration	Vertical extent	Lateral extent	Contact with host rock	Constituents of untourmalinised granite	Minerals replaced during tourmalinisation	Minerals formed during tourmalinisation
Tregarden	chloritised/ tourmalinised rock	vertical veins	>10m	1-3m	gradational	Qtz.,alkali feldspar, plag.,biotite,muscovite,(tourmaline)	Biotite,plag., (alkali feldspar)	Chlorite,muscovite, tourmaline,K-feldspar, fluorite,sulphide
Tregarden	luxullianite -type	vertical veins	>10m	2-3m	gradational	as above	as above	Tourmaline,K-feldspar, muscovite,chlorite
Venford	luxullianite -type	vertical veins	> 4m	1-3m	gradational with intervening reddened zone	Qtz., plag., alkali feldspar, biotite,(tourmaline)	Biotite,plag., (alkali feldspar)	Tourmaline,K-feldspar, hydromuscovite, apatite,(cassiterite)
Goonbarrow	tourmalinite/ greisen	vertical vein	> 3m	20cm	gradational	Qtz.,plag.,Li-mica, alkali feldspar, (tourmaline)	Li-mica, feldspar	Tourmaline,topaz, muscovite,cassiterite
Cape Cornwall	tourmalinite/ greisen	horizontal sheet	~ 6m	0.2km	gradational over greisened zone	Qtz.,plag.,alkali feldspar,biotite, (tourmaline)	Biotite, feldspar, (muscovite)	Tourmaline,fluorapatite, muscovite,sulphide, (cassiterite)

Table 2:1 Comparison of tourmalinisation processes

2.6 Discussion

Previous workers on the southwest England granites (e.g. Exley and Stone,1964) have drawn a general distinction between primary magmatic (or pre-joint) and secondary hydrothermal (or post joint) tourmaline; the former has been described as usually yellow-brown in plane polarised light, while the latter has been described as blue-green.

The tourmaline formed by hydrothermal alteration of existing minerals, at the localities investigated, shows a wide range of colours and habits. Replacive tourmaline of yellow-brown colour was observed at all localities, generally replacing feldspar by the growth of skeletal networks which gradually became infilled. Two major conclusions may thus be drawn. Firstly, it is not possible to distinguish primary, magmatic tourmalines from secondary, hydrothermal tourmalines on the basis of colour. Secondly, it appears that much of the tourmaline in 'unaltered' granites, which has hitherto been regarded as primary, may in fact be secondary (although it may have formed at an early stage, perhaps even at the assimilation stage). The view that yellow-brown tourmaline is the product of early-stage replacement is not a new one. Bonney (1877) attributed yellow-brown tourmaline to early biotite replacement; however, the present work shows that feldspar replacement is a more common mode of origin for this type of tourmaline. In the examples described in this chapter, both feldspar and biotite were replaced by both blue and brown tourmaline. It thus appears that the colour of tourmaline is a poor guide, not only to its mode of origin, but also to the identity of the minerals which it may have replaced.

A further conclusion is that the presence of tourmaline of different colours, or with successive coloured zones, does not necessarily imply several separate stages of tourmaline precipitation. Two lines of evidence support this contention. Firstly, the replacement sequence of the Venford biotite illustrates how the initial replacement products may be

polycrystalline tourmaline aggregates, and these recrystallise to form large, multiple-zoned crystals. Secondly, it appears that several modes of replacement may arise from a single tourmalinisation event: for example, the Cape Cornwall tourmalinite contains tourmalines in which brown and blue zones have accreted by the same mechanism, and apparently interchangably. It seems more likely that the alternation of colour zones in this case is due to changes in conditions during one period of tourmalinisation, rather than due to a series of events. The very common occurrence of brown centres and blue rims in the Cornubian tourmalines may represent an inherent evolutionary trend in the composition or nature of the tourmalinising fluid with time.

From the close similarities between chloritised and tourmalinised veins at Luxulyan, and the occurrence of both alteration processes in the same veins, it appears that chloritisation and tourmalinisation are essentially the same process. The relative dominance of either process must be governed by geochemical criteria such as the availability of boron, and this will be discussed further in the geochemistry chapter. Where tourmalinisation is more intense (e.g. at Goonbarrow), it may be associated with cassiterite and topaz, which represent a higher temperature assemblage. The range of mineralogical associations examined in this chapter, indicates that tourmalinisation spans a complete spectrum from the relatively low temperature chlorite/sulphide mineralisation to the higher temperature tin mineralisation, and that a rough correlation exists between the associated mineral assemblages and the intensity of tourmalinisation.

Tourmalinites have previously been interpreted by two opposing genetic theories. The view that such rocks represent products of near-total tourmalinisation of granite dates back at least to Ussher et al. (1909), and has been widely upheld since that time. Conversely, a popular concept in latter years has been that extreme magmatic differentiation

could produce quartz-tourmaline rocks. There is little doubt that tourmaline-forming fluids or 'magmas' can be differentiated and mobilised to produce tourmaline-rich pegmatites and thin, discordant quartz-tourmaline veins. However, the absence of well exposed contacts between large tourmalinite bodies and their host rocks (e.g. at Roche Rock and Hemerdon), and the lack of unequivocal replacement textures within such bodies, has made their origin difficult to prove.

Power (1968) drew geochemical distinctions between magmatic and hydrothermal tourmalines from southwest England, and concluded that the Roche Rock tourmalinite samples lay within the magmatic field. The 'magmatic' tourmalines used by Power (1968) included yellow-brown tourmaline from 'unaltered' granite; it has been shown in the present work that such tourmalines may well be replacive, and thus the geochemical evidence is not entirely conclusive.

Charoy (1979a) favoured a magmatic origin for the Cape Cornwall tourmalinite; in support of this view, he brought the experimental results of Pichavant (1979), who showed that high concentrations of boron could lower the granitic solidus, and thus increase the possibility of differentiation. However, previous experimental petrologists have only achieved tourmaline synthesis by 'hydrothermal' reactions, and not by crystallising a melt. Neither did Pichavant (1979) synthesise tourmaline from his boron-rich magmatic systems; furthermore, he used very high boron concentrations (up to 15 wt.% B_2O_3) unlikely to be encountered in natural magmas.

Charoy (1979a) also reported 'magmatic' fluid inclusion temperatures from the Cape Cornwall tourmalinite. Calculation of these temperatures involved a pressure correction based on K:Na ratios; the established methods of calculation leave room for considerable refinement (Roedder and Bodnar, 1980). A very small pressure adjustment would bring Charoy's data within the temperature range of cassiterite mineralisation, with which

the tourmalinite is in fact associated.

Field evidence and petrographic observations of transitional material, examined in the present study, show that the Cape Cornwall tourmalinite could represent the uppermost horizon of an ascending sequence of progressive tourmalinisation, ponded up against an impenetrable roof. A similar sequence is seen in the Bosworgey borehole(Ball and Basham, 1981). There is no petrographic evidence for a magmatic origin, and the arguments in favour of a magmatic origin are tenuous.

2.7 Conclusions

Tourmalinisation can produce vertical replacement veins, or horizontal replacement sheets, by hydrothermal alteration of granites. Alteration is commonly accompanied by reddening of alkali feldspars, and the formation of muscovite (or hydromuscovite). Biotite and feldspar are replaced by brown and/or blue tourmaline. Tourmalinisation covers a wide spectrum of mineral associations, from low temperature chlorite/sulphide to high temperature tin mineralisation. Chloritisation and tourmalinisation have interchangable roles.

It is not possible to distinguish primary from secondary, or magmatic from hydrothermal tourmaline on the basis of colour; neither is colour a reliable guide to the identity of replaced minerals. Multiphase tourmalines do not necessarily result from several successive tourmalinisation episodes. Much of the yellow-brown tourmaline in the Cornubian granites may be replacive after feldspar, and not primary and magmatic as was supposed.

The Cape Cornwall tourmalinite is more likely to be the uppermost horizon of an ascending progressive tourmalinisation sequence, than a product of magmatic differentiation. This may apply to other large tourmalinite bodies such as Roche Rock and Hemerdon, but does not preclude differentiation being an important process in the formation of tourmaline pegmatites and veins.

3. Analytical techniques

This chapter will be divided into two main sections, of which the first will deal with general analytical procedures, and the second will concentrate upon the techniques employed for boron determination. Except where otherwise stated, the analytical work was conducted at the Department of Mineralogy, in the British Museum (Natural History).

3.1 General analytical procedures

3.1.1 X-ray fluorescence spectrometry

One gram of each rock powder was fused with four grams of lithium metaborate flux to form two glass discs about 2.5 cm in diameter. To counteract the possible effects of water absorption by the flux, its weight lost on ignition was determined, and a commensurate weight added to each fusion. The discs were left overnight to anneal before analysis. The apparatus used for the analyses comprised a Philips PW 1540 spectrometer, a PW 1100 X-ray generator, and PW 300 series counting equipment. SiO_2, Al_2O_3 and K_2O were determined using a PE 002 crystal; CaO, TiO_2, MnO and total iron as Fe_2O_3 required a LiF 200 crystal. A Ge 111 crystal was used for P_2O_5, and RbAP for MgO. Standardisation was based upon international whole rock standards; these were not ideal, since tourmalinisation produces rather unusual chemical compositions not normally encountered in igneous and metamorphic rocks. However, it was normally possible to select standards containing approximately the correct concentrations of iron and aluminium, the proportions of which are responsible for the most significant matrix effects, and also to include the standard southwest England granite prepared by the Institute of Geological Sciences (BM(NH) standard no. S. 92). The trace elements Zr, Nb and Y were also determined by XRF in a restricted number of samples; standardisation was achieved by using one international standard rock (JG-1) doped with known concentrations of these trace elements.

Preparation for XRF allows homogenisation of rock powder without the need to dissolve the constituents: this is particularly advantageous in the case of tourmalinised rocks, which do not readily dissolve in solvents normally used for silicates (e.g. hydrofluoric acid). However, the use of lithium metaborate flux obviously precludes the determination of Li and B in the fused discs. The technique does not in any case respond well to the lighter elements, of which Na and F are also important. Hence only a partial major element analysis (Si, Ti, Al, Fe, Mn, Mg, Ca, K, P), may be obtained for tourmalinised rocks by this method.

3.1.2 Atomic absorption spectrometry

To 0.2 gram of each rock powder was added 5 ml of hydrofluoric acid, and according to the method of Langmyhr and Paus (1968), this was neutralised with 4% (w/v) boric acid solution, when dissolution of the sample was complete. Unfortunately, even after several hours in HF over the steambath, a black residue remained undissolved. Since the quantity of residue was approximately proportional to the concentration of tourmaline in each rock, though insufficient to represent the total tourmaline content, it was presumed that the tourmaline had partially dissolved, leaving an insoluble fraction. This may have been because tourmaline of several different compositions was present in each sample, particularly those which contained tourmalines with complex zoning. The residues were filtered from the neutralised solutions, the filter papers ignited, and the incombustible products fused in a 1:3 mixture of potassium carbonate and boric acid. The fusions were dissolved in a few ml of concentrated nitric acid and added to the original solutions, which were then made up to volume. Na_2O, and the trace elements Li, Rb Sr, Cu, Zn, Pb, Ba and Be were determined using a Perkin Elmer^R 403 Atomic Absorption Spectrophotometer. For sodium, international whole rock standards were used, while synthetic standards were used for trace

elements. Separated tourmalines were also analysed for trace elements by this method, and since the somewhat larger insoluble residues required greater quantities of flux for fusion, a series of appropriate standards (based upon existing synthetic standards) was specially made up for this purpose.

Although atomic absorption is a simple and convenient method for most silicate rocks, tourmalinised materials are not ideally suited to it because of the difficulties in dissolving the samples. Furthermore, boron could be determined neither by the atomic absorption equipment available, nor by an alternative method from the same solutions, since boric acid is one of the major reagents used.

3.1.3 Pyrohydrolysis for fluorine

Fluorine was determined in whole rocks and separated tourmalines by a method based on the technique of Clements et al., 1971). One gram of sample (0.5 gram, in the case of tourmaline) was thoroughly mixed, in a silica boat, with one gram of a flux containing bismuth trioxide, sodium tungstate and vanadium pentoxide in the proportions 1:1:2. The boat was placed in a fused silica tube, which instead of being heated by burners, was housed in an electric furnace according to the method of Berns and van der Zwaan (1972), and heated to 900°C. Water vapour was supplied not from a nickel boat within the tube, but from an external flask of boiling distilled water, through which was bubbled O_2-free nitrogen. The first 75 ml of the condensate was collected into an alkaline solution, which was buffered using 10 ml of sodium acetate and acetic acid (3:1),,and made up to 100 ml. Fluorine was determined by means of an ion-specific electrode, using synthetic standards.

3.1.4 C,H,N elemental analysis

The method used was that described by Din and Jones (1978). 25 mg of dried sample and 100 ($\pm$ 5) mg of flux comprising PbO, $PbCrO_4$ and CuO (10:1:1) were weighed into an expendable nickel boat, which had previously been cleaned by running through a standard analytical cycle. The loaded boat was then inserted into the Perkin-Elmer^R 240 elemental analyser by means of a quartz ladle. Phenacetin and a standard epidote (BM(NH) no. S 221) were used as standards. This is a simple, rapid and precise method of determining total hydrogen and total carbon, the very small sample size being the only major source of error.

3.1.5 Electron probe microanalysis

Polished thin sections for microprobe work were prepared from the same samples as used for whole rock analysis, and these were coated with a carbon layer approximately 150 to 200 Å thick. Electron microprobe facilities at the British Museum (Natural History) have undergone major changes during the past few years, and for this reason, the present work has involved the use of no less than four separate instruments. In the early stages of the work, a Cambridge Instruments Geoscan two-spectrometer wavelength dispersive microprobe was used. This allowed determination of only two elements simultaneously (using the method outlined by Sweatman and Long, 1969), and required manual data processing for Z.A.F. (atomic number, absorption, fluorescence) correction by the program of Mason et al., (1969). This instrument was later modified with a lithium-drifted silicon detector and Link Systems 860 multichannel analyser. The machine now operates on an energy-dispersive basis, displaying a full spectrum of elements present, and programmed to give fully corrected, fourteen element silicate analyses; cobalt is used as a base standard. This system, which was used in the later stages

of the work, was more efficient in terms of time spent on each analysis. Since it eliminates the need to return several times to the same point within a crystal, the new system also allows more reliable analysis of heterogeneous, partially altered mineral grains. In particular, the facility for simultaneous Na, K and Ca determination made possible the estimation of composition in altered feldspars which had previously given ambiguous and misleading results.

While modifications were in progress at the British Museum (Natural History), a similar energy-dispersive, Link-adapted instrument, based on the Cambridge Instruments Microscan 5 model, was used at Imperial College; this machine provided the analyses for the appended 'Quartz-cored tourmaline' paper (Lister, 1979a). Finally, the British Museum (Natural History) has now installed a new Cambridge Instruments Microscan 9, which is a wavelength-dispersive but fully computer-controlled microprobe, programmed to provide full Z.A.F. correction. Part of this system is based on the Cambridge Instruments Scanning Electron Microscope model 180, which affords high resolution imaging (e.g.Chapter 5, Plate 5:2). This instrument has all the advantages of the energy-dispersive Geoscan, with many additional features, among them the better analytical precision possible with a wavelength-dispersive system, and the facility for performing step-scans across mineral grains and grain boundaries. Opportunities for the use of this instrument in the present work were limited, but the results in Table 5:7 (Chapter 5) were thus obtained.

Tourmaline, feldspar, biotite, chlorite, muscovite and opaque minerals in samples described petrographically (Chapter 2) were analysed by microprobe. The elements determined were Si, Al, Fe, Mg, Ti, Mn, Ca, Na, K, and in some grains, also P, Cl and Sn. The electron microprobe does not respond well to low atomic number elements, and although boron determination is possible (Reed, 1975), it would have required special operating

conditions which preclude normal silicate analysis, and this was not considered feasible. Hence boron, and also fluorine and hydroxyl, were omitted from microprobe analyses, and the totals for tourmaline of around 85-86% were supplemented by figures obtained by analysis of bulk samples. Mica analyses were totalled by adding theoretical hydroxyl percentages from Deer et al. (1962).

3.2 Boron determination

In addition to its obvious importance in the investigation of tourmaline and tourmalinised rocks, boron warrants detailed examination because of the difficulties involved in its determination. Since boron is not determinable by the techniques generally used for routine silicate analysis (such as XRF and atomic absorption), alternative methods must be sought; many such methods require the sample in solution, for which the inherent problems relating to tourmaline were discussed above. Some of the methods by which boron may be determined are listed in Table 3:1, and described below. This chapter also includes a section devoted to the neutron capture method which was established as part of the present research programme.

3.2.1 Conventional chemical techniques

3.2.1.1 Spectrophotometry

Bawden (1959) reviewed the various methods available at that time for boron determination in silicate rocks and minerals, and concluded that the most suitable was a colorimetric technique using carminic acid. This method involves a sodium carbonate fusion of the sample, which is then dissolved, and following treatment in an ion-exchange column, the colour complex is developed by carmine in concentrated sulphuric acid. A modification published by Shelton and Reed (1976) omits the ion-exchange procedure,

Technique	Sample preparation	Reported sensitivity & precision	Suitability for tourmaline
Spectrophotometry			Requires solution, and gives poor accuracy; time-consuming
Carminic acid	Solution	0-0.3% B_2O_3 ± 0.002% (Shelton & Reed, 1976)	
Curcumin	Solution	not quoted	
Volumetric analysis	Solution	9-10% B_2O_3 ± 0.08% (Povondra & Čech, 1976)	Requires solution; time-consuming
Flame photometry	Solution	Sensitive to 0.02 g B ± 3.9% (Chapman & Dale, 1977)	Requires solution
Pyrohydrolysis	Powder	2-15% B_2O_3 (Williams et al.,1959) 0.002- 96% B (Morgan, 1964) precision not quoted	Potentially suitable
Plasma emission spectrometry	Solution	Sensitivity for B not yet certain Precision ± 1.5% (present work)	Suitable but needs solution
Laser-induced plasma	Polished thick section or grain mount	Not yet certain	Potentially suitable
Ion microprobe	Polished surface	Not yet certain	Potentially suitable
Nuclear microprobe	Polished surface	Not yet certain	Potentially suitable
Particle track analysis	Polished surface	Not yet certain, but can detect one atom (in theory)	Suitable if problems with lithium tracks were solved
Activation analysis	Powder	With U.L.R.C. neutron capture prompt gamma spec. equipment, 0.1 to 12.53% B_2O_3 ± 2.8% (present work)	Suitable, especially if precision at low B concs. were improved

Table 3:1. Methods for boron determination in rocks and minerals

- destructive techniques - - non-destructive -
- need specialised equipment -

but requires correction for titanium, the main interfering ion; this technique was employed to analyse one batch of samples which had also been analysed for boron using neutron capture (results are shown in Fig. 3:10. This method could probably have been made to yield acceptable results for tourmalinised rocks, but by comparison with the neutron capture method, is unduly time-consuming and cumbersome.

A further colorimetric method, based on curcumin, modified by Grinstead and Snider (1967) has been used for geological applications (e.g. by Hall, 1971). The technique investigated in the present work was based on that of the Laboratory of the Government Chemist, and requires a potassium carbonate fusion which is then dissolved in hydrochloric and glacial acetic acids. The boron complex developed with curcumin reagent is extracted in acetic anhydride and amyl alcohol. As this method did not yield repeatable results, it was abandoned in favour of other methods.

3.2.1.2 Volumetric analysis

Povondra and Čech (1976) reported a method specifically developed for tourmaline analysis. This involves the separation of boric acid from other components by ion exchange after fusion of the sample, and determination of boron by titration in the presence of mannitol (Schulek and Vastagh, 1931; 1932). Attempts were made in the early stages of the present work to use the volumetric determination of the mannito-boric complex as a basis for boron analysis. Since this would have required much repetition and modification before it could have been made to give reliable results on a routine basis, it was not used for quantitative work.

3.2.1.3 Pyrohydrolysis

Boron determination by pyrohydrolysis is described by Williams et al.(1959) and Morgan (1964). This was not attempted in the present

study, because the required equipment for heating the sample to about 1400°C was not available.

3.2.1.4 Flame spectrometry

This technique, described by Chapman and Dale (1977) was likewise not attempted.

3.2.2 Instrumental techniques

3.2.2.1 Inductively coupled plasma emission spectrometry (ICP)

This relatively new technique is based on a similar principle to that of atomic absorption spectrometry, but sprays the sample solution into an argon plasma which is heated to about 6000°K. The equipment was not available in London until the later stages of the present work, when it was possible to make comparative determinations of boron in some samples already analysed by the neutron capture method.

The Philips PV 8490 ICP Source Specrtometer in the Geology Department of King's College, London, was used for this part of the work. The performance of the instrument is described by Walsh and Howie (1980), who reported precisions better than 1-2% for major and fifteen trace elements in silicate materials. Boron had not previously been included in the analyses, but boron determination by ICP is described by Greenfield et al. (1976).

0.5 gram of each rock powder was fused with 2 grams of sodium carbonate (instead of the lithium metaborate flux normally used in routine major element analysis), and the fusions were leached in water. Four standards were used, namely N.B.S. borosilicate glass no. 92 (BM(NH) no. S.114), I.G.S. standard southwest England granite (BM(NH) no. S.92), King's College standard andesite KC10, and the same KC10 doped with a known amount of boron.

When sample preparation is complete, the ICP takes only about two minutes to produce each 31 element analysis. Boron was, however, the only element of interest, since the use of sodium carbonate invalidated existing standard solutions for other elements.

The boron calibration curve obtained is shown in Fig. 3:9. Precision is calculated to be $\pm$ 1.5%. Results for seven tourmalinised rock samples are compared with those obtained by the neutron capture method in Fig. 3:8.

The ICP is potentially a useful and relatively rapid method for determining boron in tourmalines and tourmalinised rocks, but more work is needed on standardisation before it can be used on a routine basis.

3.2.2.2 Laser induced plasma emission spectrometry

A Zeiss LMA 10 Laser Microspectral Analyser designed for use with the ICP was supplied by the manufacturers, for a trial period of one month only, to the Applied Geochemistry section in the Geology Department of Imperial College. Boron and lithium determination was attempted in a few tourmaline grains. A polished thick section or grain mount, when bombarded with the laser, emits particles which are carried into the ICP, and analysed to give a thirty element determination in a matter of minutes (manual data processing was necessary, but this could be automated). Whole rock or mineral powders, in the form of either fused or pressed discs, can also be analysed by this method, and in fact the latter were used as standards during the trial. The method is semi-destructive, since the laser produces a small crater (from about 100 μm to 1 mm in diameter and depth, depending on the matrix) in the sample; this can be useful in plotting the positions of points analysed, but the use of polished microprobe sections is precluded by the crater depth. The experiment with tourmaline grains showed that there is good potential for determining boron and lithium

quantitatively. The method would have considerable advantages over alternatives, since it incorporates the speed and precision of the plasma, and also eliminates the need to dissolve samples.

3.2.2.3 Ion microprobe

The instrument at the Department of Earth Sciences, Cambridge, has been used for a study of lithium (Wilson, 1980), and with appropriate standardisation to minimise matrix effects, boron could also be determined (J.V.P. Long and G.C.Wilson, pers. comm., 1979). Oxygen is used as an ion source, but alternatively argon could fill this role. The ion microprobe is ideally suited to the determination of low atomic number elements, and may also determine individual isotopes; it utilises polished thin sections as prepared for electron microprobe analysis, and has the advantage of allowing optical viewing of the sample in transmitted light. It could provide a supplement to electron microprobe work, and ultimately, complete analyses of individual mineral grains.

3.2.3 Radiometric techniques

3.2.3.1 Nuclear microprobe

Described by Olivier et al. (1976), this instrument has been used for the examination of boron isotope distributions in irradiated neutron absorber materials. It is not envisaged at present as a quantitative method for use in mineralogy, but could be developed as such. It would have similar advantages to the ion microprobe and laser induced plasma, but would require equipment not available to most University departments.

3.2.3.2 Particle track analysis

This is theoretically a feasible proposition for boron determination, allowing detection limits of only a few ppm. A polished surface of the

mineral is irradiated in contact with a plastic film, in which alpha tracks from the reaction $^{10}B\ (n,\alpha)^{7}Li$ are later etched and examined microscopically. A major difficulty arises in distinguishing tracks produced by the boron (n,α) reaction from those produced by the lithium reaction (Fleischer et al., 1975); this is particularly important where the minerals of interest may contain both boron and lithium, as in the present study.

3.2.3.3 Activation analysis

Methods recently utilised for boron determination include proton activation (Delmas et al., 1976, concluded that this was better for boron than neutron activation), deuteron activation (Pretorius et al., 1972), neutron absorption (de Jesus and van der Berg, 1978), and neutron capture prompt gamma spectrometry (Gladney et al., 1976; Henkelmann et al., 1976; Kerr et al., 1980). Activation methods have the advantage of providing non-destructive analysis, either of whole rocks or of single minerals. Time spent on sample preparation is usually minimal, since neither dissolution nor polishing is required.

Individual investigations in this field have, by necessity, been concerned with the application of existing systems to boron determination. The present work was likewise influenced by the particular reactor facilities available; the apparatus which had been set up at the University of London Reactor Centre by Dr. T.D. MacMahon, made possible the following study based on neutron capture prompt gamma ray spectrometry.

3.3 Neutron capture prompt gamma spectrometry

3.3.1 Introduction

This technique involved simultaneous irradiation of the sample by thermal neutrons, and measurement of the gamma radiation emitted. Nuclear states excited by neutron capture produce gamma rays with energies ranging from about 50 keV to 10 MeV, and half-lives in the order of 10^{-14} to 10^{-12} seconds (Henkelmann and Born, 1973). The sensitivity of a given nuclide depends, according to Duffey et al. (1970) upon the absorption cross section, the atomic mass, and the intensity of gamma radiation emitted (expressed as photons per 100 neutrons captured). Table 3:2 shows the gamma ray energies and sensitivities of the most prominent peaks for some elements important in silicate analysis. Most of these elements are more sensitive in the low energy range ($<$ 3 MeV). Sensitivities vary over several orders of magnitude, which means that the method is more suited to some elements than others. Good sensitivity alone does not necessarily make a given peak usable for analytical purposes, since the spectral contrast (i.e. the relative intensity of a line to that of adjacent lines) is also important; hence, although most elements produce complicated spectra with several gamma peaks, there may be only one peak which is usable for analysis. Boron is particularly suited to this analytical method, because it shows unusually high sensitivity (due to the exceptionally high neutron-capture cross-section of 3837 barns for ^{10}B). There is also comparatively good spectral contrast on the 0.478 MeV peak, the only possible interference being from the sodium peak at 0.472 MeV. Boron determination is based on the reaction $^{10}B\ (n, \gamma\ \alpha)\ ^{7}Li$, and since this requires a relatively low neutron flux, a neutron beam external to the reactor may be used as a source.

Element	Low energy range (< 3MeV)		High energy range (> 3MeV)	
	Energy (MeV)	Sensitivity ($I\sigma/A$)*	Energy (MeV)	Sensitivity ($I\sigma/A$)*
Li	2.033	0.140	-	-
B	0.478	3269.0	-	-
F	0.596	0.047	-	-
Na	0.472	1.61	6.395	0.592
Mg	2.828	0.925	3.916	0.10
Al	0.249	0.065	7.724	0.175
Si	2.093	0.153	3.539	0.453
P	2.154	0.103	3.900	0.1078
S	0.841	0.867	5.420	0.678
Cl	1.951	20.0	6.111	14.8
K	0.771	1.68	5.380	0.393
Ca	1.943	0.563	6.420	0.301
Ti	1.381	8.33	6.760	6.87
Cr	0.835	1.43	8.884	1.44
Mn	0.213	1.46	7.244	2.92
Fe	0.353	0.509	7.646 7.632	1.04 1.27
Rb	0.557	0.11	(7.624	0.016)
Sr	1.836	1.26	6.267	0.0769
Zr	0.935	0.079	6.295	0.0321

* where I = peak intensity, σ = absorption cross section, A = atomic mass

Table 3:2. Neutron-capture, gamma-ray energies and maximum sensitivities of important elements in silicate analysis. (Sensitivity quoted is that of the most prominent peak for each element, taken from Duffey et al., 1970, and Senftle et al., 1971)

3.3.2 Previous work

The determination of prompt gamma ray energies was originally undertaken for application in nuclear physics (Groschev et al., 1959). Isenhour and Morrison (1966a) developed the technique of neutron capture gamma ray measurement for quantitative analysis, by incorporating a system which removed interfering radiations; with apparatus including a 'neutron chopper', NaI detector and multichannel analyser, they were able (1966b) to measure known concentrations of boron in mixtures of boron and samarium oxide.

Garbrah and Whitley (1967a,b) further developed this method, and determined boron in several previously analysed samples of steel (1967a) and glass (1967b), for which latter material they reported a precision better than ± 1%. Henkelmann et al. (1976) reported boron determinations in standard glasses based on a similar concept, but using a ^{241}Am-Be neutron source, with analytical error less than 2.5% and a detection limit of about 10 ppm B.

Whitley et al. (1971) used neutron capture gamma ray analysis for determining boron in granitic rocks and peralkaline lavas. They reported similar performance from both NaI and Ge(Li) detectors, quoting accuracy of ± 5% at the 100 ppm level, but only ± 50% at the 10 ppm level. Results compare favourably with those obtained from the same samples by spectrophotometric methods.

Gladney et al. (1976) modified the technique by using a Ge(Li) detector surrounded by a NaI annulus; the peak to background ratio was improved by this means. From analyses of several standard reference materials including glass, steel and rock, they obtained overall, a precision of ±7%; the practical detection limit was found to be 0.5 μg B in most cases. Standardisation was achieved by two independent methods, the first involving the use of evaporated standard solutions, and the

second relying upon comparison with gamma rays from other elements of which known quantities were irradiated at the same time. Sodium interferences were noted, and a correction applied.

Kerr et al. (1980) have now applied a similar method to boron determination in sedimentary rocks. Using standards 'spiked' with known boron concentrations, they successfully determined boron in the range 10 to 350 ppm, in previously analysed shales.

The necessary apparatus for neutron capture prompt gamma spectrometry had been set up by Dr. T.D. MacMahon at the University of London Reactor Centre. This equipment had been used for qualitative studies of gamma spectra (Campbell, 1977; Thein, 1977; Massoumi, 1979), but not hitherto for quantitative analysis. The present investigation, conducted between 1977 and 1980, was designed to evaluate the possibility of using or modifying the existing apparatus for quantitative boron determination in rocks and minerals, and to establish a suitable routine method.

3.3.3 Apparatus

The (n, γ) apparatus at the University of London Reactor Centre (Fig. 3:1) is situated at the 0° through-tube of the CONSORT II Reactor (Burholt, 1977; Burholt and MacMahon, 1979), and utilises an external target geometry. The thermal neutron flux at the scattering block is approximately 1.5×10^{11} n/cm^2/sec., with a Westcott r factor of about 0.03 and a fast neutron flux of 1.0×10^{10} n/cm^2/sec. The diameter of the neutron beam may be reduced either to 2.5 cm or 1.25 cm at the shutter position, by means of a conical collimator.

The thermal neutron flux at the target position is approximately 2×10^6 n/cm^2/sec., with a thermal to epithermal ratio of 460. The target position is viewed by two lithium-drifted germanium (Ge(Li)) detectors, one vertically below the target, and the other to one side. The latter

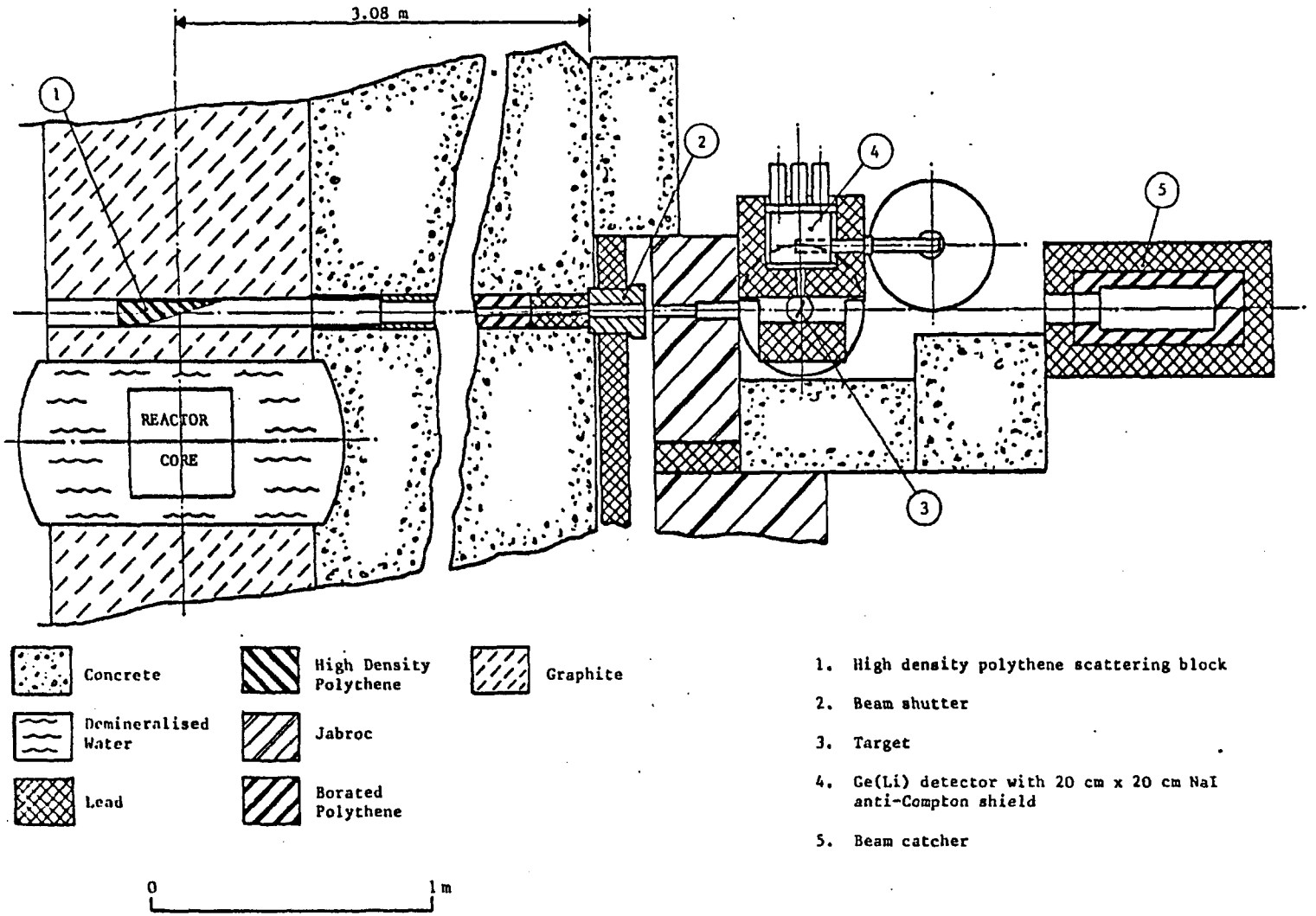

1. High density polythene scattering block
2. Beam shutter
3. Target
4. Ge(Li) detector with 20 cm x 20 cm NaI anti-Compton shield
5. Beam catcher

Fig. 3:1 Layout of (n,γ) apparatus at U.L.R.C.

(unpublished diagram drawn by Dr. T.D. MacMahon of U.L.R.C.)

detector is surrounded by a 20 x 20 cm sodium iodide anti-Compton shield; this Compton-suppression system improved the peak to background ratio, but introduces interferences that are unacceptable in certain types of study. The detectors each have a resolution of 2.1 keV (FWHM at 1.33 MeV) and efficiencies of 12%.

Signals are transmitted via a pre-amplifier, amplifier and analog digital converter to a multichannel analyser, which displays and prints the resulting spectra.

3.3.4 Method

3.3.4.1 Initial experiments

3.3.4.1.1 Self-shielding and sample geometry

The initial investigations were made using solid samples of standard materials and single crystals of tourmaline. Since calibration based on sample weight was not linear, it was suspected that differences in sample geometry might affect count rates. Boron is an effective neutron absorber, and this property results in a 'self-shielding' effect. It seemed that this effect varied according to the sample geometry, and in particular the thickness of sample through which the neutron beam had to pass. A simple experiment served to confirm that the geometry, thickness and orientation of the sample with respect to the beam were important factors. An N.B.S. (610) standard glass disc containing 500 ppm B, 3 mm thick and about 15 mm in diameter, was irradiated in positions at different angles to the neutron beam (Fig. 3:2). The highest count rate was recorded when the flat surface of the disc was at right angles to the beam. Positioning of the sample with its flat surface parallel to the beam resulted in only a 6.78% loss of counts, in spite of a 60% reduction in area exposed to the beam. It is not certain to what extent this discrepancy is due to differences in the degree of self-shielding, but any such effect was avoided by keeping subsequent samples to a constant geometry, and maintaining a constant orientation

(Neutron beam at 90° to plane of paper)

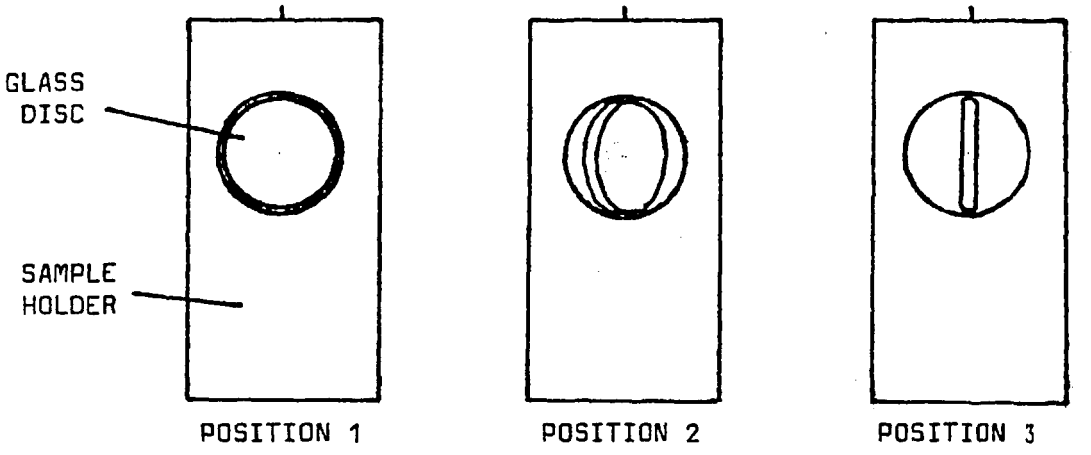

	POSITION 1	POSITION 2	POSITION 3
Total counts in 2000 secs.	32301	31276	30111
% count loss compared with position 1		3.17%	6.78%

Fig. 3:2 Relationship between sample geometry and count rate

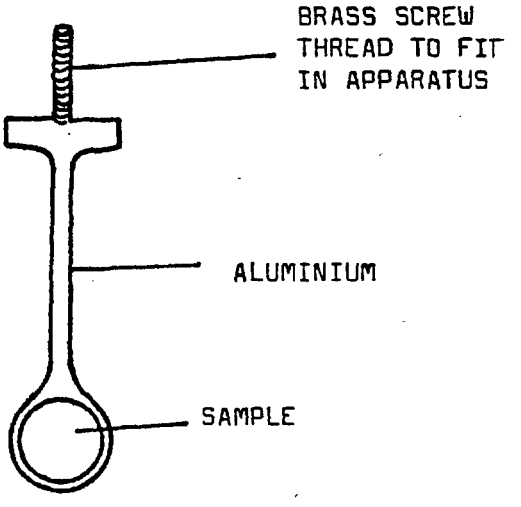

Fig. 3:3 Aluminium sample holder (actual size)

with respect to the neutron beam. Garbrah and Whitley (1967b) found that self-shielding increased with boron concentration, and overcame the problem by diluting all samples to fall within a limited boron concentration range. This practice was not attempted in the present study, since calibration was found to be linear over the total range investigated, when a constant sample size was used. Henkelmann et al. (1976) stated that between 0 and 56 weight % B_2O_3, self-absorption was not an important factor; this statement may, however, be questioned.

For quantitative boron determination, powdered samples were pressed into an aluminium holder, 10 mm in diameter and 1 mm in thickness (Fig. 3:3); the use of powdered samples also permitted the mixing of materials to produce synthetic standards. Aluminium was selected as the most suitable material for use as a sample holder, since unlike other readily available materials such as plastics and paper (which were also tried), it could be shown to contain neither traces of boron nor other interfering elements (such as sodium).

The first powdered samples and standards were made up to a constant volume, and the results corrected for weight, on the supposition that by completely filling the holder, any differences in self-shielding would be minimised. However, this only served to amplify the problem, since in the present study, the most boron-rich samples were also the most dense, and therefore required more material to fill the same volume. Subsequent samples and standards were made up to a constant weight of 37 mg, this being a quantity which would fit into the standard sized sample holder for the entire range of densities involved.

3.3.4.1.2 Sodium interference

The 0.478 MeV gamma ray from boron is symmetrically broadened by ± 7.6 keV (Neuwirth et al., 1975), due to a Doppler effect resulting

from de-excitation of the ^{7}Li nucleus. Interference from sodium was apparent in most spectra, particularly those representing low boron concentrations, and this was difficult to quantify, since the Na peak at 0.472 MeV overlaps the boron region at a position where counts tend to be highest. Samples high in sodium ($\geq\sim$10% Na_2O) increased this problem, but blank runs showed that the major interference arose from the annular sodium iodide crystal. This had not previously caused any difficulty, since other workers had been interested only in high energy gamma rays. Attempts were made to avoid this effect by lining the beam tube with a cadmium shield, which should have prevented scattered neutrons from entering the sodium iodide; interference continued, but the cadmium was left in place for future work. The vertically positioned detector without the Compton-suppression system introduced no such sodium interference, and therefore, in spite of the relatively high background arising from its use, this detector was used exclusively for the main experiments.

3.3.4.1.3 Standardisation

In order to establish a standard working curve, three standard borosilicate glasses were diluted with 'Spec-pure' silica to give twelve standards, covering a compositional range from 0.1% to 12.53% B_2O_3 (310ppm to 3.89% B). Since tourmaline contains about 10% B_2O_3 and an average southwest England granite might be expected to contain about 500 ppm elemental boron, this range was considered suitable for the intended study.

3.3.4.2 Preparation of standards and samples

The following materials were used as standards:

a) National Bureau of Standards borosilicate glass S.R.M. 93a (BM(NH) no. S.115), containing 12.53% B_2O_3.

b) Pilkington's Experimental Glass 77c 155/3, containing 5.5% B_2O_3.

c) N.B.S. standard sample (glass) no. 92 (BM(NH) no. S.114); 0.7% B_2O_3.

d) Institute of Geological Sciences standard granite (BM(NH) no. S.92), with boron determined by several conventional methods at approximately 575 ppm B.

Standards a) and b) were supplied in solid form, and first had to be cut using a Laztech diamond saw, and crushed to powder in an agate pestle and mortar. The other standards were supplied in powder form. The three borosilicate glasses (a, b and c) were used both alone, and diluted with various proportions of 'Spec-pure' silica, with which they were mixed by grinding together in agate. Standard a) yielded concentrations of 12.53%, 10.02% and 7.52% B_2O_3, while standard b) gave 5.5%, 3%, 2% and 1%, and standard c) 0.7%, 0.5%, 0.35%. 0.2% and 0.1% B_2O_3. Standard d) was used undiluted.

All powders were dried for one hour at 110°C before loading, and after cooling, were weighed directly into the aluminium sample holders, and secured by sellotape. All charges weighed 37 mg. The same procedure was employed for the preparation of spec-pure silica blanks, and of rock and mineral samples.

Standards and samples, made up as described, could be kept and irradiated several times over a period of a few weeks without any detrimental effect. However, after much handling, the powders began to settle in the holders, thus altering their geometry, so samples had to be reloaded if further irradiation was necessary.

3.3.4.3 Irradiation and counting

Samples and standards were irradiated in the external neutron beam for 1500 seconds; those containing less than 2% B_2O_3 needed 3000 seconds irradiation time to produce statistically acceptable results. Duplicate standards were measured at least three times in order to construct a calibration curve, and individual standards were remeasured at intervals, to confirm the correct functioning of the equipment and uniformity of the neutron flux.

Gamma rays produced by the $^{10}B\ (n, \gamma\ \alpha)^7Li$ reaction were received by the non-Compton suppressed Ge(Li) detector, which transmitted signals to the multichannel analyser. The 0.478 MeV peak is shown in Figs. 3:4 and 3:5.

3.3.4.4 Data processing

Attempts to process data by means of existing computer programs were unsuccessful because the peak at 0.478 MeV is non-Gaussian, and therefore cannot be fitted mathematically. The results were therefore calculated according to the following formula:

a) Resolution was checked by the relative positions in the spectrum of the main 0.478 MeV peak and other prominent peaks.

b) The same thirty-six channels were integrated for each analysis; the position of these channels was determined by the distance from the annihilation peak at 511 MeV.

c) Background was calculated by averaging counts in ten channels, i.e. five either side of the boron region.

d) Total B_2O_3 counts = sum of 36 channels $-$ $\left(\frac{\text{sum of 10 bgd. channels}}{10} \times 36\right)$

$$\times \frac{1500}{\text{counting time (secs.)}}$$

e) The totals for at least three measurements per sample were averaged.

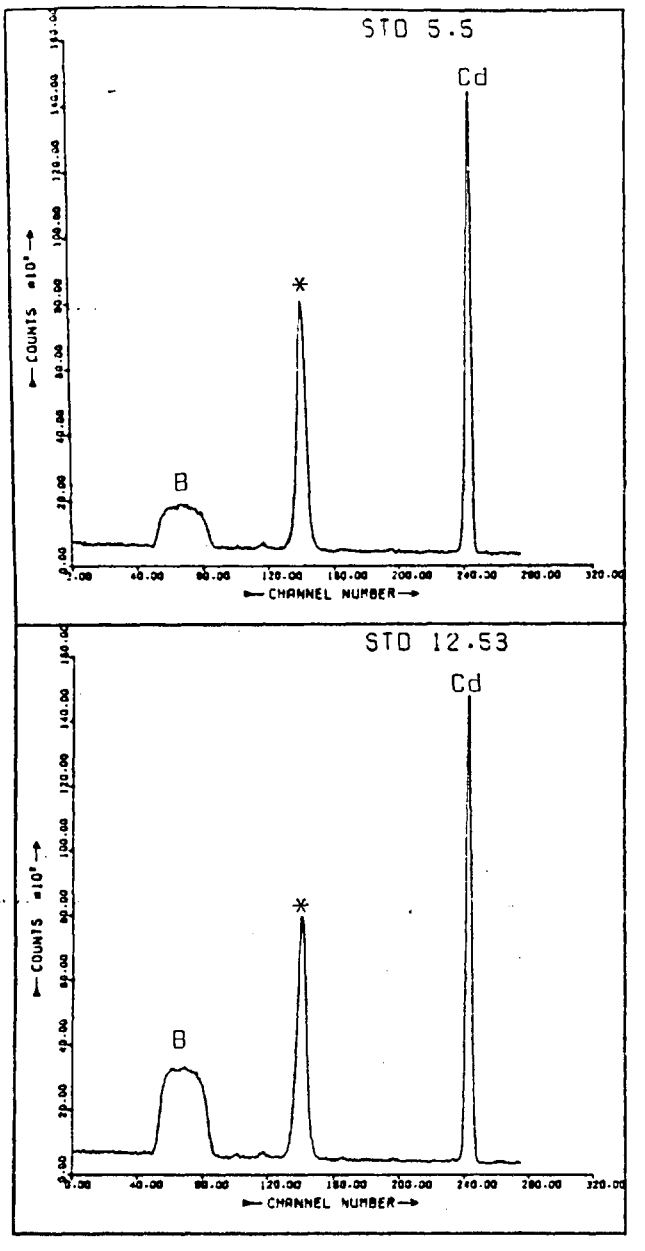

Fig. 3:4 Prompt gamma spectra for two borosilicate glass standards containing 5.5 and 12.53% B_2O_3. The boron 'peak' shows as a broad hump.

* annihilation peak

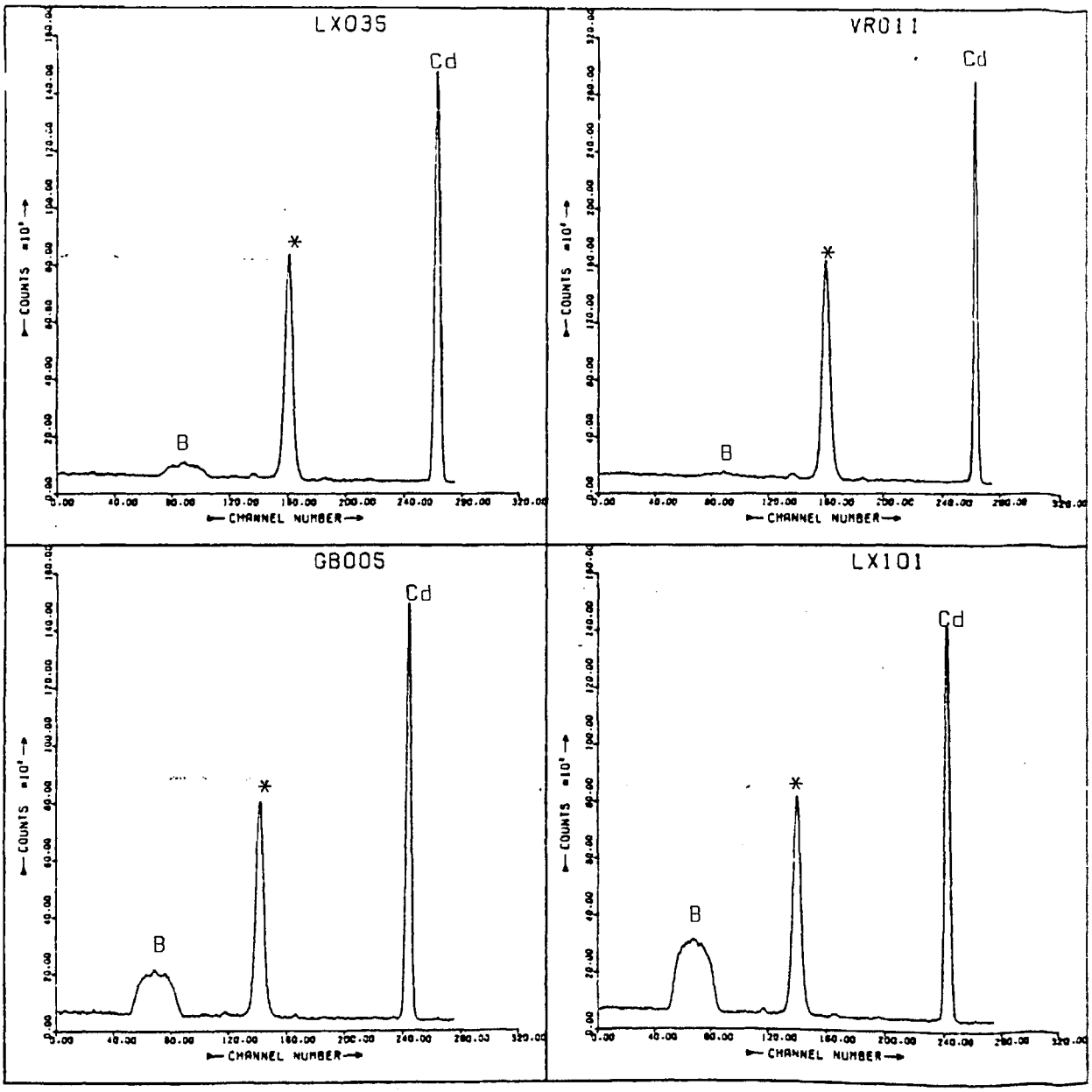

Fig. 3:5 Prompt gamma spectra for three tourmaline-bearing samples (LX035, VR011 and GB005) and one tourmaline (LX101).

* annihilation peak

f) From average count rates (per 1500 seconds) measured using the whole range of standards including the standard granite, a least squares linear regression line was derived. This was used to calculate unknown boron concentrations in samples.

3.3.5 - Results

The counting response and repeatability obtained from duplicate samples of twelve borosilicate glass standards, each measured at least three times, is shown in Table 3:3. The calibration curve for the complete concentration range from 0.1% to 12.53% B_2O_3 may be calculated mathematically as a straight line, and is drawn through the individual standard points in Fig. 3:6. The curve for the lower part of the concentration range (0.1% to 1.0% B_2O_3) is expanded in Fig. 3:7, which also shows the spread of values obtained in single 1500 second counting runs. As this spread is sometimes considerable (up to $\pm$ 6.6%), and certainly unpredictable, the necessity to average at least three results per sample is confirmed.

The boron concentrations measured in whole rock samples and separated tourmalines are included in the analyses given in Chapters 4 and 5 respectively.

3.3.6 Comparison of results obtained by neutron capture and those obtained by other methods

A batch of seven samples (VR001 to VR007), containing between 0.5% and over 3% B_2O_3, was analysed for boron by the neutron capture method and by inductively coupled plasma emission spectrometry (ICP).

Fig. 3:8 shows that the results obtained by ICP are consistently higher than those obtained by neutron capture. It is possible that the self-shielding effect discussed above could depress the boron levels recorded by the latter method; however, since this method involved

NEUTRON CAPTURE PROMPT GAMMA RAY SPECTROMETRY: response to various boron concentrations in specially prepared standard glass powders.

% B_2O_3	0.10	0.20	0.35	0.50	0.70	1.00	2.00	3.00	5.50	7.52	10.02	12.53	
Total counts	1821	2926	4650	5956	9463	13416	13308	19733	35174	49159	61205	76794	
	1678	2830	4507	6175	9241	13366	12853	19974	34628	48333	61031	77803	Sample 1.
	1329	2442	5285	6746	9118	12890	13269	19717	34890	48422	60818	77231	
				5551			12891						
				5749									
Average (3000 s)	1609	2733	4814	6035	9274	13224							
Average (1500 s)	805	1367	2407	3018	4637	6612	13080	19808	34897	48638	61018	77277	
Total counts	1622	3376	4918	6817	8918	13080	13253	19578	36809	49517	62316	78712	
	1944	2862	4422	6697	8709	13012	13084	19821	36822	48947	60711	78231	Sample 2.
	1422	2814	5100	6576	9072	12273	12814	19787	35987	47965	61318	78303	
Average (3000 s)	1663	3017	4813	6697	8900	12788							
Average (1500 s)	831	1509	2407	3348	4450	6394	13050	19729	36539	48810	61448	78415	
Average (1500 s)	818	1438	2407	3183	4544	6503	13065	19769	35718	48724	61233	77846	All results, samples 1 & 2

Table 3:3 **Counting response for boron in standard glass powder preparations, in neutron-capture prompt-gamma spectrometry.**

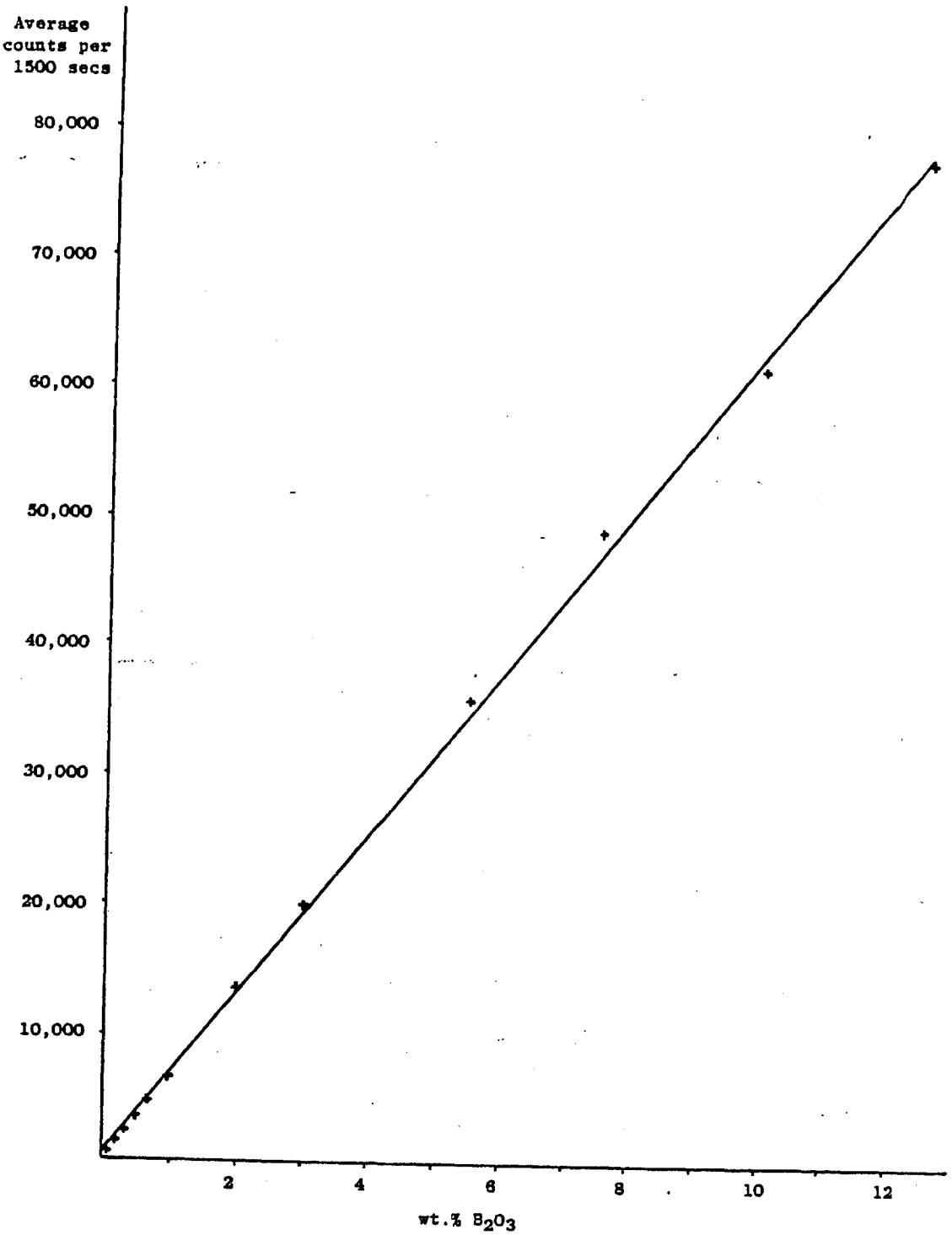

Fig. 3:6 Calibration curve for borosilicate glass standards

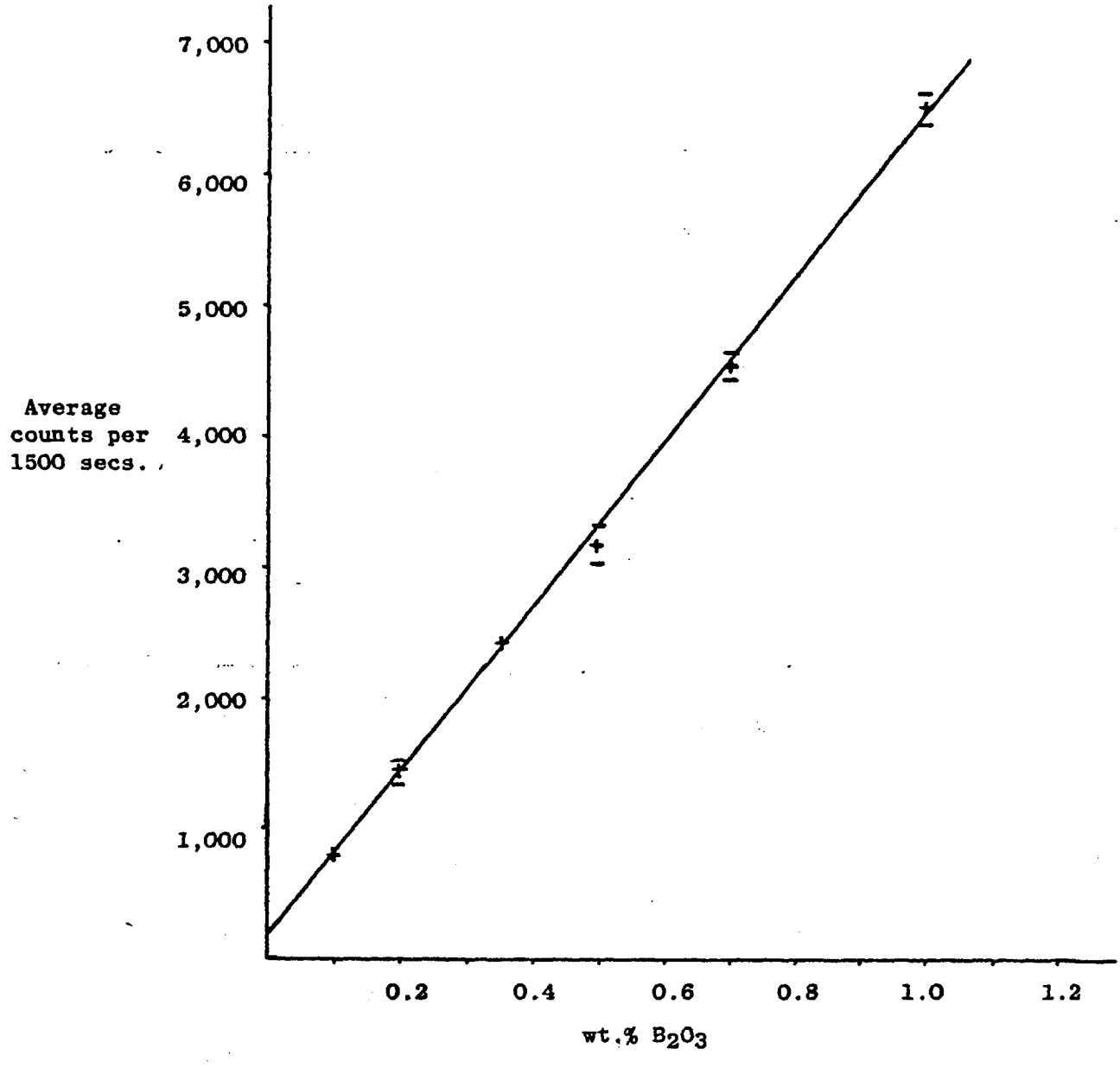

Fig. 3:7 Calibration curve for borosilicate glass standards in the range 0.1 to 1.0% B_2O_3 (error bars show max. and min. counts recorded).

standardisation using a wide range of silicate standards, such an effect should have been eliminated. Matrix differences between standards and samples could have produced inaccuracies in either method. With the neutron capture method, results for a standard granite showed that this was unlikely to be a significant source of error. However, using the ICP, high silica standards gave higher boron readings than low silica standards (Fig. 3:9); although very few data are available at present, it seems probable that matrix effects may be significant, and that further work is required to correct for such effects.

A further batch of samples containing low boron concentrations (LX201 to LX207) was analysed separately by neutron capture and by the carminic acid method of Shelton and Reed (1976). Fig. 3:10 shows that there is poor correlation between results obtained by these two methods. The possible effect of self-shielding in neutron capture can even more justifiably be discounted here, since the meutron capture method yields higher boron concentrations for several of the samples. Again, matrix effects involved in standardisation may contribute to the differences observed; Shelton and Reed's (1976) standard magnesite was used as the main standard in the carminic acid determinations, and this differs strongly from silicates. There are several other potential sources of experimental error inherent in the spectrophotometric method, including loss or boron during sample preparation, and the critical time and temperature constraints upon the development of the colour complex. It is also true to say that at the boron levels involved, the neutron capture method is close to its lower limit of accuracy. If the neutron capture method is to be viable at low concentrations, the sensitivity and precision must be improved, by perhaps extending the counting time or increasing the sample size.

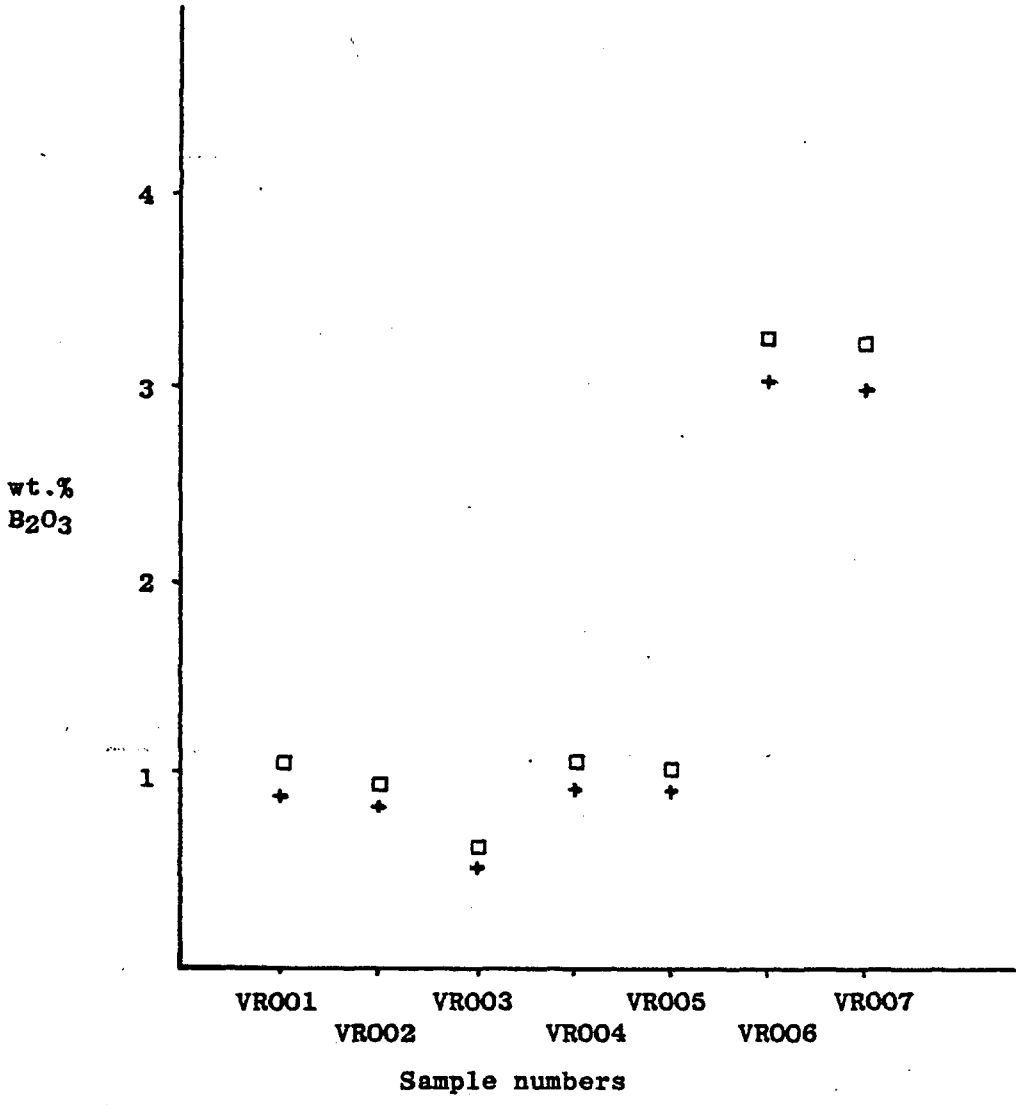

Fig. 3:8 Comparison of results obtained by neutron-capture prompt gamma spectrometry with those obtained by inductively coupled plasma-emission spectrometry (ICP), for samples containing up to 4% B_2O_3.

+ = neutron capture

□ = ICP

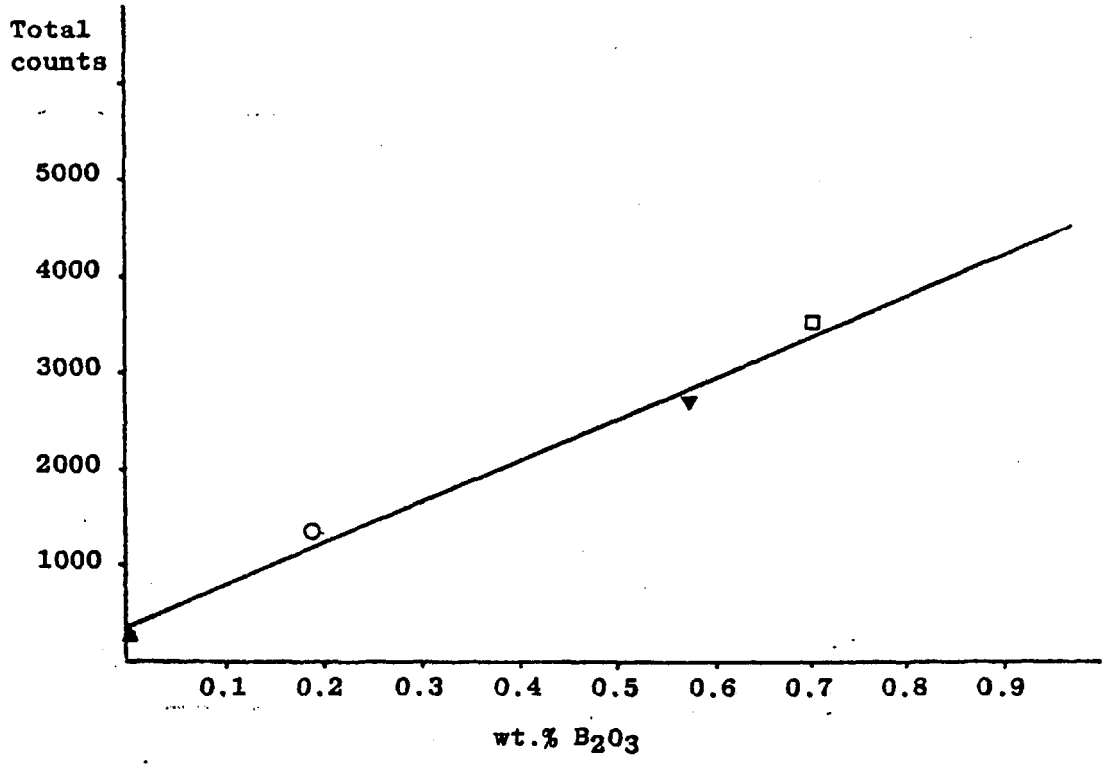

Fig. 3:9 Calibration curve for boron standards using the ICP at King's College, London.

silica-rich stds.		silica-poor stds.	
○	std. granite S.92	▲	std. basic rock KC10
□	borosilicate glass S.114	▼	KC10 spiked with B

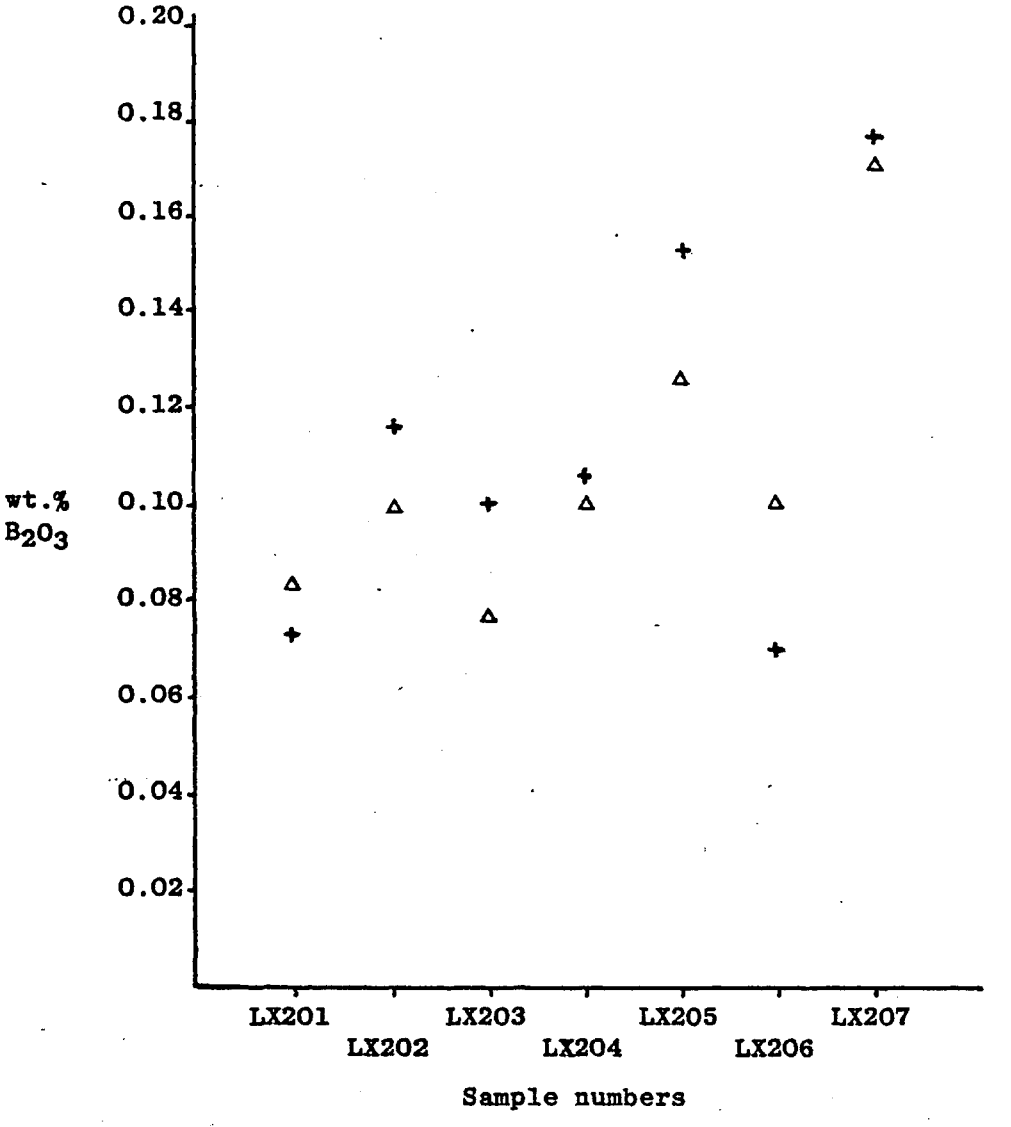

Fig. 3:10 Comparison of results obtained by neutron-capture prompt gamma spectrometry with those obtained by spectrophotometry, for samples containing low boron concentrations.

+ = neutron capture

Δ = spectrophotometry (carminic acid)

3.3.7 Conclusions

3.3.7.1 Evaluation of the neutron capture method

Neutron-capture prompt-gamma spectrometry, as employed using the equipment at the University of London Reactor Centre, offers a relatively rapid and non-destructive method of determining boron in tourmaline and tourmalinised rocks. It has the advantage of using dried rock and mineral powders without theneed for solution or chemical separation, and therefore eliminates any problems arising from incomplete dissolution of, or boron extraction from, tourmaline. Once the equipment is set up, a single analysis can be obtained in less than one hour, including manual calculation of the results.

The method can be used with confidence over the range 0.1 to 12.5% B_2O_3, where precision has been calculated from replicate measurements of standards as $\pm$ 2.8% over the complete compositional range examined, and $\pm$ 1.5% for concentrations between 1 and 12.5% B_2O_3. For rock matrices containing less than about 300 ppm B, the signal to background ratio is too low for reliable boron determination, under the operating conditions described.

3.3.7.2 Possibilities for improvement

It is probable that by changing the size of the sample (which is at present restricted by the diameter of the neutron beam), or by increasing the counting time, greater sensitivity could be achieved. The operating conditions were tailored to the needs of the present study, which involved samples containing relatively high concentrations of boron; Kerr et al. (1980) extended the sensitivity to lower boron levels encountered in shales by using larger samples and longer counting times. The thermal neutron flux available in the external reactor beam is also a restricting factor,

and one which is unlikely to change at the U.L.R.C. However, if it were possible to utilise an external beam with twice or three times the present neutron flux, much lower boron concentrations could be determined.

Using the present operating conditions, it would be possible to automate the irradiation of successive samples, by the installation of a rotating plattern or similar device. This would enable up to sixteen measurements to be made per working day, with the operator needing to spend only about ten minutes setting up the equipment. The main limiting factor is the necessity to make measurements while the reactor is running at full power (100 kw), which in the case of U.L.R.C. means a maximum period of eight hours per day. Automation of data processing would also be a considerable advantage.

4. Geochemistry of progressive tourmalinisation

The purpose of this investigation is to characterise chemically the tourmalinised sequences already examined petrographically, and to establish the chemical changes inherent in tourmalinisation of the Cornubian granites. The aim is not simply to provide analyses of tourmalinised rocks, as previous authors have done, but to examine the relationships between these tourmalinised rocks and their parent materials. Evidence for the chemical processes involved in the conversion of granite to tourmalinised rock is provided by chemical data for continuous transitions representing progressive tourmalinisation.

It has already been noted (Chapter 2) that tourmalinisation is commonly associated with other post-magmatic phenomena, such as greisening, chloritisation, or feldspar reddening, and the samples collected for the present study represent a wide spectrum of mineralogical associations. By comparison between such different tourmalinised sequences, it is possible not only to identify the chemical features attributable to tourmalinisation alone, but also, more importantly, to view tourmalinisation in its context with respect to related alteration processes. The controversial origin of the Cape Cornwall tourmalinite is also reconsidered in the light of the chemical evidence.

4.1 Previous work

Although several previous writers have analysed tourmalinised or tourmaline-bearing rocks (e.g. Matteucci and Zucchetti, 1965; Khan, 1966; Nemec, 1975; Alderton, 1976; Alderton *et al.*, 1980), published studies relating specifically to the tourmalinisation process are few. Brammall and Harwood's (1925) classic paper on tourmalinisation in the Dartmoor granite is mainly concerned with petrographic features, but does include a calculation, based on partial analyses, to show how a 'basic segregation' could be

converted to form the nucleus of a tourmaline-quartz nodule. The conclusions were that boric acid and alumina must be introduced, and potash released in the alteration process, and that '....the formation of tourmaline on the scale observed in granites .... must have appreciably disturbed the balance between potash and alumina in the magma'.

Chauris (1965, p.104-108) described tourmalinite veins produced by alteration within the St. Renan granite of Brittany. He gave a partial analysis of the tourmalinite, and major element analyses of the unaltered granite, and of a bleached zone ('granite blanchi') adjacent to the tourmalinite vein; these analyses are quoted in Table 4:1, for comparison with results from the present work. The tourmaline percentage in Chauris' tourmalinite is not stated, but his analysis (which, incidentally, lacks a boron concentration) would indicate about 60% tourmaline in the rock. The tourmalinite shows much depleted silicon, and enhanced aluminium and iron, by comparison with the unaltered granite, while the bleached zone is poor in nearly all elements except silicon, aluminium and potassium.

Hall (1973) briefly discussed tourmalinisation in southwest England, giving analyses of three different tourmalinised rocks and their untourmalinised equivalents from the same localities. These data are reproduced in Table 4:2. Analysis 3B, which according to the author corresponds with luxullianite, shows similarities with Chauris' (1965) tourmalinite, although the degree of alteration is not so great. By contrast, analyses 1B and 2B show increasing silica and decreasing alumina as a result of tourmalinisation.

Alderton (1976) examined the many aspects of mineralisation at Pendarves Mine, and other Cornubian localities, giving analyses of several altered rock types. With respect to tourmalinisation, he identified two main alteration phases, namely an earlier stage of sericitisation and K-feldspathisation, and a later stage involving tourmalinisation or

	Normal granite, unaltered	Bleached granite	Tourmalinite developed by metasomatism in the granite
SiO_2	71.60	75.80	44.56
Al_2O_3	15.45	12.45	28.15
Fe_2O_3	0.08	1.30	11.05*
FeO	1.40	0.20	
MnO	0.07	0.04	0.16
MgO	0.60	0.10	3.25
CaO	1.60	1.20	0.75
Na_2O	2.85	2.90	1.25
K_2O	6.40	5.10	1.60
TiO_2	0.50	0.25	0.45
P_2O_5	0.18	0.17	0.13
H_2O^-	0.26	0.16	0.53
H_2O^+	0.65	0.35	
			S = 0.30, WO_3 = 0.20, As = high, B_2O_3 = high.
			*Total iron as Fe_2O_3.
	99.84	100.02	

Table 4:1 Chemical analyses of unaltered granite and tourmalinite, with an intermediate bleached zone ('granite blanchi'), after Chauris (1965).

	Fresh 1A	Altered 1B	Fresh 2A	Altered 2B	Fresh 3A	Altered 3B
SiO_2	73.22	76.21	73.15	73.66	72.93	57.94
TiO_2	0.06	0.08	0.21	0.18	0.13	0.06
B_2O_3	0.11	1.28	0.08	0.78	0.33	2.69
Al_2O_3	14.67	11.80	14.42	14.09	14.67	23.67
Fe_2O_3	0.22	1.23	0.40	0.27	0.72	3.29
FeO	0.54	2.68	0.96	1.28	0.11	0.05
MnO	0.01	0.02	0.02	0.02	0.02	0.02
MgO	0.23	0.27	0.25	0.44	0.27	3.26
CaO	0.45	0.47	0.90	0.50	0.28	1.05
Na_2O	3.85	3.24	2.82	2.11	2.69	1.44
K_2O	4.75	1.39	5.31	5.22	6.12	3.54
Li_2O	0.03	0.02	0.02	0.01	0.02	0.20
P_2O_5	0.18	0.18	0.13	0.16	0.21	0.04
H_2O^+	0.79	0.84	0.61	0.96	0.81	1.51
H_2O^-	0.40	0.37	0.48	0.40	0.38	0.31
F	0.13	0.26	0.07	0.10	0.18	0.46
	99.64	100.34	99.83	100.18	99.87	99.53
$-O\equiv F$	0.05	0.11	0.03	0.04	0.08	0.19
	99.59	100.23	99.80	100.14	99.79	99.34

Table 4:2 Unaltered and tourmalinised granites from southwest England (after Hall, 1973).

1A & 1B Hingston Down, Chilsworthy, Cornwall

2A & 2B " " " " (finegrained gte)

3A & 3B Cadover Bridge, Dartmoor, Devon

chloritisation. Zoned alteration profiles associated with ore mineralisation are explained by this writer in terms of several successive and separate stages of mineral development; an example from the Harriet Lode at Pendarves shows the sequence, yellow-brown tourmaline -- orthoclase -- muscovite -- chlorite (-- biotite?) -- blue-green tourmaline (-- fluorite?).

Charoy (1979a) considered tourmalinisation with particular reference to the Cape Cornwall tourmalinite; his analyses of the tourmalinite and the underlying granites (which he regarded as separate petrographic units) are reproduced in Table 4:3. This author gave a reasoned argument for the possible origins of the tourmalinite, and favoured a magmatic rather than a hydrothermal genesis. However, the field relationships and petrographic evidence from the present study (Chapter 2) indicate that a hydrothermal origin is more likely, and that the vertical succession, culminating at the top in tourmalinite, represents a progressive tourmalinisation sequence. The chemical evidence will be reconsidered in the present chapter.

Alderton et al. (1980) investigated rare earth element behaviour during alteration in the Cornubian granites, and from their data on tourmalinised rocks (reproduced in Fig. 4:1), concluded that rare earths are depleted during tourmalinisation.

All the above authors have examined tourmalinisation by taking discrete samples of granite and of rocks showing various degrees of alteration. Where there are well-defined boundaries between the different rock types, there is no alternative to this approach. However, the samples collected for the present study offer the opportunity to trace chemical changes through continuous sequences of progressive tourmalinisation across gradational boundaries. In this respect, the present work is able to provide data relating to the tourmalinisation process, rather than to the differences between unaltered and tourmalinised rocks. The present writer provided a starting point for this study by analysis of four progressively more tourmalinised rocks from

	Priest's Cove microgranite	Tourmaline granite	Tourmalinite	
	CC 75	CC 95	CC 70	CC 98
SiO_2	73.66	74.29	71.08	74.48
Al_2O_3	13.86	14.13	15.23	12.09
Fe_2O_3	0.76	1.25	5.94	6.75
FeO	1.17	0.24	1.27	0.96
MnO	0.01	0.01	0.05	0.04
MgO	0.28	0.02	0.26	0.17
CaO	0.07	0.04	0.10	0.25
Na_2O	2.86	3.03	0.83	0.70
K_2O	4.48	4.97	0.08	0.07
TiO_2	0.21	0.09	0.17	0.14
P_2O_5	0.29	0.28	0.36	0.46
F	0.42	0.13	0.43	0.37
P.F.	1.38	1.04	1.04	0.82
	99.45	99.52	96.84	97.30
$-O\equiv F$	99.27	99.47	96.66	97.14
As	29	39	10.5	30.5
B	653	1823	1.28%	1.09%
W	< 50	< 50	< 50	540
Ba	57	102	17	16
Co	12	< 10	48	43
Cr	< 10	< 10	25	16
Cu	< 10	< 10	< 10	< 10
Ni	18	12	74	59
Sr	24	35	< 10	< 10
V	25	21	82	62
Rb	711	447	< 10	< 10
Li_2O	2101	116	340	275

Table 4:3 Chemical analyses of granites and tourmalinite from Cape Cornwall (after Charoy, 1979a).

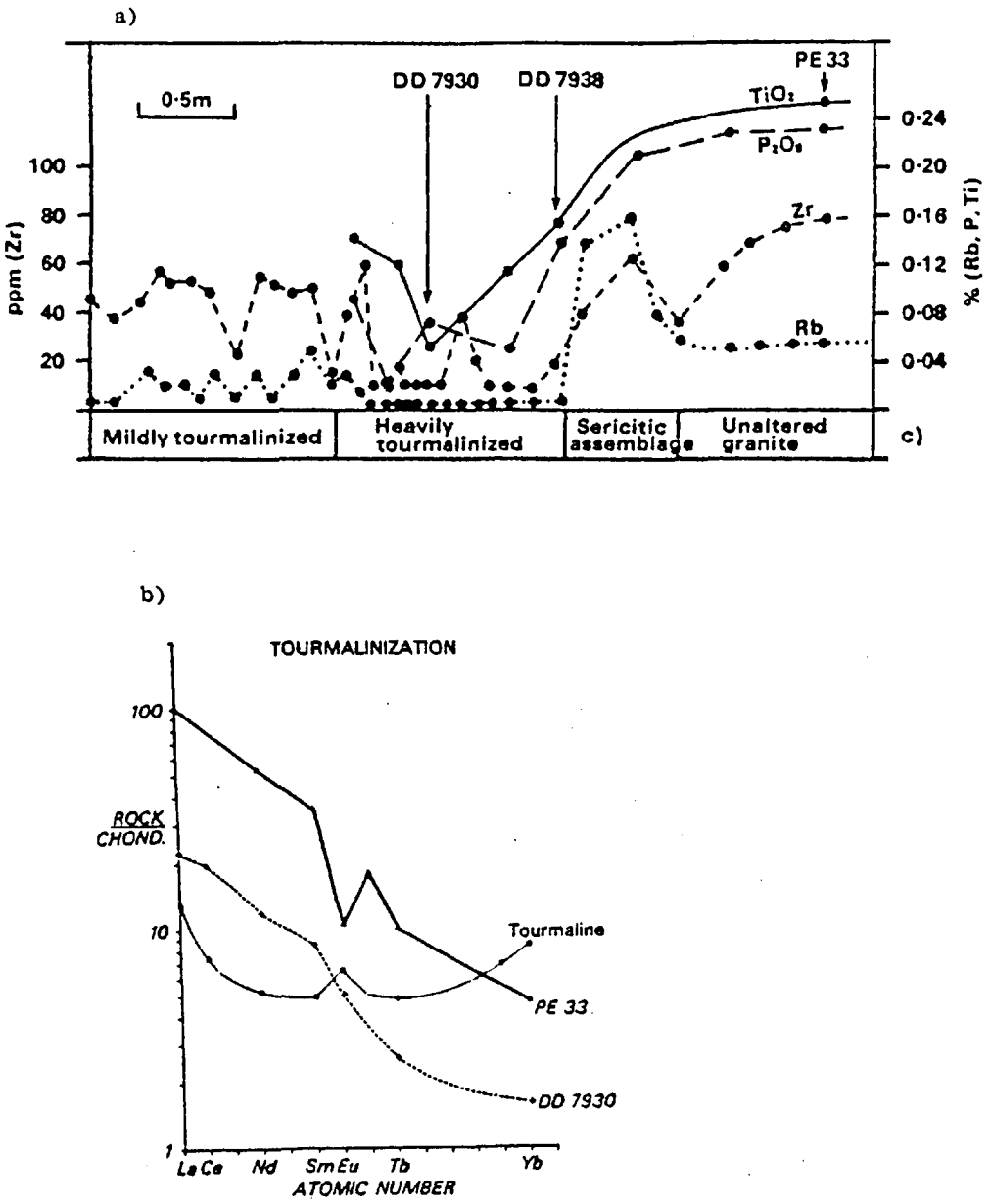

Fig. 4:1 a) Geochemical traverse from fresh into altered granite to highlight the effect of tourmalinisation on some critical elements

b) Chondrite-normalised REE patterns for a fresh granite (PE33), an adjacent tourmalinised alteration assemblage (DD7930) and a tourmaline mineral separate

(a and b after Alderton et al., 1980)

a luxullianite vein at Tregarden Quarry, Luxulyan (Lister, 1978a); data from this work are included here (Table 4:4) for comparative purposes, and will be referred to later in the text.

The association of potassium feldspar with tourmalinised rocks is common (Alderton, 1979; reply by Lister, 1979b), but it is not certain whether the processes of tourmalinisation and K-feldspathisation are inextricably linked, or independent of one another. Exley (1959) stated that potassium feldspar, unlike plagioclase, is in equilibrium with kaolinisation processes until an advanced stage, and the same seems to be true in tourmalinisation. However, tourmaline-albite associations have also been reported from Cornubia (Ussher et al., 1909). The partitioning of the alkalis between solid and fluid phases is known to be temperature dependent (Orville, 1963), such that a liquid coexisting with two feldspars will be more potassic at high temperatures but more sodic at low temperatures; this allows 'K-metasomatism' to occur in rocks as a natural consequence of thermal gradients. Thus, from a source of heat (e.g. a tourmalinising vein), potassium-rich liquid might be expected to migrate outwards, as a 'front' of K-feldspathisation. This might explain why the K-feldspar concentration is greatest at tourmalinised vein margins (as in the analyses of Lister, 1978a), and is also in accordance with the findings of Alderton (1976). The experimental work of Pichavant (1979; pers. comm.,1981) shows that the presence of boron may also increase the tendency for potassium to be partitioned into the fluid phase; this would favour the development of potassium-rich fluids, and would increase the potential for potassium metasomatism. The question of alkali changes associated with tourmalinisation will be further considered in the following pages.

Experimental work on tourmaline synthesis has shown that tourmaline is formed in weakly acid to weakly alkaline conditions. The stability field reported by Smith (1949) was in the weakly alkaline range for concen-

	Unaltered granite	vein margins Transition zone	Transition zone	Luxullianite
	LX001	LX B1-3	LX B4-6	LX008
SiO_2	72.60**	69.46	62.50	53.89
Al_2O_3	14.05	14.73	18.69	19.21
TiO_2	0.36	0.30	0.38	0.45
Fe_2O_3*	2.53	1.60	2.20	8.81
MnO	0.06	0.01	0.01	0.07
MgO	0.61	0.27	0.40	1.47
CaO	1.00	0.23	0.19	0.34
Na_2O	3.37	0.42	0.57	1.11
K_2O	4.57	11.15	13.43	9.81
P_2O_5	0.17	0.12	0.11	0.17
B_2O_3**	0.10	0.38	0.71	3.60
F**	0.27	0.06	0.07	0.07
H_2O^+ **	0.79	0.66	0.98	1.38
CO_2**	0.01	0.03	0.04	0.01
	100.32	99.42	100.28	100.39
-O=F	0.11	0.02	0.03	0.03
	100.21	99.40	100.25	100.36
Sr	82	80	88	156
Rb	469	807	971	672
Zr	156	122	150	189
Nb	24	17	18	21
Y	29	16	35	30

Table 4:4 Chemical analyses of unaltered granite, tourmalinised vein margins, and luxullianite, from Tregarden Quarry, Luxulyan (from Lister, 1978a, except for values marked **, which are unpublished data)

* Total iron as Fe_2O_3

** Unpublished values

trated solutions, but extended to the weakly acid range for very dilute solutions. Frondel and Collette (1957) synthesised tourmaline in weakly alkaline to moderately acid conditions, with the best results obtained from acid solutions. These latter authors found that strongly alkaline conditions were unfavourable to tourmaline formation, and suggested that the pH may influence the type of borate anions present in the solution, with (BO_3) groups present in the acid range, and ($B(OH)_4$) or other tetrahedral or polynuclear complexes present in the strongly alkaline range. Tourmaline contains boron in the form of (BO_3) triangles, while certain other borosilicates contain tetrahedrally co-ordinated boron; notable among the latter is reedmergnerite, which is stable in the alkaline (and tourmaline-free) environment of the Green River Formation, Utah. Fluid inclusion data from natural tourmalines (e.g. Slivko, 1973) support the contention that tourmaline forms in near-neutral pH conditions.

Tourmaline can form at very low temperatures and pressures during sedimentary diagenesis (Krynine, 1946), and has been synthesised at temperatures as low as 250°C (Morgan, 1980). Most reported tourmaline syntheses were, however, achieved at temperatures between 400 and 700°C (Frondel and Collette, 1957; Michel-Levy, 1953; Smith, 1949; Taylor and Terrell, 1967; Tomisaka, 1968). Temperatures derived from fluid inclusion geothermometry are frequently equivocal, since data are often reported without correction for pressure; however, a wide range of temperatures is indicated. Pressures of between 700 and 2000 bars have been employed to synthesise tourmalines experimentally.

4.2 Venford Reservoir Quarry, Dartmoor

4.2.1 Results

Chemical analyses of the samples described petrographically in Chapter 2 are given in Tables 4:5 and 4:6, which show major and trace elements respectively. The main sequence of samples, beginning with 'unaltered', white, biotite granite (VR022) passes through brown-stained granite (VR020) into a reddened zone some 6 metres wide (VR012 to VR010), and thence through the 15 cm vein margin (VR001 to VR005) into the zone of maximum tourmalinisation (VR006 and VR007). Samples VR023 and VR024 are from the margin and fully tourmalinised portion respectively of the smaller, cavitous tourmalinised vein at the same quarry.

The 'unaltered' granite is compositionally similar to the mean of Dartmoor granite analyses given by Edmonds et al. (1968, p.105), apart from the calcium value which is, however, within the range quoted; its composition is also compatible with the series of Dartmoor granite analyses given by Brammall and Harwood (1932, anal. 1-24). Sample VR022 may thus be considered sufficiently unaffected by local tourmalinisation to fill the role of a theoretical parent rock in the present investigation. As previously explained (Chapter 2), a totally unaltered granite, as emplaced, would be impossible to procure, since the whole southwest England province has undergone extensive post-magmatic changes.

4.2.2 Chemical changes during tourmalinisation

In the progressive tourmalinisation sequence from VR022 to VR007, the major chemical changes occur in the transition from white to reddened granite (from VR022 to VR012) and at the beginning of the maximum tourmalinisation zone (between VR005 and VR006). However, these changes are not attributable simply to an increase in tourmaline concentration, since the

	VRO22	VRO20	VRO12	VRO11	VRO10	VRO01	VRO02	VRO03	VRO04	VRO05	VRO06	VRO07	VRO23	VRO24
SiO_2	73.3	73.5	75.0	74.8	75.5	75.8	75.7	77.5	76.7	77.3	68.0	64.5	71.6	72.9
TiO_2	0.25	0.29	0.25	0.28	0.29	0.23	0.27	0.30	0.29	0.33	0.24	0.29	0.22	0.23
Al_2O_3	12.82	12.75	13.07	13.04	12.61	13.53	13.70	12.80	13.25	12.54	15.80	17.62	11.05	12.02
FeO	2.11	2.38	0.69	0.96	0.91	1.10	1.22	0.77	1.12	1.09	2.59	2.86	1.61	3.39
MnO	0.06	0.06	0.01	0.01	0.01	0.01	0.01	0.01	0.01	0.01	0.02	0.02	0.02	0.03
MgO	0.33	0.39	0.28	0.29	0.25	0.29	0.28	0.22	0.51	0.50	1.89	1.93	0.18	0.54
CaO	0.59	0.32	0.23	0.25	0.29	0.27	0.31	0.31	0.37	0.37	0.56	0.51	0.09	0.33
Na_2O	3.89	3.80	3.90	3.86	3.74	2.36	2.59	2.57	2.41	1.89	1.58	1.09	1.21	2.33
K_2O	5.23	5.52	5.25	5.31	6.62	4.63	4.40	4.34	4.10	4.43	3.95	5.96	7.71	6.12
P_2O_5	0.14	0.15	0.12	0.14	0.17	0.13	0.15	0.16	0.17	0.18	0.17	0.16	0.08	0.12
B_2O_3	0.12	0.04	0.31	0.38	0.32	0.89	0.87	0.50	0.96	0.99	3.09	3.02	0.08	1.96
H_2O^+	0.60	1.02	0.63	0.87	0.65	0.66	0.70	0.58	0.62	0.68	1.21	1.47	0.74	0.61
(H_2O^-)	(0.15)	(0.32)	(0.20)	(0.22)	(0.08)	(0.19)	(0.19)	(0.19)	(0.19)	(0.19)	(0.20)	(0.29)	(0.17)	(0.00)
CO_2	0.01	0.02	0.01	0.03	0.01	0.01	0.01	0.03	0.03	0.02	0.02	0.03	-	-
F	0.18	0.15	0.05	0.05	0.04	0.07	0.07	0.05	0.07	0.07	0.17	0.18	0.06	0.06
Others	0.10	0.09	0.03	0.04	0.03	0.04	0.04	0.05	0.04	0.05	0.07	0.08	0.10	0.09
	99.73	100.48	99.83	100.31	101.44	100.02	100.32	100.19	100.65	100.45	99.36	99.72	94.75	100.73
-O≡F	0.08	0.07	0.02	0.02	0.02	0.03	0.03	0.02	0.03	0.03	0.07	0.08	0.02	0.02
	99.65	100.41	99.81	100.29	101.42	99.99	100.29	100.17	100.62	100.42	99.29	99.64	94.73	100.71

Table 4:5 Chemical analyses of rocks from Venford Reservoir Quarry (major elements, % oxides)
* total iron as FeO - below detection limit

	VRO22	VRO20	VRO12	VRO11	VRO10	VRO01	VRO02	VRO03	VRO04	VRO05	VRO06	VRO07	VRO23	VRO24
F	1800	1545	525	450	435	657	664	480	681	742	1669	1782	585	585
Li	317	264	8	13	9	42	38	33	53	59	136	152	26	57
Rb	501	534	127	209	206	75	70	70	68	87	91	174	701	508
Sr	40	29	39	54	37	25	23	20	28	30	90	94	82	132
Ba	136	75	75	108	64	17	10	11	27	-	23	40	161	217
Zn	34	26	5	8	11	24	42	92	49	26	79	105	10	15
Cu	8	6	6	6	6	7	10	28	4	10	7	7	7	7
Be	10	14	3	4	2	3	2	1	2	2	4	5	6	6
Zr	n.d.	n.d.	n.d.	n.d.	n.d.	127	161	168	166	191	187	170	n.d.	n.d.
Nb	n.d.	n.d.	n.d.	n.d.	n.d.	31	29	37	23	24	19	22	n.d.	n.d.
Y	n.d.	n.d.	n.d.	n.d.	n.d.	35	42	34	27	29	26	28	n.d.	n.d.

Table 4:6 Chemical analyses of rocks from Venford Reservoir Quarry (trace elements, ppm)

- below detection limit n.d. not determined

reddened granite appears to be a zone not of accumulation, but of depletion in several elements.

Silica remains high and relatively constant at 73 to 76% throughout the white and reddened granites and the vein margins; the variation here is probably due to the uneven distribution of large, rounded quartz blebs. As the zone of maximum tourmalinisation is reached, there is a sudden and dramatic decrease to 64.5% silica.

Alumina also maintains its original level around 13% throughout the sequence, before increasing to nearly 16% and finally nearly 18% in the zone of maximum tourmalinisation. Aluminium is one of the essential major elements in tourmaline (which, in the schorl-dravite series, contains about 35% Al_2O_3), and hence there is a general correlation between the concentrations of boron and aluminium in the rock (Fig. 4:2). Other aluminium-rich phases present are muscovite (27% Al_2O_3) and hydromuscovite (36% Al_2O_3); their development also reflects the aluminium increase with tourmalinisation, in the already 'peraluminous' Cornubian granite.

Tourmalinisation involves a net gain in iron and magnesium, both of which are major components of the tourmaline at this locality. Both these elements are, however, depleted in the reddened granite and the vein margin (Fig. 4:3). Iron shows a decreasing trend from over 2% FeO in the unaltered granite to less than 1% FeO (or about 1% Fe_2O_3) in the reddened granite. This may be correlated with the increasing breakdown of biotite and its replacement by tourmaline. Since biotite contains up to 20% FeO, while the tourmaline at this locality contains a maximum of 15%, the total replacement of one unit of biotite by one unit of tourmaline represents a decrease in iron. The replacement process, however, appears to comprise at least two stages (Chapter 2), in the first of which, biotite becomes unstable and is partially decomposed into secondary white micas and iron oxides. In

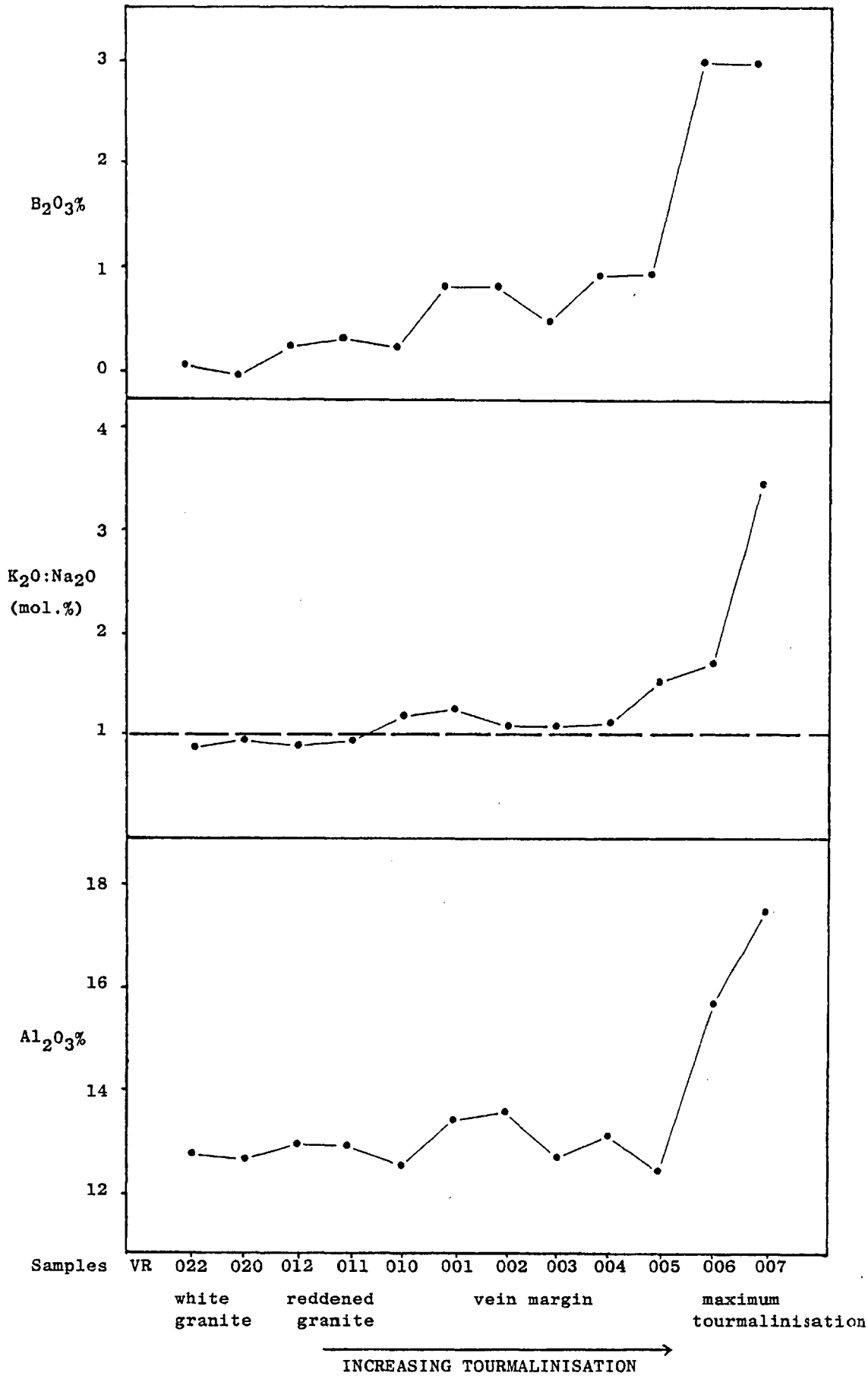

Fig. 4:2 Behaviour of boron, potassium, sodium and aluminium, in progressive tourmalinisation, Venford Reservoir Quarry.

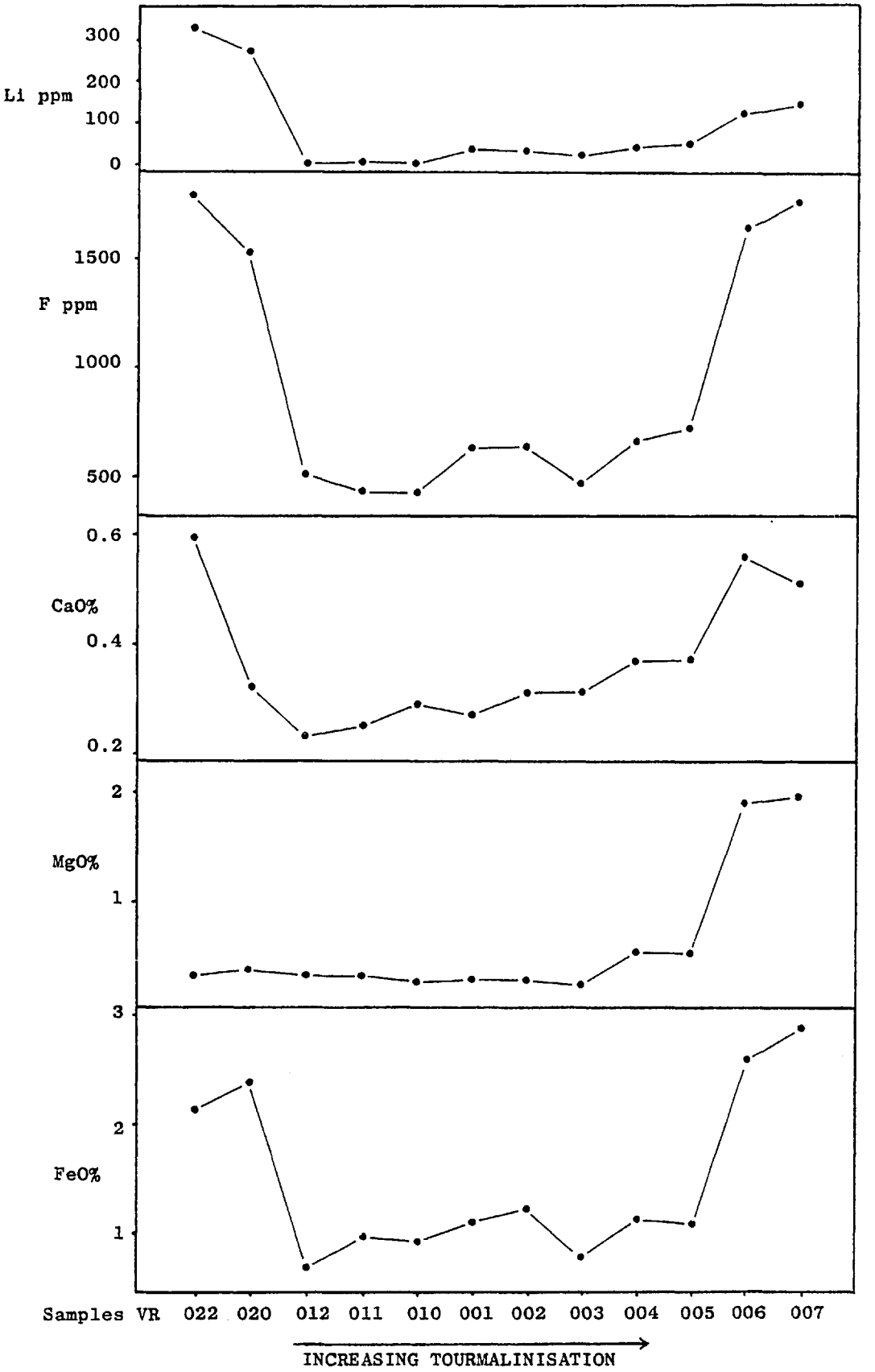

Fig. 4:3 Chemical changes during progressive tourmalinisation, Venford Reservoir Quarry: variation in Li, F, CaO, MgO, FeO.

this state, it is susceptible to replacement by tourmaline. The first, the breakdown stage, could be achieved simply by the action of aqueous fluids (Schwarz, 1958), perhaps advancing ahead of the 'tourmalinisation front', or perhaps considerably preceding it (this kind of biotite breakdown is fairly common in the 'unaltered' granites of Dartmoor, according to Edmonds et al., 1968). The associated intense reddening is presumably due to a change in the oxidation state of iron, which as Fe_2O_3 can induce considerable colouration of a rock when present in very small quantities. Once the biotite and its primary alteration products have been eliminated or made over into tourmaline (from VR001 onwards), the iron content of the rock becomes roughly proportional to its tourmaline content. Magnesium shows a similar trend to iron, although less pronounced.

Manganese is lost from the system during tourmalinisation, falling from 0.6% MnO in the white granites to 0.2% in the tourmalinised rock. The reddened granite and vein margin is even further depleted in MnO (down to 0.1%).

Calcium shows a trend of depletion from 0.59% CaO in the white granite to 0.23% in the reddened granite, but with increasing proximity to the maximum tourmalinisation zone, calcium increases and is restored to its original level (Fig. 4:3). The calcium hosts in the unaltered granite are apatites and the plagioclase rims of rapakivi feldspars; the latter are eliminated in the reddened granite. Although no calcium minerals (apart from apatite) are present in the maximum tourmalinisation zone, many tourmaline crystals contain up to nearly 2% CaO (Chapter 5), and this presumably accounts for the relatively high calcium concentration in the tourmalinised rock.

The alkali balance in this series of rocks is determined by two processes, namely the replacement of K-bearing biotite by Na-bearing tourmaline (with hydromuscovite as a by-product), and the increase in the

K:Na ratio in the feldspar. These processes result in a net increase in K_2O at the expense of Na_2O in the rock during progressive tourmalinisation, because tourmaline contains only about 2% Na_2O, compared with the much higher K_2O concentrations in both potassium feldspar and hydromuscovite. In the maximum tourmalinisation zone, the 'normative' tourmaline content of about 31% would require only about 0.6% Na_2O. Therefore, the measured Na_2O concentrations of over 1% must include some sodium resident in another mineral phase; this assumption is confirmed by microprobe analyses of feldspar indicating patches of almost pure albite. Fig. 4:2 shows that the mol. ratio K_2O:Na_2O increases with proximity to the vein centre, and that the increase may be roughly correlated with the increase in B_2O_3. The relationship between concentrations of sodium, potassium and boron in the rocks is illustrated in Fig. 4:4.

The concentrations of phosphorus and titanium remain remarkably constant throughout the white and reddened granites and into the maximum tourmalinisation zone. Although apatite has extensively recrystallised in the tourmalinisation process, the 'modal' percentage of this mineral is not essentially changed, and hence neither is the phosphorus content of the rock. By contrast, titanium changes its host mineral in the tourmalinisation process, but can to a certain extent be accommodated in tourmaline (microprobe analyses, Chapter 5, show some zones within tourmaline crystals to be extremely titaniferous). The breakdown of biotite prior to its replacement by tourmaline also releases titanium, apparently as TiO_2, which for some reason does not become depleted in the reddened granite along with iron. The chemical analyses of the reddened granites support the identification of dark brown and red, semi- to non-crystalline substances observed in thin section as titanium oxides; microprobe analyses also confirmed some opaque grains as being almost pure rutile.

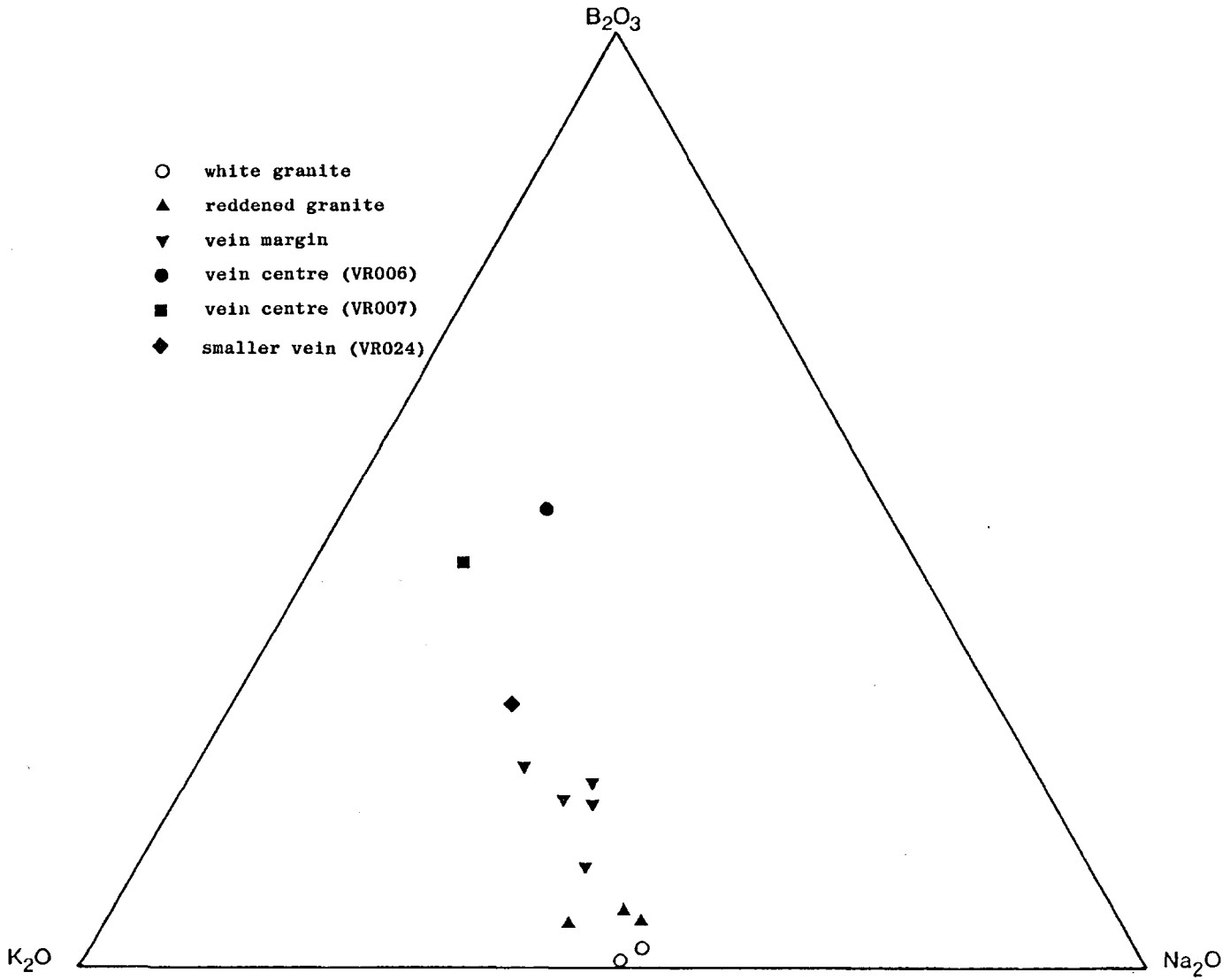

Fig. 4:4 Relationship between boron, potassium and sodium concentrations in rocks from Venford Reservoir Quarry. (mol.% B_2O_3, K_2O, Na_2O)

Boron shows a predictable increase with progressive tourmalinisation. The 0.12% B_2O_3 recorded in the unaltered granite may seem high in view of the absence of tourmaline in thin sections. However, this figure, which would represent a 'normative' tourmaline content of 1.25% in the rock, is not unrealistic, since tourmaline occurs sporadically in small pods within the granite. After the lower concentration in the brown-stained granite (VR020), boron increases in step-like increments, until a major increase to over 3% B_2O_3 is seen in VR006; this major increase coincides with the influx of the fine acicular tourmaline in the zone of maximum tourmalinisation. There is no evidence for boron depletion in the reddened granite. The low boron figure for VR003 is attributable to heterogeneities in a very coarse-grained rock, and simply represents a patch where the tourmaline concentration was slightly lower.

Fluorine shows a very similar pattern to that of iron (Fig. 4:3), becoming considerably depleted in the reddened granite and the vein margin, but increasing to its original level of about 1800 ppm in the maximum tourmalinisation zone. As no major fluorine-bearing minerals are observed either in the granite or the tourmalinised rock, the fluorine present may almost certainly be assigned to hydroxyl positions in biotite and tourmaline. Fluorine concentrations of up to 1.75% have been reported from biotite in the Dartmoor granite (Al-Saleh et al., 1977), and tourmaline from Venford Reservoir contains 0.37% F (present work, Chapter 5). The tourmaline content (about 31%) of the tourmalinised vein is insufficient to account for 1800 ppm fluorine in the rock; therefore, either some of the tourmaline present must contain more than 0.37% F, or another fluorine-bearing phase must be present (perhaps fluorapatite).

Lithium also shows depletion from over 300 ppm in the granite to about 10 ppm in the reddened zone, and rises again to 152 ppm in the tourmalinised vein (Fig. 4:3). In the white granite, biotite is probably

the host for lithium, which is easily released when the biotite breaks down. The tourmaline at this locality is lithium-poor, belonging to the schorl-dravite solid solution series, and lacking an elbaite component. A lithium concentration of 171 ppm was measured in separated tourmaline (Chapter 5); since this would not account for 152 ppm in the rock, and since no other lithium-bearing minerals were recognised, it must be presumed that some tourmaline present contains higher lithium concentrations (possibly the fine acicular needles, which were very difficult to separate).

Rubidium behaves in a similar manner to lithium, but the maximum depletion occurs in the vein margin. From over 500 ppm in the white granites, Rb drops to 70 ppm at the margin of the vein, then rises again to 174 ppm in VR007. Fig. 4:5 shows that in the reddened granites and tourmalinised rocks there is a rough correlation between rubidium and potassium, but that these rocks show a decrease in the ratio Rb:K compared with the white granites. Rubidium is therefore lost with respect to potassium at the onset of reddening. This could be due to the release of Rb from biotite, since concentrations of 3500 ppm Rb have been reported in some Cornubian biotites (Butler, 1953); if this is so, the implication is that biotite is a more important host for rubidium than feldspar.

All the other trace elements determined show a depletion in the reddened granite and/or the vein margins (although with Cu and Be, the concentrations are too low to be meaningful). Strontium and zinc show a net increase in the tourmalinised rock by comparison with the white granite; barium shows a net decrease.

Zirconium, niobium and yttrium concentrations are given in Table 4:6 for the tourmalinised vein and its margins. Nb and Y show a small decrease from the outer vein margin into the vein centre. Zr shows an increase from 127 ppm in the outer vein margin to 170 ppm in the vein centre; this latter figure is comparable to that reported by Hawkes and Dangerfield (1978) for

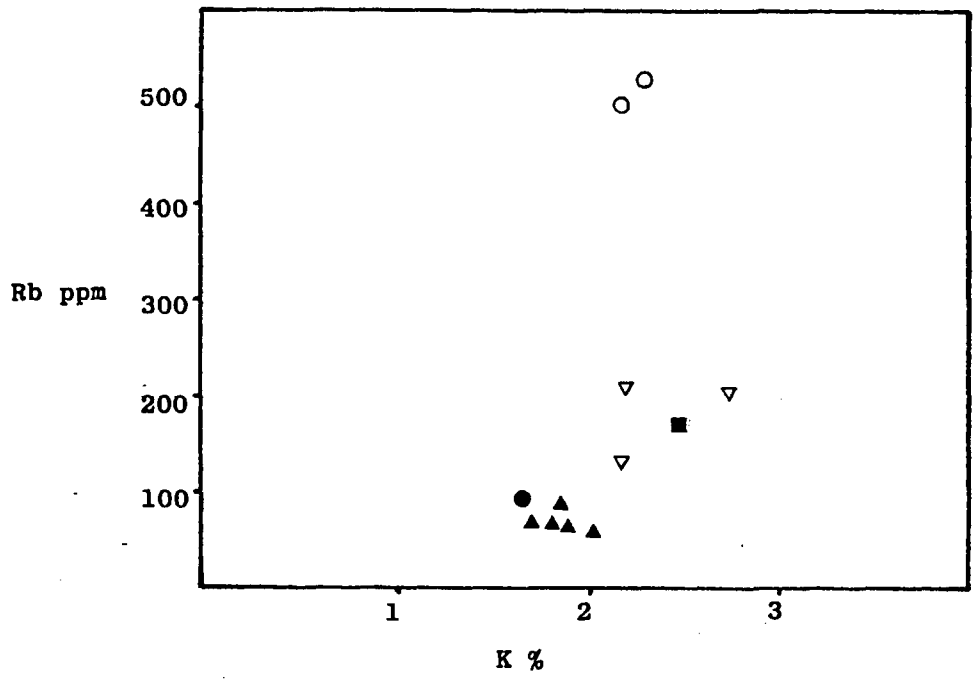

Fig. 4:5 Correlation between rubidium and potassium, Venford Reservoir Quarry.

- ○ white granite
- ▽ reddened granite
- ▲ vein margin
- ● vein centre (VR006)
- ■ vein centre (VR007)

the megacrystic granite of Dartmoor. It therefore appears that there has been no net gain or loss in zirconium as a result of tourmalinisation. The breakdown of zircon on replacement of biotite by tourmaline has been cited by Simpson et al. (1979) as a possible source of radiogenic elements for later uranium mineralisation. However, the petrographic evidence (Chapter 2) indicates that not all zircon is mobilised when its host biotite is replaced, and the chemical trend also shows that although some change in the Zr concentration in the rock is apparent, zircon is not removed from the system during tourmalinisation.

The sample from the smaller, cavitous tourmalinised vein at the same locality (VR024) contains more silica and less alumina than its counterpart in the larger tourmalinised vein centre. Although VR024 has a very black matrix in hand specimen, it is actually less tourmaliniferous than VR007, since most of the tourmaline takes the form of acicular needles and isolated prisms embedded in quartz. The smaller, cavitous vein contains 1.96% B_2O_3, which indicates about 20% tourmaline; it contains more iron and less magnesium and calcium than the larger vein, but more sodium and potassium. With respect to the white granite, fluorine, lithium and zinc are considerably depleted, while strontium and barium are enriched, and rubidium is unchanged.

4.3 Tregarden Quarry, Luxulyan

4.3.1 Results

Tables 4:7 and 4:8 show the chemical analyses, for major and trace elements respectively, of samples from the predominantly chloritised vein (LX201 to LX207). From the centre of the same vein, LX208a is a fully chloritised sample, and LX208b is more strongly tourmalinised.

Table 4:9 shows major and trace elements in the margins and centre of the predominantly tourmalinised vein (LX030 to LX036). From the boron and aluminium concentrations, sample LX035 seems to represent the maximum

	LX201	LX202	LX203	LX204	LX205	LX206	LX207	LX208a	LX208b
SiO_2	72.6	71.9	72.4	72.1	72.6	71.1	62.5	62.9	60.6
TiO_2	0.34	0.33	0.26	0.31	0.32	0.38	0.33	0.34	0.31
Al_2O_3	14.35	14.45	14.23	14.51	14.28	14.37	16.21	14.92	18.07
FeO	2.11	2.10	2.14	1.93	2.07	3.05	5.45	6.72	4.04
MnO	0.07	0.07	0.07	0.06	0.05	0.05	0.09	0.14	0.17
MgO	0.47	0.47	0.48	0.44	0.50	0.62	1.06	1.37	0.79
CaO	0.98	0.90	0.94	0.85	0.80	0.45	0.43	0.40	0.39
Na_2O	2.34	2.24	2.16	2.06	1.92	0.73	0.23	0.13	0.56
K_2O	5.30	5.70	5.36	5.89	5.66	7.69	10.81	9.79	12.24
P_2O_5	0.26	0.26	0.25	0.25	0.25	0.27	0.29	0.28	0.30
B_2O_3	0.08	0.12	0.10	0.11	0.15	0.07	0.18	0.10	1.70
H_2O^+	0.82	0.83	0.90	0.72	0.94	1.55	1.96	2.27	0.91
(H_2O^-)	(0.31)	(0.30)	(0.29)	(0.25)	(0.32)	(0.35)	(0.26)	(0.15)	(0.22)
CO_2	0.01	0.02	0.02	–	–	–	–	–	–
F	0.27	0.25	0.26	0.22	0.21	0.16	0.12	0.09	0.06
Others	0.12	0.12	0.11	0.11	0.10	0.14	0.18	0.15	0.22
	100.12	99.76	99.68	99.56	99.85	100.63	99.84	99.60	100.36
-O≡F	0.11	0.11	0.11	0.09	0.09	0.08	0.05	0.04	0.02
	100.01	99.65	99.57	99.47	99.76	100.55	99.79	99.56	100.34

Table 4:7 Chemical analyses of rocks from the chloritised and tourmalinised sequence at *Tregarden Quarry*, Luxulyan (major elements, % oxides). * total iron as FeO
- below detection limit

	LX201	LX202	LX203	LX204	LX205	LX206	LX207	LX208a	LX208b
F	2653	2518	2562	2201	2142	1602	1227	852	589
Li	188	178	168	151	155	152	81	75	17
Rb	465	449	421	465	442	608	653	572	834
Sr	90	88	85	83	68	63	73	48	128
Ba	150	217	192	208	171	295	800	594	930
Zn	73	42	51	28	28	55	67	72	105
Cu	21	16	-	-	-	5	6	9	7
Be	9	9	5	7	6	6	5	1	3
Zr	146	141	147	134	145	156	126	121	131
Nb	30	29	29	29	27	29	22	20	24

Table 4:8 Chemical analyses of rocks from the chloritised and tourmalinised sequence at Tregarden Quarry, Luxulyan (trace elements, ppm).

- below detection limit

	LX030	LX031	LX032	LX033	LX034	LX035	LX036
SiO_2	70.3	70.0	71.9	64.0	64.5	64.1	65.1
TiO_2	0.28	0.35	0.33	0.34	0.32	0.34	0.37
Al_2O_3	14.80	13.95	13.26	15.54	15.18	15.49	15.23
FeO	2.08	3.08	2.27	5.23	5.07	5.65	4.86
MnO	0.05	0.07	0.05	0.09	0.09	0.09	0.09
MgO	0.47	0.59	0.36	0.76	0.79	0.86	0.71
CaO	0.18	0.25	0.23	0.30	0.30	0.36	0.37
Na_2O	2.72	1.83	1.25	2.20	2.33	2.49	2.25
K_2O	7.38	8.02	8.28	8.88	8.58	8.67	8.91
P_2O_5	0.20	0.28	0.26	0.25	0.23	0.26	0.27
B_2O_3	0.35	0.23	0.28	1.36	1.56	1.73	1.36
H_2O^+	1.56	1.54	1.25	1.52	1.27	1.23	1.26
(H_2O^-)	(0.48)	(0.27)	(0.23)	(0.28)	(0.14)	(0.12)	(0.15)
CO_2	0.01	0.02	0.01	–	0.01	0.01	0.01
F	0.13	0.12	0.09	0.09	0.08	0.09	0.07
Others	0.11	0.14	0.13	0.16	0.15	0.15	0.15
	100.62	100.47	99.95	100.72	100.46	101.52	101.01
-O≡F	0.05	0.05	0.04	0.04	0.03	0.04	0.03
	100.57	100.42	99.91	100.68	100.43	101.48	100.98
F	1275	1185	885	885	780	855	720
Li	125	75	48	54	41	39	40
Rb	553	683	695	727	684	678	719
Sr	71	59	48	79	81	81	76
Ba	344	556	508	603	614	617	628
Zn	34	33	25	82	47	42	42
Cu	6	10	10	21	19	12	23
Be	3	3	2	2	1	1	1

Table 4:9 Chemical analyses of rocks from the tourmalinised and chloritised sequence, Tregarden Quarry, Luxulyan.

oxides %, trace elements ppm
* total iron as FeO – below detection limit

tourmalinisation product. At this locality, by contrast to Venford Reservoir, the effects of alteration are virtually confined to the lateral extent of the tourmalinised or chloritised veins, and there is no widespread reddening of the surrounding granite. The close similarity betweeen sample LX201 (Tables 4:7 and 4:8) and LX001 (unaltered granite from the same locality, Lister 1978a) shows that even as close as 15 cm to the edge of the chloritised vein, there is very little alteration of the granite.

4.3.2 Chemical changes during tourmalinisation and chloritisation

A major reduction is silica, from over 70% to 63 or 64%, accompanies tourmalinisation and chloritisation alike. The greatest reduction in silica is seen in the tourmalinised portion of the chloritised vein (LX208b) where a silica concentration of 60.6% is recorded.

Alumina increases during both alteration processes (Fig. 4:6); the increase is greater in tourmalinisation, and this is consistent with the relative concentrations of Al_2O_3 in tourmaline (about 35%) and in chlorite (less than 20%). Chloritisation without the associated tourmalinisation need therefore involve very little Al_2O_3 enrichment, although the growth of secondary muscovite (containing about 27% Al_2O_3) also enhances the alumina content of the rock.

Iron and magnesium are increased both in tourmalinisation and chloritisation. The greater increase in both these elements is seen in chloritisation (Fig. 4:6). At this locality, both tourmalines and chlorites are relatively iron-rich, with a minor magnesian component. The tourmaline (Chapter 5) can contain up to about 19% FeO and up to about 4% MgO. The chlorite, however, can contain up to about 35% FeO and up to about 8% MgO; thus one unit of chlorite results in higher iron and magnesium concentrations in the rock than does one unit of tourmaline.

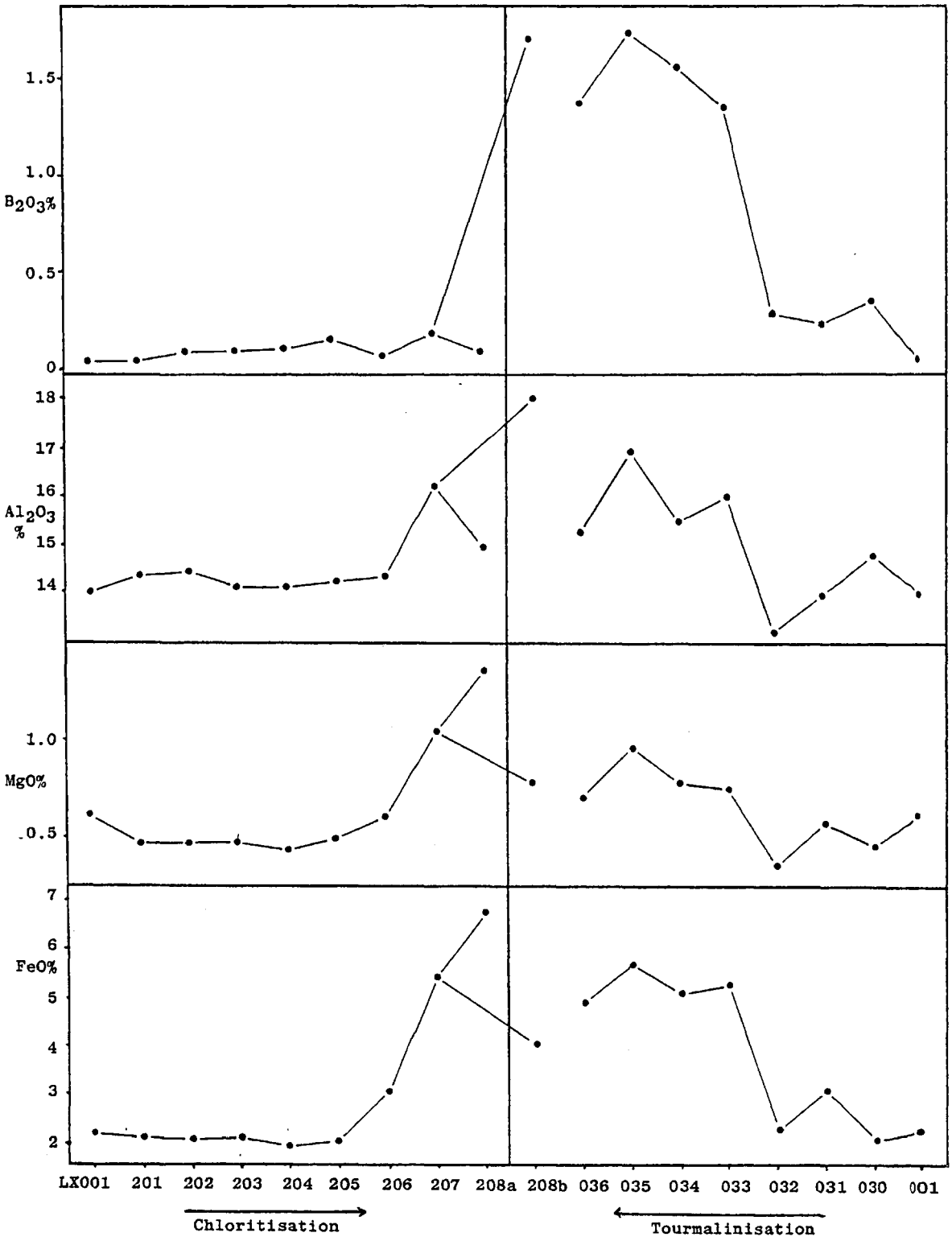

Fig. 4:6 Chemical changes in tourmalinisation and chloritisation at Tregarden Quarry, Luxulyan. (LX001 - Al_2O_3, FeO and MgO values from Lister, 1978a)

Calcium appears to be progressively decreased during chloritisation but increased during tourmalinisation. However, the final calcium concentrations are similar (about 0.4% CaO) in both chloritised and tourmalinised materials. The unaltered granite (LX001) and the outer chloritised vein margin (LX201) each contain about 1% CaO; at the outer tourmalinised vein margin (LX030) this concentration is reduced to 0.18%. Thus it seems that the tourmalinised vein margin represents a narrow zone of calcium depletion, analogous to the depleted zone at Venford. It is logical that this depletion should occur in the sequence LX030-036, since here the vein margin is iron-stained and friable, whereas the chloritised vein margin consists of coherent white granite right up to the onset of pink feldspar colouration in LX205. (The four analyses representing 'luxullianitisation' (Lister, 1978a) also indicate a zone of depletion in calcium and certain other elements at the vein margin).

In both tourmalinisation and chloritisation, potassium increases with respect to sodium. The K:Na enrichment trends are shown in Fig. 4:7, which includes the data of Lister (1978a). In both the tourmalinised sequences (culminating in LX035 and LX008) the greatest K_2O:Na_2O ratio is seen at the vein margins, not the vein centre. The chloritised sample LX208a shows the most extreme K_2O:Na_2O ratio (52:1). The alkali balance with respect to boron concentration is illustrated in Fig. 4:8, which emphasises the trend of potassium enrichment towards the chloritised vein centre and the tourmalinised vein margins. The high potassium concentrations represent the growth of K-feldspar and muscovite, while in the tourmalinised vein centres, the potassium concentrations are reduced by the development of Na-bearing tourmaline at the expense of K-bearing feldspar. These findings favour the theory of a K-feldspathisation front, perhaps advancing ahead of tourmalinisation. Since the tourmalinised vein margins are also chloritised, it

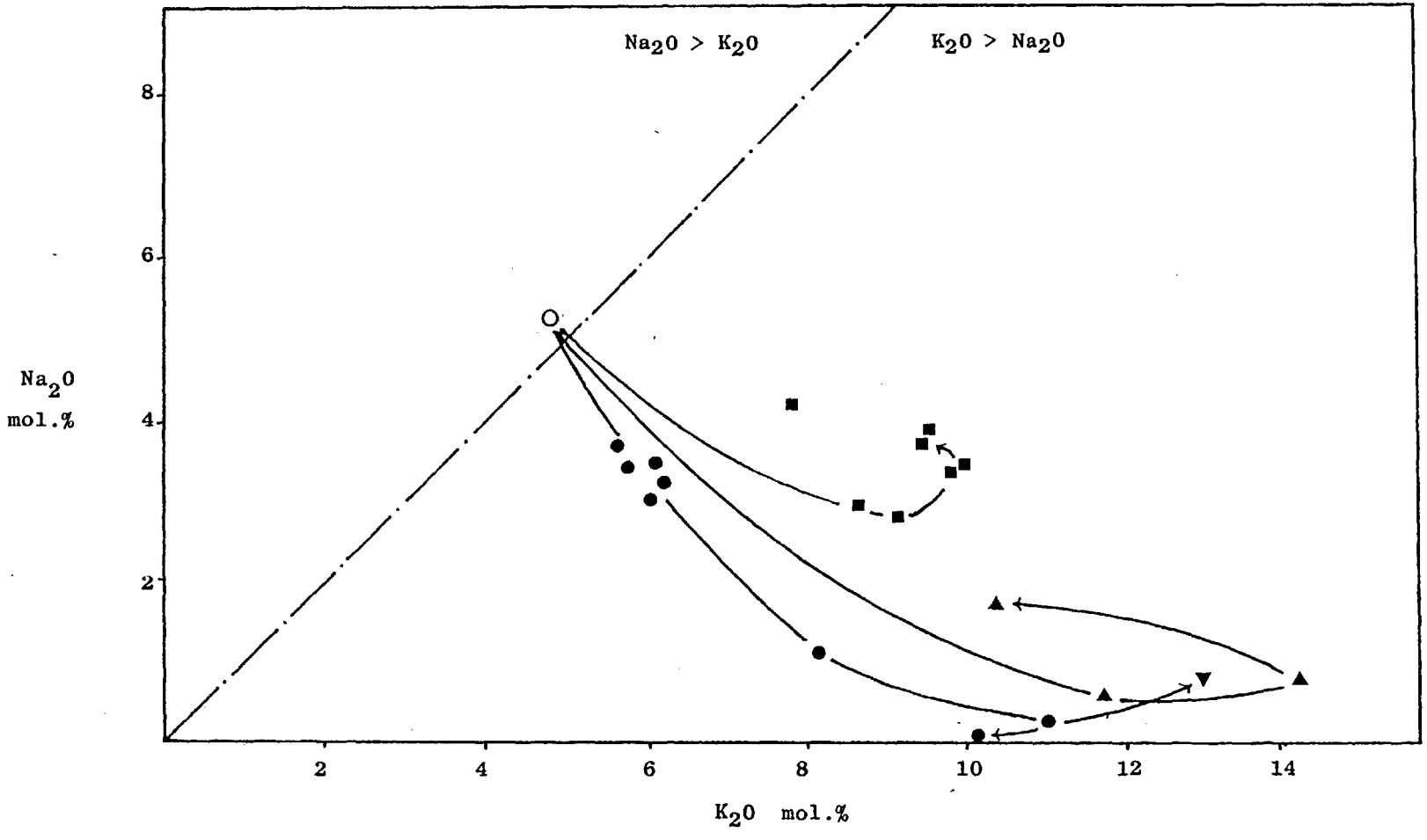

Fig. 4:7 Alkali changes in tourmalinisation and chloritisation at Tregarden Quarry, Luxulyan.
○ 'unaltered' granite ● LX201-208a (chloritised) ▼ LX208b (tourmalinised)
■ LX030-036 (tourmalinised) ▲ LX B1-3,B4-6,008 (tourmalinised; from Lister, 1978a)

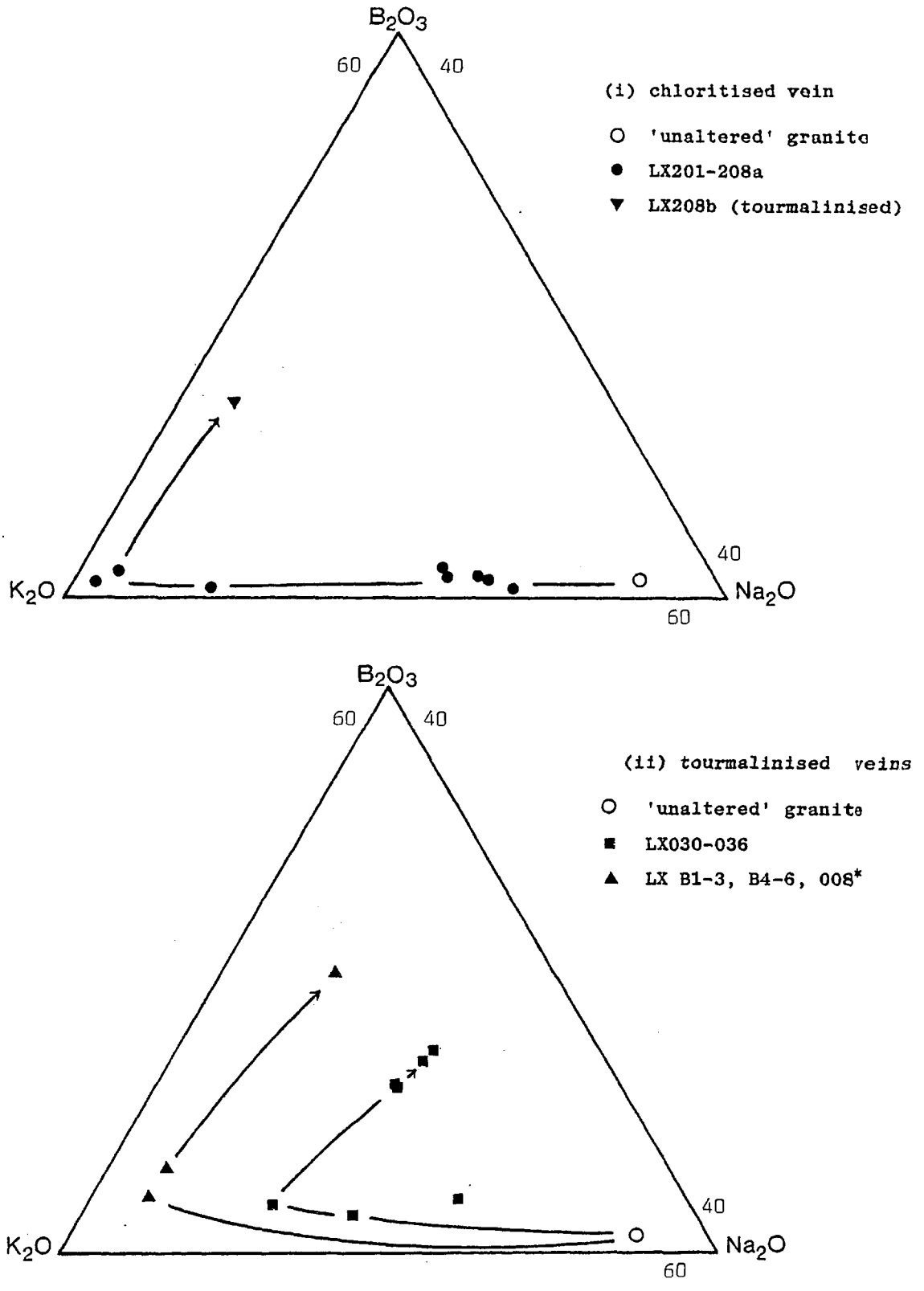

Fig. 4:8 Relationship between boron, potassium and sodium concentrations in rocks from Tregarden Quarry, Luxulyan. (mol.% B_2O_3, K_2O, Na_2O) (* values for K_2O & Na_2O from Lister, 1978a)

seems probable that a front of K-feldspathisation and chloritisation may precede tourmalinisation in this way, and that the tourmaline development may be superimposed upon K-feldspar and chlorite assemblages. However, unlike the examples of zoned alteration profiles described by Alderton (1976; 1979), the Tregarden vein margins are completely gradational, with no sharp boundaries between the products of successive phases of alteration; the phenomena observed could thus have resulted from a single alteration event.

TiO_2 fluctuates around 0.3% in both tourmalinised and chloritised sequences, showing no particular trend with increasing alteration. A few large (1 mm) crystals of almost pure TiO_2 (according to microprobe analyses) are present in the chloritised vein margin, apparently arising by exsolution from altered biotite. Since the corresponding TiO_2 concentrations in the rocks are not enhanced where such crystals occur, they must represent very localised concentrations of otherwise dispersed titanium.

In both tourmalinisation and chloritisation, the P_2O_5 concentrations remain fairly constant, but show a small net increase; presumably, although apatite recrystallises, the amount present does not change significantly.

Boron is the only major or trace element which increases substantially during tourmalinisation but not during chloritisation. This suggests that the two processes are genetically closely related, and that the local availability of boron may be the main factor determining the nature of alteration in a particular vein (or part of a vein). Concentrations of about 1.7% B_2O_3 are recorded in both LX035 and LX208b, and represent about 18% 'normative' tourmaline; as explained in Chapter 2, the actual amount of tourmaline present in these rocks is less than it appears visually, since much of the tourmaline is fine and acicular. The fully chloritised LX208a contains only 0.1% B_2O_3, which equates with about 1% tourmaline; this is

no greater than the tourmaline content of the unaltered granite in the quarry (LX001), although it includes fine, acicular tourmaline as well as the yellow-brown, prismatic variety. By comparison with the above mentioned tourmalinised rocks, luxullianite (LX008) contains 3.6% B_2O_3, which may be equated with 38% tourmaline.

Fluorine (Fig. 4:9) shows a steady decrease with both types of alteration, falling from over 2,500 ppm in the unaltered granite (LX001, and also LX201) to 600 or 700 ppm in the tourmalinised rocks, and 850 ppm in the chloritised LX208a. This trend is unexpected in view of the petrographic and field evidence (Chapter 2). In the chloritised vein margins, purple fluorite can be seen in thin section, apparently replacing biotite along its cleavage lamellae (Plate 2:22), and large (1 mm) purple fluorite crystals occur in the vein centre. Fluorite-bearing joint surfaces are fairly common in some parts of the same quarry. The inference, in the absence of chemical data, would have been that fluorine was introduced by a process perhaps related to tourmalinisation and chloritisation. However, the chemical trend observed indicates that fluorine already present in biotite is released from this mineral during its breakdown. The high fluorine concentrations (1.75%) in Dartmoor biotites (Al-Saleh et al., 1977) have been mentioned above, with reference to Venford Reservoir Quarry. Exley (1959) also reported the fluorine content of the St. Austell 'late lithionite granite' as higher than that of the 'fluorite granite', a fact which he attributed to the high fluorine concentration in micas. It has recently been suggested by Manning (1981b) that the fluorite granites may represent an early stage in the alteration of lithium-mica granite; in this case, primary micas could constitute an important source of fluorine.

Lithium also decreases as a result of tourmalinisation and chloritisation, and, as in the case of fluorine, biotite breakdown is probably the main controlling factor. From nearly 200 ppm in LX201, lithium drops to

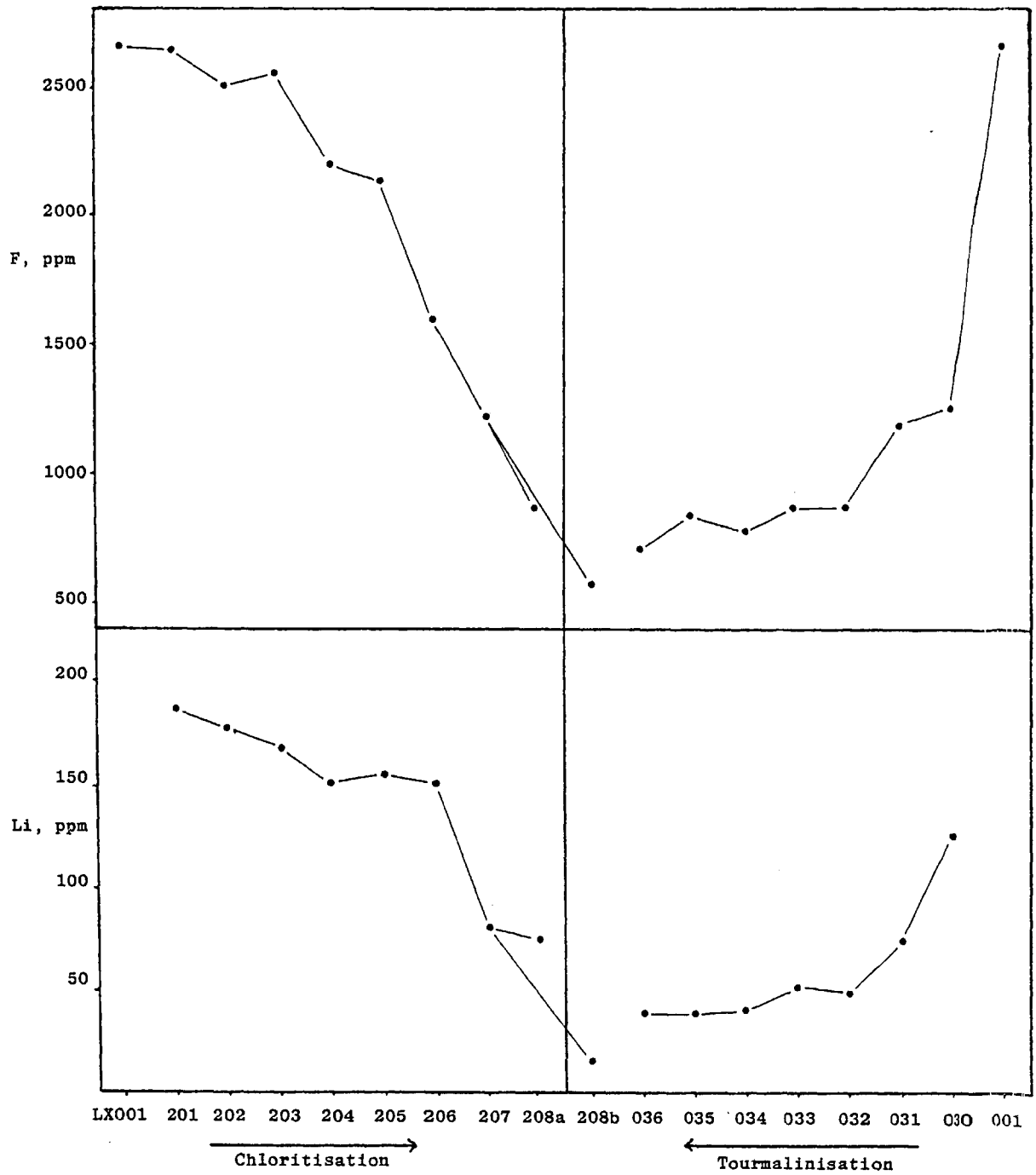

Fig. 4:9 Behaviour of fluorine and lithium in tourmalinisation and chloritisation at Tregarden Quarry, Luxulyan.

75 ppm in the chloritised LX208a, and to 39 and 17 ppm respectively in the two tourmalinised rocks, LX035 and LX208b. The separated tourmaline sample from this locality contains 124 ppm Li; thus in LX208b all the lithium present can be assigned to tourmaline, but LX035 and LX208a contain more lithium than is consistent with their tourmaline content. In the chloritised LX208a, it would be reasonable to assign some of the lithium to muscovite. It is also possible that the fine acicular tourmaline contains more lithium than the separated sample, and this contention is supported by the work of Wilson (1980), whose ion microprobe analyses of a luxullianite sample show that the lithium concentration in the blue-green tourmaline is higher than that in the yellow-brown tourmaline.

Rubidium shows a net increase during both tourmalinisation and chloritisation; the increase correlates with the behaviour of potassium, as shown in Fig. 4:10 (which includes data from Lister, 1978a). Strontium increases slightly during tourmalinisation, but decreases during chloritisation; the difference in behaviour cannot be explained by a difference in strontium content of tourmaline and chlorite, since tourmaline from this locality contains virtually no strontium.

Barium increases substantially during tourmalinisation, from 344 to 628 ppm in the LX030 - 036 sequence, and from 150 to a total of 930 ppm in the sequence LX201 - 208b. The chloritised LX208a also contains nearly 600 ppm barium. Tourmaline from this locality contains no detectable barium, so cannot be the host for this element. However, the positive correlation between barium and potassium (Fig. 4:11) indicates that barium substitution in feldspars may increase with their potassium content; the structural similarity between potassium feldspars and the barium feldspar, celsian ($BaAl_2Si_2O_8$), would facilitate this substitution. It is possible that barium may be transported with solutions responsible for K-feldspathisation, ahead of tourmalinisation fluids.

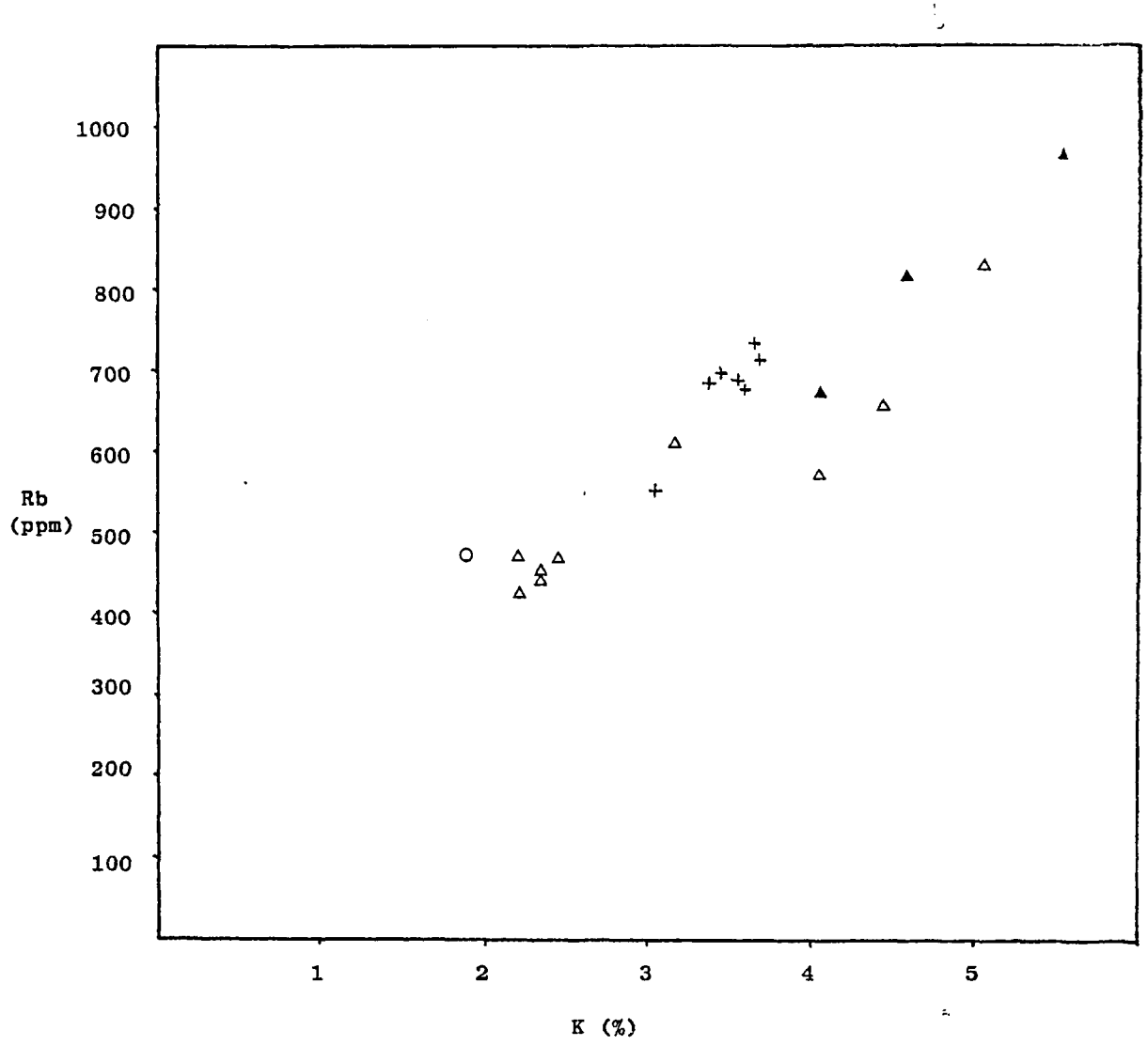

Fig. 4:10 Relationship between K and Rb behaviour in tourmalinisation, Tregarden Quarry, Luxulyan.

○ 'unaltered' granite
△ chloritisation and tourmalinisation (LX201-208a,208b)
\+ tourmalinisation (LX030-036)
▲ tourmalinisation (LX B1-3,LX B4-6, LX008, from Lister, 1978a).

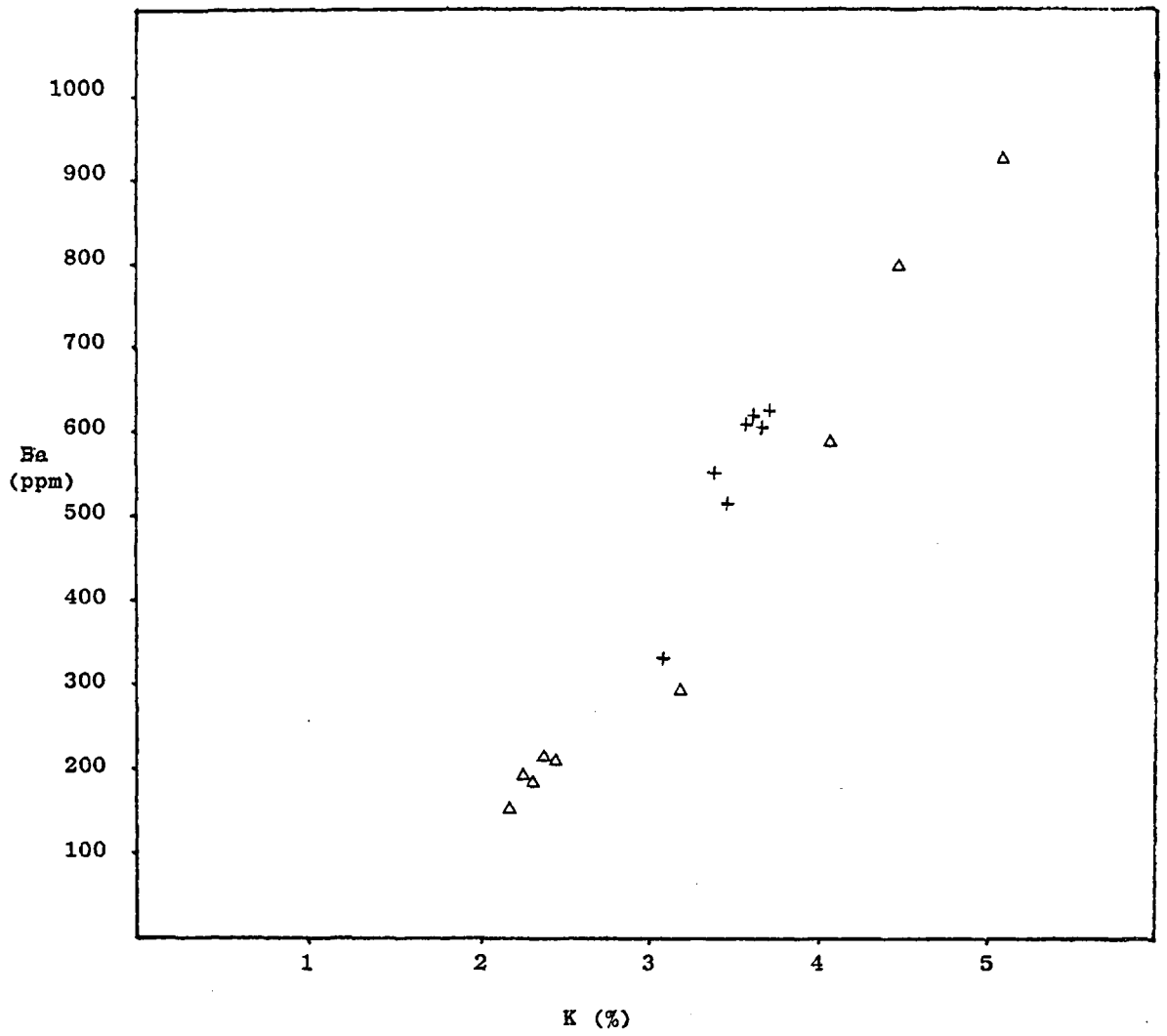

Fig. 4:11 Relationship between K and Ba behaviour in tourmalinisation, Tregarden Quarry, Luxulyan.

△ chloritisation and tourmalinisation (LX201-208a,208b)
\+ tourmalinisation (LX030-036)

Zinc fluctuates, but shows a net increase in tourmalinisation, reaching 105 ppm in LX208b. This increase is not seen in chloritisation. Tourmaline from Tregarden contains nearly 350 ppm zinc, and this could account for the concentrations measured in the whole rocks. Copper increases in the tourmalinised sequence LX030 - 036, but decreases in the chloritised sequence including LX208b. The low levels of copper measured in the rocks may be due to occasional sulphide grains, seen in hand specimen but not identified in thin section, and to the 34 ppm recorded in tourmaline from this locality.

Beryllium shows a net decrease in both sequences, but the concentrations are very low throughout. Zirconium and niobium data are only available for the sequence LX201 to 208a and 208b, which indicates a slight decrease in both elements. The decrease in Zr is too small to imply any major loss of zircon during alteration of the host biotite.

4.4 Goonbarrow China Clay Pit

4.4.1 Results

Chemical analyses of the four samples representing a tourmalinised vein and its margin are given in Table 4:10. Since the granite adjacent to the tourmalinised vein is heavily kaolinised, the exact nature of the unaltered parent granite is uncertain. However, it seems likely (Chapter 2) that the parent granite would have been of the type designated 'early lithionite granite' by Exley (1959), 'poorly megacrystic granite' by Hawkes and Dangerfield (1978), and 'small feldspar granite' by Bray (1980). Chemical data for this unaltered granite type (after Exley, 1959; Exley and Stone, 1964) are included in Table 4:10 for comparative purposes.

The tourmalinised vein represented by sample G8005 shows the combined effects of greisening, tin mineralisation, and intense tourmalinisation, and contains more tourmaline than any other sample in the present study.

	Early lithionite granite	GB002	GB003	GB004	GB005
SiO_2	73.4	72.5	73.1	70.2	43.4
TiO_2	0.10	0.09	0.08	0.09	0.14
Al_2O_3	14.8	15.11	14.22	14.51	28.90
FeO	1.32**	1.66*	1.87*	5.45*	11.17*
MnO	0.01	0.07	0.08	0.19	0.24
MgO	0.32	0.11	0.05	0.07	0.09
CaO	0.87	0.39	0.44	0.63	0.79
Na_2O	2.52	3.77	3.74	2.62	3.53
K_2O	4.63	4.52	4.63	1.86	1.51
P_2O_5	n.d.	0.30	0.31	0.39	0.48
B_2O_3	n.d.	0.77	0.94	2.78	6.34
H_2O^+	n.d.	1.00	0.96	0.87	1.88
(H_2O^-)	n.d.	(0.04)	(0.03)	(0.03)	(–)
CO_2	n.d.	–	0.01	0.01	0.01
F	0.38	0.96	0.93	2.33	3.03
Others		0.27	0.29	0.52	0.49
		101.52	101.65	102.52	102.00
-O=F		0.40	0.39	0.98	1.76
		101.12	101.26	101.54	100.24
F	3800	9600	9300	23250	30300
Li	32	1608	1792	4155	3946
Rb	813	973	1024	893	718
Sr	48	20	22	10	17
Ba	83	–	Tr.	–	–
Zn	n.d.	69	71	167	252
Cu	n.d.	9	7	7	6
Be	n.d.	5	3	3	3

Table 4:10 Chemical analyses of rocks from Goonbarrow China Clay Pit (GB002-5) and of the Early lithionite granite from the St. Austell pluton. (Early lithionite granite values from Exley, 1959; Exley and Stone, 1964).

* Total iron as FeO
** Total iron as Fe_2O_3

– below detection limit
n.d. not determined

oxides %, trace elements ppm

4.4.2 Chemical changes attributable to tourmalinisation

Silica shows a striking reduction from over 70% in the unaltered granite and vein margins to only 43.4% in the tourmalinised vein centre (GB005).

There is a massive increase in alumina from around 15% outside the vein to nearly 29% in GB005. The alumina concentration in the vein centre is in excess of that required by the tourmaline present; the excess may be assigned to topaz, which accounts for the 3% fluorine in the rock.

The increase in iron, from a little over 1% FeO to over 11% FeO is consistent with the development of tourmaline which is predominantly the almost pure iron end-member. Magnesium shows a decrease with tourmalinisation, reflecting the low magnesium concentrations in the tourmaline.

Calcium shows a trend similar to that observed at other localities, namely one of depletion across the tourmalinised vein margin, with a return in the vein centre to a concentration close to that in the unaltered granite. This effect is intensified by kaolinisation of calcic feldspars in the vein margin.

Manganese increases steadily from 0.01% MnO in the unaltered granite to 0.24% MnO in the tourmalinised vein centre. Tourmaline from this locality contains up to about 0.3% MnO, and some manganese may also be held in muscovite. The increase in manganese may be a feature of greisening rather than of tourmalinisation, since neither the Venford nor the Tregarden tourmalinised sequences show such an increase; greisens described by Hall (1971) from Cligga Head do, however, indicate a similar order of manganese increase by comparison with ungreisened granites.

Titanium and phosphorus both increase with tourmalinisation. The titanium may probably be assinged to tourmaline, since the brown variety in these rocks is titaniferous. The phosphorus increase may represent a slight increase in the proportion of apatite present.

The vein centre (G8005) contains 6.34% B_2O_3, and this concentration may be equated with over 60% tourmaline in the rock, which is therefore the most intensely tourmalinised rock examined in the present study. No boron value is available for the unaltered granite, but Exley's (1959) modal analysis figure of 3.8% tourmaline would indicate about 0.3 to 0.4% B_2O_3.

In considering the sodium and potassium concentrations, the effects of kaolinisation at the vein margin must be taken into account. Hence, at this locality, the changing ratio of K_2O:Na_2O across the vein margin does not reflect the consequences of progressive tourmalinisation alone. The mol. ratio K_2O:Na_2O decreases from over 1 in the unaltered granite to 0.28 in the tourmalinised vein centre; this trend contrasts with those observed at Venford Reservoir and Tregarden. However, a trend of decreasing potassium is unlikely to be due to kaolinisation, since Exley and Stone's (1964) analyses of kaolinised granites indicate increasing potassium. According to these authors, sodium feldspar is more susceptible to kaolinisation than is potassium feldspar, and hence kaolinised granites frequently retain K_2O while losing Na_2O, until an advanced stage of alteration is reached. In the vein centre, sodium is in excess of that required for the tourmaline present, and in the absence of other sodium-bearing minerals, may probably be assigned to residual feldspar. Muscovite may account for virtually all the potassium present in the centre and margin of the vein. It seems possible that this tourmalinised vein was associated not with K-feldspathisation, but perhaps by albitisation, which may have rendered the surrounding granite more susceptible to later kaolinisation processes.

Fluorine and lithium both show a considerable increase with tourmalinisation. The increase in fluorine from 0.38% to over 3% in the vein centre is reflected in the development of topaz. Lithium rises from about 30ppm in the granite to some 4000 ppm in the tourmalinised rock; tourmaline is, however, unlikely to be the major host for this element, for two reasons.

Firstly, the lithium concentrations do not correlate with the tourmaline contents of the rock samples. Secondly, it has been shown by Wilson (1980) that the muscovite at Goonbarrow is more lithium-rich by an order of magnitude than the tourmaline. Hence, most of the lithium present in these rocks can probably be assigned to muscovite.

Rubidium behaviour follows that of potassium. Strontium, barium, copper and beryllium are all depleted in tourmalinisation. Zinc increases from 69 ppm at the vein margin to 252 ppm in the vein centre (no zinc value is available for the unaltered granite).

4.5 Cape Cornwall

4.5.1 Results

Chemical analyses of two progressively more tourmaline-rich sequences from the Porthledden tourmalinite may be found in Tables 4:11 and 4:12. Sample CC010 is tourmaline granite, from 1 metre below the subhorizontal contact with tourmalinite. Samples CC011 to 015 span about 15 cm covering the gradational and greisened contact between the two rock types. Samples CC001 to 005 are taken from one of the layered units within the tourmalinite, and show the range of chemical composition observed. It seems possible (Chapter 2) that the parent rock for both tourmaline granite and tourmalinite may have been the 'Priest's Cove microgranite' of Charoy (1979a), and this author's chemical analysis has already been given for comparison in Table 4:3.

4.5.2 Chemical changes during progressive tourmalinisation, and the chemical variation within the tourmalinite

The tourmalinite is a very quartz-rich rock by comparison with other tourmalinised rocks examined in the present study. Within the tourmalinite, silica fluctuates between about 70% and over 88%, depending upon the relative

	CC010	CC011	CC012	CC013	CC014	CC015	CC001	CC002	CC003	CC004	CC005
SiO_2	73.1	71.3	74.1	75.4	75.4	75.6	86.6	86.1	88.4	77.2	70.5
TiO_2	0.03	0.04	0.06	0.06	0.05	0.06	0.02	0.02	0.02	0.05	0.07
Al_2O_3	14.06	16.71	13.72	12.86	12.21	13.15	5.64	6.29	4.72	11.36	14.32
FeO*	2.27	2.81	4.45	4.95	5.07	6.04	2.99	2.92	2.85	5.74	7.82
MnO	0.02	0.03	0.04	0.04	0.04	0.05	0.03	0.03	0.03	0.05	0.06
MgO	0.06	0.05	0.06	0.08	0.09	0.10	0.05	0.05	0.05	0.09	0.11
CaO	0.32	0.35	0.57	0.44	0.37	0.38	0.44	0.50	0.54	0.68	0.64
Na_2O	0.59	0.66	0.70	0.74	0.74	0.89	0.47	0.46	0.43	0.79	1.05
K_2O	7.08	5.72	2.01	1.04	1.19	0.09	0.54	0.73	0.10	–	–
P_2O_5	0.42	0.32	0.39	0.29	0.25	0.23	0.29	0.34	0.35	0.42	0.43
B_2O_3	1.13	1.46	2.48	2.71	2.83	3.45	1.61	1.69	1.60	3.29	4.21
H_2O^+	0.98	0.83	1.18	1.07	0.97	0.76	0.60	0.56	0.51	0.82	1.10
(H_2O^-)	(0.28)	(0.09)	(0.13)	(0.10)	(0.07)	(0.08)	(0.04)	(0.05)	(0.04)	(0.05)	(0.05)
CO_2	0.03	0.02	0.02	0.02	0.01	0.01	–	–	–	–	–
F	0.15	0.24	0.30	0.30	0.30	0.34	0.18	0.20	0.18	0.33	0.40
Others	0.08	0.08	0.04	0.03	0.04	0.02	0.02	0.02	0.01	0.02	0.03
	100.32	100.62	100.12	100.03	99.56	101.17	99.48	99.91	99.79	100.84	100.74
-O=F	0.06	0.10	0.13	0.13	0.13	0.14	0.08	0.08	0.08	0.14	0.17
	100.26	100.52	99.99	99.90	99.43	101.03	99.40	99.83	99.71	100.70	100.57

Table 4:11 Chemical analyses of rocks from Cape Cornwall (major elements, % oxides)

- = below detection limit * total iron as FeO

	CC010	CC011	CC012	CC013	CC014	CC015	CC001	CC002	CC003	CC004	CC005
F	1455	2355	2985	3015	2970	3435	1845	1965	1800	3285	4020
Li	42	74	90	89	86	104	65	64	57	86	108
Rb	535	569	252	154	133	11	53	70	5	-	-
Sr	21	17	7	4	5	5	5	6	5	6	7
Ba	131	69	-	-	-	-	3	-	-	-	Tr.
Zn	72	53	79	74	201	96	63	56	47	117	130
Cu	4	7	2	-	-	10	6	5	4	8	7

Table 4:12 Chemical analyses of rocks from Cape Cornwall (trace elements, ppm)

- below detection limit

proportions of quartz and tourmaline. From over 73% SiO_2 in the tourmaline granite (CC010), silica drops to just over 71% in the greisened CC011, before rising to nearly 76% in the tourmalinite sample CC015.

Alumina within the tourmalinite shows an inverse relationship with silica, and varies between 5.6% and over 14%. The variation in Al_2O_3 within the tourmalinite and across the transitional zone is compared with that of K_2O and B_2O_3 in Fig. 4:12. In order to illustrate a sequence from 'unaltered biotite granite through tourmaline granite into tourmalinite, the data of Charoy (1979a) for the Priest's Cove microgranite and the tourmaline granite are included in this diagram (for Charoy's analyses see Table 4:3 at the beginning of this chapter). Within the tourmalinite (CC014, 015, 001-005) Al_2O_3 correlates with B_2O_3, and reflects the proportion of tourmaline present In the granites and the transition zone, however, there is no such correlation. The most aluminous rock is the greisened CC011, which shows many similarities to the tourmalinised end-products at other localities, since it contains nearly 1.5% B_2O_3 and a relatively high potassium concentration. In the tourmaline granite and the transition zone, the combined effects of tourmalinisation, greisening and K-enrichment are observed; above the transition zone, where tourmalinisation is more intense, muscovite and potassium feldspar are eliminated in favour of tourmaline and quartz.

K_2O increases from the biotite granite (Priest's Cove microgranite) into the tourmaline granite, reaching its maximum concentration in the upper part of the tourmaline granite (CC010), where the feldspar is mostly potassium-rich, and muscovite is becoming an important secondary mineral. This 'K-silicate' alteration assemblage becomes potassium-depleted upwards, as the potassium-bearing phases are replaced by tourmaline and quartz. Within the tourmalinite, K_2O is strongly depleted, except where a small amount of residual feldspar or mica is present (e.g. in CC002).

The potassium-rich, greisened zone is depleted in several other major

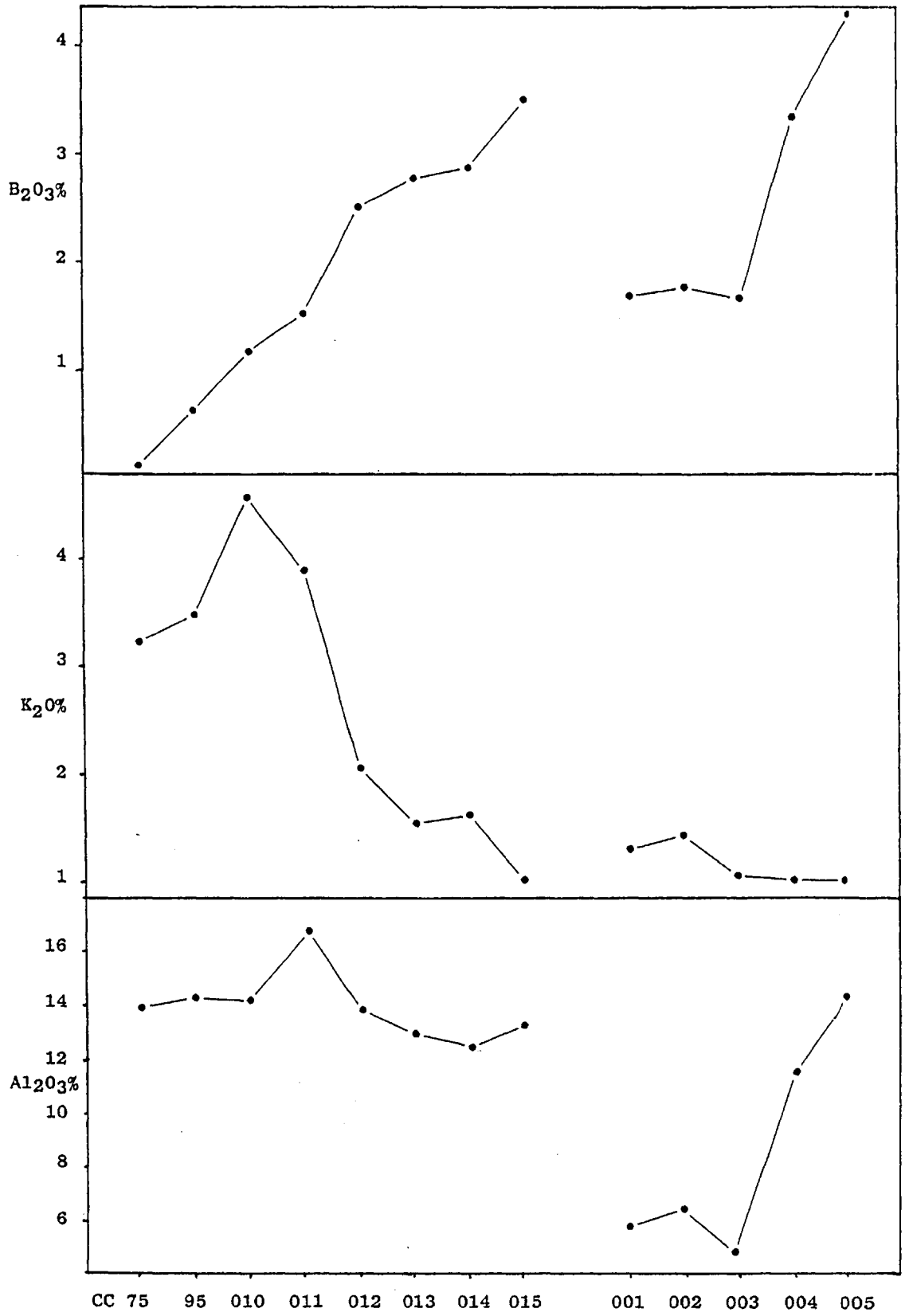

Fig. 4:12 Behaviour of boron, potassium and aluminium in progressive tourmalinisation (CC75, 95, 010-15), and within the tourmalinite (CC001-5) at Cape Cornwall.
(CC75 and CC95 from Charoy, 1979a)

and trace elements, notably sodium, iron, fluorine and lithium (Fig. 4:13). Na_2O drops from around 3% to only 0.6% in the upper part of the tourmaline granite and greisened zone; the corresponding sharp rise of K_2O indicates that a major alkali change probably occurs in the feldspars. After sodium feldspars are eliminated (CC011-015; CC001-005), the Na_2O concentration reflects the tourmaline content of the rock. FeO decreases between biotite granite and tourmaline granite, presumably as a result of biotite breakdown. Charoy(1979a) recorded $FeO > Fe_2O_3$ in the biotite granite, but $Fe_2O_3 > FeO$ in the tourmaline granite; this may account for the reddening of the tourmaline granite, and also indicates that some of the biotite has broken down to give muscovite and iron oxides, rather than being directly replaced by tourmaline. This zone of reddening, oxidation of iron, and depletion in certain elements is analogous to the reddened granite at Venford Reservoir Quarry, which likewise was found between granite and tourmalinised rock.

Fluorine and lithium (Fig. 4:13) also show similar patterns to those observed at Venford Reservoir. The biotite granite contains about 4000 ppm fluorine, and this concentration is decreased to a little over 1000 ppm in the tourmaline granite before rising to around its original level in the tourmalinite. According to Charoy (1979a), some of the fluorine in the tourmalinite is present in fluorapatite, which is most abundant in the more tourmaline-rich parts; there is a general correlation between F, CaO and P_2O_5 in these rocks (apart from the biotite and tourmaline granites), but this effect is difficult to isolate from the increasing tourmaline trend. Lithium reaches nearly 1000 ppm in the biotite granite, but drops to only about 50 ppm in the tourmaline granite, presumably due to biotite breakdown; there is then a steady rise in lithium concentration, which correlates with the amount of tourmaline in the rock. The highest Li concentration in the tourmalinite is just over 100 ppm.

Magnesium and titanium also show trends of depletion in the tourmaline

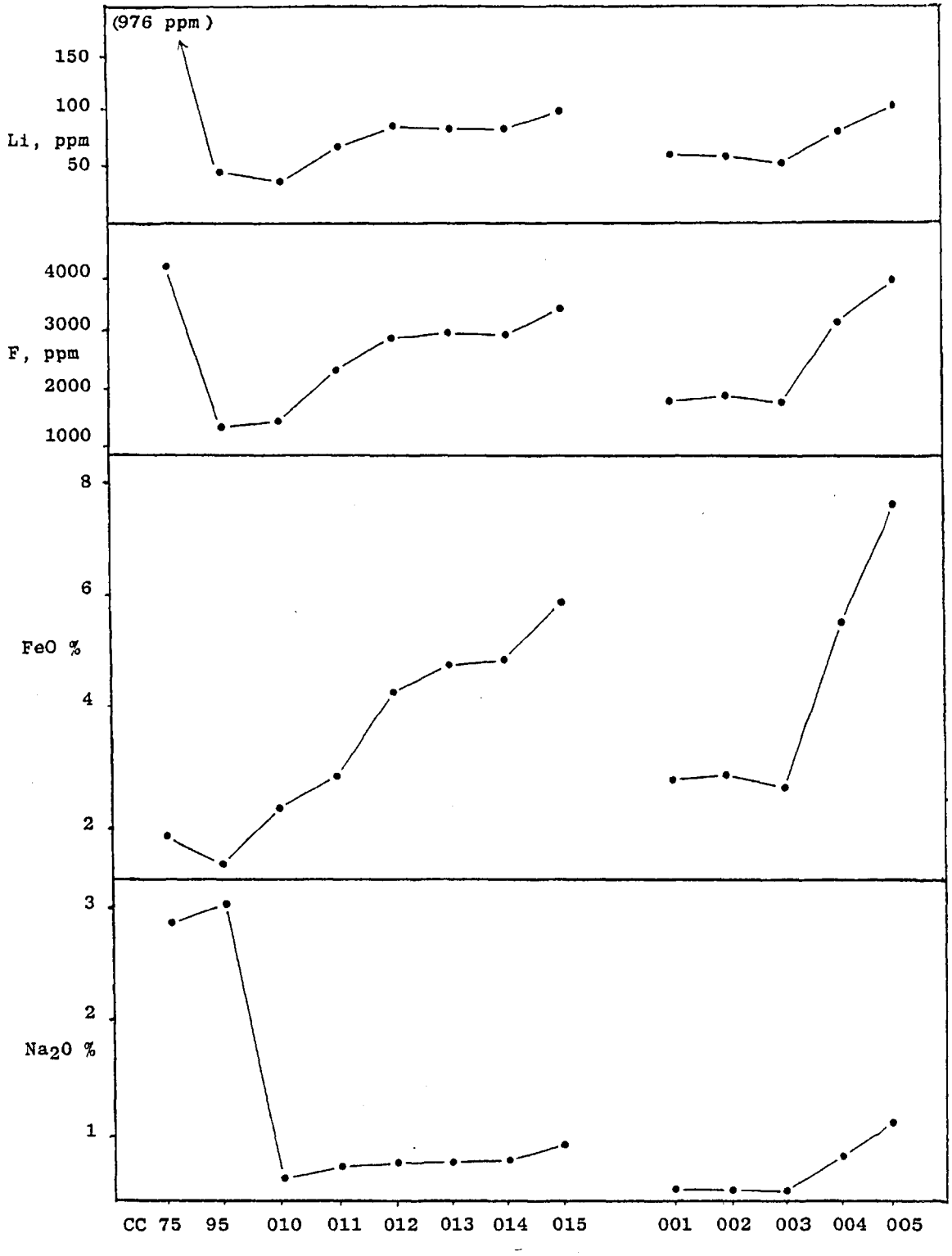

Fig. 4:13 Chemical variation in progressive tourmalinisation (CC75, 95, 010-015) and within the tourmalinite (CC001-5) at Cape Cornwall. (CC75 and CC95 from Charoy, 1979a)

granite, followed by a small but steady increase with increasing tourmalinisation. Manganese is very low in the biotite granite, and shows a steady increase throughout the sequence into tourmalinite. MgO, TiO_2 and MnO are all present in very small concentrations (nearly always less than 0.1%), and can probably be assigned to the iron-rich tourmaline.

The behaviour of rubidium follows that of potassium. Strontium and barium are depleted in tourmalinisation. Copper and zinc are present in fluctuating concentrations (zinc up to 200 ppm), which probably reflect the sporadic occurrence of sulphide grains within the tourmaline granite and tourmalinite.

4.6 Discussion of tourmalinisation geochemistry, and comparison of observations from different localities

The vertical tourmalinised veins all appear to have been formed in open systems, from which chemical components were allowed to escape (this is not necessarily true of the Cape Cornwall tourmalinite, which may have been confined beneath an impermeable roof). It may be assumed that constant volumes were maintained during alteration, since the tourmalinised rocks were formed by <u>in situ</u> modification of existing granites, with lateral dilation restricted to a maximum of a few millimetres. The chemical gains and losses observed in progressive tourmalinisation are summarised in Figs. 4:14 to 4:17.

Nearly all the tourmalinised sequences show, with progressive tourmalinisation, a decrease in silica, and an increase in Al_2O_3 and FeO + MgO, which is roughly proportional to the B_2O_3 content of the rocks. The extreme end product of this trend should be a rock consisting entirely of tourmaline, with about 35% SiO_2, 35% Al_2O_3, 10% B_2O_3, up to 20% FeO, MgO, &c., and a few % H_2O. Exceptions to this trend are shown by the smaller tourmalinised vein at Venford Reservoir, and the Cape Cornwall tourmalinite, both of which

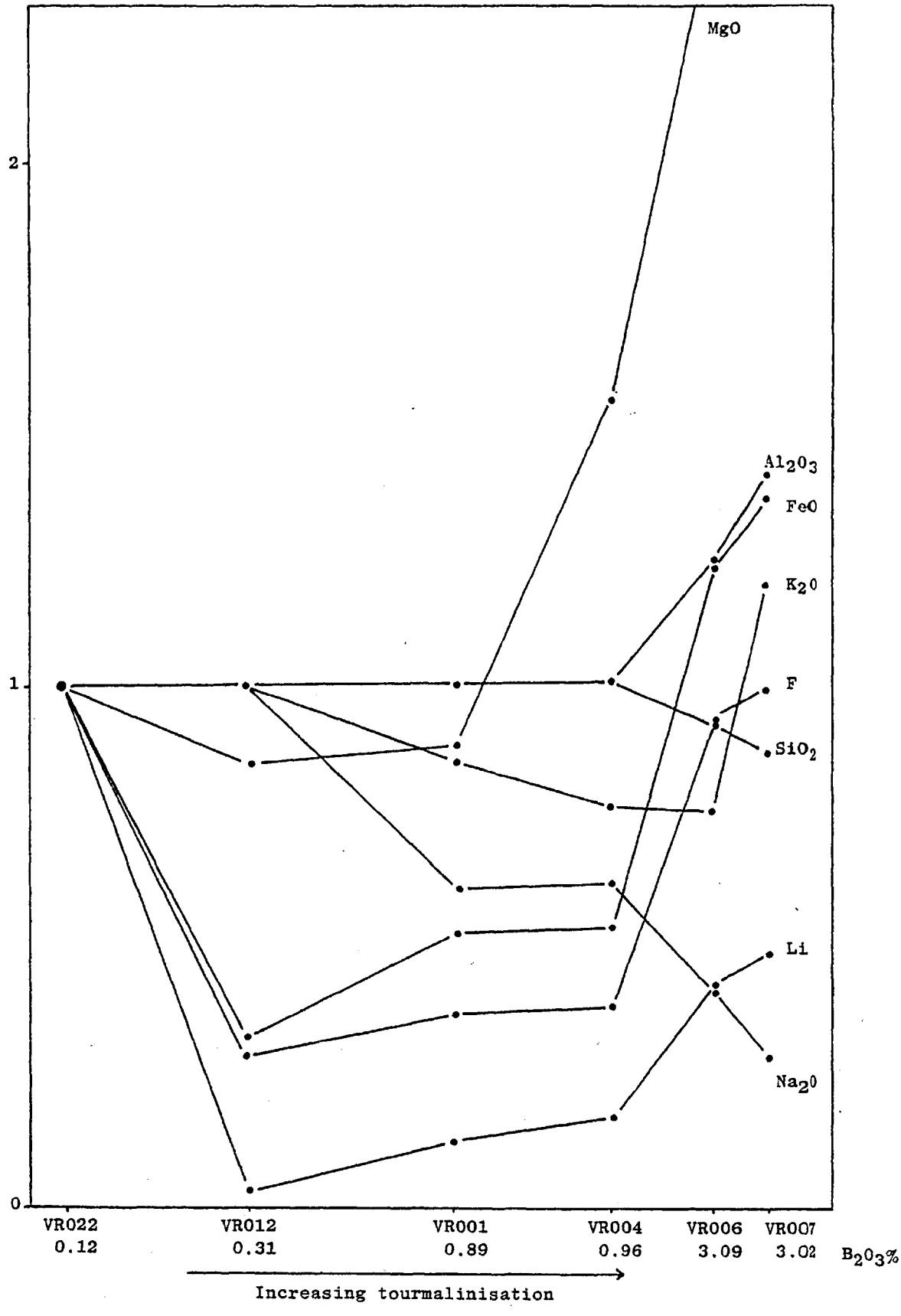

Fig. 4:14 Relative concentration changes in progressive tourmalinisation at Venford Reservoir Quarry.

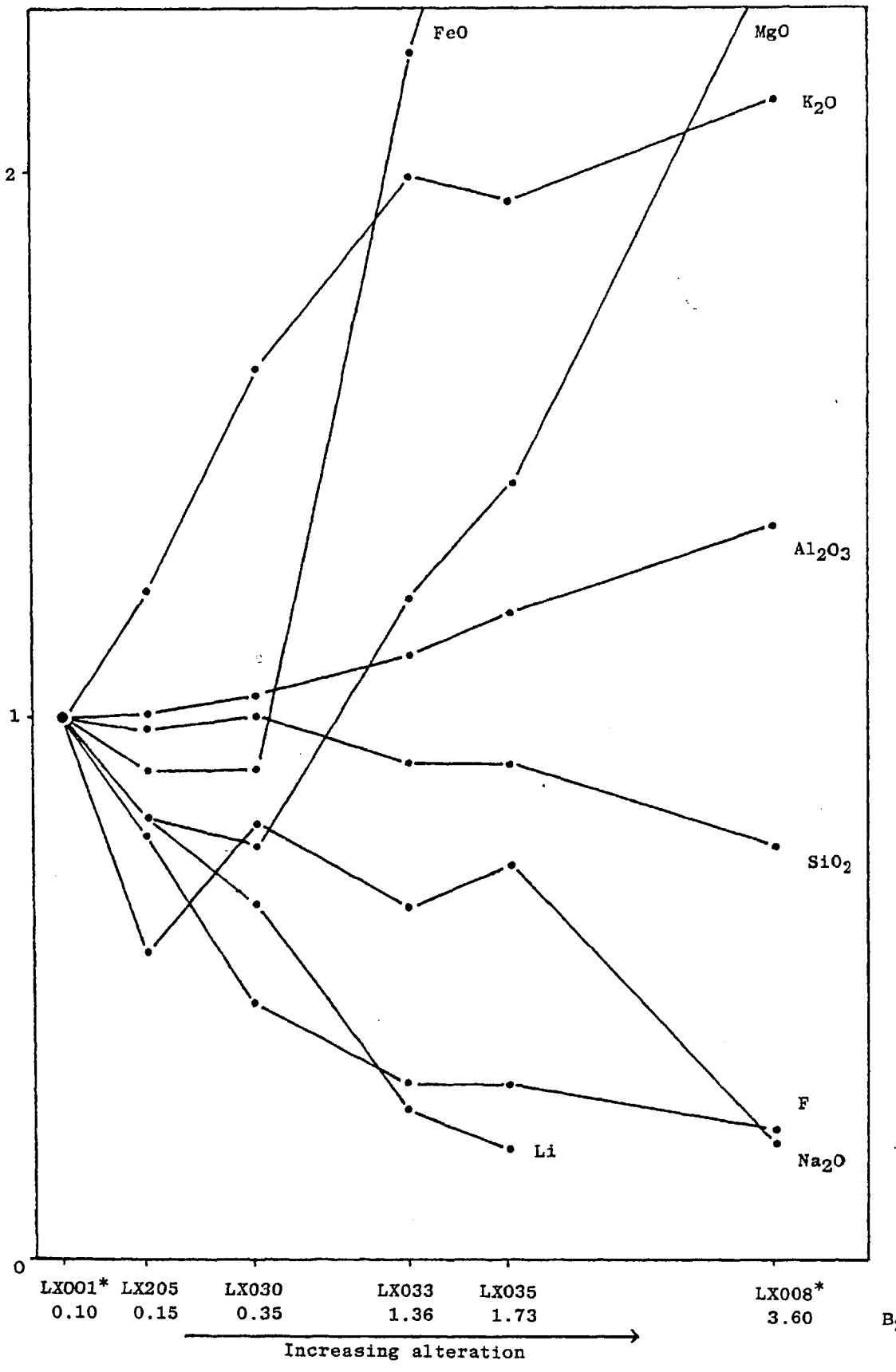

Fig. 4:15 **Relative concentration changes in tourmalinisation and chloritisation at Tregarden Quarry, Luxulyan. (LX001 values from Lister, 1978a, except SiO_2, Li and F)**

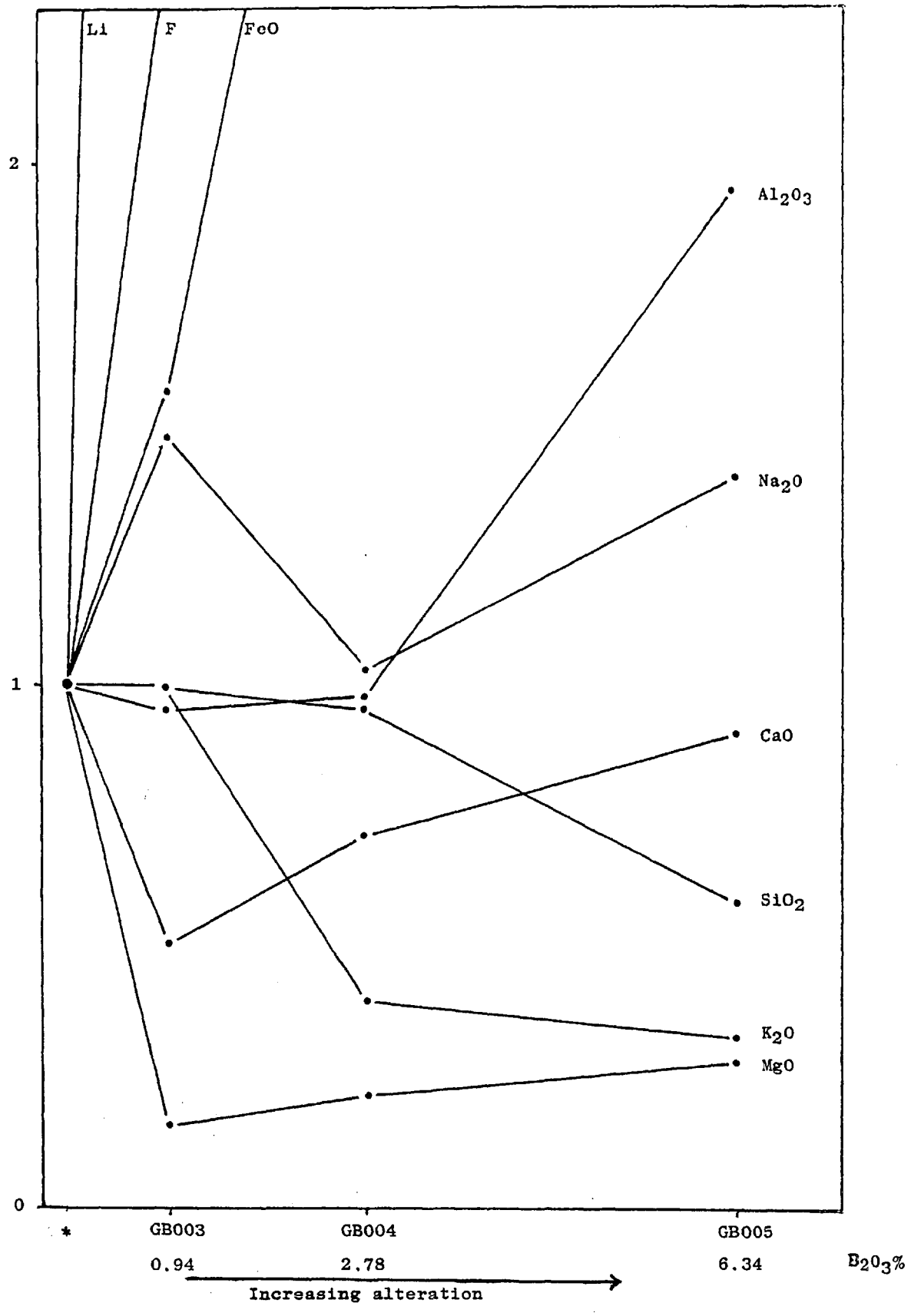

Fig. 4:16 **Relative concentration changes in tourmalinisation associated with greisening and tin mineralisation at Goonbarrow China Clay Pit.**
(* = Early lithionite granite; values from Exley, 1959, and from Exley and Stone, 1964)

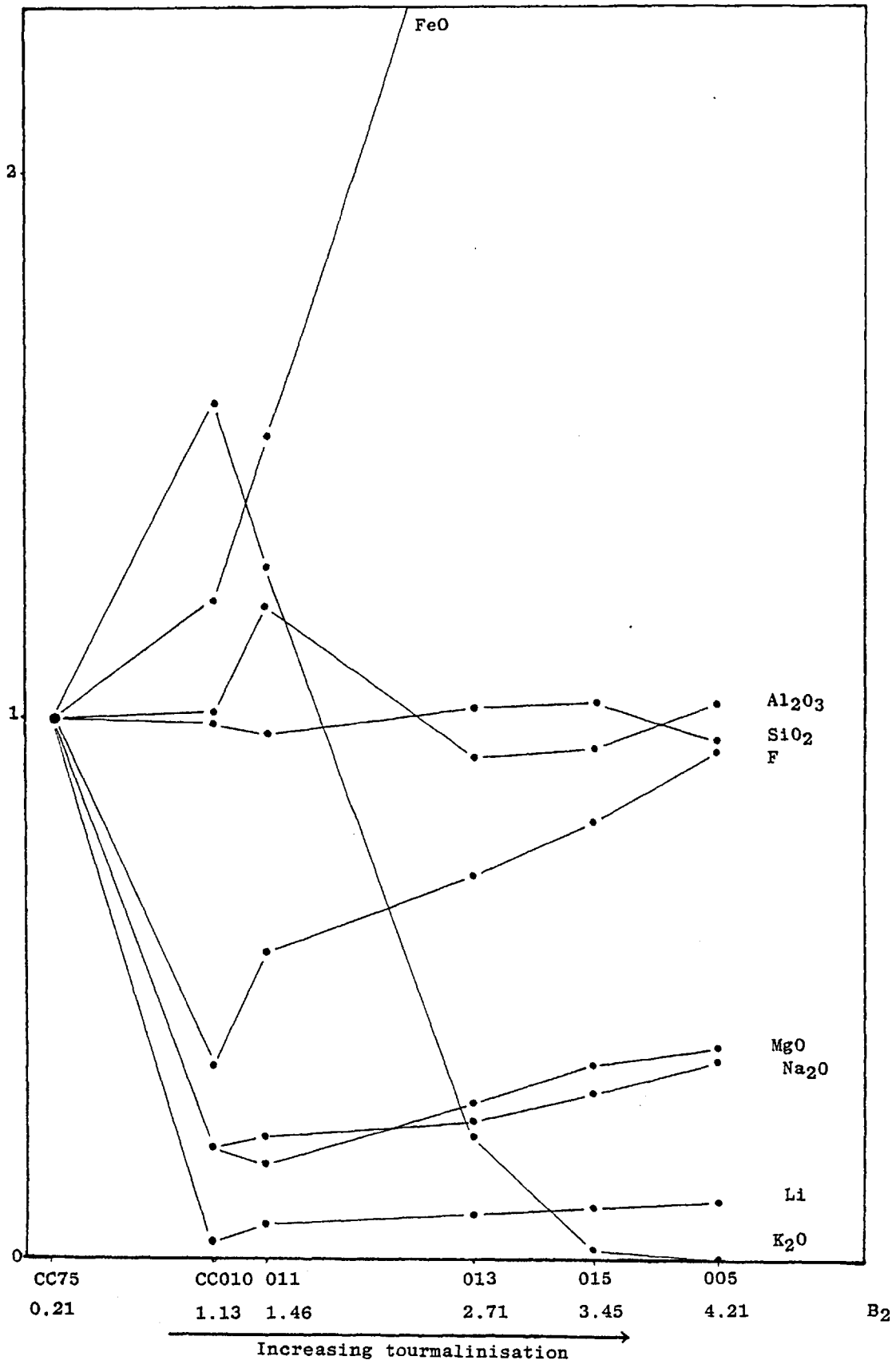

Fig. 4:17 Relative concentration changes in tourmalinisation (and silicification) at Cape Cornwall. (CC75 = Priest's Cove microgranite; values from Charoy, 1979a)

contain relatively high SiO_2 and low Al_2O_3. However, the transitional zone passing upwards into the Cape Cornwall tourmalinite has a similar composition to the tourmalinised vein material at other localities (particularly Tregarden Quarry).

The behaviour of potassium and sodium during tourmalinisation is complex. At Venford Reservoir, the K_2O:Na_2O ratio shows an increase which correlates roughly with the tourmaline content of the rock, although the most tourmaline-rich rock (VR006) is not the most potassic. At Tregarden and Cape Cornwall, the K_2O:Na_2O ratio increases with progressive tourmalinisation, up to B_2O_3 concentrations of about 1.5%; with more intense tourmalinisation, potassium bearing phases are replaced by tourmaline, so that a lower K_2O:Na_2O ratio results. At Venford Reservoir and Goonbarrow, there is evidence for the stability of sodium feldspar, in conditions of intense tourmalinisation (3% and over 6% B_2O_3 respectively, in the fully tourmalinised rocks).

Experimental work has shown that K:Na in the fluid phase increases as a function of temperature (Orville, 1963), and that this effect is intensified in the presence of chlorides (Lagache and Weisbrod, 1977) and of boron (Pichavant, 1979). If these findings are applicable to hydrothermal, tourmalinising systems, it will be logical to find albite in the centres of heavily tourmalinised veins, but orthoclase or microcline at the lower temperature vein margins and in chloritised veins. This is also consistent with the theory of a K-feldspathisation and chloritisation front preceding tourmalinisation. Evidence from Tregarden indicates that chloritisation shows close chemical similarities to tourmalinisation, and may result from the same process operating in conditions of relative boron depletion. If tourmalinising and chloritising agents rise upwards from a reservoir below the site of alteration, the same vein might be tourmalinised at depth and chloritised nearer the surface, where the boron content of the solutions had become

exhausted. High temperatures and boron concentrations at depth could raise the K:Na ratio in the fluid phase, so that the upward migration of this fluid would promote K-feldspathisation as an accompaniment to chloritisation at higher levels. Continuing tourmalinisation could superimpose a tourmaline bearing assemblage upon the precursor K-rich, chloritised assemblage. The formation of chlorite is probably restricted to conditions of low temperature and boron depletion, and hence is not apparent at Venford Reservoir, Goonbarrow or Cape Cornwall.

Enrichment in fluorine and lithium is often regarded as almost synonymous with tourmalinisation, but the present study has shown that this is not necessarily true. The tourmaline varieties in Cornubian tourmalinised rocks are mostly members of the schorl-dravite series, and although they may contain small concentrations of fluorine and lithium (Chapter 5), these concentrations are in most cases lower than those in the micas of the unaltered granite. At all localities except Goonbarrow, the tourmalinised rocks contain either less F and Li, or the same amount, by comparison with the untourmalinised rock, and the evidence indicates that these elements are not introduced, but released, by the tourmalinisation process. It is possible that the behaviour of F and Li may be controlled by the intensity of tourmalinisation, and perhaps ultimately by the temperature. Table 4:13 shows that with B_2O_3 concentrations up to 1.73% (Tregarden, and Cape Cornwall transitional zone) F and Li are both lost in tourmalinisation, while at B_2O_3 concentrations of about 3 and 4% (Venford and Cape Cornwall tourmalinite) Li is lost but F is unchanged with respect to the unaltered granite, and at a B_2O_3 concentration of 6.34% (Goonbarrow) both F and Li are increased in the tourmalinised rock.

At Venford Reservoir, the reddened zone between unaltered granite and the main tourmalinised vein shows depletion in several major and trace elements, and in this respect resembles Chauris' (1965) zone of 'blanchissement'. Oxidation of iron on biotite breakdown is probably the cause of

	Max. B_2O_3%	Chemical gains in tourmalinisation	Chemical losses in tourmalinisation
Tregarden chloritised vein	0.18	Al,Fe,Mg,K, Rb,Sr,Ba,Zn	Si,Na, F,Li
Tregarden tourmalinised vein	1.73	Al,Fe,Mg, K,Rb,Ba	Si,Na, F,Li
Venford Reservoir	3.09	Al,Fe,Mg, K,Sr,Zn	Si,Na, Rb,Li
Cape Cornwall transition zone	1.46	Al,Fe,K Ba	Si,K,Mg,Rb, Sr, F,Li
Cape Cornwall tourmalinite	4.21	Al,Fe,Zn	Na,K,Mg,Rb, Sr,Li,Ba
Goonbarrow	6.34	Al,Fe,Mg,Li, F,Mn,Zn,Sn	Si,K,Rb

Table 4:13 Chemical gains and losses associated with different tourmalinisation intensities (B_2O_3%)

reddening. Chauris' (1965) bleached zone also shows mainly ferric iron, by contrast to the mainly ferrous iron recorded in his unaltered granite; it is not clear why bleaching rather than reddening should occur in these conditions. A much narrower zone of depletion in certain elements is also seen at Tregarden, where the tourmalinised vein margin is more strongly affected than is the chloritised vein margin. The Cape Cornwall tourmaline granite and transitional zone into tourmalinite likewise show depletion in several elements by comparison with concentrations in either the biotite granite or the tourmalinite. This effect could be achieved simply by the passage of water through the system, initiating biotite breakdown prior to tourmalinisation, and leaching ions out of the rock. Where biotite replacement by tourmaline is observed (Venford Reservoir and Tregarden), this may be either a direct replacement process or a two-stage process, as described in Chapter 2. Where a two-stage process is involved, the first stage in which biotite is converted to chlorite and muscovite (Tregarden) or to hydromuscovite and alkali feldspar (Venford Reservoir) does not require the introduction of any extraneous components other than water, as shown in the following equations:

(i) $10\ \underset{\text{biotite}}{K_2(Fe,Mg,Ti)_2AlSi_3O_{10}(OH)_2} + 6H_2O \longrightarrow \underset{\text{chlorite}}{(Fe,Al,Mg)_{12}(Si,Al)_8O_{20}(OH)_{16}} + \underset{\text{muscovite}}{K_2Al_6Si_6O_{22}(OH)_4} + TiO_2 + 9K_2O + 4Fe_2O_3 + 5FeO + 18SiO_2 + 6H_2$

(ii) $10\ \underset{\text{biotite}}{K_2(Fe,Mg,Ti)_2AlSi_3O_{10}(OH)_2} \xrightarrow{H_2O} \underset{\text{hydromuscovite}}{2KAl_2(OH)_2AlSi_3(O,OH)_{10}} + \underset{\text{feldspar}}{4KAlSi_3O_8} + TiO_2 + 7K_2O + 2MgO + 8Fe_2O_3 + FeO + 12SiO_2 + 2O_2$

(In biotite, Fe:Mg:Ti = 17:2:1; in chlorite, Fe:Al:Mg = 4:2:2, & Si:Al = 6:2).

Tourmaline could form from biotite (or its breakdown products) and sodium feldspar, with the introduction of boron to the system. However, if only boron were introduced, then six units of biotite would be required to produce one unit of tourmaline, the most important constraint being the supply of aluminium. If both boron and aluminium were introduced (although not necessarily in the forms stated), the following reaction might occur:

$$10\ \underset{\text{biotite}}{K_2(Fe,Mg,Ti)_2AlSi_3O_{10}(OH)_2} + 6NaAlSi_3O_8 + 9B_2O_3 + 12Al_2O_3 \rightarrow \underset{\text{tourmaline}}{6Na(Fe,Mg)_3Al_6Si_6O_{18}(BO_3)_3(OH)_4} + \underset{\text{feldspar}}{4KAlSi_3O_8} + TiO_2 + FeO + 8K_2O + 2H_2O$$

(Biotite, Fe:Mg:Ti = 17:2:1; tourmaline, Fe:Mg = 16:2)

While this demonstrates that in theory, tourmaline could be formed by replacement of biotite and feldspar with very few chemical additions to the system, it is clear from the relative proportions of biotite and tourmaline in the rocks that the total tourmaline content of the veins could not be produced without the introduction of additional ions, especially iron and magnesium. The chemical components required for tourmaline formation could either be introduced in solution along with boron, or they could be leached from the depleted zones adjacent to tourmalinised veins and thus taken up by boron-bearing solutions. A leaching process of this kind might involve large volumes of rock, extending to a considerable depth within the granite, and therefore its feasibility is difficult to assess, simply on the evidence of the present surface exposure.

To produce the tourmalinised rocks examined in the present study, by alteration of the parent granites, the necessary additions to the system are boron, aluminium, and to a lesser extent iron and magnesium. Accepting that some iron and magnesium may be leached from surrounding granite, boron and aluminium still need to be supplied from an extraneous source, since there is no evidence that leaching of granite could produce an excess of these elements

If the Cornubian granites were formed, at least in part, by assimilation of country rocks (and there is ample evidence from xenoliths, to suggest that this was locally an important process), then the largely pelitic sediments would have supplied aluminium, perhaps in considerable excess. Boron is also well known to be more concentrated in pelitic sediments than in most other rock types, due to its adsorption onto illite and other clay minerals (Chapter 1). Intercalated volcanics of the culm synclinorium could have been an abundant source of iron and magnesium, whether themselves assimilated into the granite or subjected to hot groundwater circulation; it has already been suggested (Hosking, 1964, p.236) that certain metalliferous deposits in Cornwall could have been concentrated from such a source.

However, for boron to be assimilated into the granite along with the pelitic sediment, this element would have to be conserved within the sediment through a considerable degree of thermal metamorphism before reaching the granite-killas boundary. Boron is expelled in the transition from illite to muscovite, which, according to Muffler and White (1969), can occur at temperatures below 210°C; the adsorbed boron may thus be released into solution and carried with circulating groundwater, or may be fixed in tourmaline which can form as a metamorphic rather than a metasomatic mineral in the lower greenschist facies (Landergren and Carjaval, 1959). Since tourmaline in the Cornubian killas is generally restricted to hydrothermal occurrences, it seems unlikely that much boron was in fact fixed in tourmaline at this stage. Boron from illite conversion entering the circulating groundwater (or hydrothermal systems) could, however, be carried in solution to the granite-killas boundary to supply tourmalinising fluids within the granite. Tourmaline precipitation would be inhibited if this solution were more than weakly acid or alkaline (according to experimental work by Smith, 1949; Frondel and Collette, 1957); thus, pH conditions could be responsible for retaining tourmalinising agents in solution en route.

It is also possible that some boron is retained in clay minerals and directly assimilated into the granite, since it is known that illite can incorporate boron into its structure as well as adsorbing it on the surface. This may account for the high concentrations of tourmaline found around the margins of many xenoliths, and may also help to explain the fact that tourmaline is often abundant in the roof zones of granites. Assimilation could provide the means to produce a boron-rich magma (as opposed to a boron-rich fluid), from which differentiation products could supply tourmaline-bearing pegmatites and aplites.

There has been much debate as to whether tourmalinites such as those at Cape Cornwall and Roche Rock could be produced from such a 'magmatic' source. It seems possible that both 'magmatic' and 'hydrothermal' tourmaline could have an ultimate source in the intruded sediments, and therefore the origin of the tourmalinites would be difficult to confirm on geochemical grounds.

However, the Cape Cornwall succession from biotite granite through tourmaline granite into tourmalinite has been treated in the present chapter as a progressive tourmalinisation sequence, and as such, it shows several close geochemical similarities to tourmalinisation sequences from the other localities investigated. Chemical changes observed in passing from biotite granite upwards to the base of the tourmalinite indicate a pattern of aluminium and potassium enrichment, allied with depletion in several major and trace elements; these features correspond closely with those observed at Venford Reservoir and Tregarden. Within the tourmalinite, the only major chemical difference from other tourmalinised rocks examined is the higher proportion of silica; it seems that silica in particular was prevented from escaping from the system by an impermeable roof, and the zone of silicification forming the upper boundary of the tourmalinite supports this view. There is no chemical evidence to preclude the formation of the tourmalinite by in situ alteration of a granite such as the Priest's Cove microgranite.

4.7 Conclusions

A continuous series of tourmalinisation phenomena exists, such that tourmalinisation of relatively low intensity may be associated with chloritisation and K-feldspathisation, while more intense tourmalinisation may be associated with tin mineralisation (as at Goonbarrow).

Potassium enrichment shows an inverse relationship with the degree of tourmalinisation, so that the greatest K-feldspathisation occurs at tourmalinised vein margins, and in the centres of veins where chloritisation predominates over tourmalinisation. In strongly tourmalinised vein centres, albite is stable.

Fluorine and lithium are only enriched in conditions of very intense tourmalinisation; where alteration is less intense, these elements are often depleted by comparison with the unaltered granite concentrations. There is evidence to suggest that instead of being introduced with tourmalinising fluids, fluorine and lithium may be released from primary minerals (micas) and thus incorporated in hydrothermal systems as a result of tourmalinisation.

Tourmalinisation probably involves the advance of more than one alteration 'front'. The first of these fronts, which may consist only of water, initiates biotite breakdown, and possibly begins leaching elements from areas of rock adjacent to the source of alteration. It is not certain to what extent this first stage may be distinguished from the second, which produces chloritisation and K-feldspathisation. The final tourmalinisation front introduces sufficient boron to form a tourmaline assemblage, which may be superimposed upon chlorite and K-feldspar. Instead of chlorite, hydromuscovite may be formed in the intermediate stage, as at Venford Reservoir. The ultimate source of tourmalinising fluids is likely to be in the intruded sediments, rather than in the granites.

The Cape Cornwall tourmalinite shows no chemical evidence to preclude an origin by hydrothermal alteration of existing granite.

5. Mineral chemistry in progressive tourmalinisation

This part of the investigation is chiefly concerned with the chemistry of tourmaline from the localities discussed in preceding chapters. Major elements were determined by electron microprobe, with the exception of boron, which was determined in bulk tourmaline samples from each locality. Fluorine, lithium, water, carbon dioxide and certain trace elements were also determined in bulk tourmaline samples from Venford and Tregarden. Details of the analytical techniques used are given in Chapter 3.

Some of the minerals associated with tourmaline have also been analysed by electron microprobe, although the state of structural and chemical breakdown often encountered in such minerals precluded fuller treatment of this aspect of the work. For hydrous minerals of which the microprobe analyses are necessarily incomplete, the proportion of water is taken from Deer et al. (1962).

Detailed examination of the chemistry of tourmaline in its replacement rôle provides an insight into the mechanisms by which other minerals are replaced by tourmaline, and raises many questions concerning the mobility of elements during the tourmalinisation process, as well as the possibilities for ionic substitution within the tourmaline group.

5.1 Previous work

The difficulties of analysing tourmaline by conventional chemical techniques have been discussed in Chapter 3. Until the advent of the electron microprobe, published analyses of tourmalines were relatively few; for many years, the only analyses of Cornubian tourmalines cited by writers on the province were those of Butler,(1953). The work of Power (1968) produced much major and trace element data on tourmaline from southwest England, but this author did not publish any complete chemical analyses; Power distinguished

'magmatic' from 'hydrothermal' tourmalines, but it has been shown (Chapter 2) that many tourmalines of the type traditionally regarded as magmatic are in fact secondary in origin. Chaudhry and Howie (1976) have published analyses of tourmalines from the Meldon Aplite, Devon, but unlike tourmalines encountered in the present study, these are of the variety elbaite. The electron microprobe analyses of Lister (1979a) are of tourmalines from pegmatites at four Cornish localities, and from the Cape Cornwall tourmalinite; the analyses (in the appended paper on 'Quartz-cored tourmalines') show that the tourmalines analysed are close to the schorl end-member of the schorl-dravite series, and contain small but varying concentrations of Mg, Ca, Ti and/or Mn. Charoy (1979a) published a number of electron microprobe analyses of tourmalines from the Cape Cornwall tourmalinite, and these are also schorl with some substitution by the same cations. Wilson (1980), in a study of lithium determination by the ion microprobe, found that among Cornubian tourmalines of the schorl variety, later generations frequently contained several hundred ppm more lithium than earlier generations from the same localities; some of Wilson's figures will be quoted later in this chapter. Alderton et al. (1980) determined rare earth elements (but not major or trace elements) in Cornish tourmaline, which gave a 'basin-shaped' pattern with a small positive Eu anomaly.

None of the above writers has sought to establish the chemistry of tourmaline resulting from specific replacement processes, or to relate tourmaline chemistry to that of the replaced minerals. It is possible to do this in the present study, particularly with reference to Venford Reservoir, whence detailed petrographic evidence of the tourmalinisation process is available (Chapter 2).

5.2 Venford Reservoir Quarry

5.2.1 Tourmaline

As described in Chapter 2, several varieties of tourmaline may be distinguished optically in the Venford rocks, and these varieties fall into five main categories according to their mode of origin:

(i) Tourmaline after biotite

(ii) Tourmaline after feldspar

(iii) Acicular tourmaline (in vein centres)

(iv) Outer zones deposited on types (i), (ii) and early-formed (iii)

(v) Monomineralic tourmaline vein material

The reddened granite is characterised by type (i), and to a lesser extent, type (ii). The main tourmalinised vein margins contain both types (i) and (ii), which, owing to recrystallisation, are not always distinguishable from one another. In the maximum tourmalinisation zone (VR006 -007), all the first four varieties are present, with types (i) and (ii) now almost totally indistinguishable, forming the centres of large and often composite, zoned crystals. Type (iii) is the main constituent of the smaller, cavitous tourmalinised vein, from which types (i) and (ii) are virtually absent.

5.2.1.1 Tourmaline after biotite

The earliest stages in the replacement of biotite by tourmaline may be seen in the reddened granite sample VR012, some 6 metres from the main tourmalinised vein. The partially replaced crystal illustrated in Plate 2:6 (Chapter 2) shows a patchy colour distribution; following the initial adoption of the tourmaline structure (recognisable from optical properties), different degrees of recrystallisation have occured in different parts of the crystal. The sequence of analyses in Table 5:1 shows how the first-formed tourmaline inherits the biotite composition as closely as the tourmaline structure will

	Biotite →	Tourmaline (brown) →	Tourmaline (dark blue) →	Tourmaline (pale blue)
SiO_2	35.52	34.14	33.76	35.31
TiO_2	3.37	2.26	0.39	0.21
B_2O_3		(10.55)	(10.55)	(10.55)
Al_2O_3	18.91	22.14	27.49	27.66
FeO	24.61	20.15	15.83	13.37
MnO	0.46	0.01	0.10	0.13
MgO	3.90	4.05	4.72	5.63
CaO	0.10	1.16	1.24	1.52
Na_2O	0.46	2.40	2.26	2.05
K_2O	9.23	–	–	–
Li_2O		(0.04)	(0.04)	(0.04)
F		(0.37)	(0.37)	(0.37)
H_2O	(3.17)*	(2.74)	(2.74)	(2.74)
CO_2		(0.03)	(0.03)	(0.03)
	99.73	100.04	99.52	99.61
Less O ≡ F		.16	.16	.16
		99.88	99.36	99.45

Ions on the basis of 24 (O,OH,F) for biotite; 31 (O,OH,F) for tourmaline:

Si	5.56	6.05	5.87	6.05	
B		3.23	3.17	3.12	
Al	3.49	4.63	5.64	5.59	Z position**
Al					
Fe	3.22	2.99	2.30	1.92	
Mg	0.91	1.07	1.22	1.44	Y "
Ti	0.40	0.30	0.05	0.03	
Li		0.03	0.03	0.03	
Mn	0.06	0.00	0.01	0.02	
Na	0.14	0.82	0.76	0.68	X "
Ca	0.02	0.22	0.23	0.28	
K	1.84	0.00	0.00	0.00	
OH	3.31	3.24	3.18	3.13	
F		0.21	0.20	0.20	

Table 5:1 Replacement of biotite by tourmaline, Venford Reservoir – the initial progressive replacement sequence (bi VRO20; tour VRO1

( ) detmd. in bulk samples of separated tourmaline
( )* value from Deer et al. (1962)
– below detection limit
** structural positions in tourmaline (see Chapter 1)
total iron as FeO

allow. The exchange of potassium for sodium appears to be the major chemical transformation at this stage, along with a small adjustment between iron and aluminium. The Al_2O_3 concentration of only 22% seems very low for tourmaline, but it is now accepted that ferric iron can substitute in the octahedral aluminium position, as in the newly-designated, end-member 'ferridravite' (Walenta and Dunn, 1979). Although the total iron is measured as FeO, it is likely that in the partial breakdown of biotite prior to its replacement, some of the iron would have become oxidised. As the tourmaline recrystallises, there is an increase in aluminium and magnesium, and a decrease in iron and titanium; calcium also increases slightly, probably due to substitution for sodium, which decreases. Recrystallisation is achieved by resolution into concentric zones, thereby presumably expelling the less compatible elements from the structure. In VR012, recrystallisation is not always complete, and several tourmalines retain residual biotite lamellae (Chapter 2), and certain elements inherited from biotite become concentrated in isolated patches within some tourmalines (e.g. one analysis showed 8% TiO TiO_2!).

With increasing proximity to the main tourmalinised vein, biotite is completely eliminated, and the tourmaline which replaced it recrystallises to form large (1 mm) grains with concentric zoning. Commonly, the central areas of such crystals are very pale or almost colourless (as in Chapter 2, Plate 2:7), or sometimes brownish. In the example (from sample VR010) in Table 5:2, the central pale brown area retains some of the original biotite features, such as high titanium and low aluminium. The very pale zone adjacent to this is very strongly magnesian, while the outer blue zone is very iron-rich. Sample VR010 contains several similar examples. Since progressive stages can be detected in the development of such zoned tourmalines from the original biotite replacement products, it may be concluded that the successive zones do not represent a chronological sequence of accretion

	Tourmaline brown centre	Tourmaline v.pale zone	Tourmaline blue outer zone	
SiO_2	36.13	37.44	35.80	
TiO_2	1.50	0.36	0.12	
B_2O_3	(10.55)	(10.55)	(10.55)	
Al_2O_3	26.97	31.70	34.16	
FeO	10.16	2.33	14.67	
MnO	-	0.04	0.12	
MgO	7.86	10.49	0.68	
CaO	1.64	1.33	0.12	
Na_2O	1.60	1.97	0.99	
Li_2O	(0.04)	(0.04)	(0.04)	
F	(0.37)	(0.37)	(0.37)	
H_2O	(2.74)	(2.74)	(2.74)	
CO_2	(0.03)	(0.03)	(0.03)	
	99.59	99.39	100.39	
Less O ≡ F	.16	.16	.16	
	99.43	99.23	100.23	

Ions on the basis of 31 (O,OH,F):

Si	5.51	6.12	6.04	
B	2.78	2.98	3.07	
Al	4.85	6.00	6.00	Z position**
Al		0.11	0.80	
Fe	1.30	0.32	2.07	
Mg	1.79	2.56	0.17	Y "
Ti	1.72	0.04	0.02	
Li	0.02	0.03	0.03	
Mn	0.00	0.00	0.02	
Na	0.47	0.63	0.32	X "
Ca	0.27	0.23	0.02	
OH	2.79	2.99	3.08	
F	0.18	0.19	0.20	

Table 5:2 Replacement of biotite by tourmaline, Venford Reservoir - recrystallisation to produce concentric zones.(VR010).

( ) detmd. in bulk samples of separated tourmaline
\- below detection limit
** structural positions in tourmaline
total iron as FeO

upon a central core; instead, it seems that composite, heterogeneous tourmaline aggregates recrystallise and resolve themselves into concentrically-zoned, single crystals. The bulk composition of the zoned tourmaline crystals is not substantially different from that of the original products derived from biotite, except that the former contain more magnesium on average. Excess titanium either becomes concentrated in certain zones, or is expelled from the tourmaline structure during recrystallisation, to form rutile, which was identified by microprobe in some samples.

5.2.1.2 Tourmaline after feldspar

In the main tourmalinised vein margins, the replacement of feldspar by tourmaline takes at least two forms, firstly skeletal networks of tourmaline leaving residual 'islands' of feldspar in optical continuity, and secondly sheaf-like aggregates of acicular tourmaline needles growing outwards from nuclei in cleavage planes. The first variety of tourmaline is usually brown-yellow, and is sometimes rimmed or infilled by later blue tourmaline (Chapter 2, Plates 2:10 and 2:11). The second variety is always dark blue-green. An intermediate variety is pale blue to brown, and skeletal, but growing in the form of very irregular, fine veinlets (Plate 2:12). All varieties become resolved into single, large tourmaline crystals, recrystallising and infilling interstices, as tourmalinisation proceeds.

As for the replaced feldspar, microprobe analyses confirm that compositions range from albite to orthoclase throughout the reddened and tourmalinised rocks, with extreme heterogeneity within many individual feldspars (both megacrysts and others). Since different modes of feldspar replacement occur in the same thin sections, and often adjacent to one another, it was suspected that the nature of the feldspar might influence the habit and/or colour of the replacive tourmaline; such influence could be structural rather than purely compositional.

Table 5:3 shows the composition of feldspar which is partially replaced by acicular blue tourmaline aggregates, in sample VR005. Compositionally, this feldspar is heterogeneous, and is predominantly potassium-rich, with some more sodium-rich patches; the feldspar is in an advanced state of K-feldspathisation, and tourmaline development from a number of nuclei has left very little feldspar intact. The tourmaline thus formed contains variable proportions of iron and magnesium, but always has high calcium, in spite of the lack of calcium in the feldspar. This could be because K-feldspathisation and tourmalinisation were synchronous, and Ca released from original plagioclase became incorporated in the tourmaline. However, this seems unlikely, since almost equally high calcium concentrations are seen in tourmaline replacing biotite (Table 5:1). In view of the extreme compositional difference between feldspar and tourmaline, virtually all the necessary components for replacement must be supplied from outside the feldspar, and in all probability calcium is no exception. In any case, the amount of calcium recorded in feldspars in the same sample which had not been K-feldspathised (e.g. Table 5:4) would not have been sufficient to provide nearly 2% CaO for tourmaline.

The yellow-brown skeletal tourmaline variety is seen in sample VR005 replacing almost pure albite (Table 5:4). The tourmaline composition differs from that of the blue acicular tourmaline, in being relatively iron-rich and magnesium-poor; calcium is low, about the same concentration as in the replaced feldspar. Fibrous blue tourmaline forms a discontinuous rim upon parts of the yellow-brown, skeletal network, and this has a composition similar to that of the blue acicular variety (high Mg and Ca). A further, outer rim of almost colourless magnesian tourmaline is also present locally (both blue and colourless zones are similar to outer zone-forming tourmaline in the vein centre, and will be discussed as such below. These outer zones appear to post-date the skeletal network. Owing to the compositional

	Feldspar a (predominant)	Feldspar b (subsidiary)	Tourmaline (blue)	Tourmaline (blue)	
SiO_2	68.57	67.72	34.92	34.64	
TiO_2			0.39	0.10	
B_2O_3			(10.55)	(10.55)	
Al_2O_3	18.39	19.56	30.89	32.92	
FeO			12.36	8.76	
MnO			0.02	0.04	
MgO			3.70	5.68	
CaO	-	0.22	1.92	1.92	
Na_2O	0.31	10.47	1.60	1.30	
K_2O	16.62	1.34	-	-	
Li_2O			(0.04)	(0.04)	
F			(0.37)	(0.37)	
H_2O			(2.74)	(2.74)	
CO_2			(0.03)	(0.03)	
P_2O_5			-	0.24	
	100.89	99.31	99.53	99.33	
Less O ≡ F			.16	.16	
			99.37	99.17	
Ions on the basis of 32 (O) for feldspar; 31 (O,OH,F) for tourmaline:					
Si	11.95	11.91	5.96	5.82	
B			3.11	3.06	
Al	3.95	4.06	6.00	6.00	Z**
Al			0.22	0.52	
Fe			1.76	1.23	
Mg			0.94	1.42	
Ti			0.05	0.01	Y
Li			0.03	0.03	
Mn			0.00	0.01	
Na	0.11	3.57	0.53	0.42	
Ca	0.00	0.04	0.35	0.35	X
K	3.87	0.30	0.00	0.00	
OH			3.12	3.07	
F			0.20	0.20	

Table 5:3 Replacement of feldspar by tourmaline, Venford Reservoir - blue acicular tourmaline replacing K/Na feldspar (VR005).

( ) detmd. in bulk samples of separated tourmaline
- below detection limit
** structural positions in tourmaline
total iron as FeO

	Feldspar	Tourmaline (yellow)	Tourmaline (yellow-brown)	Tourmaline (blue infill)
SiO_2	68.32	35.15	35.48	34.59
TiO_2		0.75	0.36	0.22
B_2O_3		(10.55)	(10.55)	(10.55)
Al_2O_3	19.69	33.42	33.27	32.24
FeO		12.92	13.53	11.81
MnO		0.13	0.06	-
MgO		2.26	2.17	4.30
CaO	0.12	0.17	0.12	1.86
Na_2O	11.43	2.15	1.85	1.43
K_2O	-	-	-	-
Li_2O		(0.04)	(0.04)	(0.04)
F		(0.37)	(0.37)	(0.37)
H_2O		(2.74)	(2.74)	(2.74)
CO_2		(0.03)	(0.03)	(0.03)
P_2O_5		-	-	-
	99.56	100.68	100.41	100.18
Less O ≡ F		.16	.16	.16
		100.52	100.25	100.02

Ions on the basis of 32 (O) for feldspar; 31 (O,OH,F) for tourmaline:

Si	11.93	5.92	5.98	5.85	
B		3.06	3.07	3.08	
Al	4.05	6.00	6.00	6.00	Z**
Al		0.63	0.61	0.43	Y
Fe		1.82	1.91	1.67	Y
Mg		0.57	0.54	1.08	Y
Ti		0.10	0.05	0.03	Y
Li		0.03	0.03	0.03	Y
Mn		0.02	0.01	0.00	Y
Na	3.87	0.70	0.60	0.47	X
Ca	0.02	0.03	0.02	0.34	X
K	0.00	0.00	0.00	0.00	
OH		3.08	3.08	3.09	
F		0.20	0.20	0.20	

Table 5:4 Replacement of feldspar by tourmaline, Venford Reservoir - yellow-brown skeletal tourmaline replacing Na-feldspar (VR005).

( ) detmd. in bulk samples of separated tourmaline
\- below detection limit
** structural positions in tourmaline
total iron as FeO

similarity between the blue outer zone material and the acicular, blue tourmaline aggregates (compare Table 5:3 with Table 5:4, fourth analysis), it is possible that the acicular aggregates also postdate skeletal growth.

In tourmaline, the X position (Chapter 1) can be occupied by Na or Ca (or, theoretically, K, which is really too large). Na would be the preferred ion, but in cases of Na depletion, the divalent Ca ion can be accomodated with a coupled substitution of O for OH in the tourmaline structure. In tourmaline after Na-feldspar (e.g. Table 5:4, yellow-brown tourmalines), the X position is filled almost entirely by Na, which presumably would have been in plentiful supply from the replaced mineral. Tourmaline after K-feldspar, however, contains a higher concentration of Ca relative to Na, indicating that Na, when not supplied by the replaced feldspar, was less readily available than Ca; it is noteworthy that tourmaline after biotite is also relatively Ca-rich. It is possible that tourmaline formation after feldspar may be restricted by the availability of Na, and that for this reason, replacement of Na-feldspar may occur both more readily and earlier than the replacement of K-feldspar.

The example of replacement given in Table 5:5 is also illustrated in Chapter 2, Plate 2:13; these analyses confirm that irrespective of any chronological sequence of events, the mode of replacement by tourmaline is influenced by the feldspar composition and/or structure. Here, a single, but very heterogeneous feldspar crystal is partially replaced by both blue and brown tourmaline. Blue tourmaline predominates, and this forms a very fine intergrowth of small veinlets within the feldspar; continuous patches of both blue and brown tourmaline occur where replacement is more intense. The blue tourmaline is compositionally similar to the acicular and fibrous varieties, in having high Mg and Ca, while the brown tourmaline corresponds with the yellow-brown skeletal variety. The feldspar adjacent to the blue tourmaline is K-feldspar, with the high iron content which accompanies

	Feldspar adjacent to blue tourm.	Tourmaline (blue)	Tourmaline (blue)	Feldspar adjacent to brown tourm.	Tourmaline (brown)	
SiO_2	64.22	35.60	36.52	68.00	35.49	
TiO_2		0.63	0.35		0.62	
B_2O_3		(10.55)	(10.55)		(10.55)	
Al_2O_3	18.22	32.57	30.31	19.49	33.06	
FeO	0.31	11.91	7.73		13.87	
MnO		–	0.04		0.19	
MgO		3.51	7.63		1.76	
CaO	–	0.61	1.96	–	0.13	
Na_2O	–	1.72	1.36	9.82	1.94	
K_2O	16.41	–	–	2.88	–	
Li_2O		(0.04)	(0.04)		(0.04)	
F		(0.37)	(0.37)		(0.37)	
H_2O		(2.74)	(2.74)		(2.74)	
CO_2		(0.03)	(0.03)		(0.03)	
P_2O_5		–	–		–	
	99.16	100.28	99.63	100.19	100.79	
Less O ≡ F		.16	.16		.16	
		100.12	99.47		100.63	

Ions on the basis of 32 (O) for feldspar; 31 (O,OH,F) for tourmaline:

Si	11.95	5.99	6.10	11.90	5.97	
B		3.06	3.04		3.06	
Al	4.00	6.00	5.97	4.02	6.00	Z**
Al		0.46			0.55	Y
Fe	0.05	1.68	1.08		1.95	Y
Mg		0.88	1.90		0.44	Y
Ti		0.08	0.04		0.08	Y
Li		0.03	0.03		0.03	Y
Mn		0.00	0.01		0.03	Y
Na	0.00	0.56	0.44	3.33	0.63	X
Ca	0.00	0.10	0.35	0.00	0.02	X
K	3.90	0.00	0.00	0.64	0.00	
OH		3.07	3.05		3.07	
F		0.20	0.20		0.20	

Table 5:5 Replacement of feldspar by tourmaline, Venford Reservoir - blue and brown skeletal tourmaline replacing K/Na feldspar (VR003).

( ) detmd. in bulk samples of separated tourmaline
– below detection limit
** structural positions in tourmaline
total iron as FeO

reddening. Adjacent to the brown tourmaline, the feldspar is essentially sodic, with a small potassium component.

Hence it seems that there is a correlation between the state of the feldspar and the nature of the tourmaline which replaces it, despite the fact that the feldspar supplies very few of the chemical components for tourmaline. There may also have been two main stages of feldspar replacement, the earlier phase attacking Na-feldspar, and the later K-feldspar. If this is so, we may conclude that magnesium availability increased as tourmalinisation progressed, so that the early-formed tourmaline is Mg-poor, while the later tourmaline often contains Mg in excess of Fe. This trend also seems apparent in biotite replacement.

Is there any compositional difference between tourmaline after biotite and tourmaline after feldspar? In terms of bulk composition, the former is very similar to tourmaline after K-feldspar. However, the more extreme compositions within individual zones are confined to the tourmaline after biotite, and this seems to be a re-equilibration effect rather than an original characteristic. The early-formed tourmaline after biotite is deficient in aluminium, although this is corrected with recrystallisation; no such deficiency is seen in tourmaline after feldspar. Abnormally high titanium levels are restricted to the post-biotite tourmaline; again, recrystallisation brings the titanium to less extreme concentrations. When fully recrystallised, the products of biotite and feldspar replacement may not easily be distinguished from one another on the basis of composition.

5.2.1.3 Acicular tourmaline needles

This tourmaline variety is distinct from the sheaf-like, acicular aggregates described above, and is not regarded as a replacement product. It occurs as individual, elongate needles, which may form radiate 'swarms' (Chapter 2), within recrystallised quartz, not feldspar. The needles often

show euhedral morphology, but are very narrow, with thicknesses considerably less than the 30 μm or so of the polished thin sections. Accurate microprobe analysis is difficult, since most such crystals lie beneath the surface of the slide, and those which are exposed take a poor polish because of their fibrous texture. However, it has been possible to establish that the acicular needles in the centre of the main tourmalinised vein are predominantly megnesian, and that their composition is similar to that of the outermost colourless zone accreted upon larger grains. By contrast, the acicular tourmaline in the smaller, cavitous tourmalinised vein is essentially iron-tourmaline (Table 5:8) and appears to be unrelated to that of the larger vein.

5.2.1.4 Outer zones accreted upon existing crystals (VR006, VR007)

In the centre of the main tourmalinised vein, existing tourmalines after biotite and feldspar, as well as early-formed acicular needle swarms, have become rimmed by euhedral growth of additional outer zones. The first of these outer zones is dark blue, and the outermost is very pale, almost colourless.

Plate 5:1 shows such a crystal group, thought to be originally after biotite; the chemical variation is shown by analyses of successive zones in Table 5:6; the X-ray scan photomicrographs forming Plates 5:2 to 5:5 illustrate the complex nature of the compositional zoning in the larger crystal (hereafter referred to as 'tourmaline A'). From the distribution of colour in the lower part of Plate 5:1 (see arrows), it appears that some interaction has occurred between the different coloured zones, such that the dark blue zone, in particular, may have developed by the concentration of material already present in the crystals. Chemically, one of the major effects is the concentration of calcium towards the outer zones, and the retention of titanium in the central brown zone (Plates 5:4 and 5:5). The dark blue zone differs from the adjacent zones chiefly in its higher iron and calcium

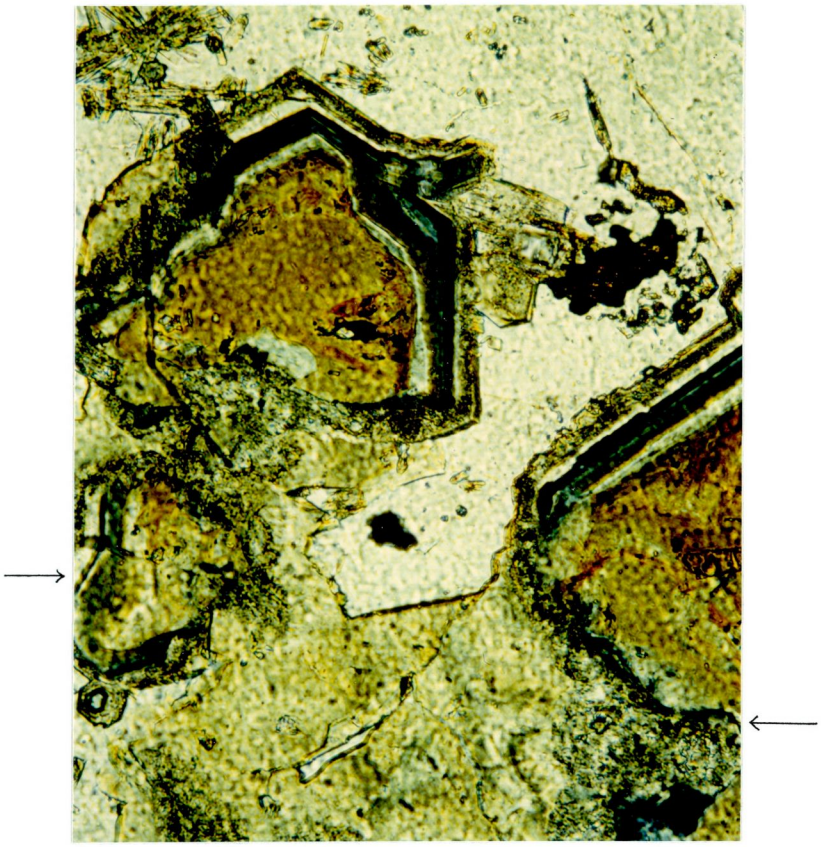

0 0.5mm

Plate 5:1 Zoned tourmaline crystal group (tourmaline A) from the centre of the main tourmalinised vein (VR007), Venford Reservoir Quarry. The central brown areas are possibly post-biotite. (p.p.l.)

	Zone 1 (brown)	Zone 2 (pale blue)	Zone 3 (dark blue)	Zone 4 (colourless)
SiO_2	34.18	35.40	34.73	36.87
TiO_2	1.12	0.84	0.42	0.41
B_2O_3	(10.55)	(10.55)	(10.55)	(10.55)
Al_2O_3	32.56	29.68	32.91	33.48
FeO	12.55	8.32	12.63	2.13
MnO	0.22	0.12	0.04	-
MgO	3.01	7.96	2.53	10.12
CaO	0.38	1.46	2.17	1.06
Na_2O	2.22	1.85	1.26	2.32
Li_2O	(0.04)	(0.04)	(0.04)	(0.04)
F	(0.37)	(0.37)	(0.37)	(0.37)
H_2O	(2.74)	(2.74)	(2.74)	(2.74)
CO_2	(0.03)	(0.03)	(0.03)	(0.03)
	99.97	99.36	100.42	100.12
Less O ≡ F	.16	.16	.16	.16
	99.81	99.20	99.26	99.96

Ions on the basis of 31 (O,OH,F):

Si	5.79	5.95	5.86	5.99	
B	3.08	3.06	3.07	2.96	
Al	6.00	5.88	6.00	6.00	Z**
Al	0.50		0.54	0.41	Y
Fe	1.78	1.17	1.78	0.29	Y
Mg	0.76	1.99	0.39	2.53	Y
Ti	0.14	0.11	0.05	0.05	Y
Li	0.03	0.03	0.03	0.03	Y
Mn	0.03	0.02	0.01	0.00	Y
Na	0.36	0.60	0.41	0.73	X
Ca	0.07	0.26	0.39	0.18	X
OH	3.10	3.07	3.08	2.97	
F	0.20	0.20	0.20	0.19	

Table 5:6 Compositional zoning in tourmaline A (Plate 5:1), from the centre of the main tourmalinised vein, Venford Reservoir.

( ) detmd. in bulk samples of separated tourmaline
\- below detection limit
** structural positions in tourmaline
total iron as FeO

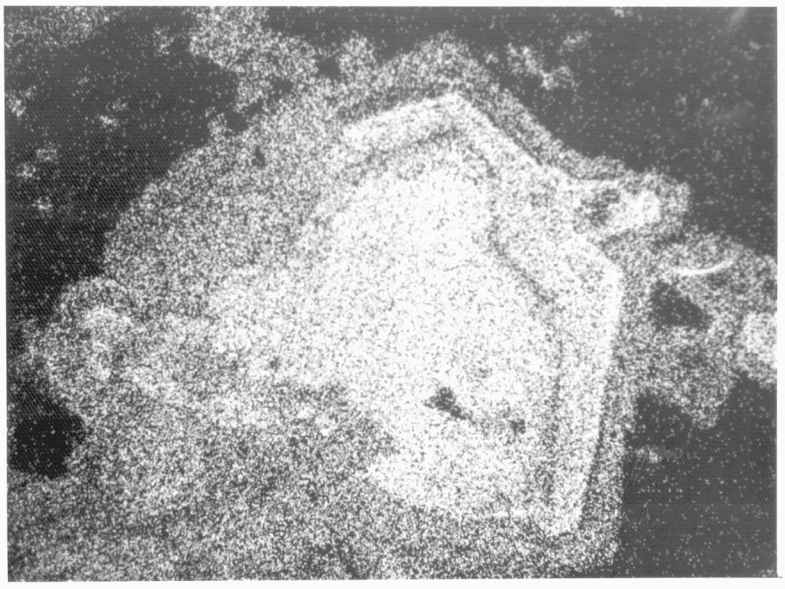

0 0.25mm

Plate 5:2 X-ray scan photomicrograph of tourmaline A (illustrated in Plate 5:1), showing distribution of iron.

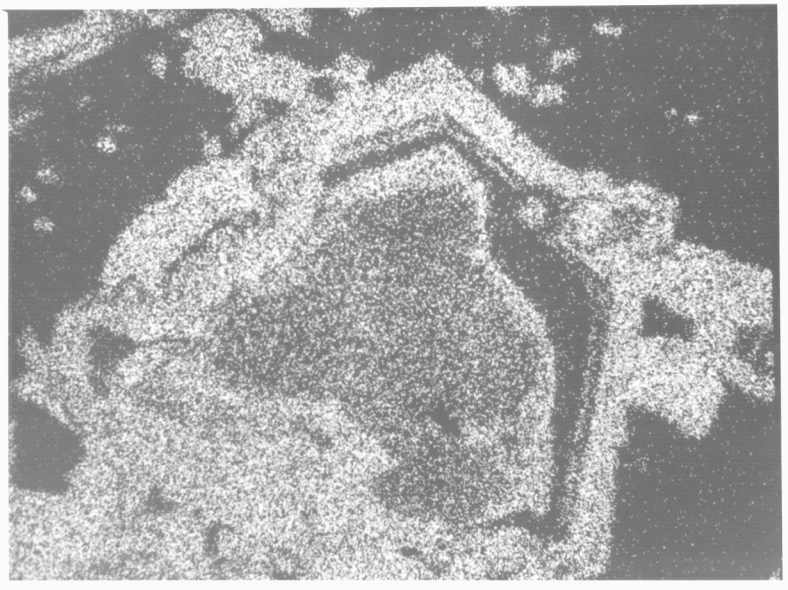

0 0.25mm

Plate 5:3 X-ray scan photomicrograph of tourmaline A, showing distribution of magnesium.

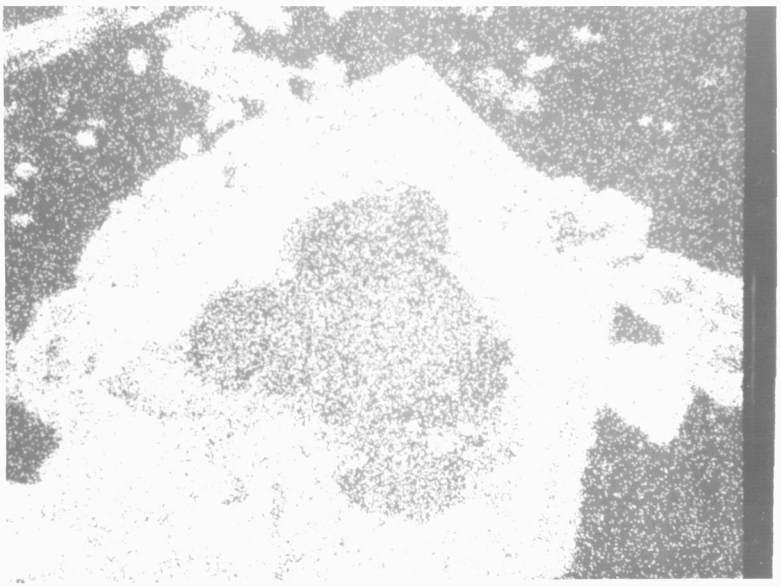

0 0.25mm

Plate 5:4 X-ray scan photomicrograph of tourmaline A, showing distribution of calcium.

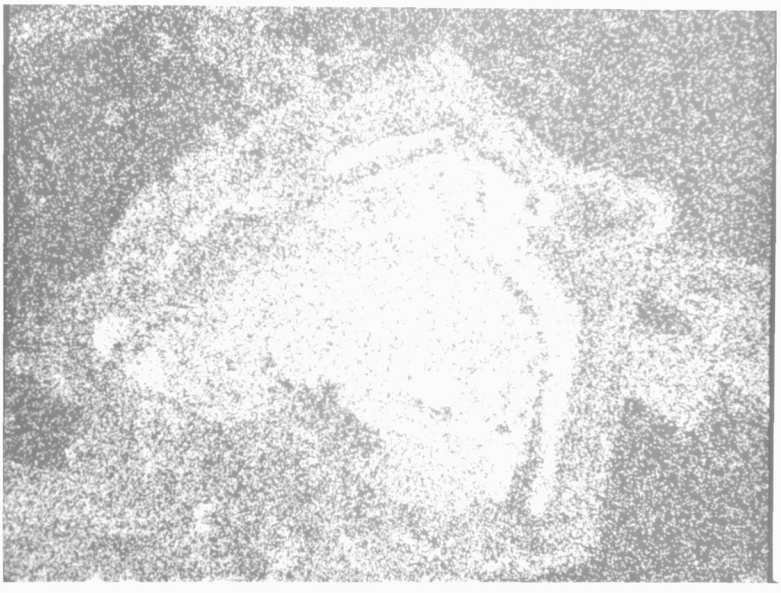

0 0.25mm

Plate 5:5 X-ray scan photomicrograph of tourmaline A, showing distribution of titanium.

concentration; in parts of this zone (Table 5:6, zone 3), calcium considerably exceeds sodium in terms of weight percent, though not in terms of numbers of ions.

Plate 5:6 shows a pale blue centred crystal group (possibly after feldspar, but its origin is uncertain); this group, 'tourmaline B', is rimmed by the same dark blue and colourless zones as seen in tourmaline A. Again, the zoning sequence is more complex than it at first appears, as demonstrated by the X-ray scan photomicrographs comprising Plates 5:7 to 5:10. Here the chemical similarity between the outer colourless zone and the acicular needles is striking, and supports their common origin. Table 5:7 gives the compositions of zones within this crystal group. It is clear that the outer zones correspond closely with those of tourmaline A. One particular characteristic common to both crystal groups is the oscillatory zoning with respect to calcium; this is also shown by iron in tourmaline B. Titanium in tourmaline B is confined to one narrow zone, where it appears to have been expelled from the central structure prior to deposition of the outermost zones.

The compositions of tourmaline in the centre of the main tourmalinised vein all lie within the schorl-dravite solid solution series, with some high calcium and titanium levels. In terms of bulk composition, there is little difference between the tourmaline within the vein and that in the vein margin. The outer zones are consistently richer in calcium, and the outermost zone is also strongly magnesian. However, there are no compositions in outer zones within the vein, which are not also present in the vein margins or in the reddened granite. On compositional grounds, there is nothing to preclude the derivation of these outer zones by remobilisation of existing tourmaline, but this process could not account for the additional volume of tourmaline in the vein itself. From the margins into the vein centre, there is an increase from about 10% 'normative' tourmaline to about 30%, and thus a considerable influx of elements into the system is indicated. The very

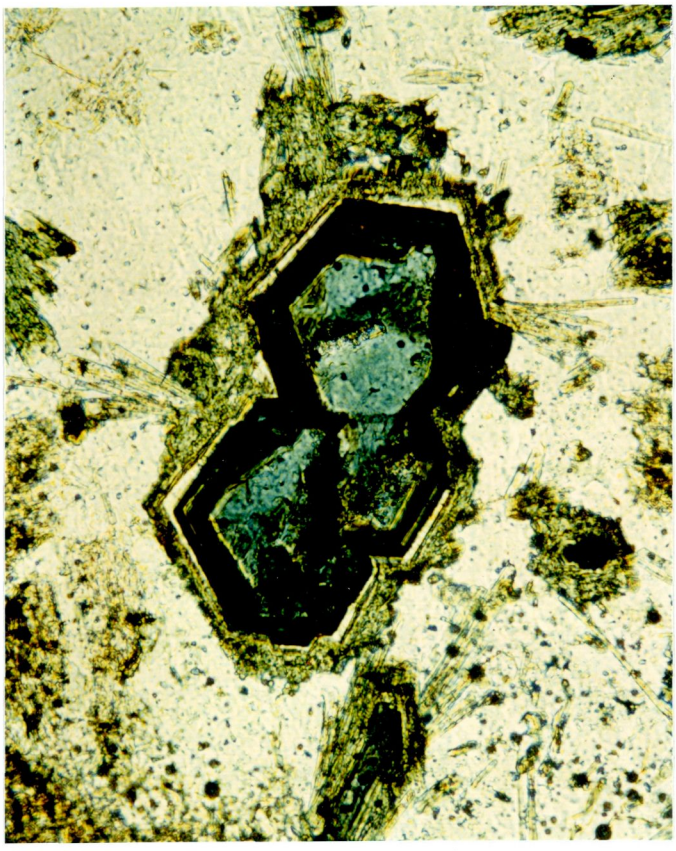

0 0.5mm

Plate 5:6 Zoned tourmaline crystal group (tourmaline B) from the centre of the main tourmalinised vein (VR007), Venford Reservoir Quarry. (p.p.l.)

	Zone 1 (pale blue)	Zone 2 (pale blue)	Zone 3 (brown)	Zone 4 (dark)	Zone 5 (dark blue)	Zone 6 (colourless)	
SiO_2	36.11	35.90	34.34	34.64	34.20	37.02	
TiO_2	0.07	0.27	1.54	0.36	0.45	0.51	
B_2O_3	(10.55)	(10.55)	(10.55)	(10.55)	(10.55)	(10.55)	
Al_2O_3	33.06	30.65	36.06	32.46	30.70	32.11	
FeO	8.87	7.88	9.83	12.23	14.51	2.82	
MnO	0.02	0.02	0.02	0.05	0.02	-	
MgO	5.64	7.97	0.72	2.63	2.50	9.87	
CaO	0.27	1.48	1.23	1.73	1.54	1.30	
Na_2O	2.49	2.07	1.54	1.36	1.81	2.15	
Li_2O	(0.04)	(0.04)	(0.04)	(0.04)	(0.04)	(0.04)	
F	(0.37)	(0.37)	(0.37)	(0.37)	(0.37)	(0.37)	
H_2O	(2.74)	(2.74)	(2.74)	(2.74)	(2.74)	(2.74)	
CO_2	(0.03)	(0.03)	(0.03)	(0.03)	(0.03)	(0.03)	
	100.26	99.97	99.01	99.19	99.46	99.51	
Less O ≡ F	.16	.16	.16	.16	.16	.16	
	100.10	99.81	98.85	99.03	99.30	99.35	
Ions on the basis of 31 (O,OH,F):							
Si	6.00	6.00	5.79	5.91	5.90	6.06	
B	3.03	3.04	3.07	3.11	3.14	2.98	
Al	6.00	6.00	6.00	6.00	6.00	6.00	Z**
Al	0.48	0.04	1.16	0.53	0.24	0.20	Y
Fe	1.23	1.10	1.39	1.75	2.09	0.39	
Mg	1.40	1.98	0.18	0.67	0.64	2.41	
Ti	0.01	0.03	0.20	0.05	0.06	0.06	
Li	0.03	0.03	0.03	0.03	0.03	0.03	
Mn	0.00	0.00	0.00	0.01	0.00	0.00	
Na	0.80	0.67	0.50	0.45	0.61	0.68	X
Ca	0.05	0.27	0.22	0.32	0.29	0.23	
OH	3.04	3.05	3.08	3.12	3.15	2.99	
F	0.19	0.20	0.20	0.20	0.20	0.19	

Table 5:7 Compositional zoning in tourmaline B (Plate 5:6), from the centre of the main tourmalinised vein, Venford Reservoir.

( ) detmd. in bulk samples of separated tourmaline
\- below detection limit
** structural positions in tourmaline
total iron as FeO

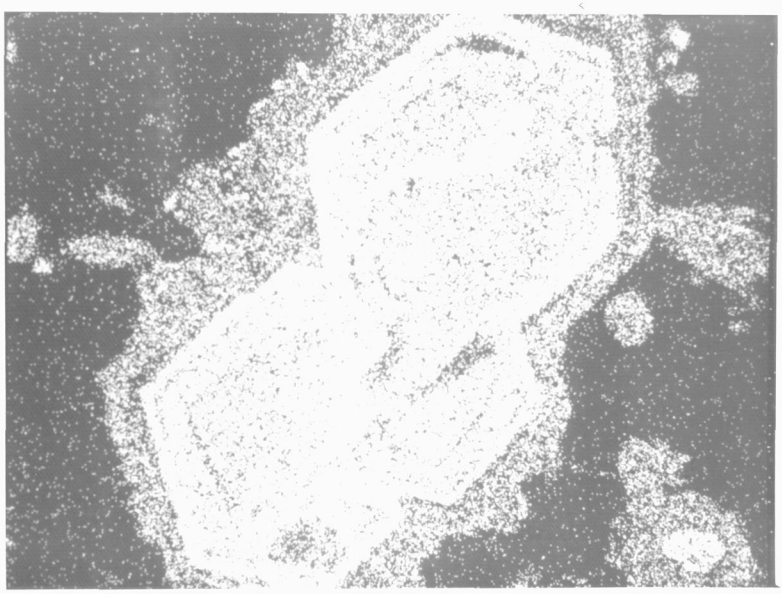

0 0.25mm

Plate 5:7 X-ray scan photomicrograph of tourmaline B (illustrated in Plate 5:6) showing distribution of iron.

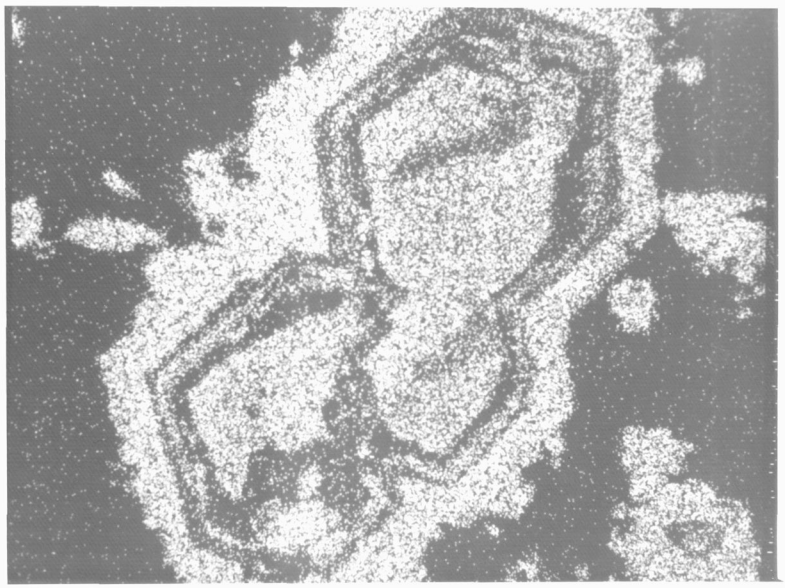

0 0.25mm

Plate 5:8 X-ray scan photomicrograph of tourmaline B, showing distribution of magnesium.

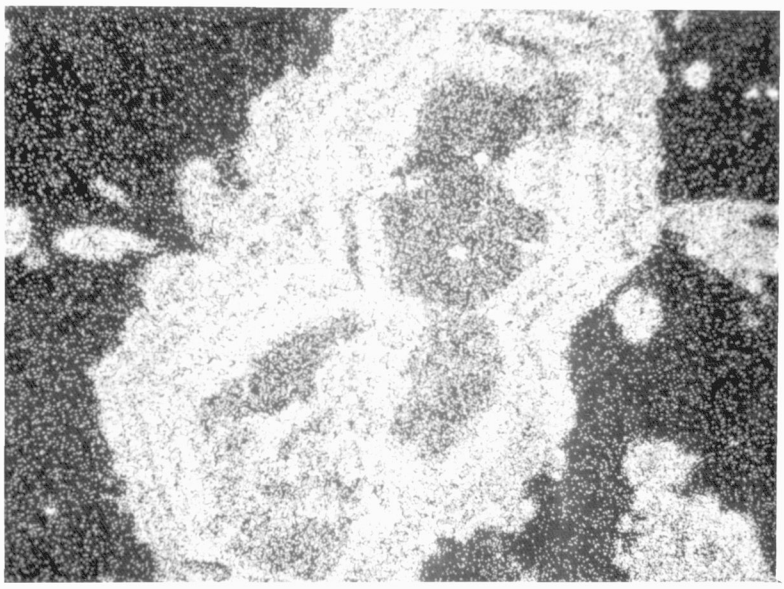

0 0.25mm

Plate 5:9 X-ray scan photomicrograph of tourmaline B, showing distribution of calcium.

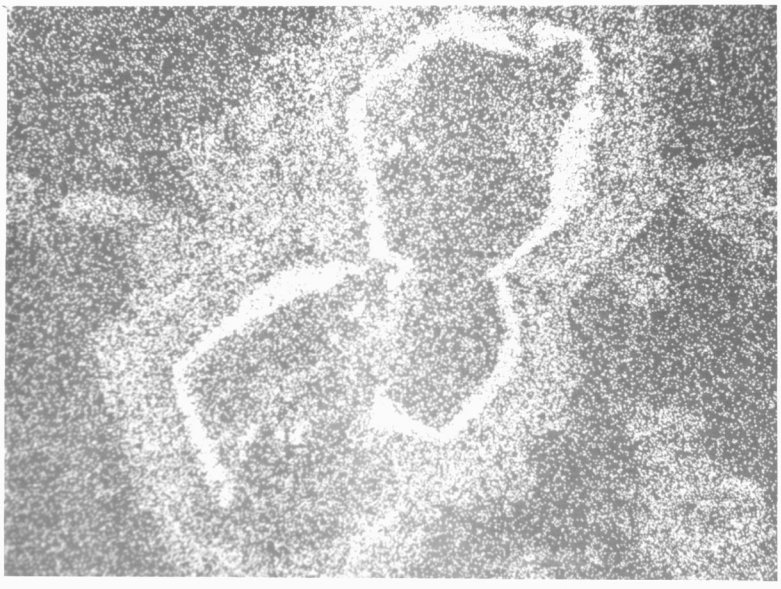

0 0.25mm

Plate 5:10 X-ray scan photomicrograph of tourmaline B, showing distribution of titanium.

magnesian nature of the acicular needles, and the outermost zones of larger crystals, suggests a continuation of the trend towards magnesium enrichment, noted in previous tourmaline analyses, and confirmed by the whole rock chemistry (Chapter 4).

Therefore, the formation of the outer zones of tourmalines within the main tourmalinised vein could represent the culmination of the same process which allowed tourmaline replacement of biotite and feldspar, rather than a distinct and separate event.

5.2.1.5 Monomineralic tourmaline veins

The large, patchy, blue-brown tourmaline masses in these veins yield compositions within the schorl-dravite series, with a minor calcium component. The average composition is more iron-rich and less calcic than the tourmaline associated with the main tourmalinised vein. A thin monomineralic vein traversing VR006 shows slightly more magnesian compositions , which might be superimposed by the later, main tourmalinised vein formation. Table 5:8 gives analyses of tourmaline from an isolated monomineralic vein, and one which cuts VR006. Also included in this table, for comparison, are analyses of the acicular tourmaline in the small, cavitous tourmalinised vein (VR024), and it is clear that this is similar to the isolated monomineralic vein material. The high iron content of both tourmaline types supports the field observation that these veins share a common orientation which differs from that of the main tourmalinised vein.

5.2.1.6 Trace elements in the Venford Reservoir tourmaline

Owing to the difficulties of separating the many closely intergrown tourmaline types for wet chemical analysis, a single bulk sample (VR021) was analysed for some trace elements, as well as boron, fluorine, bound water and carbon dioxide. The concentrations of these components are given in

	VR024 Tourm.1	VR024 Tourm.2	Tourm.vein 1,isolated	Tourm. vein 2, cutting main tourmalinised vein	
SiO_2	35.66	33.30	33.42	34.63	36.45	
TiO_2	0.52	3.09	0.56	0.67	0.07	
B_2O_3	(10.55)	(10.55)	(10.55)	(10.55)	(10.55)	
Al_2O_3	30.98	30.72	33.92	34.36	32.63	
FeO	15.40	12.87	14.00	12.17	7.18	
MnO	0.13	0.20	0.14	0.12	0.03	
MgO	2.07	3.23	1.72	2.41	7.17	
CaO	0.16	0.95	0.17	0.25	0.47	
Na_2O	2.04	1.68	2.06	2.08	2.34	
Li_2O	(0.04)	(0.04)	(0.04)	(0.04)	(0.04)	
F	(0.37)	(0.37)	(0.37)	(0.37)	(0.37)	
H_2O	(2.74)	(2.74)	(2.74)	(2.74)	(2.74)	
CO_2	(0.03)	(0.03)	(0.03)	(0.03)	(0.03)	
	100.69	99.77	99.72	100.42	100.07	
Less O = F	.16	.16	.16	.16	.16	
	100.53	99.61	99.56	100.26	99.91	
Ions on the basis of 31 (O,OH,F):						
Si	6.07	5.70	5.67	5.81	6.32	
B	3.10	3.12	3.09	3.05	3.04	
Al	6.00	6.00	6.00	6.00	6.00	Z**
Al	0.21	0.20	0.79	0.79	0.67	Y
Fe	2.19	1.84	1.99	1.71	1.04	Y
Mg	0.52	0.82	0.44	0.60	1.85	Y
Ti	0.07	0.40	0.07	0.08	0.01	Y
Li	0.03	0.03	0.03	0.03	0.03	Y
Mn	0.02	0.03	0.02	0.02	0.00	Y
Na	0.67	0.39	0.66	0.68	0.79	X
Ca	0.03	0.17	0.03	0.05	0.09	X
OH	3.11	3.07	3.10	3.06	3.17	
F	0.20	0.20	0.20	0.20	0.20	

Table 5:8 Tourmaline from the smaller cavitous tourmalinised vein (VR024) and from the monomineralic tourmaline veins, Venford Reservoir.

( ) detmd. in bulk samples of separated tourmaline
** structural positions in tourmaline
total iron as FeO

Table 5:9, where they may be compared with those in a similar bulk sample of tourmaline from Tregarden Quarry, Luxulyan. Tourmaline from these two localities is closely comparable in its trace element content, the most important trace elements being lithium and zinc in each case.

In microprobe analyses of tourmaline, tin, chlorine, phosphorus and chromium were included, but of these, only phosphorus was ever recorded above the detection limit, and that only rarely.

5.2.2 Other minerals associated with tourmalinisation at Venford Reservoir Quarry

Opaque mineral grains were identified by microprobe, but quantitative analyses were not obtained. In the reddened granite and the main tourmalinised vein margin, the predominant opaque mineral was identified as rutile, almost pure TiO_2; this did not, however, show the characteristic red colour, but was almost black. In the margin of the smaller, cavitous tourmalinised vein, the opaque grains proved to be impure iron oxides, containing small concentrations of several other elements; these grains could have been fine aggregates rather than single crystals. Also in the smaller tourmalinised vein margin (VR023), several semi-opaque grains were identified as cassiterite. This was the only cassiterite recognised at Venford Reservoir, in spite of the proximity of tin mineralisation at Hexworthy Mine, and its occurrence further supports the contention that the smaller, cavitous tourmalinised vein was not emplaced at the same time as the main tourmalinised vein.

Analyses of hydromuscovite and apatite are given in Table 5:10. The hydromuscovite contains small quantities of iron, magnesium and phosphorus. The apatite contains virtually nothing apart from calcium and phosphorus; chlorine was nearly always below the detection limit (although one analysis showed 1% MnO and 0.15% Cl), so most of the apatite present is not

	Tourmaline from Venford Reservoir	Tourmaline from Tregarden Quarry
Li	171	124
Rb	-	6
Sr	Tr.	Tr.
Ba	-	-
Be	4	1
Cu	60	34
Zn	341	349
Sn	-	-
B_2O_3	10.55	10.42
F	0.37	0.43
H_2O	2.74	2.54
CO_2	0.03	0.03

Table 5:9 Tourmaline from Venford Reservoir and Tregarden Quarry, Luxulyan: elements determined in bulk samples of separated tourmaline, by methods other than electron microprobe (traces ppm, oxides & F, %).

chlorapatite. It is not possible to distinguish hydroxyapatite from fluorapatite by microprobe, but since the fluorine in the whole rocks would not be fully accounted for by the tourmaline present (Chapter 4), some of the fluorine measured could be assigned to fluorapatite.

	Hydromuscovite	Apatite
SiO_2	47.50	
Al_2O_3	35.01	
FeO	0.66	
MgO	0.46	
CaO		55.36
K_2O	9.75	
P_2O_5	0.34	42.14
F		(3.73)*
H_2O	(6.31)*	
	100.03	101.23
Less O = F		1.57
		99.66

Table 5:10 Hydromuscovite and apatite from the main tourmalinised vein margins, Venford Reservoir Quarry.
(* from Deer et al., 1962).

total iron as FeO

5.3 Tregarden Quarry, Luxulyan

5.3.1 Tourmaline

The situation at Tregarden is less complex than at Venford, since only two main tourmaline varieties are present in the tourmalinised and chloritised veins. These are (i) yellow-brown, prismatic tourmaline, and (ii) blue-green, acicular and fibrous tourmaline. Type (i) is found in the 'unaltered' granite as well as in the veins, while type (ii) is confined to the vein centres.

5.3.1.1 Yellow-brown, prismatic tourmaline

This variety may be seen as an apparently primary mineral in the 'unaltered' granite and around xenoliths, and also in the tourmalinised and chloritised veins and margins, where it replaces feldspar; Table 5:11 shows the compositional similarity of these two modes of occurrence. It is not possible to correlate tourmaline composition with replaced feldspar composition, since all replaced feldspar is perthitic or microperthitic K-feldspar.

In both tourmalinised and chloritised vein centres, the yellow-brown tourmaline becomes fringed with either radiate acicular blue tourmaline, or oriented overgrowths of the same blue tourmaline (Plate 5:11). The composition of the yellow-brown variety is fairly constant throughout, with around 11% FeO, and minor MgO, CaO and TiO_2. The analyses of 'yellow cores' of overgrown tourmalines, given in Table 5:12, are representative of this variety.

5.3.1.2 Acicular blue-green tourmaline

Blue-green tourmaline forms very fine acicular needles in quartz (Chapter 2, Plate 2:30), sheaf-like aggregates replacing biotite and chlorite, and oriented overgrowths upon yellow tourmaline grains. The first two types

	Tourmaline (Yellow - 'primary' in granite)	Tourmaline (Yellow - after feldspar)	Tourmaline (Blue - after chlorite)	
SiO_2	35.29	34.75	35.49	
TiO_2	0.47	0.71	0.56	
B_2O_3	(10.42)	(10.42)	(10.42)	
Al_2O_3	34.86	35.32	26.62	
FeO	10.79	11.12	15.00	
MnO	-	0.12	-	
MgO	2.17	2.48	5.00	
CaO	0.18	0.23	1.50	
Na_2O	1.82	1.90	2.29	
Li_2O	(0.03)	(0.03)	(0.03)	
F	(0.43)	(0.43)	(0.43)	
H_2O	(2.54)	(2.54)	(2.54)	
CO_2	(0.03)	(0.03)	(0.03)	
	99.03	100.08	99.91	
Less O ≡ F	.18	.18	.18	
	98.85	99.90	99.73	
Ions of the basis of 31 (O,OH,F):				
Si	6.07	5.84	6.15	
B	3.10	3.02	3.12	
Al	6.00	6.00	5.44	Z**
Al	1.07	1.00	0.00	Y
Fe	1.55	1.56	2.17	Y
Mg	0.56	0.62	1.29	Y
Ti	0.06	0.09	0.07	Y
Li	0.02	0.02	0.02	Y
Mn	0.00	0.02	0.00	Y
Na	0.61	0.62	0.77	X
Ca	0.03	0.04	0.28	X
OH	2.92	2.85	2.94	
F	0.23	0.23	0.24	

Table 5:11 Tourmalines from Tregarden Quarry, Luxulyan.

( ) Detmd. in bulk samples of separated tourmaline
\- Below detection limit
** Structural positions in tourmaline
total iron as FeO

were difficult to analyse by microprobe, on account of their fibrous nature and very narrow width (only a few μm). The third analysis given in Table 5:11 indicates that the first-formed tourmaline after chloritised biotite is unusually rich in iron and magnesium, and depleted in aluminium.

In the case of oriented overgrowths, it was possible to make analyses, examples of which are given in Table 5:12. The blue 'overgrowth (i)' in each case refers to the position close to the plane of contact between yellow and blue tourmaline varieties, and this shows an increase in both iron and magnesium, compared with the central yellow part of the crystal. This increase appears to be at the expense of aluminium, which although low, still accounts for six ions in the Z position. The blue 'overgrowth (ii)' in Table 5:12 refers to a position well within the overgrowth. This shows, in each case, a large increase in iron, to as high as nearly 20% FeO, with a corresponding decrease in magnesium to below the level generally found in the yellow tourmaline. The overgrown crystal shown in Plate 5:11 is the subject of the X-ray scan photomicrographs forming Plates 5:12 to 5:15; these show that the blue overgrowth is consistently richer in iron than the yellow core of the crystal, and that a narrow zone of magnesium enrichment marks the plane of contact. Calcium distribution bears little relation to the tourmaline types, and titanium is slightly more concentrated in the yellow tourmaline, but more depleted at the plane of contact than within the overgrowth itself. The white area to the top right of Plate 5:15 indicates microcrystalline rutile.

5.3.1.3 Cored tourmalines in pegmatitic joint fill

These are described in the appended paper on 'quartz-cored tourmalines' (Lister, 1979a), which includes representative microprobe analyses. Compositions are somewhat less magnesian than the yellow-brown tourmaline in the major tourmalinised and chloritised veins, but are otherwise similar.

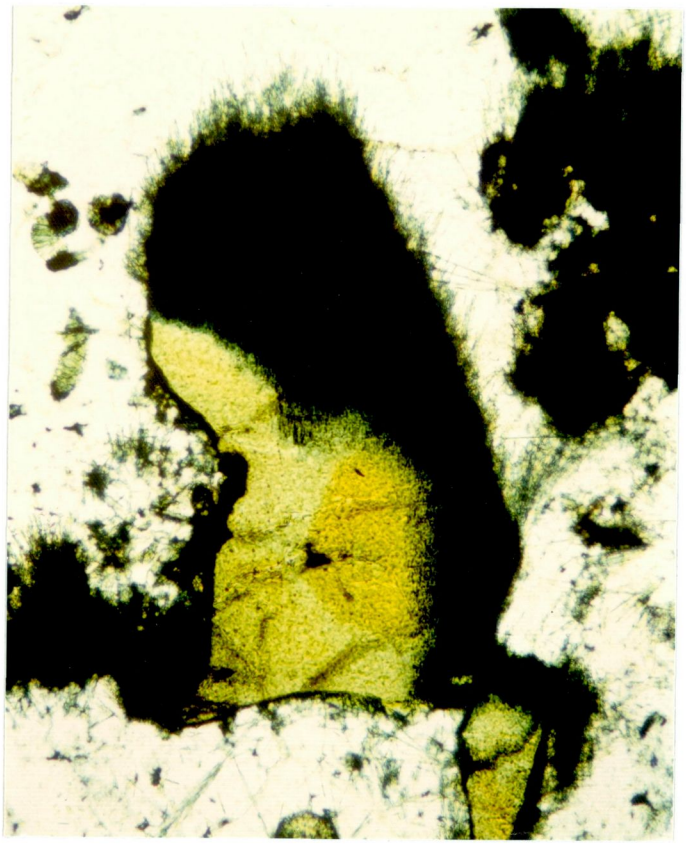

0 1mm

Plate 5:11 Yellow-brown tourmaline with blue-green acicular overgrowth in optical continuity, Tregarden Quarry Luxulyan. (LX207, p.p.l.)

	Yellow core	Blue overgrowth (i)	Blue overgrowth (ii)	Yellow core	Blue overgrowth (i)	Blue overgrowth (ii)	
SiO_2	35.02	34.73	34.59	34.94	34.70	34.44	
TiO_2	0.43	0.13	0.16	0.61	0.09	0.05	
B_2O_3	(10.42)	(10.42)	(10.42)	(10.42)	(10.42)	(10.42)	
Al_2O_3	34.73	29.40	29.05	33.81	29.40	29.09	
FeO	11.17	15.24	18.90	10.92	15.44	19.45	
MnO	0.08	0.31	0.13	0.14	0.17	0.08	
MgO	2.40	3.22	1.05	3.23	4.24	2.01	
CaO	0.17	0.11	0.11	0.16	0.37	0.36	
Na_2O	1.73	2.53	2.17	1.96	2.18	2.15	
Li_2O	(0.03)	(0.03)	(0.03)	(0.03)	(0.03)	(0.03)	
F	(0.43)	(0.43)	(0.43)	(0.43)	(0.43)	(0.43)	
H_2O	(2.54)	(2.54)	(2.54)	(2.54)	(2.54)	(2.54)	
CO_2	(0.03)	(0.03)	(0.03)	(0.03)	(0.03)	(0.03)	
	99.18	99.12	99.61	99.22	100.04	101.05	
Less O≡F	.18	.18	.18	.18	.18	.18	
	99.00	98.92	99.43	99.02	99.86	100.87	
Ions on the basis of 31 (O,OH,F):							
Si	5.93	6.04	6.07	5.92	6.00	5.99	
B	3.04	3.13	3.16	3.05	3.11	3.13	
Al	6.00	6.00	6.00	6.00	5.99	5.96	Z**
Al	0.93	0.03	0.01	0.76			Y
Fe	1.58	2.22	2.77	1.55	2.23	2.83	Y
Mg	0.61	0.84	0.27	0.82	1.09	0.52	Y
Ti	0.05	0.02	0.02	0.08	0.01	0.01	Y
Li	0.02	0.02	0.02	0.02	0.02	0.02	Y
Mn	0.01	0.05	0.02	0.02	0.03	0.01	Y
Na	0.57	0.85	0.74	0.64	0.73	0.72	X
Ca	0.03	0.02	0.02	0.03	0.07	0.07	X
OH	2.87	2.95	2.97	2.87	2.93	2.94	
F	0.23	0.24	0.24	0.23	0.23	0.24	

Table 5:12 Compositions of two tourmaline crystals with oriented overgrowths, Tregarden Quarry, Luxulyan.(sample LX207).

( ) detmd. in bulk samples of separated tourmaline
** structural positions in tourmaline
total iron as FeO

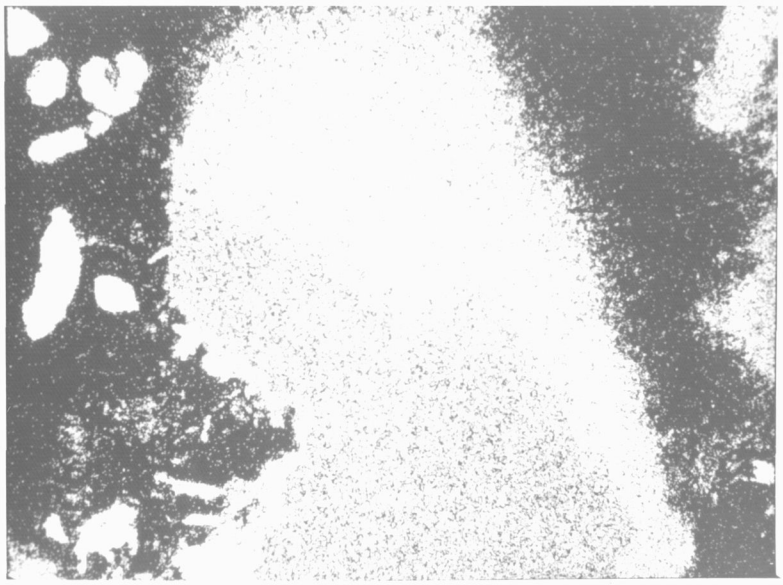

0 0.5mm

Plate 5:12 X-ray scan photomicrograph of tourmaline with oriented overgrowth (illustrated in Plate 5:11), showing distribution of iron.

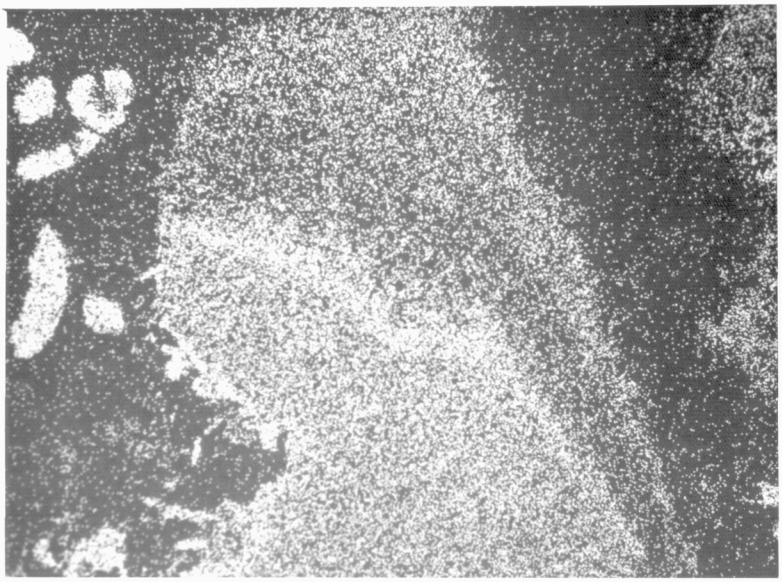

0 0.5mm

Plate 5:13 X-ray scan photomicrograph of tourmaline with oriented overgrowth, showing distribution of magnesium.

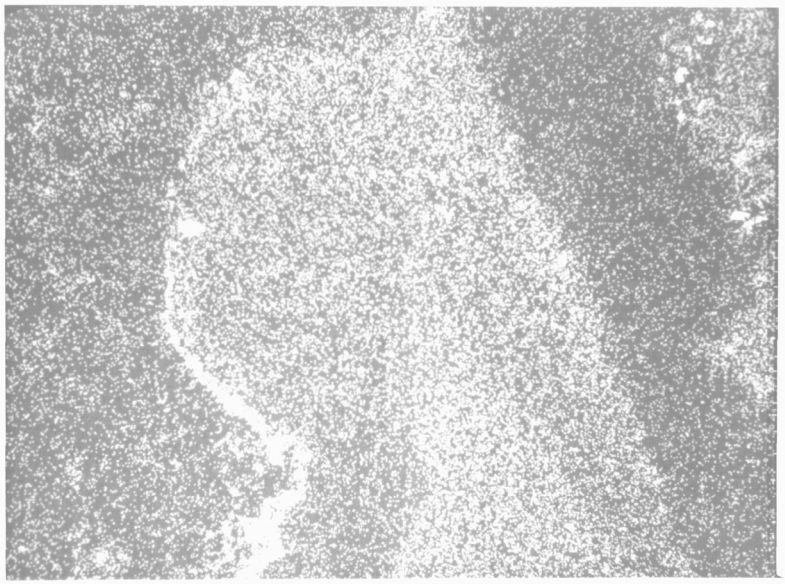

0 0.5mm

Plate 5:14 X-ray scan photomicrograph of tourmaline with oriented overgrowth, showing distribution of calcium.

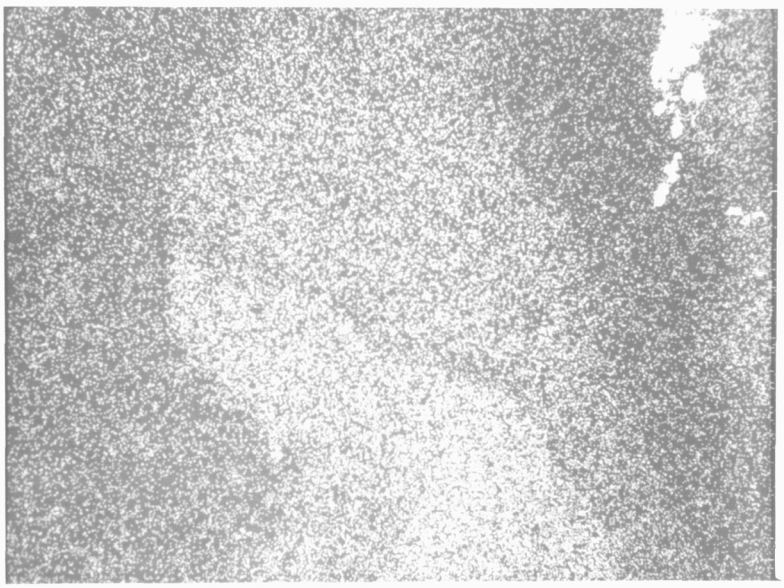

0 0.5mm

Plate 5:15 X-ray scan photomicrograph of tourmaline with oriented overgrowth, showing distribution of titanium. The light area at top right represents titanium oxides.

5.3.2 Other minerals associated with tourmalinisation and chloritisation

The conversion of biotite to chlorite involves a major reduction in potassium and silicon; magnesium shows a slight increase, but iron shows a much greater increase, since the chlorites at Tregarden are unusually iron-rich (up to 35% FeO). Iron-rich chlorites have also been reported from the chloritic wall-rock assemblages of Pendarves Mine, by Alderton (1976). Some of the Tregarden chlorites are also quite manganiferous, containing over 1% MnO. Titanium appears to be lost in the change from biotite to chlorite, and this finding is consistent with the appearance of titanium oxides which were identified in the chloritised vein margin.

Muscovites analysed were low in iron and titanium. Opaque minerals identified by microprobe proved to be ilmenite in the chloritised vein margin and arsenopyrite in the chloritised vein centre.

Feldspars in the veins and margins were predominantly potassic, but some areas within individual feldspar crystals showed extreme heterogeneity resulting from perthitic and microperthitic textures. Plagioclase was proved to be absent from the chloritised and tourmalinised veins.

5.4 Goonbarrow China Clay Pit

5.4.1 Tourmaline

In the tourmalinised vein at Goonbarrow, the tourmalines are yellow-brown with pale blue rims, and appear to be formed by skeletal replacement of feldspar. If biotite was ever present, no trace of it remains, either in the vein or its margin. Cored brown tourmalines with blue rims are found in the Stockscheider pegmatite at the boundary between two granite facies in the same pit.

5.4.1.1 Tourmalinised vein

Table 5:13 shows that the brown cores and blue rims of these tourmalines are very iron-rich, and close to the schorl end-member. Significant concentrations of magnesium, calcium or titanium are found only in the darker areas of the brown cores, and many of the outer blue zones contain none of these elements, although they do contain manganese in concentrations up to about 0.3% MnO. Tin, chlorine, chromium and phosphorus were included in the microprobe analyses, but were below the detection limit. The chief replacement process observed is the fine skeletal replacement by tourmaline of predominantly sodic feldspar. The resulting tourmaline is distinctive by its depletion in cations other than Fe, occupying the Y position (see Chapter 1 for structure). Tourmaline after Na-feldspar at Venford shows a similar, but less marked, depletion, by comparison with tourmaline after biotite or K-feldspar.

5.4.1.2 Cored tourmalines in pegmatite

Analyses given in the 'quartz-cored tourmaline' paper (Lister, 1979a) show that the tourmalines in the earlier formed pegmatite contain more magnesium and titanium than those in the tourmalinised vein.

5.4.2 Other minerals associated with tourmalinisation in the tourmalinised vein

The presence of topaz and cassiterite was confirmed by microprobe, but quantitative analyses were not obtained. Feldspars were too strongly kaolinised to give reliable microprobe analyses.

	Brown core	Brown core	Blue rim	Blue rim	
SiO_2	35.21	35.96	35.66	35.96	
TiO_2	0.73	0.08	0.06	-	
B_2O_3	(9.92)	(9.92)	(9.92)	(9.92)	
Al_2O_3	34.35	34.42	33.90	33.52	
FeO	13.00	14.33	14.40	14.90	
MnO	0.15	0.26	0.33	0.30	
MgO	1.73	-	0.15	-	
CaO	0.36	0.02	0.05	0.06	
Na_2O	2.07	2.17	2.31	1.96	
Li_2O	(0.03)*	(0.03)*	(0.03)*	(0.03)*	
F	(0.43)*	(0.43)*	(0.43)*	(0.43)*	
H_2O	(2.54)*	(2.54)*	(2.54)*	(2.54)*	
CO_2	(0.03)*	(0.03)*	(0.03)*	(0.03)*	
	100.55	100.19	99.76	99.65	
Less O ≡ F	.18	.18	.18	.18	
	100.37	100.01	99.58	99.47	
Ions on the basis of 31 (O,OH,F):					
Si	5.96	6.12	6.10	6.17	
B	2.90	2.91	2.93	2.94	
Al	6.00	6.00	6.00	6.00	Z**
Al	0.86	0.91	0.84	0.78	Y
Fe	1.84	2.04	2.06	2.14	Y
Mg	0.44	0.00	0.04	0.00	Y
Ti	0.09	0.01	0.01	0.00	Y
Li	0.02	0.02	0.02	0.02	Y
Mn	0.02	0.04	0.05	0.04	Y
Na	0.68	0.72	0.77	0.65	X
Ca	0.07	0.00	0.01	0.01	X
OH	2.87	2.88	2.90	2.91	
F	0.23	0.23	0.23	0.23	

Table 5:13 Tourmalines from the tourmalinised vein (GB005) at Goonbarrow China Clay Pit.

( ) detmd. in bulk samples of separated tourmaline
( )* values from bulk sample of Tregarden tourmaline
- below detection limit
** structural positions in tourmaline
total iron as FeO

5.5 Cape Cornwall

5.5.1 Tourmaline

Tourmaline at Cape Cornwall occurs in the layered tourmalinite and tourmaline granite of Porthledden, and also in pegmatite veins in the neighbouring Priest's Cove.

5.5.1.1 Cape Cornwall tourmalinite

The tourmalines are mostly yellow-brown or pale blue; occasionally, discontinuous dark blue outer rim portions are present. The tourmaline to which a definite mode of origin can be assigned is all after feldspar. The appearance of tourmalines so formed is similar to some of those in the vein at Goonbarrow, and Table 5:14 shows that the compositions also compare closely with those of the brown and blue zones at Goonbarrow. All varieties are iron-rich, and close to the schorl end-member. The pale blue variety is virtually pure schorl; no cations attributable to the Y position other than Fe were detected by microprobe. The yellow-brown zones always contain titanium, and often magnesium and calcium as well. The rare dark blue outer rims contain magnesium and sometimes calcium, but no titanium. The replaced feldspar is mainly potassic, but the resulting tourmaline has the compositions of tourmaline after sodic feldspar elsewhere (e.g. Venford Reservoir, and Goonbarrow); it is, however, quite distinct from any tourmaline after biotite examined at other localities.

5.5.1.2 Cored tourmalines from the pegmatite, Priest's Cove

Chemical analyses in the appended 'quartz-cored tourmaline' paper (Lister, 1979a) show that the corresponding zones in these cored tourmalines are very similar to those in the tourmalinite, except that the brown zones are somewhat less magnesian. The compositional variation within a single cored crystal is shown in Table 2 of the above mentioned paper.

	Brown core	Brown core	Pale blue rim	Dark blue rim
SiO_2	33.99	34.65	34.43	34.03
TiO_2	0.55	0.49	–	–
B_2O_3	(10.72)	(10.72)	(10.72)	(10.72)
Al_2O_3	35.24	35.09	34.74	34.72
FeO	13.92	14.26	15.16	14.94
MnO	–	–	–	–
MgO	0.72	–	–	–
CaO	0.25	–	–	0.14
Na_2O	1.63	1.47	1.44	1.62
Li_2O	(0.03)*	(0.03)*	(0.03)*	(0.03)*
F	(0.43)*	(0.43)*	(0.43)*	(0.43)*
H_2O	(2.54)*	(2.54)*	(2.54)*	(2.54)*
CO_2	(0.03)*	(0.03)*	(0.03)*	(0.03)*
	100.05	99.71	99.52	99.20
Less O ≡ F	.18	.18	.18	.18
	99.87	99.53	99.34	99.02

Ions on the basis of 31 (O,OH,F):

Si	5.77	5.89	5.89	5.84	
B	3.14	3.15	3.16	3.17	
Al	6.00	6.00	6.00	6.00	Z**
Al•	1.05	1.03	1.00	1.03	Y
Fe	1.98	2.03	2.17	2.14	Y
Mg	0.18	0.00	0.00	0.00	Y
Ti	0.07	0.06	0.00	0.00	Y
Li	0.02	0.02	0.02	0.02	Y
Mn	0.00	0.00	0.00	0.00	Y
Na	0.54	0.48	0.48	0.54	X
Ca	0.05	0.00	0.00	0.03	X
OH	2.88	2.88	2.90	2.91	
F	0.23	0.23	0.23	0.23	

Table 5:14 Tourmalines from the Cape Cornwall tourmalinite (sample CC005).

( ) detmd. in bulk samples of separated tourmaline
( )* values from bulk samples of Tregarden tourmaline
– below detection limit
** structural positions in tourmaline
total iron as FeO

5.6 Discussion

5.6.1 Compositional range and distribution

All tourmalines analysed in the present study fall essentially within the schorl-dravite solid solution series, and all except the Venford Reservoir tourmalines represent predominantly the schorl end-member of the tourmaline group. The pale blue tourmaline zones of Goonbarrow and Cape Cornwall are close to pure schorl in composition. Most brown or yellow tourmalines from all localities contain small concentrations of magnesium, calcium and titanium, in addition to iron. The greatest compositional variation is seen at Venford Reservoir, where tourmalines of very variable appearance yield compositions anywhere between almost pure dravite and almost pure schorl, sometimes with high proportions of calcium and titanium. Fig. 5:1 shows the general compositional range encountered in Venford Reservoir tourmalines, and Fig. 5:2 shows that the range of composition at other localities is considerably more restricted.

Tourmaline forming as an initial replacement product of biotite may be recognised by its high titanium, calcium and magnesium, and by depletion in aluminium compensated by iron entering the Z position in the structure. Extreme compositions showing significant departure from the schorl-dravite solid solution series are attributable either to replacement of biotite or to direct precipitation from an incoming fluid, but not generally to replacement of feldspar.

Tourmaline after sodium feldspar is predominantly schorl. Tourmaline after potassium feldspar may show a wider range of composition, including significant magnesium, and often large amounts of calcium (up to 2% CaO) in partial substitution for sodium; this substitution is not universal, and probably depends upon the supply of sodium from outside the feldspar crystal.

Recrystallisation obscures the origin of replacement tourmalines, by concentrating certain elements in well-defined concentric zones, and giving

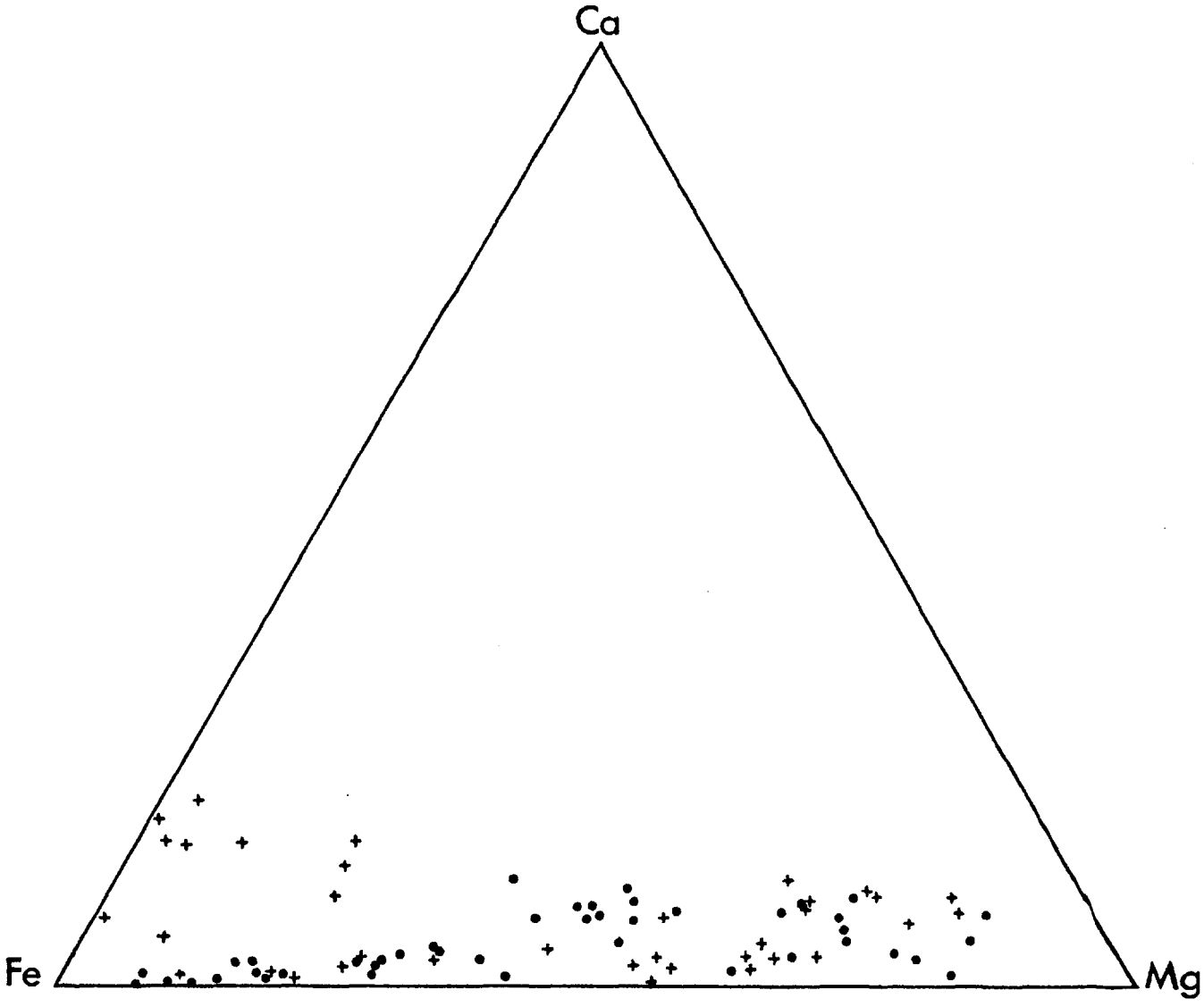

Fig. 5:1 Compositions of tourmaline at Venford Reservoir Quarry.

- • tourmaline in reddened granite and vein margins
- + tourmaline in main tourmalinised vein centre

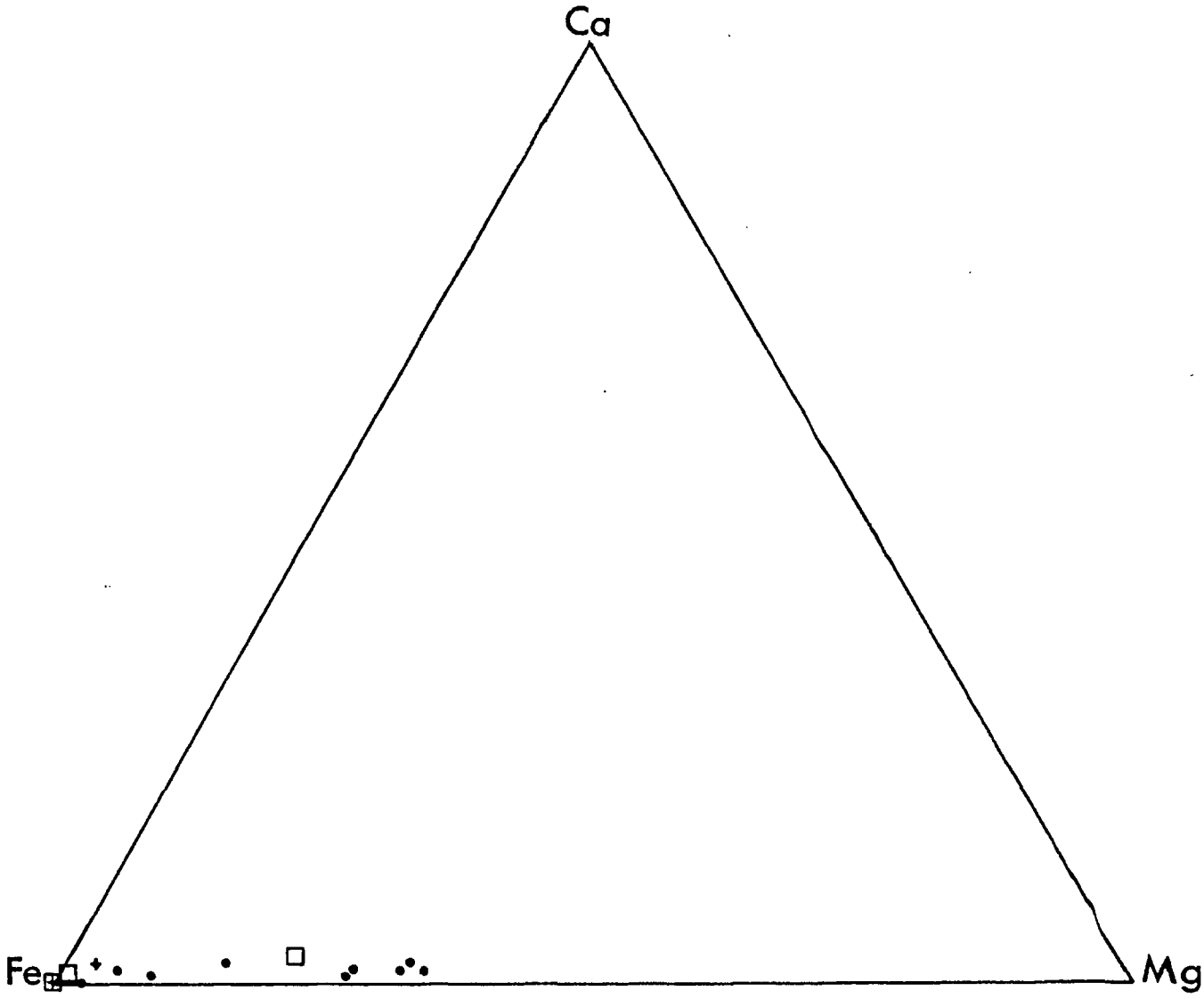

Fig. 5:2 Compositions of tourmaline at Tregarden Quarry, Goonbarrow, and Cape Cornwall.

- • Tregarden
- □ Goonbarrow
- + Cape Cornwall

tourmalines of disparate origins a similar appearance. Chemical composition also becomes less distinctive for the different tourmaline types, as recrystallisation proceeds, although characteristics such as high titanium may be retained.

Tourmaline precipitating directly from a fluid is not constrained by extant mineral compositions, but has characteristics reflecting the fluid composition, which may be iron-rich or magnesium-rich.

Colours shown by tourmaline in plane polarised light do not necessarily represent particular compositions or modes of origin. However, in general, it seems that titanium-bearing tourmalines are yellow, brown or occasionally almost black, while iron tourmalines lacking titanium are clear blue, and magnesian tourmalines when fairly pure are almost colourless. Combinations of these compositions produce a wide range of colours in plane polarised light.

On the basis of many chemical analyses of Cornubian tourmaline, Power (1968) concluded that magmatic and hydrothermal tourmaline could be distinguished by, in particular, the higher magnesium content of the latter. The present study has proved that hydrothermal tourmaline can in fact show a very wide range of composition, which overlaps that of magmatic tourmaline. It was shown in Chapter 2 that in any case, the criteria for identification of magmatic tourmaline are in doubt; however, there are grounds for regarding pegmatitic tourmaline (e.g. Lister, 1979a) as magmatic. The Tregarden and Goonbarrow hydrothermal tourmalines contain less magnesium than their magmatic counterparts, and the Venford Reservoir tourmalines, which are all hydrothermal, show every composition between schorl and dravite. At Cape Cornwall, similar compositions are found in both the tourmalinite and the pegmatites. It is, therefore, not possible to draw a simple chemical distinction between magmatic and hydrothermal tourmaline in Cornubia. The popular misconception that dravite is indicative of sedimentary tourmaline is also called into question by the occurrence of almost pure dravite zones at Venford Reservoir.

5.6.2 Enrichment trends

At all the localities examined, more than one tourmalinisation or tourmaline-producing event can be recognised, although the chronology of these events is not always certain.

At Venford Reservoir, tourmalines in the later, large tourmalinised vein are magnesium-enriched compared with those of the earlier, cavitous tourmalinised vein and monomineralic tourmaline veins. Within individual crystals in the main tourmalinised vein, the high magnesium concentrations in outermost zones support the theory of magnesium-enrichment with time.

Tregarden tourmalines show the opposite trend. Although the relative ages of the tourmalinised/chloritised veins and the pegmatitic joint fill are not certain, both contain tourmalines more iron-rich than those of the 'unaltered' granite. Compositions of tourmalines with oriented overgrowths, found in the tourmalinised and chloritised vein centres, support a trend of iron-enrichment with time, since the overgrowths are more iron-rich than the cores.

At Goonbarrow Pit, the tourmalinised vein presumably post-dates the Stockscheider pegmatite. Vein tourmalines are more iron-rich than pegmatite tourmalines, and individual crystals also have more iron-rich outer zones, indicating a chronological iron-enrichment trend.

The relative ages of the Cape Cornwall tourmalinite and the Priest's Cove pegmatites are not clear. However, tourmalines in both rocks have pale blue outer zones which are more iron-rich than the yellow-brown inner zones.

Therefore, while Venford Reservoir shows a trend of magnesium-enrichment with time, all the other localities examined indicate iron-enrichment or magnesium-depletion. At Venford Reservoir, the trend can reasonably be attributed to the evolution of a tourmalinising fluid. At other localities, this would not necessarily be a valid assumption, since the pegmatites and tourmalinised rocks are unlikely to have originated by the same mechanism.

5.6.3 Implications for tourmaline solid solution

As outlined in Chapter 1, tourmaline is not a single mineral species, but a group of minerals. While this group was originally thought to comprise three end-members (Fe; Mg; Li,Al), many additional actual or theoretical end-members are now known.

Most of the tourmalines examined in the present study fall within the schorl-dravite field, and the continuous range of compositions encountered confirms that this is a complete solid solution series. Some of the departures from Fe-Mg compositions illustrate the ability of the tourmaline structure to accomodate different cations.

Calcium is presumed to substitute for sodium in the tourmaline structure, giving the Ca-Mg end-member uvite (Dunn et al., 1977b) and the Ca-Li-Al end-member liddicoatite (Dunn et al., 1977a). In the Venford Reservoir tourmalines, calcium frequently appears in excess of sodium by weight, although the ionic proportion is always lower. Many of the very calcic tourmaline zones also contain considerably higher iron than magnesium (e.g. Table 5:6, zone 3), so that the possibility of a ferrous iron analogue of uvite and liddicoatite is implied. The absence of such an end-member may be due to the fact that axinite forms preferentially when the necessary elements are available. It has been suggested (R.A. Howie, pers. comm., 1979) that axinites generally contain manganese, and that this may be one of the factors causing axinite rather than calcic tourmaline to be formed. However, ferrous tourmalines can also contain manganese, and there is a theoretical manganese end member tourmaline (tsilaisite). The conditions required for a Ca-Fe end-member tourmaline might be difficult to fulfil in normal geological circumstances. Such conditions could be met in boron metasomatism of calcareous ironstones, or at the contact between an iron-rich igneous body and a limestone. Even then, the formation of axinite would need to be inhibited in some way, for tourmaline of this composition to form.

Kunitz (1936) named 'Titanturmalin' in a paper describing various titaniferous minerals analogous to titanaugite. Titantourmaline appears to have become adopted as a recognised mineral name (Hey, 1962), although the titanium concentrations upon which the appellation was based are apparently quite small (less than 1% TiO_2). Black (1971) reported one tourmaline with over 2% TiO_2 from New Zealand schists, and concentrations determined in the present study are sometimes over 3%, with one analysis of a narrow zone registering a staggering 8% TiO_2. If titanium entered tourmaline as Ti^{4+}, the possibilities for substitution either in the Y or Z position would be limited on account of the high charge, although this might assist its capture by tourmaline if other ions were deficient. Titanium incorporated in the tourmaline structure as Ti^{4+} could perhaps substitute for Al^{3+} in the Z position, if the charges were balanced by dehydroxylation in favour of oxygen. It is possible that the incorporation of titanium might create stresses within the crystal, which would facilitate recrystallisation, or resolution into narrow, concentric zones, in an effort to expel the incompatible ions. Very high titanium levels are restricted to narrow zones and small areas within tourmalines containing otherwise more normal concentrations The possibility of a titanium end-member is remote, since to produce a stable tourmaline structure, titanium would have to adopt a lower oxidation state than is usual, and would also have to be available in excess of iron and magnesium.

The initial replacement products of biotite at Venford Reservoir are deficient in aluminium, but contain excess iron compared with most tourmaline. An extreme example of this kind of composition is seen in the recently described ferridravite (Walenta and Dunn, 1979), which contains ferric iron substituting for aluminium in the Z position. While this feature is most likely to be found in oxidising, sedimentary conditions, it is not incompatible with biotite breakdown, which is essentially an oxidation reaction.

It has been noted (Chapter 2) that biotite breakdown precedes its replacement by tourmaline, and (Chapter 4) that this is probably accompanied by oxidation of iron in the reddened granite at Venford Reservoir. The Fe^{3+} thus made available could enter the Z position of tourmaline in the initial state of aluminium depletion. Later recrystallisation in the presence of aluminium eliminates this iron-rich tourmaline in favour of the more stable aluminous forms.

Chromium was not detected in any tourmalines in the present study; chromian dravites are generally restricted to ultramafic environments. Tin would have been a more likely candidate for inclusion in the Cornubian tourmalines, but none was recorded above the detection limit. When tin is present, as at Goonbarrow and the smaller Venford vein, it seems to form cassiterite rather than entering tourmaline. The tin levels reported by Nemec (1973) in tourmaline are all below 0.05%. The few hundred ppm of zinc determined in the Venford and Tregarden tourmalines seem surprisingly high in view of the absence of other metals. Lithium is present in the tourmalines examined, but only in trace concentrations.

5.7 Conclusions

Tourmalines analysed fall within the schorl-dravite solid solution series. The Venford Reservoir tourmalines show wide compositional variation, including some high titanium and calcium levels, and some examples of aluminium depletion; extreme compositions are normally attributable to biotite replacement, which involves several stages of recrystallisation.

It is not possible to distinguish magmatic from hydrothermal tourmaline on the basis of its chemistry. The colour of tourmaline in plane polarised light reflects the proportions of iron, magnesium and titanium.

Magnesium-enrichment with time is seen at Venford Reservoir, but the other localities show evidence of iron-enrichment with time.

6. Fluid inclusions in progressive tourmalinisation

The geochemical data discussed in Chapter 4 show that, in addition to the elements necessary for tourmaline formation, several other elements are also mobile during the tourmalinisation process. Alkali exchange phenomena, and the introduction or removal of halogens such as fluorine, indicate that tourmalinisation of granite takes place in an open system, from which components playing perhaps an important rôle in the alteration process, are allowed to escape.

The partitioning of the alkalis between solid and fluid phases during crystallisation shows a reciprocal relationship dependent upon temperature and pressure (Orville, 1963; Lagache and Weisbrod, 1977), with K:Na in the solid (feldspar) increasing with decreasing temperature. It is to be expected that fluid inclusions trapped at the time of crystallisation (or the last recrystallisation) will represent the composition of the concomitant fluid phase involved, either in magmatic processes, or, as in the present case, in metasomatic alteration.

Furthermore, fluid inclusion geothermometry could help elucidate two major problems. Firstly, in view of the very low temperatures required for tourmaline crystallisation in the diagenetic environment, it is important to consider whether metasomatic tourmalinisation can also take place at relatively low temperatures. Secondly, the question of interdependence between tourmalinisation and alkali metasomatism has been examined from the evidence of whole rock geochemistry (Chapter 4); fluid inclusions can provide data on the composition, and in particular the K:Na ratio, of the fluid phase mobile during tourmalinisation.

Fluid inclusion populations were examined microscopically in quartz and tourmaline from both granite and tourmalinised veins at all four localities, in order to identify common features, and to select one locality for more detailed and more quantitative study.

6.1 Previous work

Interest in the fluid inclusions found in tourmaline and tourmalinised rocks is by no means new. Sir David Brewster investigated fluid inclusions in minerals in the early nineteenth century, and according to Sorby (1897), he noted in fluid inclusions within tourmaline an unidentifiable liquid phase, which Sorby suggested was 'liquid carbonic acid'. Although an aqueous phase is dominant in most inclusions studied, it appears from the work of several authors (e.g. Karwowski, 1973; Motorina and Bakumenko, 1968; Slivko, 1965) that tourmaline quite commonly contains liquid CO_2 - bearing fluid inclusions. Solid NaCl and KCl daughter phases are also fairly common in aqueous fluid inclusions within tourmaline (Slivko, 1955). However, tourmaline has been the subject of relatively few fluid inclusions studies in the literature, by comparison with other commonly occurring minerals such as quartz, fluorite, apatite, or even topaz. One reason for this, as will be discussed below, is probably the tendency of tourmaline to heal its own crystal defects, and therefore rarely to retain primary fluid inclusions. Hence, workers on tourmaline-bearing rocks (e.g. Charoy, 1979a) have tended to favour the associated quartz for quantitative fluid inclusion studies, since it usually contains many more probable primary inclusions than does tourmaline. Those authors who have described fluid inclusions in tourmaline have been concerned not with the tourmalinisation process, but with the rôle of tourmaline either in a pegmatite body (e.g. Motorina and Bakumenko, 1968; Slivko, 1952 et seq.; Weis, 1953), or in an ore deposit (e.g. Dolmanova, 1976

On the subject of tourmalinisation, Sorby (1858, p.475) reported on material from Trevalgan, Cornwall: 'the removal of the feldspar from the centre of the surrounding, fine-grained granite, and the introduction of the quartz, mica, and schorl, cannot I think be explained except by the action of water. In this quartz are many interesting fluid cavities, and in some parts nearly all contain small cubic crystals.....'. Sorby crushed,

dissolved and analysed the contents of these fluid cavities to identify the cubic phase as 'chloride of sodium', and a further daughter mineral as 'sulphate of lime'. He also estimated, from the size of vapour bubbles in these inclusions, a heat of formation of 220°C, but suggested that this should be much higher owing to the influence of considerable pressure. It would have been difficult to add to these observations until the development of more accurate heating and freezing methods, and more sensitive analytical techniques. Indeed, even with the equipment now available, and in the light of the large amount of fluid inclusion data that has been amassed since Sorby's time, the nature and behaviour of fluids involved in tourmalinisation have not been fully described or understood.

Much of the more recent work in this field has been concerned with tourmalinised rocks that are closely associated with metalliferous mineralisation. The current interest in hydrothermal breccia pipes has generated fluid inclusion data relating to tourmalinisation, and involving some very saline fluids (Sillitoe and Sawkins, 1971; Grant et al., 1976; 1980). Most of the fluid inclusion studies relevant to tourmalinisation in southwest England have also dealt with tourmalinised rocks formed as a by-product of ore mineralisation (e.g. Alderton, 1976), or formed in association with ore-bearing veins and kaolinisation (e.g. Bray, 1980). These studies show that tourmalinisation can occur over a wide range of temperatures, and that tourmalinising fluids were probably chloride-rich. However, since these examples also show the effects of other alteration and mineralisation processes, it is difficult to isolate the features which are attributable to tourmalinisation alone.

The recent study by Charoy (1979a) on fluid inclusions in the Cape Cornwall tourmalinite has provided valuable data concerning fluids involved in tourmaline formation. This author reported magmatic temperatures, which support an origin for the tourmalinite by magmatic differentiation. Although

there is petrographic and geochemical evidence (from the present work) against such an origin, Charoy's fluid inclusion data indicate that perhaps the tourmalinite is not a typical example of a tourmalinised rock.

Thus, in order to characterise the fluids involved in tourmalinisation of granite, an example needs to be examined which is uncomplicated by any metalliferous mineralisation, and which has an unequivocal hydrothermal origin. A progressively tourmalinised sequence should be particularly valuable, by indicating the extent to which tourmalinising fluids affect the rocks adjacent to a tourmalinised vein.

6.2 Fluid inclusions in tourmaline

Tourmalines from all the localities discussed in previous chapters were examined microscopically for fluid inclusions. In all samples, and in all tourmaline types, the fluid inclusion populations are sparse, and are unsuitable for geothermometry owing to frequent 'necking-down', leakage, and absence of the vapour phase.

The acicular tourmaline varieties are virtually devoid of any fluid inclusions. The other tourmaline varieties contain monophase (usually liquid occasionally gas) and biphase (gas-liquid) inclusions; daughter minerals are rare. No CO_2-bearing inclusions have been recognised. Inclusions are often very irregular in shape, with re-entrant outlines, but show a tendency to elongation parallel to the main crystallographic axis of the host crystal. They occur either as isolated individuals, or in 'swarms' in which all inclusions are aligned parallel to one another and to the c-axis of the tourmaline. In the latter instance, the parallel inclusions are often disposed 'en echelon' (Fig. 6:1), apparently following a former growth surface or fracture plane; growth surfaces demarcated by such inclusion swarms may be parallel to the present crystal face or to a zone boundary. Where fibrous overgrowth occurs upon an existing tourmaline crystal (as at Tregarden),

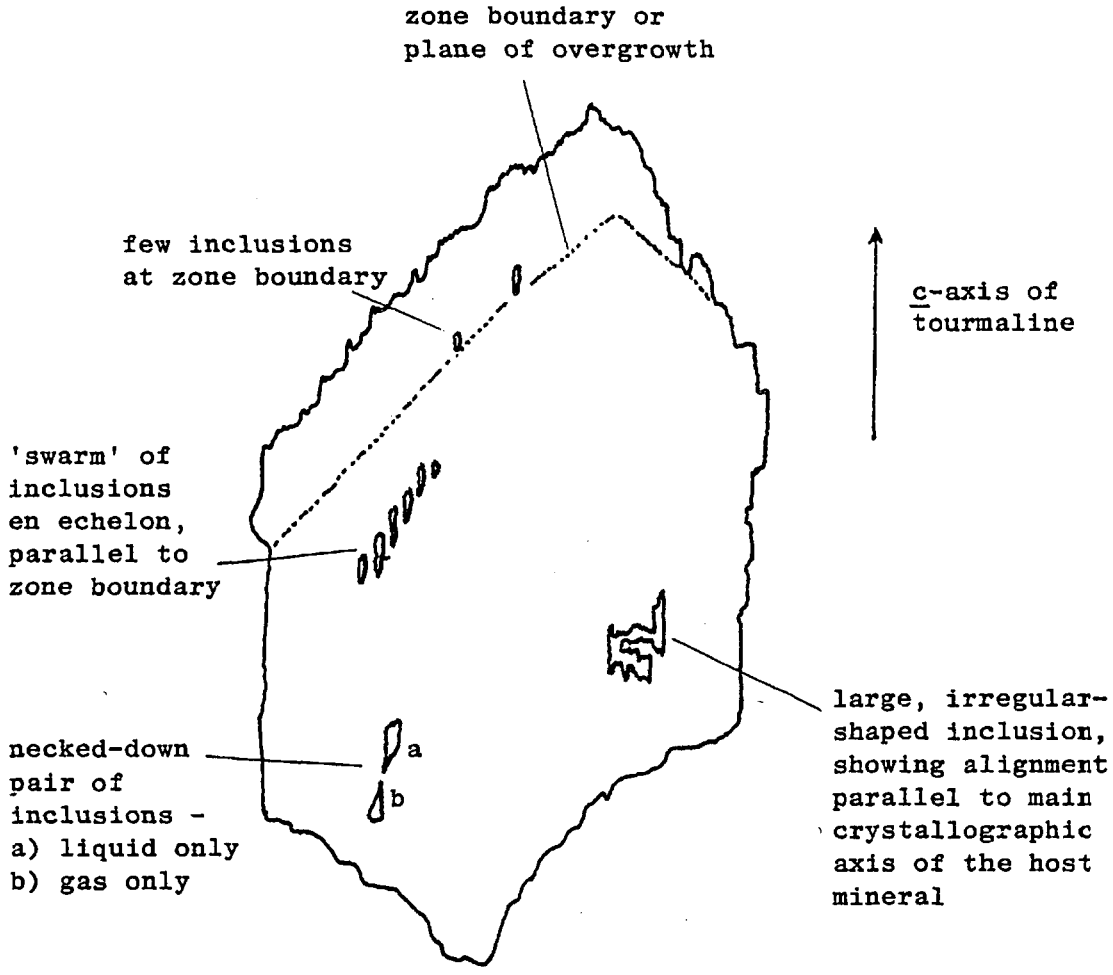

Fig. 6:1 Distribution and types of fluid inclusions in tourmaline from Venford Reservoir Quarry. (Crystal about 1 mm across)

similar swarms of parallel, elongate, monophase (liquid) inclusions occasionally appear along the plane of contact between crystal and overgrowth; where observed, such inclusions are usually so narrow as to be almost indistinguishable from the parallel, fibrous texture of the tourmaline. Although the plane of overgrowth is potentially a preferential site for fluid inclusions in tourmaline (Slivko, 1965), inclusions are no more prevalent here than along other, less prominent, internal growth planes. It is possible that any inclusions which were trapped at these compositional boundary sites have subsequently been reduced or eliminated.

An estimate was made of the abundance and variety of fluid inclusions in the tourmaline by comparison with those in the quartz in the same samples. Prismatic tourmaline from the main tourmalinised vein margin at Venford Reservoir Quarry (sample VR004) was selected as being representative (there was really very little difference between samples in this respect). A random count was made of inclusions visible in several fields of view, covering a total area of $1mm^2$. The following fluid inclusions were observed in this area of tourmaline:

(i) Three pairs of inclusions necked-down from three individuals; one of each pair contains liquid only, the other mostly vapour. Shape is irregular; size ranges from 10 to 30 μm.

(ii) Three isolated, irregular-shaped inclusions containing liquid only. All about 5 μm in size.

(iii) One 10 μm inclusion, almost entirely filled with vapour.

(iv) One inclusion containing a cubic daughter phase (probably halite) in liquid, with no vapour bubble. 15 μm in length.

(v) 'Swarm' of nine narrow, single-phase (liquid) inclusions, elongated parallel to the c-axis of the tourmaline. A few of the inclusions are over 30 μm long, but very narrow indeed (less than 1 μm).

Thus, the 1mm^2 area of tourmaline examined contains a total of twenty fluid inclusions, nearly all of which show evidence of change since trapping, and none of which could be used for geothermometry. The figure of 20 inclusions per mm^2 would be a generous estimate of the overall abundance in tourmaline, since not all crystals contain swarms of inclusions, and some contain no recognisable inclusions at all. The strong body colour of many tourmalines also makes the observation of fluid inclusions difficult. By contrast, the quartz in sample VR004 contains about 120 fluid inclusions (larger than 1 μm) per mm^2 (Fig. 6:2), and many of these are possible primary inclusions.

The general paucity of fluid inclusions in tourmaline compared with those in quartz in these rocks is difficult to explain. In the case of primary inclusions, their abundance would indicate rapid crystal growth, while an absence of such inclusions would imply slower growth (Roedder, 1979a, p.688). The large, prismatic tourmalines which have grown by steady replacement of other minerals might be expected to contain very few inclusions, by reason of their slow accretion. However, the fine acicular tourmaline has a crystal habit which indicates the very rapid crystallisation consistent with a sudden change in conditions (such as pressure release). This line of evidence is thus contradictory. Cavity healing and fluid leakage may also influence the abundance of fluid inclusions. Most minerals undergo a certain amount of recrystallisation and/or resolution after their initial formation (Roedder, 1979a). In tourmaline, this kind of change seems particularly prevalent, as evidenced by the frequency of necking-down phenomena in which one of a pair of necked-down inclusions contains no vapour bubble (this indicates that separation occurred after cooling to normal temperatures). The tendency to heal crystal defects by partial or total recrystallisation is indicated by other phenomena observed in tourmaline. For example, the capacity to develop euhedral crystals starting from fibrous overgrowth upon rounded grains is well known from the diagenetic environment (Krynine, 1946);

recrystallisation of fibrous tourmaline after biotite, to form single, larger tourmaline crystals, is also described in the present work (Chapter 2). It seems probably that these properties help to eliminate or reduce the original fluid inclusions, lattice defects, and fractures.

In view of the difficulties in finding suitable fluid inclusions in tourmaline, it was decided that the fluids associated with tourmalinisation would be better studied by examining the abundant fluid inclusions in the cogenetic quartz.

6.3 Fluid inclusions in quartz

Where quartz and tourmaline are intergrown, as in the maximum tourmalinisation zones at Venford Reservoir and Tregarden, the formation of the two minerals may with reasonable certainty be regarded as synchronous and cogenetic. Primary fluid inclusions in the quartz should therefore reflect conditions prevailing during tourmalinisation. Quartz in the granite outside the tourmalinised veins might be expected to contain both primary inclusions trapped during the original crystallisation of this mineral, and possibly also secondary inclusions superimposed upon the original populations as a result of nearby tourmalinisation.

6.3.1 Tregarden Quarry, Luxulyan

Quartz in the 'unaltered' granite contains about 55% two-phase (gas-liquid) inclusions, and 15% gas inclusions, the remainder comprising vapour + liquid + solid daughter minerals. Of the solid constituents, halite is minor compared with an unidentified, anhedral, birefringent phase. At the margins of both the tourmalinised and the chloritised veins, the proportion of solid-bearing inclusions decreases in favour of the two-phase variety; gas inclusions also become less abundant. In the zones of maximum alteration,

the abundance and size of fluid inclusions is drastically reduced, especially adjacent to strong tourmaline enrichment. Inclusions containing solid phases now comprise 11% of the total in the predominantly chloritised vein, and 19% in the mainly tourmalinised vein (compared with 30% in the unaltered granite) Two-phase inclusions now account for nearly 70% of the total; those with a gas bubble occupying less than 20% of the inclusion's volume (estimated visually) are much more common than in the unaltered granite, where inclusion with a larger vapour bubble predominate. This would imply lower homogenisation temperatures within the altered veins than in the granite, and is consistent with the theory that alteration occurred at lower than magmatic temperatures. In the same quarry, the pegmatitic joint fill containing quartz-cored tourmalines (LX052) yields a fluid inclusion assemblage similar to that of the tourmalinised vein margins, with two-phase inclusions of the vapour-rich variety forming nearly 60% of the total; no halite-bearing inclusions were observed in LX052.

6.3.2 Goonbarrow China Clay Pit

Bray (1980) conducted an extensive fluid inclusion study on kaolinised granite, mineralised veins, and elvans, from Goonbarrow Pit. He concluded that the quartz/tourmaline $\pm$ cassiterite/wolframite veins were intruded at 450°C, 450 bars (1.7 km depth) and 10 wt. % NaCl equivalent, and that by boiling and irreversible adiabatic expansion, the fluids cooled to 200°C and increased their salinity to 40 wt. % NaCl equivalent. The pressure under which the veins were formed could be calculated, because boiling inclusion assemblages were present.

Samples from the tourmalinised vein, G8002 - 005, were examined microscopically for fluid inclusions, but this locality was not envisaged as a suitable subject for quantitative studies, firstly because of the thorough investigation by Bray (1980), and secondly because the close association of

tourmalinisation with metalliferous mineralisation and kaolinisation would have precluded an appraisal of tourmalinisation alone. It was noted, however, that in the tourmalinised vein quartz, the predominant fluid inclusion types are two-phase (vapour-liquid) inclusions, with vapour occupying between 10 and 50% of the total volume. Halite-bearing inclusions make up about 10% of the total fluid inclusion population. In the Stockscheider pegmatite, which contains skeletal tourmalines, fluid inclusions in the quartz are two-phase and three-phase, and some contain halite + an additional, unidentified daughter mineral. The abundance of inclusions is greater in the pegmatite than in the tourmalinised vein.

6.3.3 Cape Cornwall

The Cape Cornwall tourmalinite was the subject of a major fluid inclusion study by Charoy (1979a), who reported vapour-liquid, halite-bearing, and halite + sylvite inclusions in the quartz (he also mentioned gas inclusions but did not investigate these). Salinities are between 30 and 40 equiv. wt. % NaCl in the three-phase inclusions. Halite + sylvite inclusions yield an average composition of 35% NaCl and 15% KCl. Homogenisation temperatures of 140 to 300°C need a pressure correction to obtain trapping temperatures of 650-700°C in accordance with the K:Na ratios. Hence, Charoy (1979a) proposed a magmatic rather than a metasomatic origin for the tourmalinite. Roedder and Bodnar (1980) have since published a criticism of the accepted methods of calculating pressure corrections for homogenisation temperatures, and have suggested a new method, which might possibly allow a reconsideration of pressures involved in the formation of the tourmalinite.

Samples CC010, 011-015, and 001-005 from the present study, all contain quartz of what appears to be the same generation, and very similar fluid inclusion populations are present throughout the sequence from tourmaline granite through the transition zone into tourmalinite. About 60 to 70%

of the inclusions present in the quartz are the two-phase (vapour-liquid) type, and between 6 and 18% are halite-bearing. The abundance of fluid inclusions is relatively low, all samples containing around 60 inclusions (> 2 μm) per mm^2, of which nearly 90% are less than 10 μm in diameter.

6.3.4. Venford Reservoir Quarry

This locality is a particularly suitable subject for a detailed fluid inclusion study of tourmalinisation, firstly because it is the only example examined in which a well-defined and extensive intermediate zone (reddened granite) exists between unaltered granite and tourmalinised rock, and secondly because in most samples the quartz contains very abundant and often very large fluid inclusions (up to 0.02 mm). A preliminary microscopic examination showed a predominance of halite-bearing inclusions throughout, with salinities (estimated from volumes) up to 50 wt. % NaCl. Unidentified second and even third daughter phases are present in some inclusions, notably the following types: (i) irregularly-shaped, birefringent crystals with low relief, and (ii) an elongate, birefringent phase (possibly either gypsum, or an iron chloride). Type (i) remains undissolved when heated to over 500°C, while type (ii) dissolves as described later in this chapter. Occasionally, sylvite appears, accompanying halite and other phases, but never alone. Monophase gas inclusions are also present, but since these sometimes form fracture-filling trails, they may be secondary. Passing from the reddened granite into the zone of maximum tourmalinisation, the most striking feature is a reduction in the abundance and size of fluid inclusions, and this coincides with the complete recrystallisation of quartz around minute tourmaline needles in the centre of the vein. The centre of the smaller, cavitous tourmalinised vein, incidentally, contains hardly any fluid inclusions at all The reduction in size and numbers of fluid inclusions in the main progressive

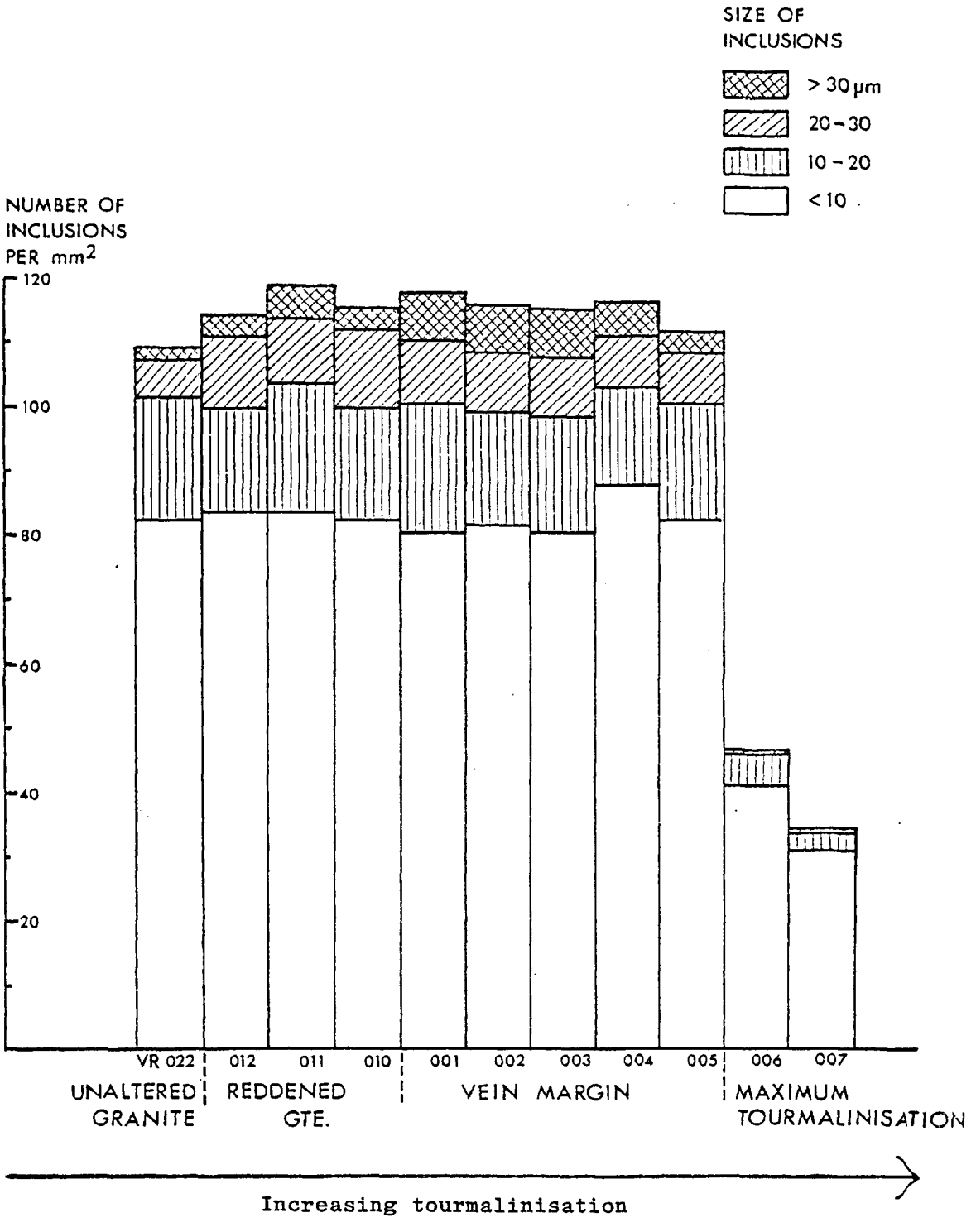

Fig. 6:2 Size and abundance of fluid inclusions in quartz at Venford Reservoir Quarry.

tourmalinisation sequence is shown diagrammatically in Fig. 6:2. The distribution of fluid inclusion types in each sample is illustrated in Fig. 6:3. In Fig. 6:3, the halite-bearing inclusions are differentiated into three types, namely type 2 in which halite is the only solid phase, type 2a which contain halite plus a further solid phase, and type 2b containing halite + sylvite ± further solid phases (the latter type is rare, and is restricted to samples external to the maximum tourmalinisation zone). Although the proportions of these saline inclusions types differ markedly between the unaltered granite (VR022) and the maximum tourmalinisation zone (VR006-007), the total percentage of inclusions containing halite remains fairly constant throughout, as do the salinities estimated from halite volumes. Two-phase inclusions may be divided visually into those containing either large or small vapour bubbles (the distinction being made, for convenience, at 20% of the total fluid inclusion volume); the proportion of two-phase inclusions containing a small vapour bubble increases as the maximum tourmalinisation zone is reached.

6.3.5 Comparison of observations at different localities

All the above examples of tourmalinisation are associated with aqueous fluid inclusions, and varying concentrations of sodium chloride. The salinities may be a feature of the general post-magmatic environment, since there is evidence (A.H.Rankin and D.H.M.Alderton, pers. comm., 1981) that fluid inclusion populations in quartz of the 'unaltered' Cornubian granites show a distribution of salinities which reflects the degree of local mineralisation. Dartmoor as a whole is rich in saline fluid inclusions, as to a lesser extent is the Land's End granite, while the eastern St. Austell pluton is relatively poor in saline fluid inclusions. Areas of intense metalliferous mineralisation are often characterised by fluid inclusions of relatively low salinity. Salinity is therfore not a diagnostic feature for tourmalinisation.

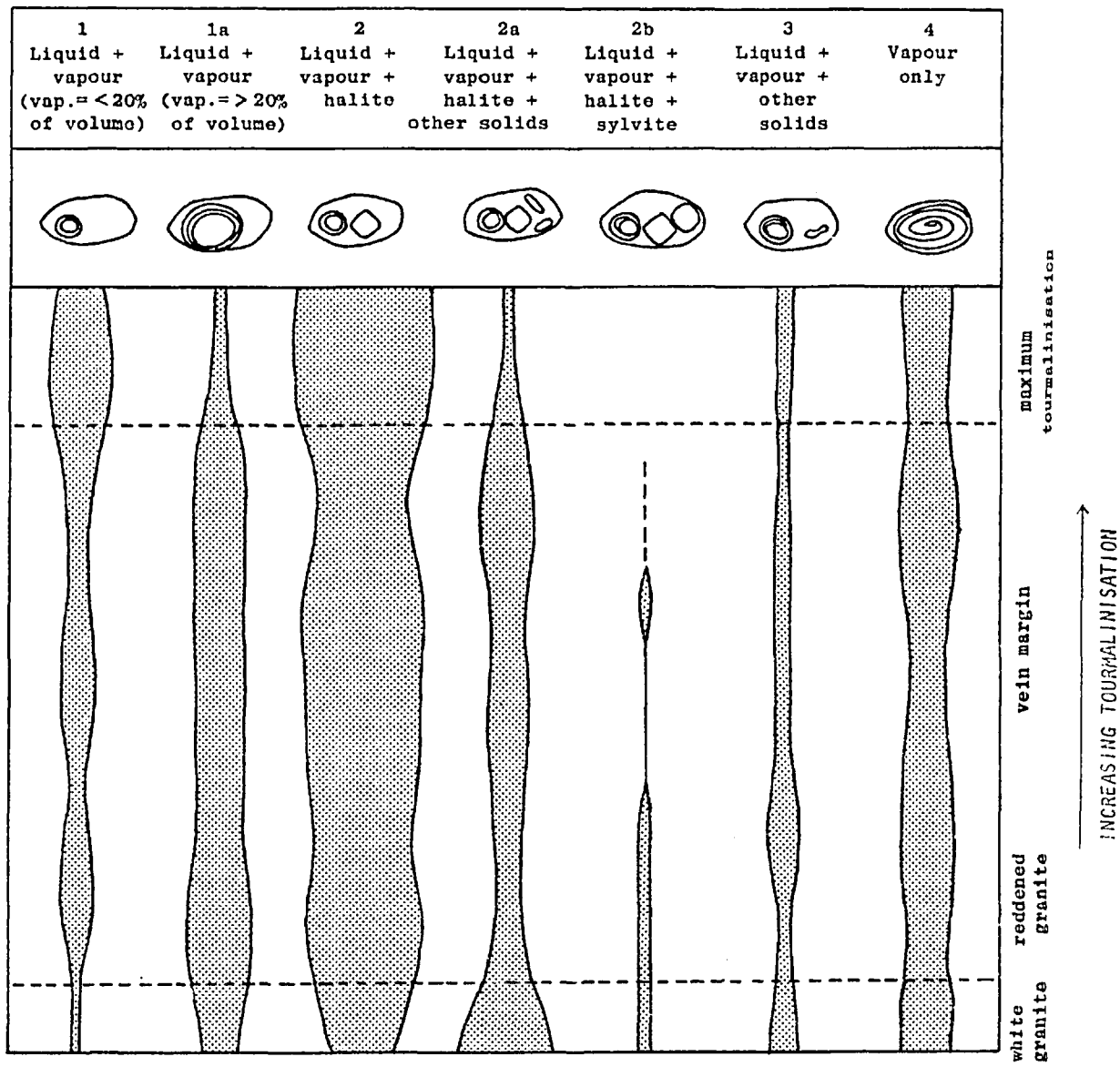

Fig. 6:3 **Distribution of fluid inclusion types in the progressive tourmalinisation sequence at Venford Reservoir Quarry.**

10%

20%

50% of total fluid inclusion population

Tourmalinisation often appears to be accompanied by a depletion in fluid inclusions; this is particularly noticeable at Tregarden and Venford, where complete progressive tourmalinisation sequences may be examined. Salinities are often similar in tourmalinised and untourmalinised rocks. The decrease in the size of vapour bubbles in two-phase inclusions at both Tregarden and Venford should imply lower homogenisation temperatures within the tourmalinised veins than outside.

The quantitative experimental work described below will relate exclusively to the main tourmalinised sequence at Venford Reservoir Quarry, as this, of the localities examined, most fully represents progressive tourmalinisation, and provides the most suitable material for such a study.

6.4 Experimental procedures

6.4.1 Geothermometry

The work was conducted in the Mining Geology Section of the Geology Department, Royal School of Mines, Imperial College.

6.4.1.1 Sample preparation

Thin slices of the rock samples, between 50 and 100 μm in thickness, and polished on both sides, were kindly prepared by Mr. B. Foster. Mounted in a polyester resin, the samples were ground, lapped and polished using a series of diamond pastes; the first polished surface was mounted face-down on a glass slide with a low melting point wax, and the sample cut off at about 150 μm using a WOCO macro-precision saw, so that the opposing surface could also be polished. By operating the equipment at slow rates, care was taken to avoid rupturing or overheating the inclusions during sample preparation. Small grains were detached from the polished slices for the experiments described below.

6.4.1.2 Apparatus

Minimum trapping temperatures and salinities were determined using a Leitz binocular microscope (allowing up to 512 X magnification), with a Linkam TH 600 heating/freezing stage and temperature control unit. The sample chamber may be sealed during heating or cooling, and has the facility for passing chilled gas over the sample for freezing purposes. The sample is placed on a 0.03 mm thick, glass cover slide, above a thermocouple which monitors the temperature; thermostatic control allows both the heating rate to be regulated, and the stage to be held at a fixed temperature for an indefinite period during operation. The image may either be viewed through the binocular optics of the microscope, or transmitted to a Hitachi closed circuit television screen. To allow for the inevitable differences in temperature between the actual inclusions and the monitoring device, Dr. A.H. Rankin had calibrated the system using a series of melting point standards; the correction factors, which increase with temperature, are listed in Appendix 2. With the application of these corrections, the accuracy may be reckoned as follows (Rankin, pers. comm., 1980): below -30°C generally better than $\pm$ 0.5°, between -30°C and 0°C better than $\pm$ 0.3°, between 0°C and 200°C about $\pm$ 2°, from 200°C to 400°C better than $\pm$ 5°, and above 400°C better than $\pm$ 8°. The accuracy is limited by variable heating rates allowing insufficient time for equilibration, as well as differences in vertical distance between the inclusion and the thermocouple, and uncertainties in the determination of last melting temperatures for calibration standards.

6.4.1.3 Methods

Salinities of two-phase (vapour-liquid) inclusions are determined by freezing. A small (1 or 2 mm) grain of the polished sample is suitably positioned on the glass slide, and the specimen chamber sealed. Nitrogen gas, chilled by passage through a copper coil surrounded by liquid nitrogen

at -196°C, is passed into the sample chamber until one of the previously selected two-phase inclusions is completely frozen. The flow of gas is then reduced while the stage is re-warmed to room temperature at a rate not greater than 1°C per minute, and both the first melting temperature (T_{fm}) and the last melting temperature (T_{lm}) of the ice are determined according to the method of Roedder (1962). In the determination of T_{lm}, the last melting point is confirmed by refreezing the final ice crystal before it disappears. It is usually possible only to observe one inclusion at a time with accuracy, but unlike heating, the procedure can normally be repeated without detriment to the sample, for the observation of further two-phase inclusions. The initial melting temperature (Tfm) gives a qualitative estimate of the composition of dissolved salts, by comparison with pure NaCl brine which begins to melt at -21.1°C. The temperature at which the final ice crystal melts may be directly related to the equivalent weight percent NaCl, using the diagram of Rankin (1978)(from data of Weast,1971).

Heating is used to determine both the gas-liquid homogenisation temperatures (which represent the minimum temperature of formation of each inclusion), and the equivalent weight percent NaCl in inclusions containing a solid halite daughter phase. With the sample positioned as for freezing, the stage is heated at a rate not exceeding 20°C per minute, until a temperature close to that of the first expected homogenisation or solution is reached; then the rate of heating may be slowed down to 10°C or less, to allow closer observation and more precise temperature monitoring. For two-phase (vapour-liquid) inclusions, the temperature of homogenisation to a single phase (T_h) is recorded. In the present study, all such inclusions homogenised to liquid by the disappearance of the gas bubble. For inclusions containing daughter minerals, both the gas-liquid homogenisation temperature and the solution temperature(s) of the daughter phase(s) are recorded. The solution temperature of halite (T_s) may be related to the equivalent weight

percent NaCl by the diagram of Sourirajan and Kennedy (1962). The same sample can be cooled and reheated for the observation of further inclusions, but this was not normally done in the present study, since particularly where high temperatures are involved, leakage from inclusions can affect the results obtained on subsequent heating. However, the comparatively large size and high concentration of inclusions in some samples allowed the simultaneous observation of several individuals in the same field of view during a single heating run. The practice normally followed was to detach the smallest possible fragment of sample and to heat this once only, taking a new fragment for further determinations.

6.4.2 Chemical analysis

This part of the work was conducted in the Department of Mineralogy, British Museum (Natural History).

The purpose of analysis was to determine the relative proportions of K and Na, and to obtain indications as to the possible presence of Ca and/or Fe in inclusions. Attempts at quantitative determination of these elements, by dissolving the quartz in hydrofluoric acid, showed such a vast potential for error that this method was abandoned in favour of a purely qualitative technique, aimed at indicating ratios only. The method used was similar to that of Alderton (1976, pp.236-7), and involved crushing the quartz sample and leaching the soluble fraction in deionised water. Theoretically, only the saline fluid inclusion contents become dissolved, since quartz itself and any other silicates present are, to all intents and purposes, insoluble in water. This proved to be a more satisfactory approach, particularly in view of the degree of intergrowth between quartz and other minerals, which made the separation of pure quartz virtually impossible.

About 0.3 gram of quartz was hand picked under the microscope. The actual weight was unimportant, since only molecular ratios of elements were

sought. The quartz grains were boiled in conc. nitric acid to remove surface contamination, then after washing, any small adherent particles were removed by agitation in an ultrasonic bath; the sample was then oven-dried at about 50°C. The cleaned quartz was crushed under deionised water in an agate mortar that had previously been tested for possible contamination (deionised water left to stand in the same mortar was used as a blank for each sample. The resulting material was centrifuged, and the liquor poured off and made up to volume. Na, K, Ca and Fe were determined using atomic absorption spectrometry, and ratios of these elements rather than actual concentrations were calculated.

6.5 Results

6.5.1 Geothermometry

6.5.1.1 Two-phase inclusions

Consisting of liquid with a vapour bubble, these inclusions were present in all samples, but formed only between 20 and 30% of the total fluid inclusion populations. In some samples, it was difficult to find any two-phase inclusions which were suitable for homogenisation, and some which contained a large proportion of vapour failed to homogenise within the temperature range of the equipment (operable up to 550°C).

For each two-phase inclusion, both freezing and heating data were obtained (in that order). On freezing, the first melting temperatures were all well below -21.1°C, and as low as -49°C, indicating that components other than NaCl must also have been present. By the additional presence of KCl, the first melting point could only be depressed to -22.9°C (Roedder, 1971, phase diagram p.114). Calcium salts, however, even in small quantity, can depress this temperature considerably; since the system H_2O - NaCl - KCl - $CaCl_2$ has a quaternary eutectic point at -56°C (Konnerup-Madsen, 1979), the temperatures measured could be explained by compositions including some

calcium (and/or possibly magnesium, whose behaviour is similar). It is not possible at the present time to quantify compositions from first melting data, but for a two-phase inclusion to exist at room temperature with no solid components, the liquid phase cannot contain more than either 26.3% NaCl, 19.54% KCl, or 30% $CaCl_2$. Calcium chloride would only be expected to form a solid phase (the hydrate, according to Konnerup-Madsen, 1979) at extremely high concentrations, and none was recognised in the present study. The following salinity determinations derived from final melting temperatures are based on data for pure NaCl solutions, since the presence of other chlorides is unlikely to cause any substantial departure from the known behaviour of the system NaCl - H_2O.

Final ice-melting temperatures, for those inclusions melting congruently, were all below -10°C, indicating concentrations between 13 and 25 equiv. wt. % NaCl. However, several inclusions, which at room temperature were bi-phase, crystallised either halite or hydrohalite ($NaCl.2H_2O$) when frozen and remelted. Halite, when crystallised thus, survived subsequent heating to at least 0°C, and occasionally to over 200°C, yielding salinities as high as 34 wt.% NaCl; the inclusions behaving in this manner must, presumably, have been trapped in a metastable state, due perhaps to the lack of internal nucleation points. Hydrohalite, which frequently crystallised during the melting of ice, always dissolved below 0°C; its formation requires salinity between 23.3 and 26.3 wt.% NaCl in a pure NaCl brine, and the actual salinity may be determined from the hydrohalite melting temperature (using the phase diagram of Roedder, 1962).

Salinities determined from freezing data are incorporated in Fig. 6:4, which shows that in most samples the two-phase and the halite-bearing inclusions yield a continuous range of salinities, from 10 to 50 equiv. wt.% NaCl.

Homogenisation temperatures range from 192 to 427°C, showing close

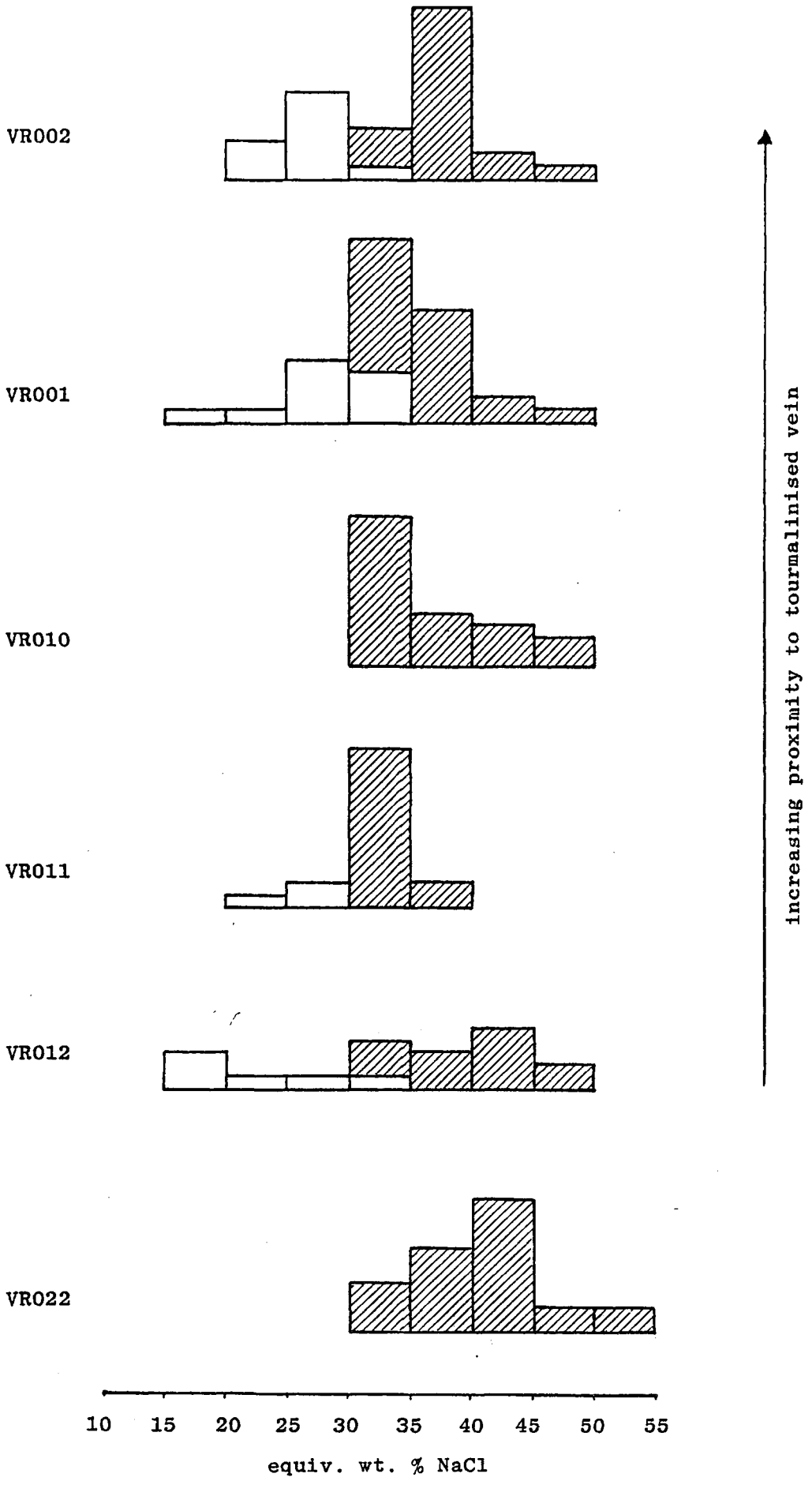

Fig. 6:4a Salinities of fluid inclusions from Venford Reservoir Quarry.

(Vertical scale = number of inclusions)

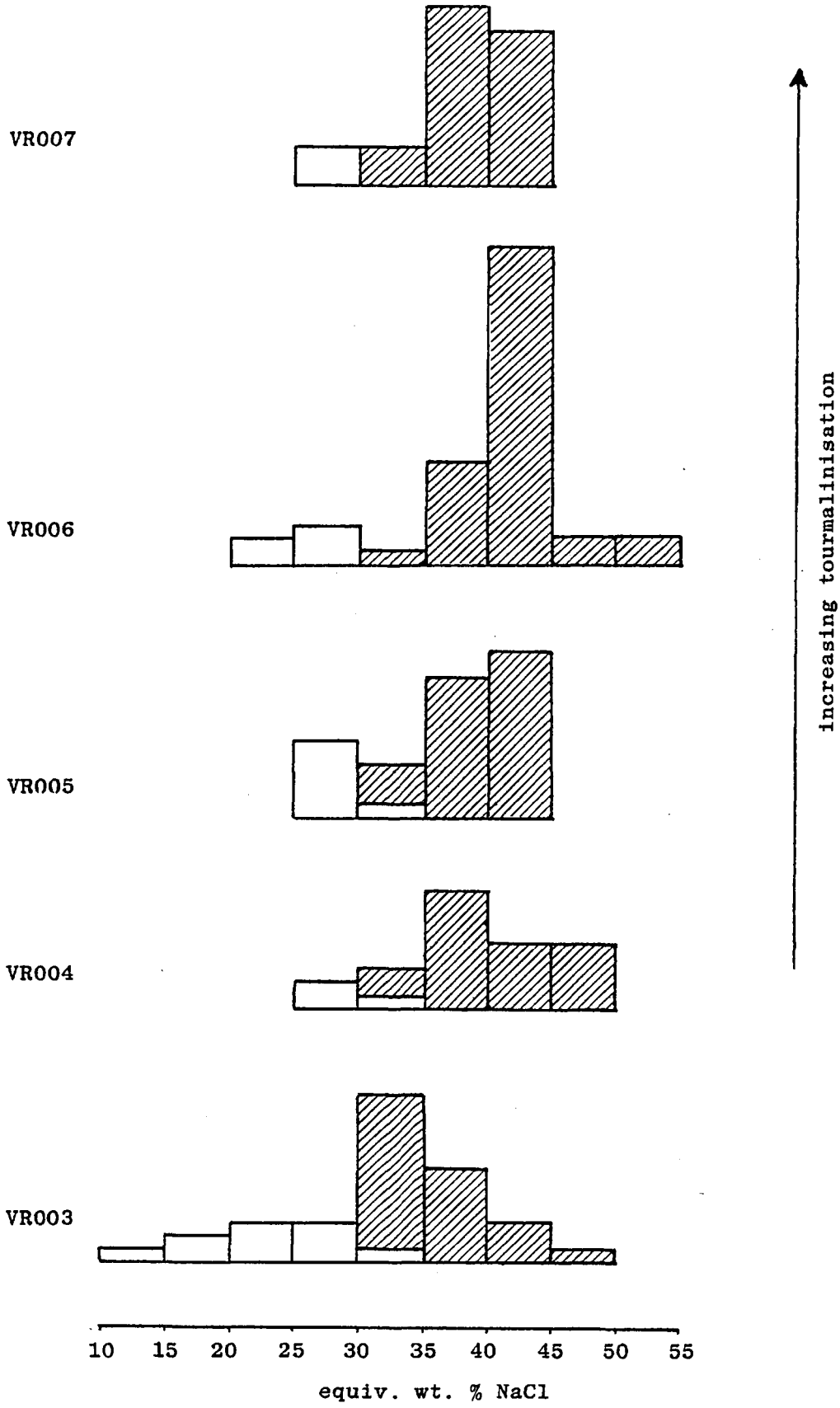

Fig. 6:4b Salinities of fluid inclusions from Venford Reservoir Quarry.

(Legend as for fig. 6:4a)

correlation with the halite-bearing inclusions in most samples. In the zone of maximum tourmalinisation, however, this correlation is less marked, the few two-phase inclusions examined giving somewhat higher T_h than their halite-bearing counterparts. The distribution of homogenisation data is shown in Fig. 6:5, and will be discussed more fully in the following section.

6.5.1.2 Halite-bearing inclusions

As well as liquid and vapour phases, these also contained a cube of halite which occupied generally between 5 and 20% of the inclusion's volume (Plate 6:1). Some halite-bearing inclusions contained additional, unidentified daughter minerals, and occasionally sylvite (KCl). This latter mineral is distinguishable from halite not only by a difference in refractive index and a tendency towards a slightly rounded-edged cubic morphology, but also by its much greater solubility coefficient on heating. Sylvite-bearing inclusions are discussed separately below.

For all three-phase (halite-bearing) inclusions, both gas-liquid homogenisation temperatures and halite solution temperatures were recorded. Freezing was unnecessary since both these quantities could be determined in a single heating run (although the presence of halite could be confirmed by its reaction with water to form hydrohalite, at temperatures below 0°C).

Salinities up to 50 equiv. wt. % NaCl are recorded throughout the sequence of granites and tourmalinised rocks, as shown in Fig. 6:4. The occurrence of the highest measured salinites in the zone of maximum tourmalinisation (VR006) and also in the unaltered granite (VR022) must be fortuitous, since no particular trend of salinity change emerges in passing from granite into tourmalinised material. In the maximum tourmalinisation zone, the majority of halite-bearing inclusions yielded salinities between 35 and 45 equiv. wt. % NaCl. However, if salinity is interpreted in terms of density, the maximum tourmalinisation zone is characterised by fluids which are considerably more dense than those outside the tourmalinised vein, since

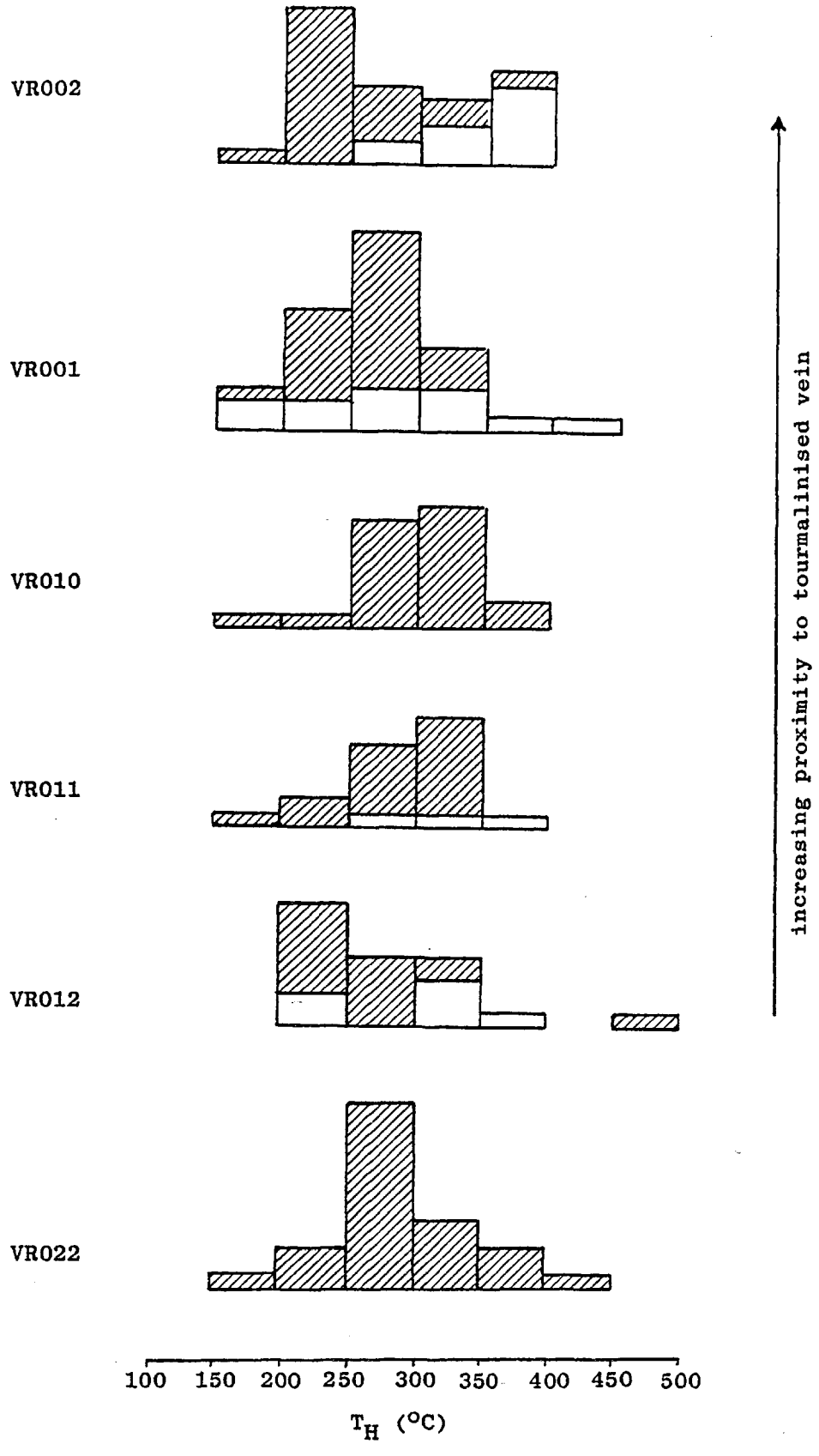

Fig. 6:5a Gas-liquid homogenisation temperatures for fluid inclusions from Venford Reservoir Quarry.

(Legend as for fig. 6:4a)

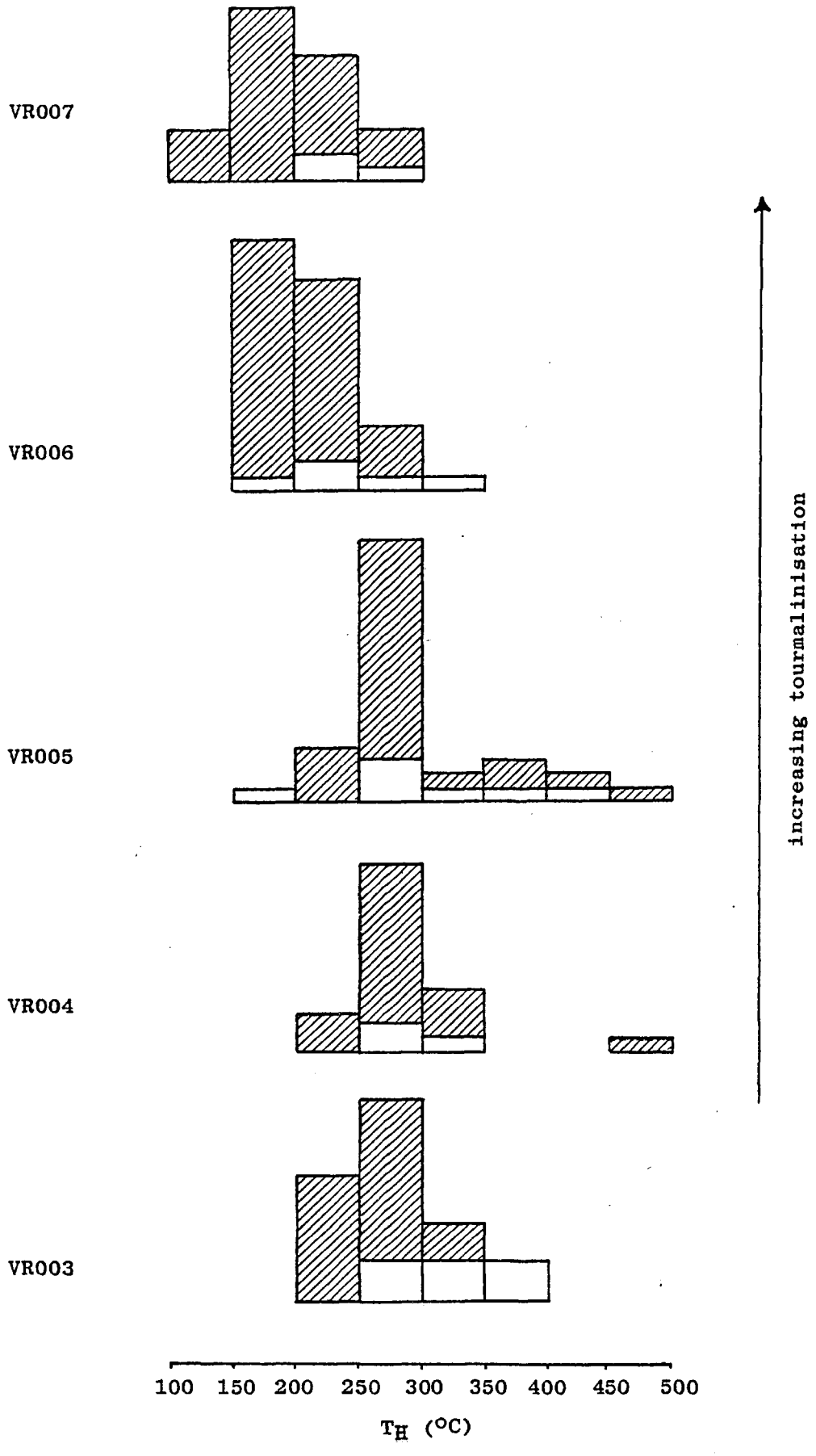

Fig. 6:5b Gas-liquid homogenisation temperatures for fluid inclusions from Venford Reservoir Quarry.

(Legend as for fig. 6:4a)

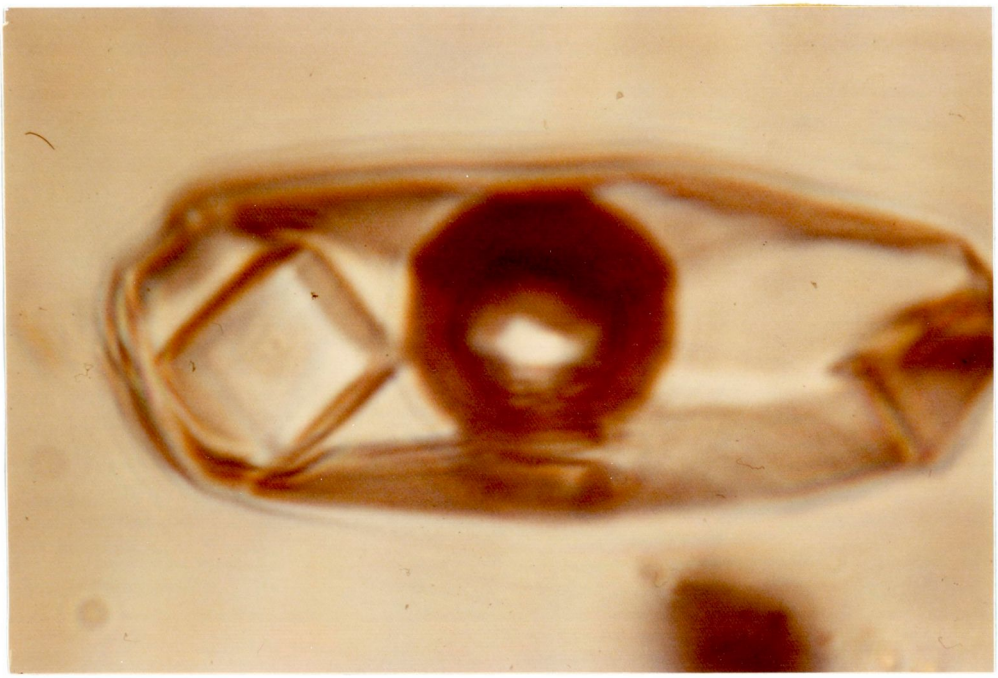

0 10μm

Plate 6:1 Halite-bearing fluid inclusion in quartz from the tourmalinised vein margin, Venford Reservoir Quarry. (Sample VR004)

similar salinities are associated with greater liquid:vapour ratios. This density trend is illustrated in Fig. 6:6.

Gas-liquid homogenisation temperatures are lowest in the zone of maximum tourmalinisation. Here the majority of inclusions homogenised to the liquid phase at around 200°C, by contrast to the higher T_h measured outside the vein (Fig. 6:5), and in fact a steady trend of decreasing homogenisation temperatures is seen with increasing tourmalinisation (Fig. 6:7). Most inclusions in the maximum tourmalinisation zone show $T_s > T_h$; it has, however, been noted (Charoy, 1979a) that a single fluid may evolve across the halite saturation curve to give two types of inclusions, namely those with $T_s > T_h$ and those with $T_h > T_s$.

6.5.1.3 Multiphase inclusions

A few inclusions contained halite, sylvite, and sometimes third and fourth solid phases (Fig. 6:8). Sylvite-bearing inclusions were rare, but all those seen were heated to determine the KCl:NaCl ratios; where additional soluble daughters were present, sylvite always dissolved first and halite last. The samples containing these multiphase inclusions were all external to the maximum tourmalinisation zone, namely in the unaltered granite (VR022), the reddened granite (VR012) and the margin of the tourmalinised vein (VR003). Although the very few measurements made must represent a biased sample of the whole fluid inclusion population, a progressive increase in the ratio KCl:NaCl with increasing distance away from the tourmalinised vein is indicated. Assuming that the observed behaviour is consistent with that within the system KCl - NaCl - H_2O, the relative proportions of these components may be determined from the phase diagram (Fig. 6:9) of Roedder (1971; 1979b). Concentrations range from 23 wt. % NaCl and 35 wt. % KCl in the unaltered granite, to 38 wt. % NaCl and 17 wt. % KCl in the tourmalinised vein margin. Details are given in Fig. 6:8, where the inclusions are also illustrated. Fig. 6:10 shows that while the KCl concentration increases away from the vein, the total chloride concentration remains similar.

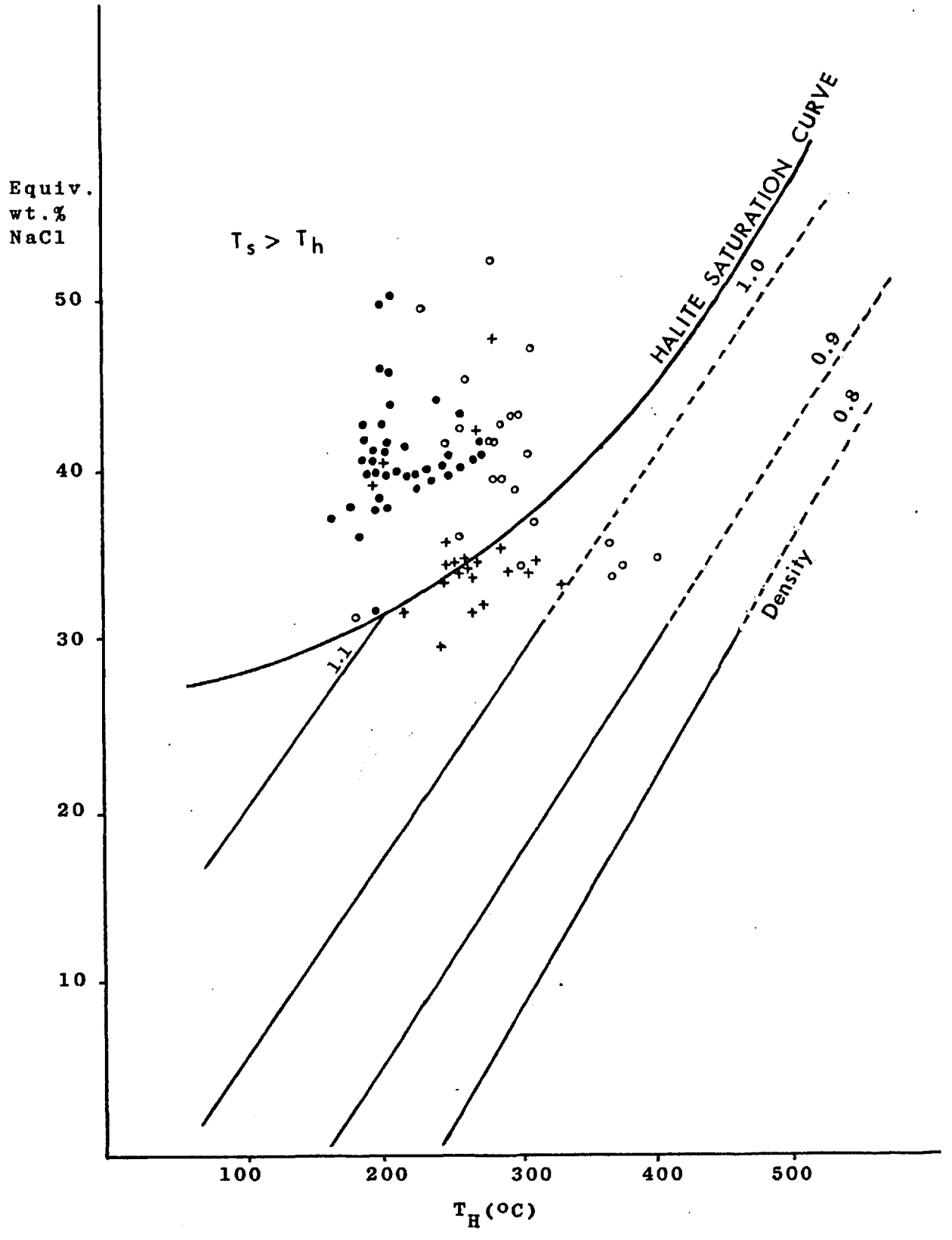

Fig. 6:6 Densities of fluid inclusions at Venford Reservoir Quarry

Legend:
- o VR022 ('unaltered' granite)
- + VR001 (reddened vein margin)
- • VR006 (maximum tourmalinisation zone)

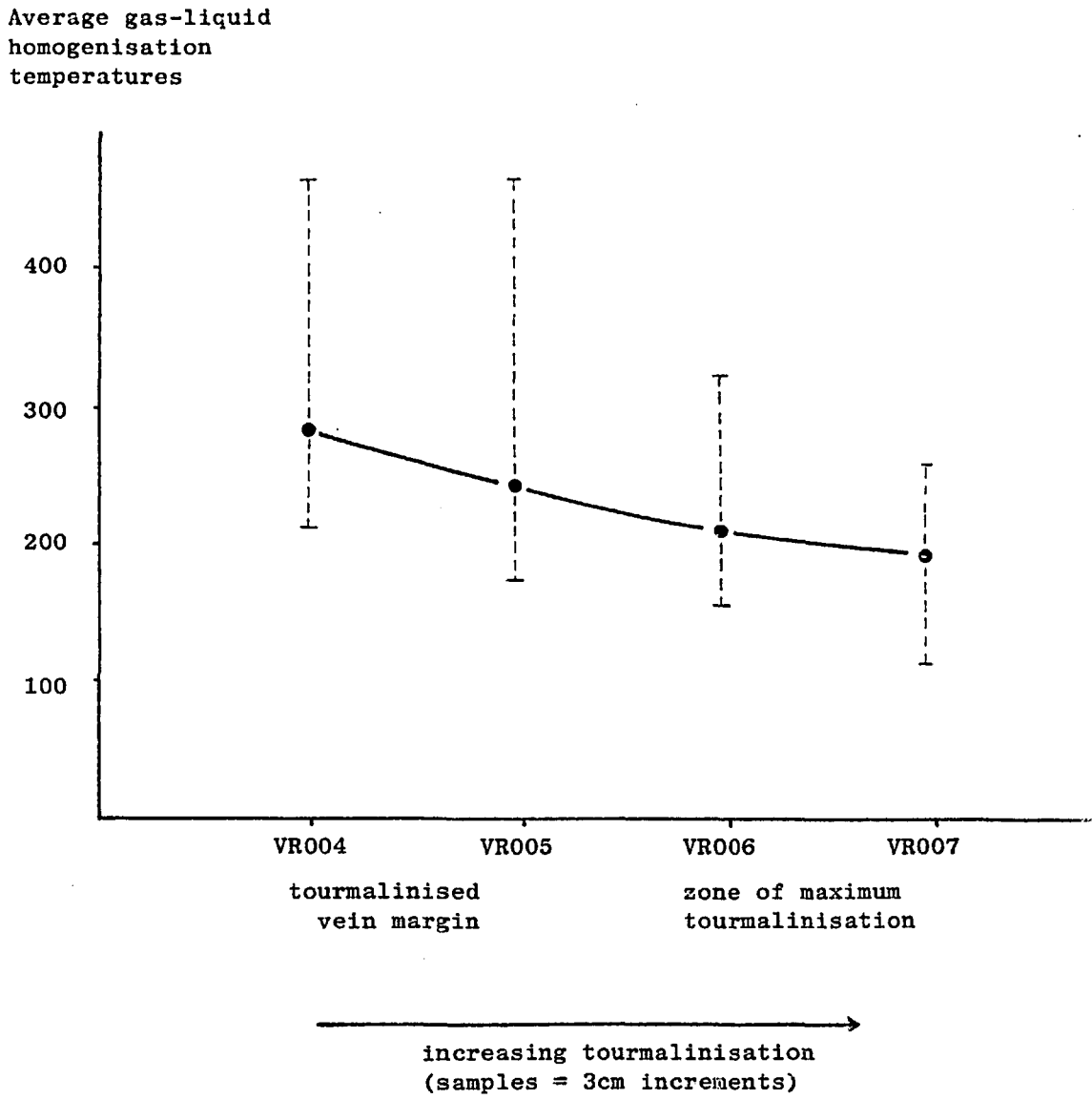

Fig. 6:7 Decrease in gas-liquid homogenisation temperatures with increasing tourmalinisation at Venford Reservoir Quarry

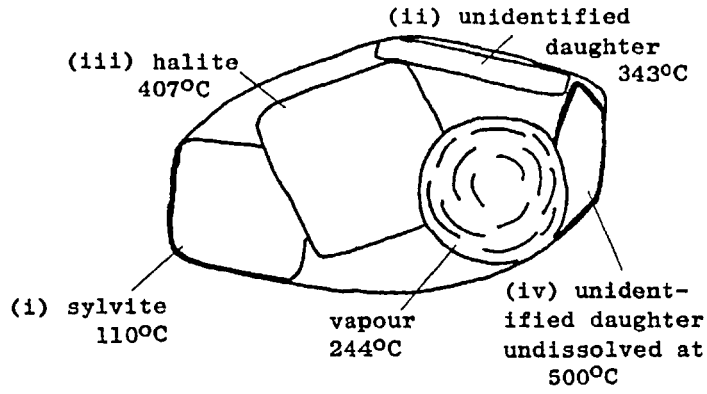

VR003

1. NaCl 38wt.%
   KCl 17 "
   H_2O 45 "

2. (not illustrated)
   NaCl 31wt.%
   KCl 21 "
   H_2O 48 "

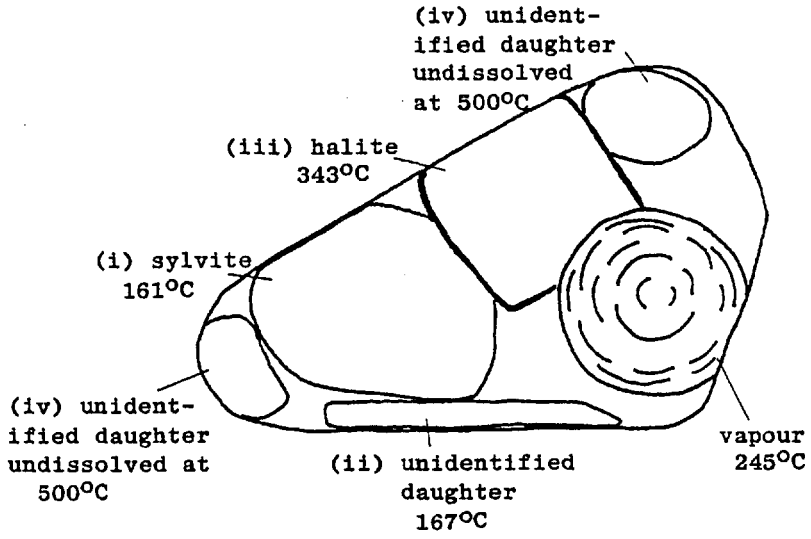

VR012

1. NaCl 28wt.%
   KCl 25 "
   H_2O 47 "

2. (not illustrated)
   NaCl 27wt.%
   KCl 24 "
   H_2O 47 "

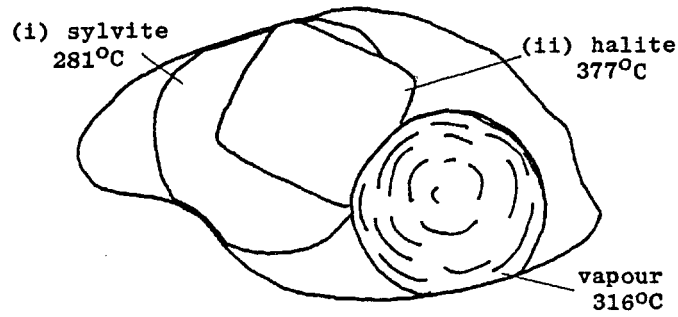

VR022

NaCl 23wt.%
KCl 35 "
H_2O 42 "

Fig. 6:8 Multiphase fluid inclusions from Venford Reservoir Quarry, showing order of dissolution and solution temperatures for solid phases, and T_H for vapour phase. Salinities in the system NaCl - KCl - H_2O are calculated from the phase diagram in Fig. 6:9.

Fig. 6.9. Phase diagram for the system NaCl - KCl - H_2O after Roedder (1971; 1979b)

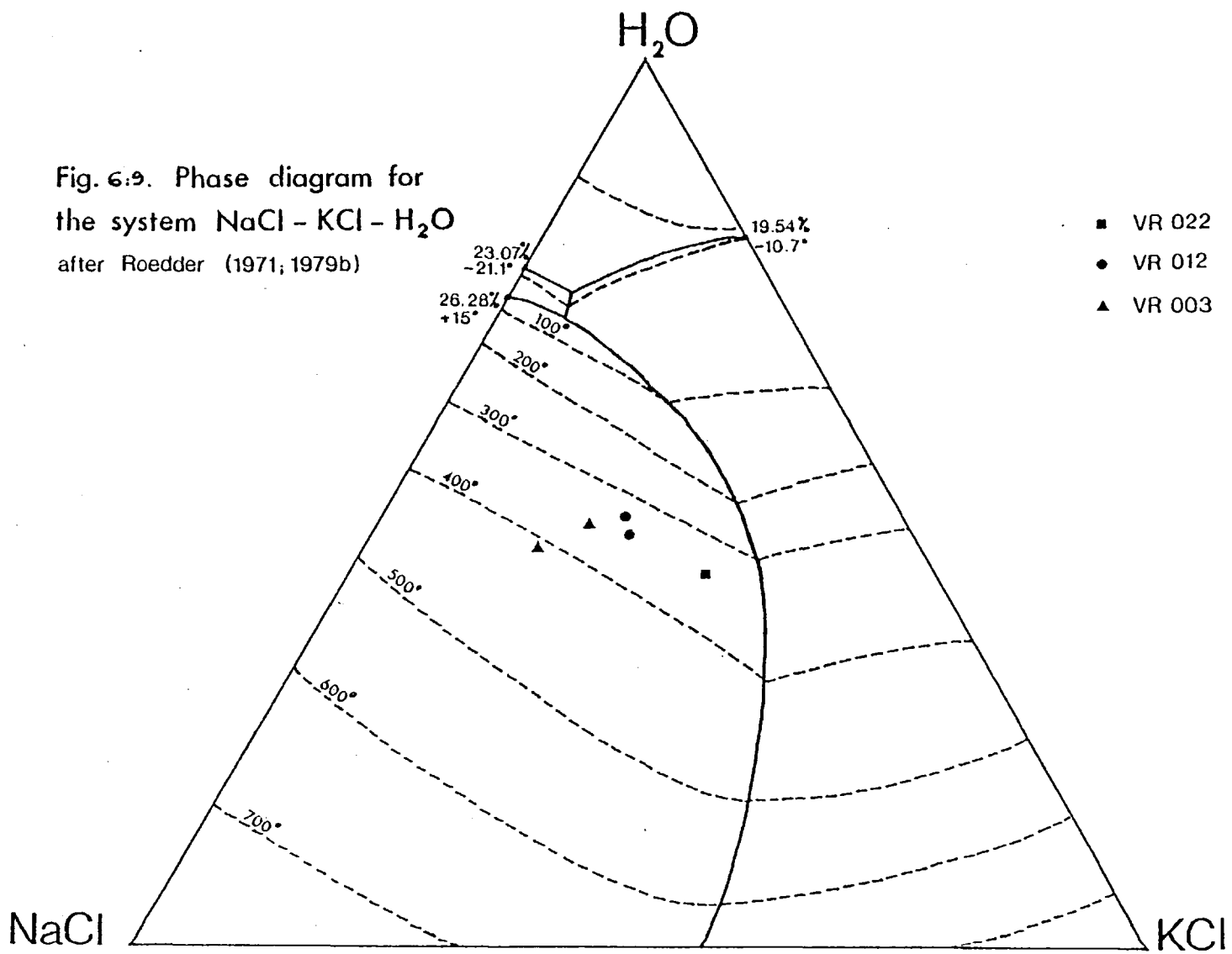

6.5.2 Analytical determination of chloride ratios

Na, K, Ca and Fe were measured by means of the crushing and leaching method described above, and are here expressed as chlorides. Quartz samples used were from the unaltered granite (VR022), the reddened granite (VR010) and the marginal tourmalinised vein material (VR003 and VR004). As stated previously, ratios rather than actual concentrations were of interest.

Table 6:1 shows the ratios of KCl:NaCl, and of each chloride to x, where x = the sum of other chlorides measured.

	KCl:NaCl	NaCl: x	KCl: x	$CaCl_2$: x	$FeCl_2$: x
VR022	0.248	1.794	0.190	0.103	0.117
VR010	0.223	2.246	0.183	0.129	0.041
VR003	0.195	2.600	0.164	0.114	0.036
VR004	0.192	2.623	0.161	0.109	0.040

Table 6:1 Chloride ratios of fluid inclusions in quartz, Venford Reservoir Quarry. (Arrow indicates increasing proximity to the main tourmalinised vein).

The ratios of KCl:NaCl decrease steadily with increasing proximity to the tourmalinised vein. Fig. 6:10 shows how these ratios, which represent the total fluid inclusion population of each sample, indicate the same trend as that implied by heating experiments on the very few halite + sylvite inclusions present. NaCl: x shows a progressive increase, and KCl: x a corresponding decrease with proximity to the vein.

$CaCl_2$ is present in all samples in about the same ratio to the other chlorides. Since the ratio of $FeCl_2$ to the remaining chlorides is greater in the unaltered granite (VR022) than in the other samples, it is possible that this may account for some of the numerous unidentified daughter minerals accompanying halite in the inclusions.

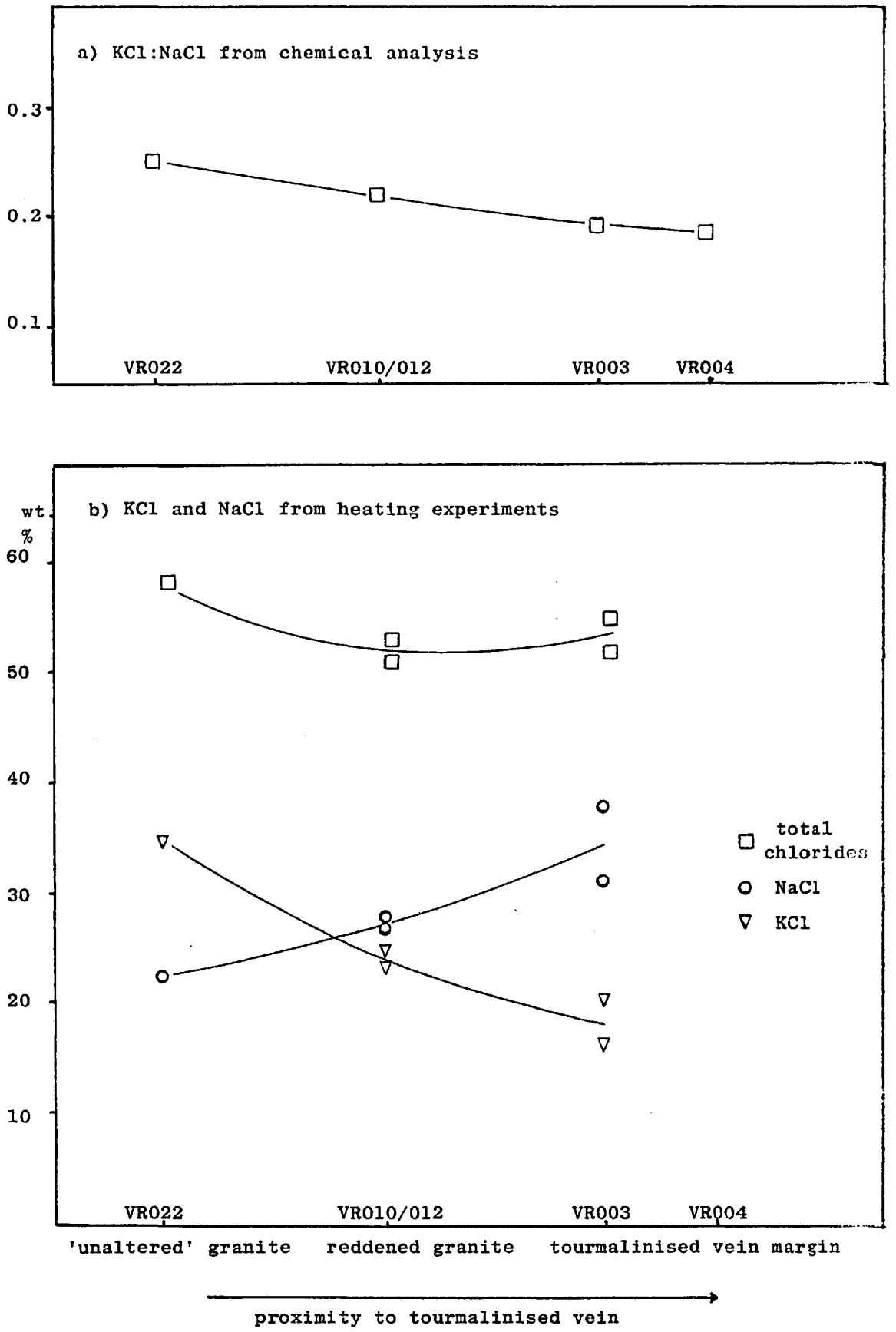

Fig. 6:10 Proportions of KCl and NaCl in fluid inclusions from Venford Reservoir Quarry

(KCl:NaCl from heating experiments is based on a few individual inclusions, and is therefore not representative of the total fluid inclusion population, although indicating the same general trends)

6.5.3 Pressure correction

The temperatures at which primary fluid inclusions homogenise to a single phase on heating represent the minimum crystallisation temperatures of the enclosing mineral grains. Unless there is evidence that crystallisation occurred in the absence of any appreciable overburden, and/or in a boiling environment, the actual temperature of formation will be higher than the minimum, due to the effect of pressure. The necessary correction may be estimated from circumstantial evidence relating to the pressure of overburden at the time of formation, or calculated either from K:Na ratios or from densities of inclusions.

Since all the Venford Reservoir samples contain some gas inclusions, it is possible that boiling did occur at some stage during the evolution of these rocks, and it is tempting to equate this with a pressure release which could have resulted in rapid growth of acicular tourmalines. However, the proportion of gas inclusions is small, and their linear alignment implies that they may be secondary. One cannot therefore postulate a boiling system prevailing throughout tourmalinisation, so some pressure correction is required.

Estimation of the lithostatic pressure due to overburden is subject to many uncertainties. The exact date of tourmalinisation is not known, and although it is generally supposed to be part of the late magmatic cycle, it has also been suggested (Dangerfield and Hawkes, 1969) that a considerable removal of overburden could have preceded mineralisation on Dartmoor.

According to the data of Lagache and Weisbrod (1977), the KCl:NaCl ratio measured in inclusions from the unaltered granite (VR022) would be consistent with a mean trapping temperature of about 600°C, if equilibrium were attained between water and rock. The ratio in the reddened granite (VR010) would indicate quartz crystallisation at about 550°C, and in the vein margin (VR003 and VR004) the temperature would be about 500°C. Since

all these samples gave average homogenisation temperatures around 300°C, this means that a progressively greater pressure must have prevailed with increasing distance from the vein. This is a reasonable concept, considering that the tourmalinised vein and its margins were probably pathways for the passage of fluids and for the escape of several components (Chapter 4). Although there is no K:Na ratio available for inclusions in the maximum tourmalinisation zone, a continuation of the trend towards K depletion may be anticipated, both from optical observation of daughter minerals, and from the marked increase in the whole-rock K:Na (Chapter 4), which should have a reciprocal relationship to the fluid inclusion K:Na. Therefore, the trapping temperature for inclusions in the maximum tourmalinisation zone can be estimated to be considerably less than 500°C, and probably around 400°C.

Alternatively, pressures could be calculated by the method of Klevtsov and Lemmlein (1959), which is based on densities of inclusions according to their volumes and compositions; this method is applicable to inclusions which, like the majority examined, show halite solution temperatures above gas-liquid homogenisation temperatures. However, Roedder and Bodnar (1980) have shown that the basic parameters upon which this method was erected are likely to be erroneous, and therefore that the method is invalid. Roedder and Bodnar (1980) outlined a new method by which pressures may more accurately be calculated from densities and volumes. Unfortunately, application of this new method to data from the present study required a degree of extrapolation which introduced unacceptable potential for error, and the results obtained were incompatible with conclusions implied by the K:Na ratios. The only conclusion to be drawn is that the minimum lithostatic pressure prevailing in the maximum tourmalinisation zone would be in the order of 1000 bars, which would represent an overburden of about 3km; if this is reliable, then tourmalinisation in the Dartmoor granite must have occurred at a very early stage in the denudation of the Variscides.

6.6 Discussion

There is little doubt that that quartz within the maximum tourmalinisation zone is genetically related to tourmalinisation, since it is intimately intergrown with acicular tourmaline. Outside the tourmalinised vein, however, the quartz appears to be of a different generation, but still shows evidence of recrystallisation (Chapter 2).

The fluid inclusion populations of quartz in the tourmalinised vein centre are characterised by low T_h values, low KCl:NaCl ratios, and inclusions which are both small in size and few in number, by comparison with populations in quartz outside the vein. It seems that the fluid inclusion assemblage in the vein centre is superimposed upon an existing assemblage in the white and reddened granite. However, it is possible that both quartz types and both fluid inclusion assemblages may be related to tourmalinisation.

From white granite, through reddened granite into the tourmalinised vein, fluid inclusions in quartz show a progressive decrease in the K:Na ratio, while maintaining a fairly constant salinity averaging about 40 equiv. wt. % NaCl. The K:Na ratio in the fluid inclusions is roughly reciprocal to that in the feldspar, and this relationship implies a genetic association between quartz recrystallisation and K-feldspathisation. It has been suggested (Chapter 4) that 'alkali metasomatism' affecting feldspars may have preceded tourmalinisation, although the two processes are genetically related. It therefore seems possible that the recrystallisation of quartz, to produce large, globular quartz aggregates in the reddened and white granites, may have accompanied K-feldspathisation as a precursor to tourmalinisation. A further quartz recrystallisation, this time restricted laterally to the extent of the tourmalinised vein, would then have accompanied tourmalinisation itself.

If both quartz types are thus related to tourmalinisation, this implies that tourmalinisation fluids have affected even the 'unaltered' granite. Over much of Dartmoor, the granite contains rounded, globular quartz, which is rich

in saline fluid inclusions; this quartz type is particularly prevalent in wall rock alteration zones adjacent to tourmaline-bearing metalliferous lodes (e.g. Birch Tor, and Hexworthy Mine; R. Scrivener, pers. comm., 1978), where it might be interpreted as a 'sweating out' effect. Of the Cornubian plutons, Dartmoor is probably the most heavily tourmalinised, and is also (A.H.Rankin and D.H.M.Alderton, pers. comm., 1980) the richest in saline fluid inclusions in quartz of the 'unaltered' granite. Post-magmatic K-enrichment is extensive, producing rapakivi feldspars (Hawkes, 1967) in areas of granite which appear in other respects unaltered. It is possible that although these effects may not be exactly contemporaneous with a major tourmalinisation episode, the general quartz recrystallisation and potassium enrichment within the pluton may be a part of the tourmalinisation cycle.

The positive correlation between T_h and K:Na in the fluid should be expected from the results of Orville (1963). There is an inverse relationship between these factors and the boron content of the rock, but it is not possible, from the data available, to say whether the boron concentration has influenced alkali behaviour (as found experimentally by Pichavant, 1979), since this could simply be temperature dependent. Average temperatures and salinities outside the vein probably represent the sum of more than one fluid inclusion assemblage.

Pressure calculations are ambiguous and contradictory, so will have to be disregarded for the present purposes. It is probable that any pressure correction to T_h would not substantially alter the trends observed. Pressure in the tourmalinised vein could have been lower than that in the granite, because the vein was partially fluidised and therefore subject to a combination of hydrostatic and lithostatic pressure at the time of formation; this would mean a larger pressure correction should apply to T_h measured in the granite than to T_h measured in the vein, and thus a trend of decreasing T_h towards the vein would remain valid.

6.7 Conclusions

Tourmalinisation at Venford Reservoir occurred at a temperature close to 400°C, in the presence of saline fluids containing up to 50 equiv. wt. % NaCl. The tourmalinised vein centre is characterised by a major reduction in the size and numbers of fluid inclusions in the quartz, by comparison with quartz outside the vein.

The K:Na ratio in fluid inclusions decreases with proximity to the tourmalinised vein, while the K:Na ratio in the solid phase (feldspar) shows a progressive increase. Throughout the progressive tourmalinisation sequence, however, sodium is the dominant cation determined in fluid inclusions, with potassium, calcium and iron also present. The highest concentration of iron is in inclusions in the 'unaltered' granite.

Alteration took place in at least two stages, the first of which may have been responsible for quartz recrystallisation extending into the white granite. K-feldspathisation may have commenced at this stage. Tourmalinisation followed, superimposing a new fluid inclusion assemblage in the centre of the tourmalinised vein. These two stages need not be regarded as two separate events, but could represent the evolution of a single hydrothermal system.

7. Conclusions and their wider implications

7.1 Conclusions

By the hydrothermal alteration of granites, tourmalinisation in southwest England has produced vertical replacement veins (e.g. at Venford Reservoir, Tregarden Quarry, and Goonbarrow) and subhorizontal replacement sheets (e.g. the Cape Cornwall tourmalinite). All the tourmalinised rocks examined are similar in terms of texture and grain size to their presumed parent material, and all contacts between granite and tourmalinised rock are gradational. Alteration is commonly accompanied by reddening of alkali feldspars, and the formation of muscovite (or hydromuscovite); these effects may extend several metres beyond the sites of maximum tourmalinisation, as at Venford Reservoir, or may be restricted to the tourmalinised rocks, as at Tregarden.

Table 7:1 summarises the major mineralogical and geochemical features of tourmalinisation at the four localities examined, and gives estimates of the temperature ranges applicable. Conclusions arising from the comparison of these tourmalinisation phenomena may be outlined as follows.

(i) Tourmalinisation and chloritisation are essentially the same process, requiring similar geochemical constraints apart from the availability of boron. The petrographic and geochemical evidence from Tregarden indicate that the two types of alteration are interchangable, and that every gradation can exist between complete tourmalinisation and complete chloritisation.

(ii) Tourmalinisation is often associated with potassium enrichment at the expense of sodium (as at Venford Reservoir, Tregarden and Cape Cornwall, but not at Goonbarrow, where subsequent kaolinisation has redistributed alkalies). The K:Na ratio is not quite proportional to the boron content of the rock, the greatest K concentration occuring

	Tourmalinisation product(s)	Constituents of untourmalinised granite	Minerals replaced during tourmalinisation	Minerals formed during tourmalinisation	Max. B_2O_3%	Chemical gains	Chemical losses	Temperature (& source of temp. data)
Tregarden	Chloritised/ tourmalinised rock	Qtz.,alkali felds., plag., biotite, muscovite,(tourm.)	Biotite,plag., (alkali felds.)	Chlorite,muscovite, tourmaline,fluorite, K-feldspar,sulphide	0.18	Al,Fe,Mg, K,Rb,Sr, Ba,Zn	Si,Na, F,Li	230-350°C (Alderton,1976, on similar assemblages from Pendarves)
Tregarden	Luxullianite-type rock	as above	as above	Tourmaline,K-felds., muscovite,chlorite	1.73	Al,Fe,Mg, K,Rb,Ba	Si,Na, F,Li	
Venford Reservoir	Luxullianite-type rock	Qtz.,plag.,alkali felds.,biotite (tourmaline)	Biotite,plag., (alkali felds.)	Tourmaline,K-feldspar, hydromuscovite, apatite,(cassiterite)	3.09	Al,Fe,Mg, K,Sr,Zn	Si,Na, Li,Rb	400°C (present work)
Goonbarrow	Tourmalinite/ greisen	Qtz.,plag.,Li-mica, alkali feldspar, (tourmaline)	Li-mica, feldspar	Tourmaline,topaz, muscovite,cassiterite	6.34	Al,Fe,Mg, Li,F,Mn, Zn,Sn	Si,K, Rb	450°C (Bray,1980)
Cape Cornwall	Tourmaline granite/greisen	Qtz.,plag., alkali feldspar, biotite	Biotite,plag.	Tourmaline,muscovite, K-feldspar	1.46	Al,Fe,K	Si,Na, Li,F	no data
Cape Cornwall	Tourmalinite	as above	Feldspar	Tourmaline,qtz., fluorapatite,muscovite, sulphide,(cassiterite)	4.21	Si,Fe,Na Zn	K,Mg,Rb, Sr,Ba,Li	> 650°C (Charoy,1979a)

Table 7:1 Summary of mineralogy, geochemistry and geothermometry involved in tourmalinisation at Tregarden, Venford Reservoir, Goonbarrow and Cape Cornwall.

in chloritised veins, and tourmalinised vein margins. Alkali behaviour may be interpreted in terms of an alteration process in which chloritisation and K-feldspathisation are necessary precursors to tourmalinisation, moving along joints ahead of the boron-rich fraction of the fluid.

(iii) A zone of geochemical depletion occurs between granite and tourmalinised rock. The intensely reddened zone at Venford Reservoir is characterised by a decrease, not an increase, in iron; the cause of reddening is a change in the oxidation state of the iron present. Depletion in Fe, Mg, Ca, Li and F across this intermediate zone may possibly be due to leaching of ions towards the tourmalinised veins.

(iv) Fluorine and lithium are not prerequisites to tourmalinisation, as has often been assumed. Both elements may actually be depleted by the tourmalinisation process. On the breakdown of biotite or lithionite micas, F and Li are released, but only small concentrations of these elements are accommodated in tourmaline of the schorl-dravite series. At Tregarden, fluorine derived from biotite forms fluorite, although the whole-rock fluorine concentration is reduced on biotite breakdown.

(v) Yellow/brown tourmaline in the Cornubian granites is not necessarily primary, but may be formed by replacement of feldspar. Evidence for this replacement process is seen at all four localities examined.

(vi) Blue/green tourmaline can be formed by replacement of either biotite or feldspar.

(vii) The geochemical distinction between primary and secondary (or magmatic and hydrothermal) tourmaline is not a simple one. Hydrothermal tourmaline is not necessarily more magnesian, as has previously been thought, but can be exceptionally iron-rich. Some hydrothermal

tourmaline is iron-rich and aluminium-depleted. The range of composition seen in hydrothermal tourmaline from a single locality can be enormous; at Venford Reservoir, compositions range from almost pure schorl to almost pure dravite, and calcium and titanium are also important components.

(viii) Complex compositional zoning in hydrothermal tourmalines does not necessarily represent the influx of several successive fluids, but can result from recrystallisation of polycrystalline tourmaline, as seen at Venford Reservoir.

(ix) The Cape Cornwall tourmalinite probably represents a vertical, progressive tourmalinisation sequence, with the biotite granite of Priest's Cove as the parent material, and the tourmaline granite and greisen as intermediate stages. These intermediate stages show similar mineralogical and geochemical characteristics to the fully tourmalinised rocks at other localities.

(x) A direct correlation exists between the boron concentration in tourmalinised rocks, their associated mineral assemblage, and the probable temperature of formation (Table 7:1). Tourmalinisation thus spans a complete range of hydrothermal conditions, from those of chloritisation at low temperatures, to those associated with tin mineralisation at higher temperatures.

(xi) Fluid inclusion work at Venford Reservoir shows that a) the most intensely tourmalinised rocks are characterised by a relative absence of fluid inclusions, b) the minimum trapping temperature of about 400°C in the tourmalinised vein is lower by about 100°C than that in the granite outside the vein, and c) salinities are around 40 equiv. wt.% NaCl, but the K:Na ratio of inclusions systematically decreases with proximity to the vein, and correlates inversely with K:Na in feldspars.

(xii) The ultimate source of tourmalinising fluids in Cornubia is probably in the intruded sediments. The necessary chemical components for tourmalinisation (and also for saline fluid inclusions) could be derived either by assimilation and subsequent differentiation, or by mobilisation of elements within sediments surrounding the granites under the influence of a high geothermal gradient. It is possible that both these processes may have contributed.

7.2 Summary of the tourmalinisation process in Cornubia

Tourmalinisation of the Variscan granites in Cornubia is related more closely to the intruded sediments than to the tectonic environment. Interaction between granite and sediment began at an early stage, with extensive assimilation by the granites of xenolithic material. Xenolith margins are common sites for 'primary' tourmaline development, and assimilation probably contributed the components for the 'magmatic' tourmaline of Cornubia.

Differentiation of tourmaline-rich fractions within the granites may locally have produced unusual 'magmas', the existence of which is evidenced by the occasional emplacement of discordant tourmalinite dykes. Tourmaline-bearing pegmatites, metalliferous lodes and breccia pipes could have been fed by such magmas, since these bodies are generally discordant within the granite, and the tourmaline may be seen to have crystallised directly from a magma or from a fluid, rather than to have formed by replacement of existing minerals.

In the case of <u>in situ</u> replacement veins, the secondary (or hydrothermal) origin of the tourmaline is in no doubt, since partially-replaced mineral grains may be observed at the vein margins. Such veins are joint-controlled, and involve no appreciable crustal extension, the feeder joint being opened to a width of perhaps a few millimetres, and the major tourmaline growth occurring within the adjacent granite to a lateral distance of up to a few metres. The

vertical extent of the veins is not known, but they are generally continuous within the area of outcrop; it is probable that the degree of tourmalinisation within vertical veins varies with depth. It is presumed that tourmalinisation in veins represents reaction within an open system, from which components are allowed to escape. If no escape of components is possible, (e.g. owing to an impermeable roof, the by-products of tourmalinisation (chiefly silica) are ponded up to form a horizontal, sheet-like tourmalinite body, such as the highly silicified Cape Cornwall tourmalinite.

The fluid responsible for tourmalinisation probably derives boron and other constituents ultimately from a sedimentary source, either by remobilisation of assimilated material, or by circulating waters becoming enriched in certain ions leached from unassimilated sediment. It is well known that the latter mechanism can be generated by the heat of an igneous body, and can draw ions in solution from the intruded sediment into the igneous mass. Boron would be released from clay minerals and therefore could be carried by circulating hydrothermal systems, at the temperatures of 200 to 300°C reached during low-grade regional metamorphism accompanying granitic intrusion in Cornubia. The pathways for circulating waters might be influenced by the horizontal, sheet-like structure of northern Dartmoor (and possibly other plutons), proposed by Bott et al. (1958).

Whatever the mechanism for its production, the tourmalinising fluid must contain, at least, boron, aluminium, iron and/or magnesium, and possibly potassium. It is not necessary for such a fluid to contain all the chemical components for tourmaline, since the remainder can be derived by replacement of minerals within the granite; some of the iron and magnesium could also be supplied by leaching from adjacent granite, as evidenced by the zone of geochemical depletion at Venford Reservoir. Tourmalinising fluids need not contain lithium or fluorine, since these elements can be more abundant in the unaltered granite than in tourmalinised veins.

The first influx of fluid mobilised along the newly-formed joint systems in the granite breaks down biotite to produce either muscovite and chlorite, or hydromuscovite and K-feldspar, plus Fe and Ti oxides. It has been shown (Chapter 4) that these transformations can be achieved without the introduction of any extraneous chemical components (other than water), and that biotite breakdown is a common precursor to its replacement by tourmaline. Fluorine held in biotite can be released at this stage to form fluorite.

The circulating fluid becomes enriched in elements such as iron, magnesium and calcium, which are leached from the granite and surrounding sediment. Potassium also becomes concentrated in the fluid, which promotes K-feldspar development as an immediate precursor to tourmalinisation; potassium in the fluid exchanges with sodium in existing feldspars, so that sodium is partitioned into the fluid phase, which is represented by saline fluid inclusions in recrystallised quartz. Two factors may encourage potassium enrichment in the fluid preceding tourmalinisation agents. Firstly, the breakdown of biotite contributes potassium to the fluid phase. Secondly, since potassium is partitioned into the fluid phase at high temperatures and the solid phase (feldspar) at lower temperatures, it is likely that water-rock interaction at depth within the cooling plutons would generate potassium-rich fluids. The experimental work of Pichavant (pers. comm., 1981) suggests that concentrations of boron may also increase the partitioning of potassium into the fluid phase; this finding supports the contention that K-rich fluids might emanate from a centre of tourmalinisation, and might precede tourmalinising fluids in their path through the granitic joint system. These precursors are effective over a larger area than the tourmalinising medium itself, since the latter has a strong tendency to precipitate tourmaline as close to the source as possible, except at relatively high temperatures. It is possible that tourmalinisation precursor fluids

are responsible for the extensive K-feldspathisation, quartz recrystallisation and biotite breakdown, which are particularly prevalent in those plutons showing maximum tourmalinisation (principally Dartmoor).

If the boron content of the fluid remains low, then any remaining biotite becomes converted to chlorite. With increasing availability of boron, biotite is tourmalinised instead of chloritised; biotite which has already been chloritised can also become tourmalinised at a later stage. Every gradation may be observed between complete chloritisation and complete tourmalinisation, and it is likely that the predominantly chloritised assemblages require lower temperatures than the predominantly tourmalinised.

Tourmaline after biotite (or chloritised biotite) is initially polycrystalline, and contains low aluminium and high iron and titanium; the initial replacement products then recrystallise to produce single, optically and compositionally zoned crystals. Tourmalinisation of feldspar involves the replacement of plagioclase as well as alkali feldspars by either skeletal or acicular tourmaline, and it seems possible that the tourmaline habit depends upon the feldspar composition at the time of replacement. Fine, acicular tourmaline needles also form within recrystallised quartz, sometimes nucleating at feldspar margins. A wide variety of tourmaline compositions can result from replacement, ranging from almost pure schorl to almost pure dravite, with sometimes significant calcium and/or titanium.

Cassiterite mineralisation may be associated with cases of intense tourmalinisation involving high boron concentrations and relatively high temperatures. It is only in very intense tourmalinisation (e.g. Goonbarrow vein) that lithium and fluorine become important constituents of the hydrothermal system. A complete spectrum of tourmalinised vein phenomena may be observed, ranging from the high-temperature Sn-Li-F type to the low-temperature chloritised type.

Tourmalinisation of granite involves a loss of silica from the system,

so that tourmalinised veins are generally silica-depleted. If, however, the by-products of tourmalinisation are unable to escape, a highly silicified tourmalinised rock will result. The tourmalinite body at Cape Cornwall may be interpreted as the product of tourmalinisation with silicification due to confinement within an impermeable roof structure. It is possible that such tourmalinite material, once formed, can be mobilised as a 'magma'; the existence of tourmalinite dykes (e.g. at Porthmeor Cove) supports this theory. There is thus a continuum between tourmaline-bearing rocks derived by replacement and those derived by differentiation.

The tourmalinisation story in southwest England is highly complex. Although all the tourmaline probably has an ultimate source in the crust, with a major contribution from sediments, there is almost certainly more than one mechanism by which this can be derived and emplaced. The simple distinction between primary and secondary, or magmatic and hydrothermal tourmaline is insufficient to explain the wide variety of tourmaline-bearing rocks.

7.3 Cornubia in the context of global tourmaline distribution

Some of the world's major tourmaline occurrences are listed in Table 7:2, which shows in general terms their paragenesis and age. Since tourmaline is almost a ubiquitous mineral worldwide, this table is restricted to a few noteworthy examples in which tourmaline is an important component of the assemblage. There is an inevitable bias towards those areas covered most extensively in the existing literature.

Tourmaline is found in rocks of all ages, and major occurrences are generally associated with contemporaneous magmatism. Most reported tourmaline assemblages are, however, younger than about 1200my, an exception being the rather unusual ultramafic association at Otokumpu, Finland. Tourmaline of Precambrian age is commonly found either in sedimentary terrains, or in pegmatites, and it is noteworthy that several Precambrian tourmaline pegmatites

Locality/area	Dominant paragenesis	Age	Tourmaline varieties
Europe			
Cornubia, England	post-magmatic alteration and metallisation	Variscan	mostly schorl
Erzgebirge, Czech.	metalliferous mineralisation	Variscan	mostly schorl
Massif Central, France	post-magmatic alteration	Variscan	mostly schorl
Elba, Italy	pegmatites	Alpine	schorl, elbaite
Varutrask, Sweden	rare-metal pegmatites	Late Precambrian	schorl, elbaite
Otokumpu, Finland	serpentinite, massive sulphide, granite	1800my (granite)	chromian dravite
Orave, Austria	gneiss	? Alpine	dravite
Africa			
Congo, Katanga, Rhodesia, Rwanda, Uganda	rare-metal pegmatites	about 1100my	schorl, elbaite
Mocambique, Tsumeb (SW Africa)	rare-metal pegmatites	about 550my	elbaite
Nigeria	pegmatites	Precambrian	schorl
Ethiopia	metalliferous min.	'basement'	schorl
Antsirabe, Malagasy	pegmatites, incl. some rare-metal assns.	Late Precambrian	schorl, elbaite, tsilaisite, uvite, liddicoatite
Americas			
California	pegmatites	Tertiary	schorl, elbaite
S. Dakota	pegmatites	Precambrian	schorl, elbaite
Mariposa Co., California	schists	?	vanadian dravite
S. Cordillera, Canada, & other locs.	sediments	Proterozoic	schorl-dravite s.s.
Bolivia & Chile	metalliferous min.	Mesozoic, Tertiary	schorl
Minas Gerais, Brazil, & vicinity	pegmatites, metalliferous min.	Mesozoic	schorl, elbaite
Asia			
Malaysia	metalliferous min., pegmatites	Mesozoic	mostly schorl
India, several locs.	sediments	Precambrian	mostly schorl-dravite
Swat, Pakistan	ultramafic contact	Precambrian	chromian dravite
Ilkwang Mine, Korea	metalliferous min.	69my $\pm$ 3	? schorl
Transbaikalia, USSR	metalliferous min.	Precambrian	schorl
Australasia			
W. Australia	schists	Proterozoic	dravite
New Zealand	metasediments	Tertiary	schorl-dravite s.s.

Table 7:2 Paragenesis and age of some major tourmaline occurrences

are also rare metal bearing (e.g. those of Varuträsk, Sweden, and a number of African examples). By contrast, most of the major tourmaline provinces associated with tin, tungsten or copper mineralisation (such as Cornubia, Czechoslovakia, South America and Malaysia) are Variscan or younger. This apparent trend could have more than one interpretation. It could be a feature of differential erosion, exposing lower portions of the earth's crust in Precambrian than in younger terrains. Alternatively, it could be because processes producing tourmaline-tin-tungsten-copper mineralisation have become more prevalent during Phanerozoic time.

It has been noted (Chapter 1) that geochemistry and mineralisation in granites show a general relationship to the tectonic environment, but that tourmaline occurs in granitic provinces associated with strongly contrasted tectonic settings. According to Watson (1978), the present-day plate tectonic regime became established around 1000my ago, between middle and late Proterozoic; tin mineralisation is concentrated in the Phanerozoic, and although examples occur prior to 1000my, these are mostly anorogenic in origin. Other authors (e.g. O'Nions and Pankhurst, 1978) suggest that mantle-derived granites, and therefore plate tectonic processes, may be traced back as far as 2800my. Whether or not plate tectonic processes were operative in the Precambrian, it is possible that the tourmaline-bearing rare metal assemblages were generated by intra-cratonic magmatism, rather than by subduction. According to Briden and Gass (1974), sporadic rare earth element and rare metal concentrations through time may be due to pauses in continental drift over particular points in the mantle, and could therefore, by inference, occur in the absence of plate movement.

Tourmalinisation associated with tin, tungsten or copper mineralisation occurs in the Variscan granite areas of Europe, the Mesozoic of Malaysia, the Mesozoic and Tertiary of the Andean province, and the Tertiary of Korea. Although distinct Sn-W and Cu-Mo granitic provinces have been delineated

worldwide (Ishihara, 1977), and are supposed to represent different tectonic environments (Chapter 1), extensive tourmalinisation is associated with both types of metalliferous deposit. The European Variscan province encompasses Cornubia, the Erzgebirge and the Massif Central, and is predominantly a tin-tungsten province, with granites having a greater crustal than mantle affinity. By contrast, the copper deposits of Korea are part of an active subduction system, producing mantle-derived plutons. The Andean belt features both porphyry copper and tin deposits, and has granites showing either crustal or mantle characteristics; both types of mineralisation and both types of granite are associated with extensive tourmalinisation. Tourmalinite rocks have been reported from the Variscan and Andean provinces, and tourmaline-cemented hydrothermal breccia pipes have been described from Cornubia, Korea and Bolivia (for references, see Chapter 1).

It thus appears that tourmalinisation is probably independent of the tectonic environment, and of the source of the associated igneous rocks. This conclusion supports the contention that tourmalinising fluids can derive their principle chemical components, not from granite, but from intruded sediment. One factor common to the Cornubian and Andean tourmalinised provinces is the nature of sediments intruded by granites, namely shales, greywackes and quartzites, which had not been regionally metamorphosed to the extent of losing their original geochemical characteristics, principally their boron content. Plant et al. (1980) found that mineralised granites in Scotland were associated with low-grade metasediments, and it seems likely that the degree of tourmalinisation affecting granitic plutons in any tectonic setting depends to a large extent upon the characteristics of their sedimentary envelope.

Cornubia is thus one of a number of tourmalinised provinces of Variscan age or younger, which feature granitic intrusions, metalliferous mineralisation of Sn-W or Cu-Mo type or both, and tourmaline of predominantly schorl composition.

7.4 Tourmaline parageneses and their representatives in Cornubia

The details of paragenesis given in Table 7:2 are much simplified, but it is clear that pegmatites, metalliferous deposits and metasediments are the most common hosts for members of the tourmaline group. Global tourmaline parageneses are classified in Table 7:3, and within this classification, the tourmalinised and tourmaline-bearing rocks of Cornubia are represented by types 1a, 1b, 1c, 2a, 2b, 2c, and minor 3b.

In the first category, type 1a ('primary', accessory tourmaline) occurs in all the main granite masses. Its abundance (summarised from previous work in Exley and Stone, 1964, Table 10) ranges from <1 to >4 modal percent, and is greatest in certain facies of the Dartmoor, St. Austell, Tregonning and Land's End granites. It is debatable whether all the so-called primary tourmaline can be regarded as truly magmatic in origin, and this problem has been discussed earlier in the present work.

Tourmalinites such as those at Cape Cornwall and Roche Rock have been assigned to the category of extreme differentiation products on the evidence of Power (1968) and Charoy (1979a), but it has been shown in the present work that the Cape Cornwall example probably has a replacement origin. The emplacement of tourmalinite dykes (e.g. Porthmeor Cove) does, however, show that tourmalinite 'magmas' can be differentiated and mobilised.

Pegmatites containing schorl of a magmatic rather than a replacement origin include those at Megiliggar Rocks and at Cape Cornwall (Lister, 1979a). The Goonbarrow pegmatite (Badham and Stanworth, 1976; Bray, 1980; Lister, 1979a) can also be assigned to the primary magmatic category, although it is not an intrusion but a Stockscheider pegmatite, formed at the junction between two granite facies. Also within category 1c should be included the only reported example of elbaite in the Meldon Aplite (Chaudhry and Howie, 1976).

Paragenesis	Reported tourmaline varieties
1. Primary magmatic (granitic & related rocks)	
a) Accessory mineral in granite	schorl; schorl-dravite s.s.
b) Extreme differentiation products	schorl; schorl-dravite s.s.
c) Late-stage minor intrusions, esp. pegmatites	schorl; elbaite; uvite; liddicoatite; tsilaisite
2. Alteration of magmatic/volcanic rocks	
a) Sporadic secondary grains/spots/pods	schorl; schorl-dravite s.s.
b) In-situ replacement veins	schorl; schorl-dravite s.s.
c) Discordant veins/pipes ± brecciation, ± metalliferous mineralisation	schorl; schorl-dravite s.s.
d) Fissure coating in rhyolite	buergerite
3. Alteration of sediments/metasediments	
a) Igneous contact ± metasomatism	
(i) granites &c.	schorl; elbaite
(ii) mafic/ultramafic rocks	dravite; chromian dravite; vanadian dravite
b) Metasomatism	schorl; dravite; ferridravite
4. Isochemical diagenesis/metamorphism of sediments	
a) Authigenic growth/overgrowth	schorl; dravite; elbaite; others implied not proved
b) Metamorphism	schorl; dravite

Table 7:3 CLASSIFICATION OF TOURMALINE PARAGENESES

Category 2a is described at length by Brammall and Harwood (1925), who attributed the tourmaline pods in the Dartmoor granite to preferential replacement of basic segregations or xenoliths. This category overlaps to a certain extent with type 1a (accessory tourmaline), since many of the supposed primary minerals in the Cornubian granites may have developed by early-stage alteration.

In situ replacement veins (2b) are relatively common within the granites, and the examples at Venford Reservoir, Tregarden Quarry, and Goonbarrow Pit have been the subject of the present work.

Discordant veins (2c) include tourmaline-bearing dykes, tourmaline-bearing metalliferous lodes which are widespread throughout the province, and tourmaline-cemented hydrothermal breccia pipes as described by Allman-Ward et al. (1981) and by Goode and Taylor (1980).

The unique occurrence of dravite in adinoles and associated rocks at Dinas Head falls into category 3b; since no granite contact is visible or detectable in the vicinity, Agrell (1941) envisaged boron metasomatism emanating from a granite at depth.

Hence, the majority of tourmalinised and tourmaline-bearing rocks in the Cornubian province are directly associated with the granites, either as magmatic or alteration products. Apart from the isolated occurrences of elbaite and dravite, most tourmaline (whatever the origin) is either schorl, or belongs to the schorl-dravite solid solution series. Other end-members of the tourmaline group are absent from Cornubia, although these may have been reported from similar parageneses elsewhere.

7.5 Future work

The major line of investigation which emerges from the present work is that of confirming the relative roles of granite and sediment, and of mantle and crust, in the production of tourmaline and other peraluminous

minerals in Cornubia.

There is much circumstantial evidence to suggest a sedimentary source for tourmalinising fluids, but direct evidence is sparse. $^{18}O/^{16}O$ data are available for some of the Cornubian granites (Sheppard, 1977), but not for tourmalinised or tourmaline-bearing rocks, and it is not clear to what extent the high values measured in the granites represent crustal contamination and/or post-magmatic processes. The single published $^{87}Sr/^{86}Sr$ result for the St. Austell granite (Harding and Hawkes, 1971) is highly equivocal, and again does not provide information concerning the tourmalinisation process.

Thus, an isotopic study of tourmalinised and tourmaline-bearing rocks from different localities, along with a parallel study of the granites and sediments, would not only confirm or refute theories for the tourmalinisation process, but would also have implications for ore genesis in tourmalinised regions.

REFERENCES CITED

AGRELL, S.O. 1941 Dravite-bearing rocks from Dinas Head, Cornwall. Mineralog. Mag. 26, 81-93.

AGYEI, E.K. and McMULLEN, C.C. 1968 A study of the isotopic abundance of boron from various sources. Can. J. Earth Sci. 5, 921-927.

ALDERTON, D.H.M. 1976 The geochemistry of mineralisation at Pendarves, and other Cornish localities. PhD Thesis, University of London, 417pp. (unpublished)

ALDERTON, D.H.M. 1979 Luxullianite *in situ* within the St. Austell granite, Cornwall: a discussion. Mineralog. Mag. 43, 441-442.

ALDERTON, D.H.M., PEARCE, J.A. and POTTS, P.J. 1980 Rare earth element mobility during granite alteration: evidence from southwest England. Earth Planet. Sci. Lett. 49, 149-165.

ALLMAN-WARD, P., HALLS, C., RANKIN, A.H. and BRISTOW, C.M. 1981 An intrusive hydrothermal breccia body at Wheal Remfry in the western part of the St. Austell pluton, Cornwall. In Evans, A.M. (ed.) Problems of Metallisation Associated with Acid Magmatism, Proc. Conference, Exeter, Dec. 1979, in press.

AL-SALEH, S., FUGE, R. and REA, W.J. 1977 The geochemistry of some biotites from the Dartmoor granite. Proc. Ussher Soc. 4, 37-48.

ARFVEDSON, A. 1818 Untersuchung einiger bei der Eisen-Grube von Utö vorkommenden Fossilien und von einem darin gefundenen neuen feuerfesten Alkali. J. für Chemie u. Physik XXII, 93-120.

AUGUSTITHIS, S.S. 1973 Atlas of the textural patterns of granites, gneisses and associated rock types. Amsterdam, Elsevier, 378pp.

BADHAM, J.P.N. and STANWORTH, C.W. 1976 The curved-crystal pegmatite, Goonbarrow. Proc. Ussher Soc. 3, 441-447.

BADHAM, J.P.N., STANWORTH, C.W. and LINDSAY, R.P. 1976 Postemplacement events in the Cornubian batholith. Econ. Geol. 71, 534-539.

BALL, T.K. and BASHAM, I.R. 1981 The petrochemistry of the Bosworgey granitic cust and its implications for ore genesis. Proc. Ussher Soc. 5, in press.

BARTON, R. Jr. and DONNAY, G. 1966 Absolute orientation of tourmaline by anomalous dispersion of X-rays. Geol. Soc. Am. Ann. Mtg., San Francisco, Abstr.,12.

BASSETT, H. 1953 A vanadiferous variety of tourmaline from Tanganyika. Rec. Geol. Surv. Tang. 3, 93-96.

BAWDEN, M.G. 1959 Distribution of boron in rocks. MSc Thesis, University of Birmingham. (unpublished)

BECKINSALE, R.D. 1979 Granite magmatism in the tin belt of South-east Asia. In Atherton, M.P. and Tarney, J. (eds.) Origin of granite batholiths, Shiva Publishing, 1-8.

BELOV, N.V. and BELOVA, E.N. 1949 Crystal structure of tourmaline. Doklady Acad. Sci. USSR 69, 185-188. (In Russian)

BERGMAN, T. 1779 Recherches chymiques sur la terre des pierres précieuses ou gemmes. Observations sur la Physique, sur l'Histoire Naturelle et sur les Arts (later became Jour. de Phys.) 14, 257-280.

BERNS, E.G. and VAN DER ZWAAN, P.W. 1972 The pyrohydrolytic determination of fluoride. Anal. Chem. 59, 293-297.

BLACK, P.M. 1971 Tourmalines from Cuvier Island, New Zealand. Mineralog. Mag. 38, 374-376.

BLYTH, F.G.H. 1949 A 'luxullianite' from East Dartmoor. Geol. Mag. 86, 175-179.

BLYTH, F.G.H. 1962 The structure of the north-eastern tract of the Dartmoor granite. Q. J. Geol. Soc. Lond. 118, 435-453.

BONNEY, T.G. 1877 On the microscopic structure of luxullianite. Mineralog. Mag. 1, 215-221.

BOOTH, B. 1966 Petrogenesis of the Land's End granites. PhD Thesis, University of Keele. (unpublished)

BOTT, M.H.P., DAY, A.A. and MASSON-SMITH, D. 1958 A geological interpretation of gravity and magnetic surveys in Devon and Cornwall. Phil. Trans. R. Soc. Lond. A 251, 161-191.

BRADLEY, J.E.S. and BRADLEY, O. 1953 Observations on the colouring of pink and green zoned tourmaline. Mineralog. Mag. 30, 26-38.

BRAMMALL, A. 1926 The Dartmoor granite. Proc. Geol. Assn. 37, 251-277.

BRAMMALL, A. and HARWOOD, H.F. 1923 The Dartmoor granite: its mineralogy, structure and petrology. Mineralog. Mag. 20, 39-53.

BRAMMALL, A. and HARWOOD, H.F. 1925 Tourmalinisation in the Dartmoor granite. Mineralog. Mag. 20, 319-330.

BRAMMALL, A. and HARWOOD, H.F. 1927 The temperature range of formation of tourmaline, rutile, brookite and anatase in the Dartmoor granite. Mineralog. Mag. 21, 205-220.

BRAMMALL, A. and HARWOOD, H.F. 1932 The Dartmoor granites: their genetic relationships. Q. J. Geol. Soc. Lond. 88, 172-237.

BRAY, C.J. 1980 Mineralisation, greisenisation and kaolinisation at Goonbarrow China Clay Pit, Cornwall, U.K. PhD Thesis, University of Oxford, 174pp, appendices, 53 figs. (unpublished)

BREWSTER, Sir David 1830 The Edinburgh Encyclopaedia. Edinburgh, William Blackwood, 18 vols.

BRIDEN, J.C. and GASS, I.G. 1974 Plate movement and continental magmatism. Nature 248, 650-653.

BRISTOW, C.M. 1968 Kaolin deposits of the United Kingdom of Great Britain and Northern Ireland. Proc. 23rd Int. Geol. Cong. 15, 275-288.

BROOKS, C., HART, S.R. and WENDT, I. 1972 Realistic use of the two-error regression treatments as applied to rubidium-strontium data. Rev. Geophys. & Space Phys. 10, 551-577.

BUERGER, M.J., BURNHAM, C.W. and PEACOR, D.R. 1962 Assessment of the several structures proposed for tourmaline. Acta Cryst. 15, 583-590.

BURHOLT, G.D. 1977 A description of the reactor facilities. University of London Reactor Centre Report OPS/4, 14pp. (unpublished)

BURHOLT, G.D. and MacMAHON, T.D. 1979 The University of London Reactor Centre, Ascot, England. J. Radioanal. Chem. 53, 365-372.

BUTLER, J.R. 1953 The geochemistry and mineralogy of rock weathering (1) The Lizard area, Cornwall. Geochim. Cosmochim. Acta 4, 157-178.

CAMPBELL, J. 1977 The (n, γ) capture reaction in the analysis of biological samples. MSc Thesis, University of Surrey. (unpublished)

CHAPMAN, J.F. and DALE, L.S. 1977 Improved sensitivity for boron and silicon in flame spectrometry by a fluoride evolution technique. Anal. Chim. Acta 89, 363-368.

CHAPPELL, B.W. and WHITE, A.J.R. 1974 Two contrasting granite types. Pacific Geology 8, 173-174.

CHAROY, B. 1979a Définition et importance des phénomènes deutériques et des fluides associés dans les granites. Conséquences métallogéniques. Sciences de la Terre, Mem. 37, 364pp., 7pl.

CHAROY, B. 1979b Greisenisation, minéralisation et fluides associés à Cligga Head, Cornwall (sud-ouest de l'Angleterre). Bull. Minéral. 102, 633-641.

CHAUDHRY, M.N. and HOWIE, R.A. 1976 Lithium tourmalines from the Meldon aplite, Devonshire, England. Mineralog. Mag. 40, 747-751.

CHAURIS, L. 1965 Les minéralisations pneumatolytiques du Massif Armoricain. Mem. B.R.G.M. 31, 218pp.

CHAYES, F. 1955 Potash feldspar as a by-product of the biotite-chlorite transformation. J. Geol. 63, 75-82.

CHORLTON, L.B. and MARTIN, R.F. 1978 The effect of boron on the granite solidus. Can. Min. 16, 239-244.

CHRIST, C.L. 1965 Substitution of boron in silicate crystals. Norsk. Geol. Tidds. 45, 423-428.

CLEMENTS, R.L., SERGEANT, G.A. and WEBB, P.J. 1971 The determination of fluorine in rocks and minerals by a pyrohydrolytic method. Analyst 96, 51-54.

COLEMAN, R.G. 1967 Low-temperature reaction zones and alpine ultramafic rocks of California, Oregon and Washington. U.S.G.S. Bull. 1247, 49pp.

COOKSON, J.A., McMILLAN, J.W. and PIERCE, T.B. 1979 The nuclear microprobe as an analytical tool. J. Radioanal. Chem. 48, 337-357.

COSSA, A. and ARZRUNI, A. 1883 Ein Chromturmalin aus den Chromeisenlagern des Urals. Zeit. Krist. 7, 1-16.

DANA, E.S. 1892 The system of mineralogy of James Dwight Dana, 1837-1868. Descriptive mineralogy, 6th ed. New York, John Wiley, 1134pp.

DANA, J.D. 1868 A system of mineralogy. Descriptive mineralogy, 5th ed. New York, John Wiley, 827pp.

DANGERFIELD, J. and HAWKES, J.R. 1969 Unroofing of the Dartmoor granite and possible implications with regard to mineralization. Proc. Ussher Soc. 2, 122-131.

DANGERFIELD, J., HAWKES, J.R. and HUNT, E.C. 1980 The distribution of lithium in the St. Austell granite. Proc. Ussher Soc. 5, 76-80.

DEER, W.A., HOWIE, R.A. and ZUSSMAN, J. 1962 Rock forming minerals. London, Longman, Green & Co., 5 vols.

DE JESUS, A.S.M. and VAN DER BERG, G.W.J. 1978 Determination of low-boron concentrations in various matrices with a neutron source. Radiochem. Radioanal. Letters 36, 183-192.

DE LA BECHE, Sir H.T. 1839 Report on the geology of Cornwall, Devon and West Somerset. London, Longmans, xxviii, 648pp.

DELMAS, R., BARRANDON, J.N. and DEBRUN, J.L. 1976 Analyse de traces dans divers minéraux, par activation avec des protons de 10 MeV et spectrométrie γ directe. Analusis 4, 339-346.

DIN, V.K. and JONES, G.C. 1978 The determination of total carbon and combined water in solicates using a C,H,N elemental analyser. Chem. Geol. 23, 347-352.

DOLMANOVA, E.I. 1976 The chemical composition of gas-liquid inclusions in minerals of tin-ore deposits. Sbornik Nauchn. Trudov, Moscov. Otdel., Vses. Mineral. Obshch., March 1974, 176-177. (In Russian, published 1976). (Translated in Fluid Inclusion Research 9,162-164).

DONNAY, G. and BUERGER, M.J. 1950 The determination of the crystal structure of tourmaline. Acta Cryst. 3, 379-388.

DONNAY, G., INGAMELLS, C.O. and MASON, B. 1966 Buergerite, a new species of tourmaline. Am. Mineral. 51, 198-199.

DONNAY, G. and BARTON, R. Jr. 1972 Refinement of the crystal structure of elbaite and the mechanism of tourmaline solid solution. Tscher. Min. Pet. Mitt. 18, 272-286.

DUFFEY, D., EL-KADY, A. and SENFTLE, F.E. 1970 Analytical sensitivities and energies of thermal-neutron-capture gamma rays. Nucl. Instr. & Methods 80, 149-171.

DUNN, P.J. 1977 Chromium in dravite. Mineralog. Mag. 41, 408-410.

DUNN, P.J., APPLEMAN, D.E. and NELEN, J.E. 1977(a) Liddicoatite, a new calcium end-member of the tourmaline group. Am. Mineral. 62 1121-1124.

DUNN, P.J., APPLEMAN, D., NELEN, J.A. and NORBERG, J. 1977(b) Uvite, a new (old) common member of the tourmaline group and its implications for collectors. Min. Record 8, 100-108.

DUPARC, L., WUNDER, M. and SABOT, A. 1910 Les mineraux des pegmatites des environs d'Antsirabe a Madagascar. Chapitre XI - les tourmalines. Mem. Soc. Phys. & Hist. Nat. de Geneve 36, 381-401.

EDMONDS, E.A., WRIGHT, J.E., BEER, K.E., HAWKES, J.R., WILLIAMS, M., FRESHNEY, E.C. and FENNING, P.J. 1968 Geology of the country around Okehampton. Mem. Geol. Surv. G.B., Explanation of sheet 324, 256pp. London, H.M.S.O.

EDMONDS, E.A., McKEOWN, M.C. and WILLIAMS, M. 1975 South-West England. British Regional Geology, 136pp. London, H.M.S.O.

EDMONDS, E.A., WILLIAMS, B.J. and TAYLOR, R.T. 1979 Geology of Bideford and Lundy Island. Mem. Geol. Surv. G.B. for 1:50,000 sheet 292, New Series, with sheets 275, 276 291 and part of sheet 308, London, H.M.S.O., 143pp.

ERD, R.C. 1980 The minerals of boron. In Supplement to Mellor's Comprehensive Treatise on Inorganic and Theoretical Chemistry, 5 (A), 7-71.

ETHIER, V.G. and CAMPBELL, F.A. 1977 Tourmaline concentrations in Proterozoic sediments of the southern Cordillera of Canada and their economic significance. Can. J. Earth Sci. 14, 2348-2363.

EXLEY, C.S. 1959 Magmatic differentiation and alteration in the St. Austell granite. Q. J. Geol. Soc. Lond. 114, 197-230.

EXLEY, C.S. and STONE, M. 1964 The granitic rocks of southwest England. In Hosking, K.F.G. and Shrimpton, G.J. (eds.) Present Views of some aspects of the Geology of Cornwall and Devon. Roy. Geol. Soc. Cornwall, 131-184.

FITCH, F.J. and MILLER, J.A. 1964 The age of the paroxysmal Variscan orogeny in England. In The Phanerozoic Time Scale, Q.J. Geol. Soc. Lond. 120S, 159-175.

FLEISCHER, R.L., PRICE, P.B. and WALKER, R.M. 1975 Nuclear tracks in solids: principles and applications. Berkeley, California, University of California Press, 605pp.

FLETT, Sir J.S. 1946 Geology of the Lizard and Meneage, 2nd ed. (reprinted with additional refs., 1973). Mem. Geol. Surv. G.B., Explanation of sheet 359, London, H.M.S.O., 212pp.

FLOYD, P.A. 1972 Geochemistry, origin and tectonic environment of the basic and acidic rocks of Cornubia, England. Proc. Geol. Assn. 83, 385-404.

FOIT, F.F. and ROSENBERG, P.E. 1977 Coupled substitutions in the tourmaline group. Contrib. Mineral. Petrol. 62, 109-127.

FOIT, F.F. and ROSENBERG, P.E. 1979 The structure of vanadium-bearing tourmaline and implications regarding tourmaline solid solutions. Am. Mineral. 64, 788-798.

FORTIER, S. and DONNAY, G. 1975 Schorl refinement showing composition dependence of the tourmaline structure. Can. Min. 13, 173-177.

FRONDEL, C. and COLLETTE, R.L. 1957 Synthesis of tourmaline by reaction of mineral grains with NaCl-H_3BO_3 solution, and its implications in rock metamorphism. Am. Mineral. 42, 754-758.

FRONDEL, C., BIEDL, A. and ITO, J. 1966 A new type of ferric iron tourmaline. Am. Mineral. 51, 1501-1505.

GARBRAH, B.W. and WHITLEY, J.E. 1967a Determination of boron by thermal neutron capture gamma-ray analysis. Anal. Chem. 39, 345-349.

GARBRAH. B.W. and WHITLEY, J.E. 1967b Determination of boron in glass by thermal neutron capture gamma-ray analysis. Glass Technol. 8, 154-156.

GARMANN, 1707 Curiöse Speculationes bei Schlaflosen Nächten - von einem Liebhaber, der immer gern speculiert. Chemnitz & Leipzig. (cited by Hintze, 1897, q.v.)

GHOSH, P.K. 1927 Petrology of the Bodmin Moor granite (eastern part). Mineralog. Mag. 21, 285-309.

GHOSH, P.K. 1934 The Carnmenellis granite: its petrology, metamorphism and tectonics. Q. J. Geol. Soc. Lond. 90, 240-276.

GIESECKE, Sir C.L. 1832 A descriptive catalogue of a new collection of minerals in the Museum of the Royal Dublin Society, to which is added an Irish Mineralogy. Dublin, Royal Dublin Society, 268pp.

GLADNEY, E.S., JURNEY, E.T. and CURTIS, D.B. 1976 Non-destructive determination of boron and cadmium in environmental materials by thermal neutron - prompt gamma-ray spectrometry. Anal. Chem. 48, 2139-2142.

GMELIN, C.G. 1827 Chemische Untersuchung über den Turmalin. Annalen der Physik und Chemie (= Poggendorf's Annalen) 9, 172-177.

GOLDSCHMIDT, V.M. and PETERS, C. 1932 The geochemistry of boron, I and II. Nachr. Ges. Wiss. Gottingen, Math-Physik. Kl., 1932, 402-407 and 528-545.

GOODE, A.J.J. 1973 The mode of intrusion of Cornish elvans. Inst. Geol. Sci. Report 73/7, 8pp, 2pl. London, H.M.S.O.

GOODE, A.J.J. and TAYLOR, R.T. 1980 Intrusive and pneumatolytic breccias in south-west England. Inst. Geol. Sci. Report 80/2, 23pp, 4pl. London, H.M.S.O.

GRANT. J.N., HALLS, C., AVILA, W. and AVILA, G. 1976 Igneous geology and the evolution of hydrothermal systems in some subvolcanic deposits of Bolivia. In Volcanic Processes in Ore Genesis. Joint Meeting Volcanic Studies Gp. of Geol. Soc. Lond. and Instn. of Min. & Met. London, 21-22 Jan. 1976, pp.117-126.

GRANT, J.N., HALLS, C., SHEPPARD, S.M.F. and AVILA, W. 1980 Evolution of the porphyry tin deposits of Bolivia. In Ishihara, S. and Takenouchi, S. (eds.) Granitic Magmatism and Related Mineralization (Mining Geology Special Issue no. 8), 151-173.

GREEN, D.H. 1964 A re-study and re-interpretation of the geology of the Lizard peninsula, Cornwall. In Hosking, K.F.G. and Shrimpton, G.J. (eds) Present Views of some aspects of the Geology of Cornwall and Devon, Roy. Geol. Soc. Cornwall, 87-114, 2pl.

GREENFIELD, S., McGEACHIN, H.McD. and SMITH, P.B. 1976 Plasma sources in analytical spectroscopy - III. Talanta 23, 1-14.

GRINSTEAD, R.R. and SNIDER, S. 1967 Modification of the curcumin method for low level boron determination. Analyst 92, 532-533.

GROSCHEV, L.V., LUTSENKO, V.N., DEMIDOV, A.M. and PELEKHOV, P.I. 1959 Atlas of gamma ray spectra from radiative capture of thermal neutrons. Oxford, Pergamon, 198pp.

HALL, A. 1971 Greisenisation in the granite of Cligga Head, Cornwall. Proc. Geol. Assn. 82, 209-230.

HALL, A. 1973 Geochimie des granites varisques du sud-ouest de l'Angleterre. Bull. Soc. Geol. Fr., Ser. 7, 15, 229-238.

HALL, A. and JACKSON, N.J. 1975 Summer field meeting in West Cornwall. Proc. Geol. Assn. 86, 95-102.

HALLS, C., RANKIN, A.H., FERRIDAY, I.L., BLAIN, C.F., BRISTOW, C.M. and GRONOW, C. 1978 A tourmalinised hydrothermal intrusion breccia at Wheal Remfry in the western part of the St. Austell pluton, Cornwall. Jl. Geol. Soc. Lond. 135, 256.

HARDER, H. 1959 Contribution to the geochemistry of boron, I: Boron in minerals and igneous rocks. Nachr. Akad. Wiss. Gottingen: II Math-Physik. Kl., no. 5, 67-122.

HARDING, R.R. and HAWKES, J.R. 1971 The Rb:Sr age and K/Rb ratios of samples from the St. Austell granite, Cornwall. Inst. Geol. Sci. Report 71/6, 10pp. London, H.M.S.O.

HAÜY, R.J. 1801 Traité de Mineralogie. Paris, Conseil des Mines, 4 vols. + Atlas.

HAWKES, J.R. 1967 Rapakivi texture in the Dartmoor granite. Proc. Ussher Soc. 1, 270-272.

HAWKES, J.R., HARDING, R.R. and DARBYSHIRE, D.P.F. 1975 Petrology and Rb:Sr age of the Brannel, South Crofty and Wherry elvan dykes, Cornwall. Bull. Geol. Surv. G.B. 52, 27-42.

HAWKES, J.R. and DANGERFIELD, J. 1978 The Variscan granites of South-west England: a progress report. Proc. Ussher Soc. 4, 158-171.

HENKELMANN, R. and BORN, H-J. 1973 Analytical use of neutron-capture gamma-rays. J. Radioanal. Chem. 16, 473-481.

HENKELMANN, R., HUBER, A., SPECHT, S. and STARK, H. 1976 Einsatz verschiedener Neutronquellen zur analytischen Nutzung prompter Neutronenanfanggammastrahlung. J. Radioanal. Chem. 32, 265-274.

HEY, M.H. 1962 An index of mineral species and varieties arranged chemically, 2nd ed. London, BM(NH), xx, 609pp.

HICKLING, G.H. 1908 China-clay: its nature and origin. Trans. Instn. Mining Eng. 36, 10-33.

HINTZE, C. 1897 Handbuch der Mineralogie, vol. 2, pp.311-367. Leipzig, Verlag von Veit & Comp.

HOLGATE, N. 1977 Tourmaline from amphibolized gabbro at Hanter Hill, Radnorshire. Mineralog. Mag. 41, 124-127.

HOSKING, K.F.G. 1964 Permo-carboniferous and later primary mineralisation of Cornwall and south-west Devon. In Hosking, K.F.G. and Shrimpton, G.J. (eds.) Present Views of some aspects of the Geology of Cornwall and Devon, Roy. Geol. Soc. Cornwall, 201-245.

ISENHOUR, T.L. and MORRISON, G.H. 1966b Determination of boron by thermal neutron activation analysis using a modulation technique. Anal. Chem. 38, 167-169.

ISENHOUR, T.L. and MORRISON, G.H. 1966a Modulation technique for neutron capture gamma ray measurements in activation analysis. Anal. Chem. 38, 162-167.

ISHIHARA, S. 1977 The magnetite-series and ilmenite-series granitic rocks. Mining Geology 27, 293-305.

ITO, T. and SADANAGA, R. 1951 A Fourier analysis of the structure of tourmaline. Acta Cryst. 4, 385-390.

JACKSON, N.J. 1974 Gryll's Bunny, a 'tin floor' at Botallack. Proc. Ussher Soc. 3, 186-188.

JANNASCH, p. and CALB, G. 1889 Über die Zusammensetzung des Turmalins. Ber. deutsch. Chem. Ges. 22, 216-221.

KARWOWSKI, L. 1973 Greisens of the Mladz-Kamien-Pobieda area of the Izera Upland (Sudetes). Acta Geol. Polon. 23, 329-340, 6pl. (Polish with English Abstract).

KERR, S.A., PRESTWICH, W.V., KENNETT, T.J. and SHAW, D.M. 1980 The determination of boron in sedimentary rocks by neutron irradiation and prompt γ-ray spectrometry. J. Radioanal. Chem. 57, 525-533.

KHAN, S.A. 1966 The analysis of boron, fluorine amd lithium in silicate rocks and minerals. PhD Thesis, University of Exeter. (unpubl.)

KLEVTSOV, P.V. and LEMMLEIN, G.G. 1959 Determination of the minimum pressure of quartz formation as exeplified by crystals from the Pamir. Zap. Vses. Miner. Obshch. 85, 661-666. (In Russian)

KONNERUP-MADSEN, J. 1979 Fluid inclusions in quartz from deep-seated granitic intrusions, south Norway. Lithos 12, 13-23.

KREBS, W. 1977 The tectonic evolution of Variscan Meso-Europe. In Ager, D.V. and Brooks, M. (eds.) Europe from crust to core. London, Wiley, 119-139.

KRYNINE, P.D. 1946 The tourmaline group in sediments. J. Geol. 54, 65-87.

KUNITZ, W. 1929 Die Mischungsreihen in der Turmalingruppe und die genetischen Beziehungen zwischen Turmalinen und Glimmern. Chemie der Erde 4, 208-251.

KUNITZ, W. 1936 Die Rolle des Titans und Zirconiums in den gesteinsbildenden Silikaten. Neues Jahrb. Mineral. Abh. 70, 385-466.

LACROIX, A. 1893 Minéralogie de la France et de ses Colonies. Paris, Librairie Polytechnique, 1, 102-105.

LAGACHE, M. and WEISBROD, A. 1977 The system: two alkali feldspars - KCl - NaCl - H_2O at moderate to high temperatures and low pressures. Contrib, Mineral. Petrol. 62, 77-101.

LANDERGREN, S. 1964 On the geochemistry of deep-sea sediments. Rep. Swedish Deep Sea Exped., 1947-1948, X (5) 57-154.

LANDERGREN S. and CARVAJAL, M.C. 1969 Contribution to the geochemistry of boron. III The relationship between boron concentration in marine clay sediments and the salinity of the depositional environments expressed as an adsorption isotherm. Arkiv. för Min. och Geol. 5, 11-22.

LANGMYHR, F.J. and PAUS, P.E. 1968 The analysis of inorganic siliceous materials by atomic absorption spectrophotometry and the hydrofluoric acid decomposition technique. Part I. The analysis of silicate rocks. Anal. Chim. Acta. 43, 397-408.

LAURENT, R. 1972 The Hercynides of South Europe, a model. Proc. 24th Int. Geol. Cong., Montreal, 363-370.

LE NEVE FOSTER, C. 1879 A rock resembling luxullianite from St. Just; and on some globular masses of schorl-rock from Ding-Dong Mine. Trans. Roy. Geol. Soc. Cornwall 10, 8-9.

LINNAEUS, C. 1768 Systema Naturae. 12th ed., Holmiae, 2 vols.

LISTER, C.J. 1978a Luxullianite in situ within the St. Austell granite, Cornwall. Mineralog. Mag. 42, 295-297.

LISTER, C.J. 1978b Some tourmalinised rocks from Cornwall and Devon. Proc. Ussher Soc. 4, 211-214.

LISTER, C.J. 1979a Quartz-cored tourmalines from Cape Cornwall and other localities. Proc. Ussher Soc. 4, 402-418.

LISTER, C.J. 1979b Luxullianite in situ within the St. Austell granite, Cornwall: a reply (to discussion by D.H.M. Alderton). Mineralog. Mag. 43, 442-443.

McCURRY, P. 1971 The relationship between optical properties and occurrence of some black tourmalines from Nigeria. Mineralog. Mag. 38, 369-373.

MANNING, D.A.C. 1981a The application of experimental studies in determining the origin of topaz-tourmaline-quartz rock (St. Mewan Beacon) and tourmaline-quartz rock (Roche Rock). Proc. Ussher Soc. 5 (2). (in press)

MANNING, D.A.C. 1981b An experimental study of the effects of fluorine on the crystallisation of granitic melts. In Evans, A.M. (ed.) Problems of Metallisation Associated with Acid Magmatism. Proc. Conference, Exeter, Dec. 1979. (in press)

MASON, B., DONNAY, G. and HARDIE, L.A. 1964 Ferric tourmaline from Mexico. Science 144, 71-73.

MASON, P.K., FROST, M.T. and REED, S.J.B. 1969 B.M. - I.C. - N.P.L. computer program for calculating corrections in quantitative x-ray microanalysis. N.P.L. Report no. 1, 91pp.

MASSOUMI, R. 1979 Thermal neutron capture in ^{107}Ag. PhD Thesis, University of London, 149pp. (unpublished)

MATTEUCCI, E. and ZUCCHETTI, S. 1965 Studio del sistema di filoni di tormalinite di Busachi (Sardegna Centrale). Boll. Assoc. Miner. Subalpina II, 381-396.

MICHEL-LEVY, M.C. 1953 Reproduction artificielle de minéraux qui apparaisant dans la métamorphisme de contact du granite. Bull. Soc. Fr. Min. Crist. 76, 237-293.

MILLER, J.A. and MOHR, P.A. 1964 Potassium-argon measurements on the granites and some associated rocks from southwest England. Geol. J. 4, 105-126.

MOORE, J.McM. 1975 A mechanical interpretation of the vein and dyke systems of the southwest England orefield. Mineralium Deposita 10, 374-388.

MORGAN, L. 1964 The determination of boron by a pyrohydrolysis technique. Analyst 89, 621-623.

MORGAN, V. 1980 Boron geochemistry. In Supplement to Mellor's Comprehensive Treatise on Inorganic and Theoretical Chemistry 5 (A),72-152.

MOTORINA, I.V. and BAKUMENKO, I.T. 1968 Genesis of tourmaline in pegmatites of the Borshchevochny Ridge. In Yermakov, N.P. (ed.) Mineralogical Thermometry and Barometry, vol. 2, Moscow, Nauka Press, 196-201. (Abstract in Fluid Inclusion Research 2, 58, 1969).

MUFFLER, L.J.P. and WHITE, D.E. 1969 Active metamorphism of Upper Cenozoic sediments in the Salton Sea geothermal field and the Salton Trough, SE California. Geol. Soc. Amer. Bull. 80, 157-182, 2 pl.

NANCE, R.M. 1955 A Cornish-English dictionary. Federation of Old Cornwall Societies, 104pp. (reprinted London, Pitman, 1971).

NEMEC, D. 1973 Tin in tourmalines. Neues Jahrb. Mineral. Monatsh. (2), 58-63.

NEMEC, D. 1975 Genesis of tourmaline spots in leucocratic granites. Neues Jahrb. Mineral. Monatsh. (7), 308-317.

NEUWIRTH, W., PIETSCH, W., RICHTER, K. and HAUSER, U. 1975 Electronic stopping cross sections of elements and compounds for swift Li ions. Z. Physik A275, 209-214.

NUBER, B. and SCHMETZER, K. 1979 Die Gitterposition des Cr^{3+} im Turmalin: Strukturverfeinerung eines Cr-reichen Mg-Al Turmalins. Neues Jahrb. Mineral. Abh. 137, 184-197.

OFTEDAHL, I. 1964a Contributions to the mineralogy of Norway. No. 29: vesuvianite as a host mineral for boron. Norsk Geol. Tidds. 44 377-383.

OFTEDAHL, I. 1964b On the occurrence and distribution of boron in pegmatite. Norsk Geol. Tidds. 44, 217-225.

OLIVIER, C., MacMILLAN, J.W. and PIERCE, T.B. 1976 An investigation into the use of the nuclear microprobe for examining distributions of boron isotopes. J. Radioanal. Chem. 31, 515-523.

O'NIONS, R.K. and PANKHURST, R.J. 1978 Early Archaean rocks and geochemical evolution of the earth's crust. Earth Planet Sci. Lett. 38, 211-236.

ORVILLE, P.M. 1963 Alkali ion exchange between vapour and feldspar phases. Am. J. Sci. 261, 201-237.

OSMAN, C.W. 1928 The granites of the Scilly Isles and their relation to the Dartmoor granites. Q. J. Geol. Soc. Lond. 84, 258-292.

PENFIELD, S.L. and FOOTE, H.W. 1899 On the chemical composition of tourmaline. Am. J. Sci., 4th Series, 7 (38), 97-125.

PHILLIPS, F.C. 1964 Metamorphism in South-west England. In Hosking, K.F.G. and Shrimpton, G.J. (eds.) Present Views of some aspects of the Geology of Cornwall and Devon, Roy. Geol. Soc. Cornwall, 185-200.

PICHAVANT, M. 1979 Etude expérimentale à haute température et 1 kbar du rôle du bore dand quelques systèmes silicatés. Intérêt pétrologique et métallogenique. Thèse pour Docteur de Specialité (3^e cycle), Institut National Polytechnique de Lorraine, 153pp + 40pp unpaginated + 3pl.

PISANI, F. 1864 Sur quelques nouveaux minéraux de Cornouailles. Comptes Rendus des Séances de l'Academie des Sciences, Paris, 59,912-913.

PITCHER, W. 1979 Comments on the geological environments of granites. In Atherton, M.P. and Tarney, J. (eds.) Origin of granite batholiths. Shiva Publishing, 1-8.

PLANT, J., BROWN,G.C., SIMPSON, P.R. and SMITH, R.T. 1980 Signatures of metalliferous granites in the Scottish Caledonides. Trans. Instn. Ming. Metall. (Sect.B: Appl. earth sci.) 89, B198-B210.

POVARENNYKH, A.S. 1970 The connection of IR-Spectra of minerals with crystallochemical factors. Mineral. Sbornik (L'vov) 24, 12-29. (In Russian, with English summary).

POVONDRA, P. and ČECH, F. 1976 A method for the chemical analysis of tourmalines. Acta Univ. Carolinae - Geologica (3), 209-241.

POWER, G.M. 1968 Chemical variation in tourmalines from South-west England. Mineralog. Mag. 36, 1078-1089.

PRENDEL, R. 1892 Analyse des Turmalin von der Urulga. Zeit. Krist. 20, 93.

PRETORIUS, R., ODENDAHL, F. and PEISACH, M. 1972 Deuteron activation analysis of geological samples. J. Radioanal. Chem. 12, 139-149.

PRYCE, W. 1778 Mineralogia Cornubiensis; a treatise on minerals, mines and mining. London, James Phillips, 331pp. (reprinted Truro, D. Bradford Barton, 1972)

RANKIN, A.H. 1978 User school on fluid inclusion equipment and methods, Imperial College, London, 30 March to 1 April 1978. Course notes, 20pp + 28pp unpaginated. (unpublished)

READ, H.H. 1944 Meditations on granite: part 2. Proc. Geol. Assn. 55, 45-93.

REED, S.J.B. 1975 Electron microprobe analysis. Cambridge, C.U.P., 400pp.

REID, C. and FLETT, J.S. 1907 The geology of the Land's End district. Mem. Geol. Surv. G.B., Explanation of sheets 351 and 358. London, H.M.S.O., 158pp, VI pl.

REID, C., BARROW, G., SHERLOCK, R.L., MacALISTER, D.A., DEWEY, H. and BROMEHEAD, C.N. 1912 The geology of Dartmoor. Mem. Geol. Surv. G.B., Explanation of sheet 338, London, H.M.S.O., 102pp,2pl.

REYNOLDS, R.C. 1965 The concentration of boron in Precambrian seas. Geochim. Cosmochim. Acta 29, 1-16.

RICKARD, M.J. 1964 Metamorphic tourmaline overgrowths in the Oak Hill Series of Southern Quebec. Can. Min. 8, 86-91.

ROEDDER, E. 1962 Studies of fluid inclusions I: low temperature application of a dual-purpose freezing and heating stage. Econ. Geol. 57, 1045-1061.

ROEDDER, E. 1971 Fluid inclusion studies on the porphyry-type ore deposits of Bingham, Utah, Butte, Montana, and Climax, Colorado. Econ. Geol. 66, 98-120.

ROEDDER, E. 1972 Composition of fluid inclusions. U.S.G.S. Prof. Paper 440-JJ, 164pp, 12pl.

ROEDDER, E. 1979a Fluid inclusions as samples of ore fluids. In Barnes, H.L. (ed.) Geochemistry of hydrothermal ore deposits, 2nd. ed. New York, Wiley, 684-737.

ROEDDER, E. 1979b Natural occurrence and significance of fluids indicating high pressure and temperature. Paper presented at Nobel Symposium on Chemistry and Geochemistry of Solutions at High Temperature and Pressure, Sept. 17-21. (Manuscript)

ROEDDER, E. and BODNAR, R.J. 1980 Geologic pressure determinations from fluid inclusion studies. Ann. Rev. Earth Planet. Sci. Lett. 8, 263-301.

SCHMETZER, K., NUBER, B. and ABRAHAM, K. 1979 Zur Kristallchemie Magnesium-reicher Turmaline. Neues. Jahrb. Mineral. Abh. 136, 93-112.

SCHULEK, E. and VASTAGH, G. 1931 Beiträge zur quantitativen Bestimmung der Borsäure. Zeit. Anal. Chem. 84, 167-184.

SCHULEK, E. and VASTAGH, G. 1932 Beiträge zur quantitativen Bestimmung der Borsäure. II. Abhandlung. Bestimmung der Borsäure in natürlichen und künstlichen Silikaten. Zeit. Anal. Chem. 87, 165-172.

SCHWARTZ, G.M. 1958 Alteration of biotite under mesothermal conditions. Econ. Geol. 53, 164-177.

SENFTLE, F.E., MOORE, H.D., LEEP, D.B., EL-KADY, A. and DUFFEY, D. 1971 Analytical sensitivities and energies of thermal neutron capture gamma rays, II. Nucl. Instr. and Methods 93, 425-459.

SHELTON, N.F.C. and REED, R.A. 1976 The determination of boron in magnesites using carminic acid. Analyst 101, 396-403.

SHEPPARD, S.M.F. 1977 The Cornubian batholith, S.W. England: D/H and $^{18}O/^{16}O$ studies of kaolinite and other alteration minerals. Jl. Geol. Soc. Lond. 133, 573-591.

SILLITOE, R.H. and SAWKINS, F.J. 1971 Geologic, mineralogic and fluid inclusion studies relating to the origin of copper-bearing tourmaline breccia pipes, Chile. Econ. Geol. 66, 1028-1041.

SIMPSON, P.R., BROWN, G.C., PLANT, J. and OSTLE, D. 1979 Uranium mineralization and granite magmatism in the British Isles. Phil. Trans. R. Soc. Lond. A291, 385-412.

SLIVKO, M.M. 1952 On the subject of polychromatic tourmalines. L'vov. Geol. Obshch. Mineral. Sbornik. 6, 211-220. (In Russian)

SLIVKO, M.M. 1955 Investigations of tourmalines from certain deposits in the USSR. Izd. L'vov. Univ., 127pp, 4pl. (In Russian)

SLIVKO, M.M. 1965 On inclusions of solutions in crystals of tourmaline. In Yermakov, N.P. et al. Research on the nature of mineral-forming solutions. Oxford, Pergamon, 626-634.

SLIVKO, M.M. 1973 Comparative physico-chemical characteristics of solutions of inclusions in tourmalines of micaceous and rare-metal pegmatities. Abstracts of papers at Fourth Regional Conference on Thermobarochemistry of Mineral-forming Processes, 24-30 Sept. 1973: Rostov, Rostov Univ. Press, 183-185. (In Russian; translated in Fluid Inclusion Research 7, 212).

SMITH, D.C. 1971 A tourmaline-bearing eclogite from Sunnmore, Norway. Norsk Geol. Tidds. 51, 141-147.

SMITH, F.G. 1949 Transport and deposition of the non-sulphide vein minerals. IV. Tourmaline. Econ. Geol. 44, 186-192.

SNETSINGER, K.G. 1966 Barium-vanadium muscovite and vanadium tourmaline from Mariposa County, California. Am. Mineral. 51, 1623-1639.

SORBY, H.C. 1858 On the microscopical structure of crystals, indicating the origin of minerals and rocks. Q. J. Geol. Soc. Lond. 14, 453-500, 3pl.

SORBY, H.C. 1897 Fifty years of scientific research. Sheffield Lit. & Phil. Soc. Report 1897, 3-14.

SOURIRAJAN, S. and KENNEDY, G.C. 1962 The system H_2O - NaCl at elevated temperatures and pressures. Am. J. Sci. 260, 115-141.

SOWERBY, J. 1811 British Mineralogy. London, Richard Taylor & Co., 4 vols.

STONE, M. 1975 Structure and petrology of the Tregonning-Godolphin granite, Cornwall. Proc. Geol. Assn. 86, 155-170.

STONE, M. and AUSTIN, W.G.C. 1961 The metasomatic origin of the potash feldspar megacrysts in the granites of southwest England. J. Geol. 69, 464-472.

STYLES, M.T. and KIRBY, G.A. 1980 New investigations of the Lizard complex, Cornwall, England and a discussion of an ophiolite model. In Ophiolites: Proc. Int. Ophiolite Symposium, Cyprus, 1979. Cyprus Geol. Survey Dept., 517-526.

SWEATMAN, T.R. and LONG, J.V.P. 1969 Quantitative electron-probe microanalysis of rock-forming minerals. J. Petrol. 10, 332-379.

TAYLOR, A.M. and TERRELL, B.C. 1967 Synthetic tourmalines containing elements of the first transition series. J. Crystal Growth 1, 238-244.

THEIN, M. 1977 A study of the prompt and delayed gamma rays following thermal neutron capture in ^{107}Ag and ^{109}Ag. PhD Thesis, University of London, 235pp. (unpublished)

TOMISAKA, T. 1968 Syntheses of some end-members of the tourmaline group. Mineralogical Journal 5, 355-364.

TSCHERMAK, G. von 1883 Lehrbuch der Mineralogie. Wien, Hölder, ix, 589pp. (published 1881 to 1884, but cited in later literature, e.g. Dana, 1892, as 1883).

TUREKIAN, K.K. and WEDEPOHL, K.H. 1961 Distribution of the elements in some major units of the earth's crust. Geol. Soc. Am. Bull. 72, 175-192.

USSHER, W.A.E. 1888 The granite of Dartmoor. Parts 1 & 2. Trans. Devon. Assn. 20, 141-157.

USSHER, W.A.E., BARROW, G. and MacALISTER, D.A. 1909 The geology of the country around Bodmin and St. Austell. Mem. Geol. Surv. G.B., Explanation of sheet 347, London, H.M.S.O., 201pp.

VERNADSKY, W. 1913 Über die chemische Formel der Turmaline. Zeit. Krist. 53, 273-288.

WAGER, L.R. and BROWN, G.M. 1966 Layered igneous rocks. Edinburgh, Oliver and Boyd, 588pp.

WALENTA, K. and DUNN, P.J. 1979 Ferridravite, a new mineral of the tourmaline group from Bolivia. Am. Mineral. 64, 945-948.

WALSH, J.N. and HOWIE, R.A. 1980 An evaluation of the performance of an inductively coupled plasma source spectrometer for the determination of the major and trace constituents of silicate rocks and minerals. Mineralog. Mag. 43, 967-974.

WANG, S. and HSU, X. 1966 A new variety of dravite and its significance in mineralogy. Kexue Tongbao 17, 91-96. (In Chinese)

WASKOWIAK, R. 1969 Contribution to the geochemistry of boron in the crystalline rocks of Ruhla-Brotterode (Thuringerwald). Geologie (Berlin) 18, 432-440.

WATSON, J.V. 1978 Ore-deposition through geological time. Proc. R. Soc. Lond. A362, 305-328.

WEAST, R.C. (ed.) 1971 Handbook of chemistry and physics, 52nd. ed. Cleveland, Ohio, Chemical Rubber Company.

WEIS, P.L. 1953 Fluid inclusions in minerals from zoned pegmatites of the Black Hills, South Dakota. Am. Mineral. 38, 671-697.

WELLS, M.K. 1946 A contribution to the study of luxullianite. Mineralog. Mag. 27, 186-194.

WHITE, D.E. and WARING, G.A. 1963 Volcanic emanations. U.S.G.S. Prof. Paper 440-K, v, 29pp.

WHITLEY, J.E., BOWDEN, P. and ANGUS, N.S. 1971 The determination of trace elements in igneous rocks by nuclear techniques. In Activation analysis is geochemistry and cosmochemistry, NATO Advanced Study Institute, Kjeller, Norway, 1971, 55-64.

WILLIAMS, J.P., CAMPBELL, P.E. and MAGLIOCCA, T.S. 1959 Determination of boric oxide in glass by pyrohydrolysis separation. Anal. Chem. 31, 1560-1563.

WILSON, B. 1762 Observations upon some gems similar to Tourmalin. Phil. Trans. R. Soc. Lond. 52, 443-447.

WILSON, G.C. 1980 Ion microprobe techniques, with applications to analysis of lithium in Cornish granites. PhD Thesis, University of Cambridge. (unpublished)

WODZICKI, A. 1971 Migration of trace elements during contact metamorphism in the Santa Rosa Range, Nevada, and its bearing on the origin of ore deposits associated with granitic intrusions. Mineralium Deposita 6, 49-64.

WORTH, R.N. 1887a The igneous and altered rocks of south-west Devon. Trans. Devon. Assn. 19, 467-497.

WORTH, R.N. 1887b On trowlesworthite, and certain granitoid rocks near Plymouth. Trans. Roy. Geol. Soc. Cornwall 10, 177-179.

WOULFE, P. 1779 Experiments on some mineral substances. Phil. Trans. R. Soc. Lond. 69, 11-34.

APPENDIX 1: List of samples to which reference is made

Venford Reservoir Quarry

VR022	white biotite granite	
VR020	iron-stained biotite granite 7m from large tourmalinised vein	
VR012	reddened granite 5m " " " "	
VR011	" " 2m " " " "	
VR010	" " 0.5m " " " "	
VR001	large tourmalinised vein margin	approaching large tourmalinised vein in 3cm increments
VR002	" " " "	
VR003	" " " "	
VR004	" " " "	
VR005	" " " "	
VR006	maximum tourmalinisation zone in large tourmalinised vein	
VR007	" " " " " " "	
VR023	smaller tourmalinised vein centre	
VR024	smaller tourmalinised vein margin	
VR026	monomineralic tourmaline vein	

Tregarden Quarry, Luxulyan

LX201	chloritised & tourmalinised vein margin
LX202	" " " " "
LX203	" " " " "
LX204	" " " " "
LX205	" " " " "
LX206	" " " " "
LX207	maximum alteration zone in chloritised & tourmalinised vein
LX208a	" " " " " "
LX208b	tourmalinised part of chloritised and tourmalinised vein
LX030	tourmalinised and chloritised vein margin
LX031	" " " " "
LX032	" " " " "
LX033	" " " " "
LX034	maximum alteration zone in tourmalinised and chloritised vein
LX035	" " " " " "
LX036	" " " " " "

LX001	white biotite-muscovite granite	(from Lister, 1978a)
LX 81-3	luxullianite vein margin	
LX 84-6	" " "	
LX008	luxullianite	
LX051	cored tourmaline-bearing pegmatite	(from Lister, 1979a)

Goonbarrow China Clay Pit

G8002	tourmalinised & greisened vein margin
G8003	" " " "
G8004	" " " "
G8005	maximum alteration zone in tourmalinised & greisened vein
G8001	Stockscheider pegmatite (from Lister, 1979a)

Cape Cornwall

CC010	tourmaline granite
CC011	transition zone from tourmaline granite into tourmalinite
CC012	" " " " " " "
CC013	" " " " " " "
CC014	tourmalinite
CC015	"
CC001	layered unit within tourmalinite
CC002	" " " "
CC003	" " " "
CC004	" " " "
CC005	" " " "
CC021	margin of tourmalinite vein within tourmaline granite
CC022	" " " " " "
CC023	tourmalinite vein
CCPC001	tourmaline pegmatite, Priest's Cove (from Lister, 1979a)
CCPC002	" " " "
CC75	Priest's Cove microgranite (from Charoy, 1979a)
CC95	tourmaline granite

APPENDIX 2: Correction factors for fluid inclusion geothermometry

Measured T_h or T_s (°C)			To Deduct (°C)
−30	to	+50	0
50	"	70	1
70	"	90	2
90	"	110	3
110	"	140	4
140	"	160	5
160	"	190	6
190	"	210	7
210	"	230	8
230	"	250	9
250	"	270	10
270	"	290	11
290	"	310	12
310	"	330	13
330	"	350	14
350	"	370	15
370	"	400	16
400	"	430	18
430	"	480	20
480	"	510	22
510	"	540	24
540	"	580	26
> 580			30

APPENDIX 3: Copies of publications, submitted in support of candidature for the Degree of PhD.

(i) Luxullianite *in situ* within the St. Austell granite, Cornwall. Mineralog. Mag. 42, 295-297, 1978.

(ii) Some tourmalinised rocks from Cornwall and Devon. Proc. Ussher Soc. 4, 211-214, 1978.

(iii) Quartz-cored tourmalines from Cape Cornwall and other localities. Proc. Ussher Soc. 4, 402-418, 1979.

(iv) Luxullianite *in situ* within the St. Austell granite, Cornwall: a reply (to discussion by D.H.M.Alderton). Mineralog. Mag. 43, 442-443, 1979.

MINERALOGICAL MAGAZINE, JUNE 1978, VOL. 42, PP. 295-7

Luxullianite *in situ* within the St. Austell granite, Cornwall

LUXULLIANITE has long been regarded as a petrological curiosity, unique to its type locality at Luxulyan, near St. Austell. Distinctive in appearance, it consists of pink alkali feldspar phenocrysts in a black groundmass of tourmaline and quartz, and is characterized texturally by radiate 'suns' of acicular tourmaline. Previous descriptions, however, relate exclusively to loose boulders of luxullianite found in fields (e.g. Bonney, 1877; Wells, 1946). Examples of superficially similar tourmalinized rocks have been described *in situ* in other localities (e.g. Blyth, 1949), but these lack the fine acicular tourmaline developed in luxullianite *sensu stricto*.

This note reports the discovery of several veins of luxullianite currently exposed *in situ* in a granite quarry near Luxulyan, both in the working face and in the quarry floor. The veins take the form of vertical sheets within the granite, and range from a few centimetres to about one metre in thickness. Their SW.-NE. orientation corresponds with local joint directions. One of the largest luxullianite veins is laterally discontinuous, dividing into three parallel veins with a total thickness of 2 m, before reuniting into a single vein that narrows and disappears altogether. The total length of this vein system, exposed as quarrying progressed, was about 25 m. The contacts between luxullianite and granite are gradational, and it is clear from field and microscopic evidence that the luxullianite results from metasomatic alteration of granite *in situ*, and not from the emplacement within the granite of a late stage magma.

For the first time it has been possible to examine petrographically the material that is transitional between luxullianite and its parent granite, and to observe the intermediate stages of progressive tourmalinization. The unaltered granite adjacent to the veins contains phenocrysts of white orthoclase microperthite up to 3 cm in length, with equigranular oligoclase, biotite, muscovite, brown tourmaline, and quartz as the other major constituents. The luxullianite consists of pink orthoclase, quartz, muscovite, chlorite, a little topaz and pyrite, and blue acicular tourmaline needles both in radiate (tourmaline sun) configuration and as overgrowths upon primary brown tourmaline.

FIGS. 1-3: FIG. 1 (*top*). Tourmaline needles forming upon biotite cleavage flake. FIG. 2 (*centre*). Feather-like development of tourmaline along cleavage plane of biotite. FIG. 3 (*bottom*). Oriented overgrowth of secondary tourmaline needles upon primary brown tourmaline. (*c*-axis horizontal.)

Particular interest lies in the mineralogical changes taking place across the transition zone. In passing from granite to luxullianite, over a zone about 0·25 m wide, the following processes were observed:

Transitional rock showed progressive reddening of the alkali feldspars, caused by minute specks of iron oxides within the feldspar crystals. At the same time, replacement of both alkali feldspar and plagioclase by tourmaline and quartz was taking place, with new tourmaline appearing around their margins and along their cleavage planes. As a result of this latter process, most of the K-feldspar phenocrysts were reduced to smaller, corroded fragments in optical continuity, while the plagioclase crystals, which originally were much smaller and fewer, seem to have been completely eliminated in favour of tourmaline and quartz. Along the cleavage planes of the biotite crystals, the growth of radiating acicular tourmaline (figs. 1 and 2) began with the appearance of minute blue tourmaline needles (less than 0·1 mm in length). Eventually the biotite became converted entirely to blue tourmaline of radiate and feather-like habit, associated in some specimens with chlorite, and surrounded by quartz. Existing brown tourmaline crystals became fringed with secondary blue tourmaline needles, growing in optical alignment with the primary phase (fig. 3). Muscovite, primary tourmaline, and accessories such as apatite, zircon, and opaque iron oxides remained stable throughout, while quartz appears to have recrystallized around the secondary tourmaline.

From the present study of *in situ* relationships, it has been possible to reconsider previous petrographic interpretations (Bonney, 1877; Wells, 1946). However, it should be noted that neither of these authors had seen the parent rock. Bonney suggested that the large *brown tourmaline* crystals in luxullianite were derived by replacement of biotite, while Wells envisaged brown tourmaline instead of biotite as a primary constituent of the parent material. The parent granite here under consideration contains biotite in addition to primary brown tourmaline, and the former mineral may be seen in the process of conversion not to brown tourmaline, but directly to the acicular blue variety. According to Bonney, the *acicular blue tourmaline* was formed from feldspar, liberating free silica in the process. Wells, however, proposed that some of the secondary blue tourmaline was formed by replacement of primary tourmaline (evidenced by corrosion of primary tourmaline and parallel optical alignment of the two tourmaline phases). The parent and transitional material examined in the present study contains primary tourmaline as irregular in outline as that in the luxullianite. Therefore, no corrosion during tourmalinization need be invoked to explain its present embayed shape. The alignment of the secondary phase parallel to the *c*-axis of the primary (fig. 3) may be considered comparable with the type of overgrowth seen in sedimentary authigenic tourmalines (as described by Krynine, 1946). Hydrothermal overgrowth upon existing tourmalines appears to have caused the chemical differences between inner and outer zones of large tourmaline crystals, reported by Power, 1968.

Chemical changes, determined in the whole rocks by X-ray fluorescence and tabulated in Table I, differ from those inferred by previous authors. Both Wells and Bonney assumed an increase in silica with tourmalinization; Wells proposed removal of K and Na, and Exley and Stone (1964), referring in general terms to the Cornubian Province, stated that K was displaced during tourmalinization. In the present investigation, it was possible to analyse four samples, namely unaltered St. Austell granite (LX 001), outer

TABLE I. *Partial chemical analyses*

	LX 001	LX B1-3	LX B4-6	LX 008		LX 001	LX B1-3	LX B4-6	LX 008
SiO_2	69·38	69·46	62·50	53·89	Sr	82	80	88	156
Al_2O_3	14·05	14·73	18·69	19·21	Rb	469	807	971	672
TiO_2	0·36	0·30	0·38	0·45	Zr	156	122	150	189
Fe_2O_3*	2·53	1·60	2·20	8·81	Nb	24	17	18	21
MnO	0·06	0·01	0·01	0·07	Y	29	16	35	30
MgO	0·61	0·27	0·40	1·47					
CaO	1·00	0·23	0·19	0·34					
Na_2O	3·37	0·42	0·57	1·11					
K_2O	4·57	11·15	13·43	9·81					
P_2O_5	0·17	0·12	0·11	0·17					
	96·10	98·30	98·48	95·33					

LX 001 unaltered granite; LX B1-3 transition zone; LX B4-6 advanced transition zone; LX 008 luxullianite. Major oxides %; trace elements ppm.

* Total iron as Fe_2O_3.

transition zone (LX B1-3), inner transition zone (LX B4-6), and luxullianite (LX 008). From the results of the partial chemical analyses shown in Table I, it may be seen that about 15% silica by weight is lost in the transition from granite to luxullianite, and that aluminium and iron constitute the main additions to the system. Based on the behaviour of K and Na, an alkali exchange mechanism is proposed, that results in a net increase in K at the expense of Na.

Acknowledgements. I am grateful to Dr. Ian L. Gibson for the use of facilities at Bedford College, London, and to Miss Giselle Marriner at Bedford College for XRF determinations. The work was carried out while I was a student at King's College, London.

Department of Mineralogy
British Museum (Natural History)
Cromwell Road, London SW7

REFERENCES

Blyth (F. G. H.), 1949. *Geol. Mag.* **86**, 175-9.
Bonney (T. G.), 1877. *Mineral. Mag.* **1**, 215-21.
Exley (C. S.) and Stone (M.), 1964. In *Present Views of Some Aspects of the Geology of Cornwall and Devon* (Roy. Geol. Soc. Cornwall), 132-84.
Krynine (P. D.), 1946. *J. Geol.* **54**, 65-87.
Power (G. M.), 1968. *Mineral. Mag.* **36**, 1078-89.
Wells (M. K.), 1946. *Mineral. Mag.* **27**, 186-94.

[*Manuscript received 17 October 1977; revised 25 November 1977*]

© *Copyright the Mineralogical Society*

CAROL J. LISTER

EXTRACT
PROCEEDINGS
OF THE
USSHER SOCIETY

VOLUME FOUR

PART TWO

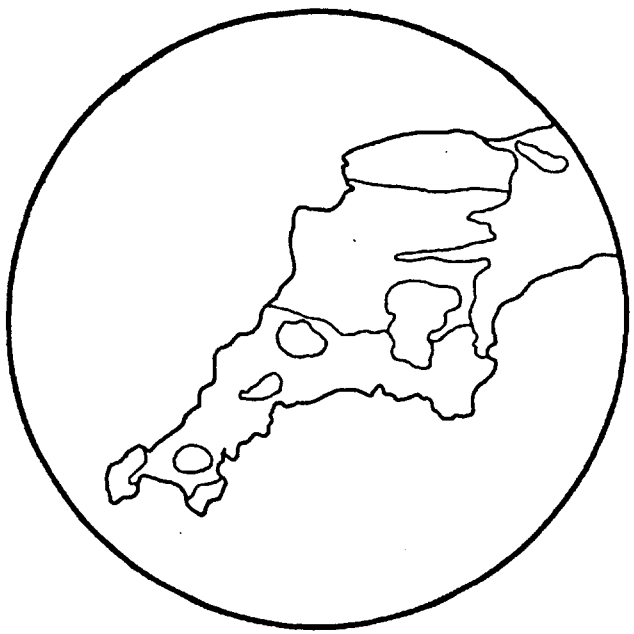

1978

SOME TOURMALINISED ROCKS FROM CORNWALL AND DEVON

by Carol J. Lister

Abstract. Contrasts are drawn between tourmaline habits and textures observed in two different luxullianite veins, one in the St Austell granite and one on Dartmoor.

1. Introduction

Luxullianite is one of the less common varieties of tourmalinised granite found in south-west England. Material previously described has generally been taken from loose boulders, rather than observed *in situ* within the parent granite (Bonney 1877; Wells 1946).

Two *in situ* occurrences of luxullianite-type rocks have been described, one from the eastern part of the St Austell granite close to the type locality (Lister 1978), and one from east Dartmoor (Blyth 1949). In both localities the tourmalinised rock occurs as vertical veins up to 2 metres wide, within potassium feldspar megacryst bearing granite. The Dartmoor vein lies within a larger zone of reddened granite containing pink feldspar megacrysts and large rounded quartz crystals in a finer-grained matrix; this texture is reminiscent of those found in zones of wall rock alteration associated with metalliferous lodes in the vicinity (R. Scrivener, personal communication, 1978). In the St Austell example, however, the reddening is confined to the luxullianite veins.

The mineralogy of the tourmalinised material is superficially similar in each case, with pink alkali feldspar, quartz and tourmaline forming the major components. However, the tourmalines show definite textural differences, reflecting their mode of formation (Blyth referred to "luxullianite" in inverted commas, presumably to imply this textural difference). The tourmalinisation process has in each case been studied by microscopic examination of material transitional between granite and its alteration product; thus it has been possible to observe mineral grains at various stages of transformation, and to suggest possible origins for the tourmaline varieties present.

2. St Austell luxullianite

In the St Austell luxullianite, two distinct tourmaline phases coexist, namely primary tourmaline which is brown in thin section, and secondary (hydrothermal) tourmaline which is blue and acicular. The brown variety is present in the parent granite as unzoned prismatic crystals up to several millimetres in length, and as clusters of fragmental or interstitial tourmaline in optical continuity. The colour and habit persist from the unaltered granite into the luxullianite veins. The blue acicular tourmaline occurs only in the luxullianite, both as "tourmaline suns" and as oriented hairlike overgrowths upon existing brown tourmalines. By reference to the material transitional between granite and luxullianite, this secondary phase may be seen to arise, at least in part, from the hydrothermal breakdown of biotite with minute tourmaline needles growing between the cleavage planes of biotite crystals (this is described and illustrated by Lister, 1978).

3. Dartmoor "luxullianite"

The Dartmoor "luxullianite"contains tourmalines of quite different habits and textures. All the tourmaline crystals are strongly zoned, comprising both brown and blue tourmaline in the central portions, and often with a dark blue rim. Most are euhedral to subhedral, ranging in size from 0.5 mm to 10 mm; some of the larger crystals are skeletal, or consist of several smaller individuals linked by the subsequent addition of outer zones. By contrast with the St Austell material, acicular "tourmaline sun" development is virtually absent, as is acicular overgrowth (Fig. 1).

Examination of the transitional rock between the reddened granite and "luxullianite" reveals four tourmaline varieties:

1. Pale brown short prismatic tourmalines 0.5 mm to 2 mm in length, are very similar to primary magmatic tourmalines seen elsewhere in the south-west England granites. Towards the centre of the "luxullianite" vein, these become zoned by the addition of a dark blue variety.
2. Pale blue, elongate (up to 3 mm) prismatic crystals, often adopting a radiate configuration, lie within and at the margins of feldspar grains, and are perhaps derived from them (an origin suggested by Wells, 1946, for St Austell radiate tourmaline). These blue tourmalines are not fine and acicular like their St Austell counterparts; rather they resemble the prismatic tourmalines forming radiate structures in quartz-schorl rocks (e.g. Hemerdon, Dartmoor). As these incipient "tourmaline suns" do not generally appear to persist into the centre of the "luxullianite" vein, it is possible that they became incorporated in the larger composite tourmaline crystals as tourmalinisation progressed.
3. Sub-radiate aggregates of brown and blue tourmaline, showing relict biotite structures (Fig. 2), are also present. Within an outer fringe of dark blue tourmaline, the core region consists of parallel dark brown, pale greenish-brown and blue lamellae, cutting straight across the tourmaline alignment. These lamellae are considered to represent residual biotite cleavage planes; indeed, the structure closely resembles some of the biotite replacement phenomena seen in the St Austell transitional zone. In the central part of the "luxullianite" vein, such residual structures are absent, but many of the larger tourmalines still show a rather patchy colour distribution in their cores.
4. Dark blue tourmaline forms continuous zones around the periphery of the tourmaline crystals already described, and this is itself frequently rimmed by a paler blue variety. In many crystals several concentric zones are present, indicating multistage growth, while in St Austell only one stage of secondary tourmaline formation is in evidence. The margins of the Dartmoor tourmalines are nearly all sharp and continuous, lacking the fine hairlike overgrowth common in the St. Austell luxullianite.

Fig.1 Large composite and zoned tourmaline from Dartmoor

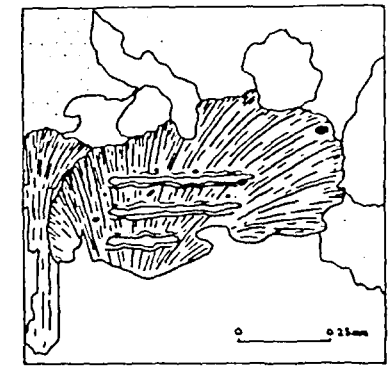

Fig.2 Residual biotite lamellae within sub-radiate tourmaline

Legend: Feldspar stippled, quartz blank, opaques solid, tourmaline all other symbols.

4. Conclusions

The tourmalines found in rocks of luxullianite type may be said to develop by various processes, though individual grains all seem to range between schorlite and magnesian schorlite in their bulk composition. Primary brown tourmaline is present in the parent granites in both the examples described. Replacement of biotite also seems an important source, both of radiate structures (St Austell and Dartmoor), and of large patchy tourmaline grains (Dartmoor only). Growth within feldspar (perhaps associated with K-feldspathisation of Na-bearing feldspar) is a further possibility for the origin of radiate configurations in the Dartmoor material; however, these structures do not seem to persist as such with continuing tourmalinisation. Finally, blue tourmaline, either introduced in solution or mobilised within the veins, accretes upon or around existing tourmaline grains, building up zoned crystals in the Dartmoor example and hairlike overgrowths in St Austell.

The formation of the St Austell luxullianite may be explained as a single stage process, producing one type of secondary tourmaline. However, the Dartmoor "luxullianite" appears to represent a somewhat more complex tourmalinisation history.

5. References

BLYTH, F.G.H. 1949. A "luxullianite" from east Dartmoor. *Geol. Mag.*, **86**, 175-179.

BONNEY, T.G. 1877. On the microscopic structure of luxullianite. *Mineral. Mag.*, **1**, 215-221.

LISTER, C.J. 1978. Luxullianite *in situ* within the St Austell granite, Cornwall. *Mineral. Mag.*, **42**, 295-297.

WELLS, M.K. 1946. A contribution to the study of luxullianite. *Mineral. Mag.*, **27**, 186-194.

Carol J. Lister,
Dept. of Mineralogy,
British Museum (Natural History),
Cromwell Road,
London SW7.

EXTRACT

PROCEEDINGS

OF THE

USSHER SOCIETY

VOLUME FOUR

PART THREE

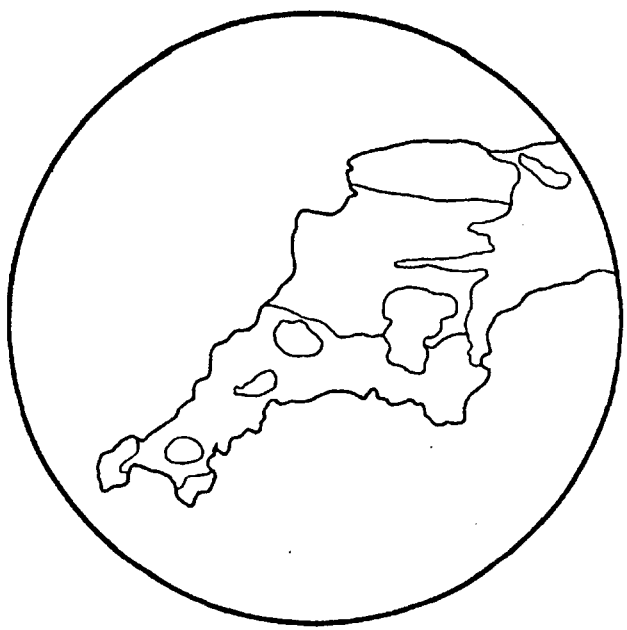

1979

QUARTZ-CORED TOURMALINES FROM CAPE CORNWALL AND OTHER LOCALITIES

by Carol J. Lister

Department of Mineralogy, British Museum (Natural History), Cromwell Road, London SW7

Abstract. Cored tourmalines from four Cornish localities have been examined and analysed for major elements. An origin by skeletal growth from a pegmatitic fluid is suggested as an alternative to origin by replacement; chemical analyses of individual zones within Cape Cornwall tourmalines are presented in support of this view.

1. Introduction

Although the phenomenon of cored tourmalines has been noticed by several workers, detailed studies in the literature are few, and no analytical data appear previously to have been published. Quartzcored, euhedral tourmaline, showing negative tourmaline morphology within, was described from Nigeria by McCurry (1971), who considered the internal quartz to have replaced the cores of originally solid, zoned tourmalines. Brammall and Harwood (1925) described quartz and feldspar inclusions in large irregular masses of Dartmoor tourmaline, postulating an autopneumatolytic origin whereby tourmaline replaced the original groundmass of the rock.

The present work gives the results of an examination of some Cornish cored tourmalines which resemble in appearance those illustrated by McCurry, and considers their possible modes of formation.

2. Location and geological setting of samples

Samples were taken from
(i) Priest's Cove (SW 352317) and Porthledden Cove (SW 354321), both at Cape Cornwall (Land's End granite)
(ii) Tregarden Quarry, Luxulyan (SX 054590) (St Austell granite)
(iii) Megiliggar Rocks (SW 612266) (Tregonning granite)

(iv) Goonbarrow China Clay Pit (SX 007583) (St Austell granite)
There is no reason to suppose that these are the only localities in southwest England where cored tourmalines occur.

All samples containing cored tourmalines came from pegmatitic veins, sheets or joint infillings, and comprise very similar mineralogical assemblages of quartz, black tourmaline, alkali feldspar and muscovite. The Cape Cornwall specimens were collected from near-vertical pegmatite veins up to 30 cm across within granite, in Priest's Cove (similar cored tourmalines were also observed on joint planes of the granite at the same locality); the Tregarden material forms pegmatitic joint infillings about 5 cm wide, showing ill-defined boundaries with the porphyritic granite on either side. At both localities (i) and (ii), tourmaline occurring within the main body of the host granite was apparently uncored. At Megiliggar Rocks a classic horizontal contact is exposed between pegmatite and aplite sheets below and hornfelsed killas above; samples of pegmatite containing vertical tourmaline needles were collected from immediately below this contact. The Goonbarrow samples were taken from the 'curved crystal pegmatite' of Badham and Stanworth (1976).

3. Descriptions of cored tourmalines

(i) Cape Cornwall (Figs. 1, 6)

Tourmaline crystals range between 0.5 mm and nearly 10 mm in diameter (basal section), the longest recorded individual reaching over 10 cm in length. Most are euhedral to subhedral, elongate, hollow, trigonal prisms; subparallel alignment to the vein sides is common. All the large crystals are brown in thin section, many individuals bearing narrow and discontinuous zones of pale blue tourmaline around their outer margins and sometimes also upon their inner surfaces adjacent to their quartz cores. Dark blue tourmaline occassionally forms very small (e.g. 0.1 mm wide) extensions at the periphery of the pale blue material, and a few clusters of fine blue tourmaline needles are also present in the slides. The cores, consisting usually of polycrystalline aggregates of optically discontinuous quartz, are bounded by the internal tourmaline margins, which although often stepped or ragged, still reflect the morphology of the external faces, as do zone boundaries within the crystals.

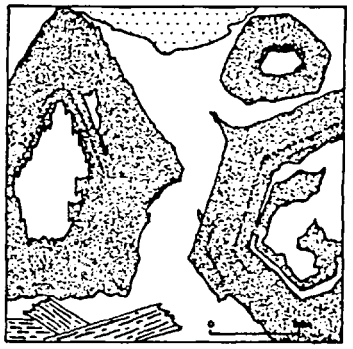

Fig.1 Cape Cornwall

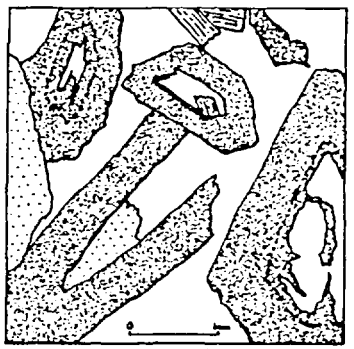

Fig.2 Tregarden

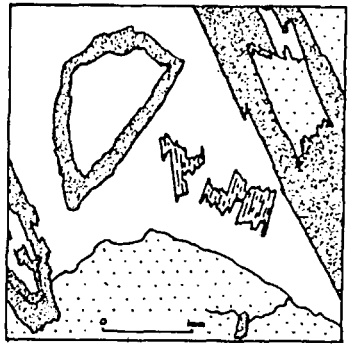

Fig.3 Megiliggar Rocks

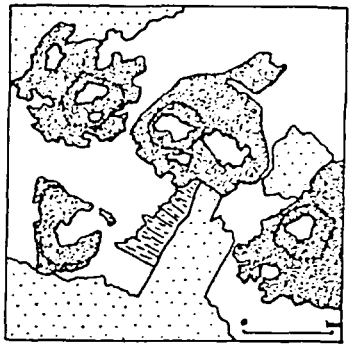

Fig.4 Goonbarrow

Legend:- Tourmaline, zone boundaries; quartz; feldspar; muscovite.

(ii) Tregarden (Fig. 2)

Tourmalines about 2-5 mm in diameter and a few cm in length appear to radiate from origins between the joint walls. In thin section they are all brown; they are mostly subhedral trigonal prisms with sharp outer margins and often stepped or ragged inner margins. Blue tourmaline is absent, but the inner zones adjacent to the cores frequently appear paler brown or slightly greenish compared with the bulk of the crystals, while the core material itself comprises polycrystalline quartz and/or feldspar with the occasional flake of muscovite. Some tourmalines, cut in longitudinal section, prove to be open at one end.

(iii) Megiliggar Rocks (Fig. 3)

Tourmaline needles are 1 or 2 mm across and up to 10 cm long, and thin sections show many to be almost perfect trigonal euhedra, often forming but a narrow shell around their quartz or feldspar cores. All crystals are brown in thin section, with no blue zoning; longitudinal sections show paler centres and stepped inner margins.

(iv) Goonbarrow (Fig. 4)

These tourmalines, which show slight curvature and radiate configuration, are about 1-3 mm in diameter and up to 5 cm in length, and although in hand specimen many appear to have euhedral outlines, thin sections reveal embayments and multiple quartz cores (features reminiscent of Brammall and Harwood's replacive texture). Apart from blue haloes surrounding minute inclusions, all crystals are brown in thin section, with paler brown centres, zone boundaries often showing euhedral form. Quartz is the only core material observed.

4. Chemical analyses

(i) *Methods.* Eleven major elements were determined simultaneously by electron microprobe analysis, of which Cr and Ni are omitted here since neither was detected in any sample. Boron was determined in bulk samples of hand-picked, finely powdered and dried tourmaline, by neutron capture prompt gamma ray spectrometry (details of which will be described in a future publication); it was not possible to separate sufficient quantities of individual crystals or material from zones within crystals, to equate with those analysed in detail by microprobe. Values for H_2O^+ were averaged from published results (Deer and others 1962), to complete the analyses.

(ii) *Results.* All tourmalines analysed fall within the schorl field; examples of compositions found are given in Table 1. Each locality yielded analyses falling into distinct populations with respect to their relative FeO, MgO and TiO_2 contents, as shown in Fig. 5 (for comparison, this diagram also includes some uncored tourmalines from two of the same localities). All brown crystals and zones, without exception, contain titanium, which is always absent from the blue zones at Cape Cornwall, and is is possible that this element contributes to the brown colouration seen in thin section; brown titaniferous tourmalines have also been reported by Black (1971). At Tregarden and Goonbarrow, dark brown outer zones differed from paler inner zones by containing calcium in addition. It was suspected that the more complex colour zoning in the Cape Cornwall tourmalines might provide evidence for their mode of origin, so this was studied in more detail.

5. Chemistry of the Cape Cornwall tourmalines

A particularly large crystal was sectioned at right-angles to its *c*-axis, at intervals along its length. Two such sections, shown in Fig. 6, revealed (a) a sequence of zones adjacent to the quartz core, from dark blue in the centre through pale blue to shades of brown (enlarged in Fig 6a), and (b) a similar sequence of zones progressing inward from the external rim (enlarged in Fig. 6b). Using the electron proble microanalyser, traverses were made across these regions, and analyses made of each coloured zone.

A striking similarity of composition was found between these two zone sequences; the results are tabulated in Table 2, and are shown diagrammatically with respect to certain elements in Fig. 7. It may be seen that the central zones mirror those on the outer rim, chemically as well as visually.

To confirm these findings, blue rims and centres of several other quartz-cored tourmalines from this locality were also analysed. The dark blue zones are not present in all crystals, and where present are often too narrow to 'probe' accurately; hence only one further rim and centre of dark blue colour were analysed, their compositions proving similar to the first. Pale blue tourmaline is fairly common forming both rims and centres; four such rims and five cores were analysed in a total of six crystals, all of which yielded a quite distinctive pure iron end-member composition, as did the pale blue zones in the original crystal.

Slide no.	Cape Cornwall, Priest's Cove CCPC001		CCPC002		Tregarden, Luxulyan LX051			
Grain	T1 Brown	T1 Blue centre	T6 Brown	T6 Blue rim	T1 Pale brown centre	T1 Dark brown	T4 Pale brown centre	T4 Dark brown
Na_2O	1.91	1.11	1.73	1.74	1.62	1.99	1.12	1.96
MgO	0.45	0.00	0.44	0.00	1.97	1.75	1.96	2.11
Al_2O_3	34.84	35.35	33.32	33.02	34.65	34.62	34.95	34.41
SiO_2	34.84	34.86	34.84	35.11	35.60	35.12	36.26	34.45
K_2O	0.00	0.00	0.00	0.00	0.00	0.00	0.00	0.00
CaO	0.00	0.00	0.00	0.00	0.00	0.14	0.00	0.24
TiO_2	0.21	0.00	0.26	0.00	0.20	0.38	0.22	0.48
MnO	0.00	0.00	0.00	0.00	0.00	0.00	0.00	0.00
FeO*	13.41	13.74	15.48	15.61	11.56	11.87	11.29	11.40
B_2O_3	10.72	10.72	10.72	10.72	10.52	10.52	10.52	10.52
H_2O^+	(3.37)	(3.37)	(3.37)	(3.37)	(3.37)	(3.37)	(3.37)	(3.37)
	99.75	99.15	100.16	99.57	99.49	99.76	99.69	98.94

Slide no.	Megiliggar Rocks MR001				Goonbarrow GB001			
Grain	T1 Brown	T2 Brown	T3 Brown	T4 Brown	T1 Pale brown centre	T1 Dark brown	T2 Pale brown centre	T2 Dark brown
Na_2O	1.62	1.50	1.84	1.41	1.17	1.96	1.87	2.00
MgO	0.00	0.00	0.00	0.18	0.86	1.10	1.22	1.16
Al_2O_3	34.64	34.68	33.93	34.97	35.12	34.29	35.06	34.36
SiO_2	34.86	34.52	34.61	35.43	35.65	34.90	35.37	34.78
K_2O	0.00	0.00	0.00	0.00	0.00	0.00	0.00	0.00
CaO	0.13	0.00	0.00	0.13	0.00	0.19	0.00	0.16
TiO_2	0.34	0.30	0.49	0.34	0.33	0.63	0.40	0.52
MnO	0.00	0.00	0.29	0.00	0.00	0.00	0.00	0.00
FeO*	14.45	14.63	14.80	12.97	12.55	13.33	12.27	12.78
B_2O_3	10.36	10.36	10.36	10.36	9.92	9.92	9.92	9.92
H_2O^+	(3.37)	(3.37)	(3.37)	(3.37)	(3.37)	(3.37)	(3.37)	(3.37)
	99.77	99.36	99.69	99.16	98.97	99.69	99.48	99.05

*Total iron as FeO

Table 1. Analyses of cored tourmalines from Cornwall

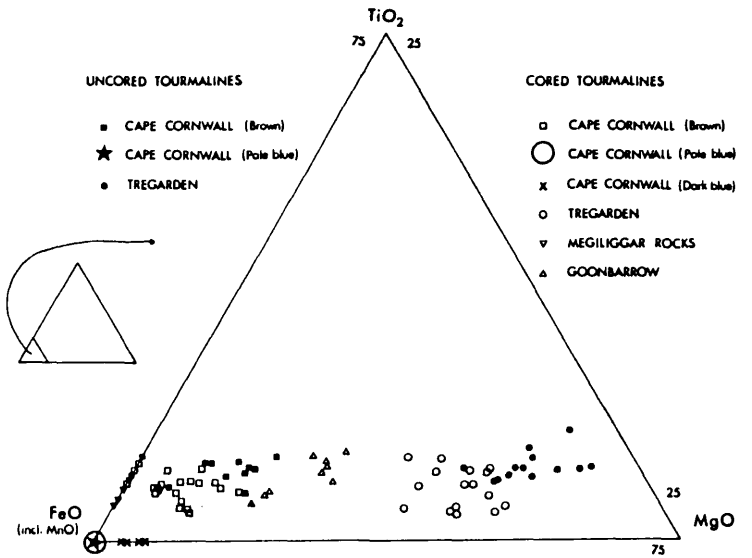

Fig. 5. FeO, MgO and TiO_2 proportions in some cored and uncored tourmalines.

From their chemical similarity, it appears that the pale blue rims and centres both belong to a single generation or depositional phase; likewise the dark blue zones may be said to represent a further single generation. It should be stressed that this need not necessarily imply a series of separate hydrothermal events (which, incidentally, would not detract from the present argument), since tourmaline crystals frequently do form by the addition of successive zones, reflecting changes in the composition of the surrounding fluid. If rims and centres of cored tourmalines are in fact coeval, it follows that they must have been deposited upon a hollow or skeletal crystal.

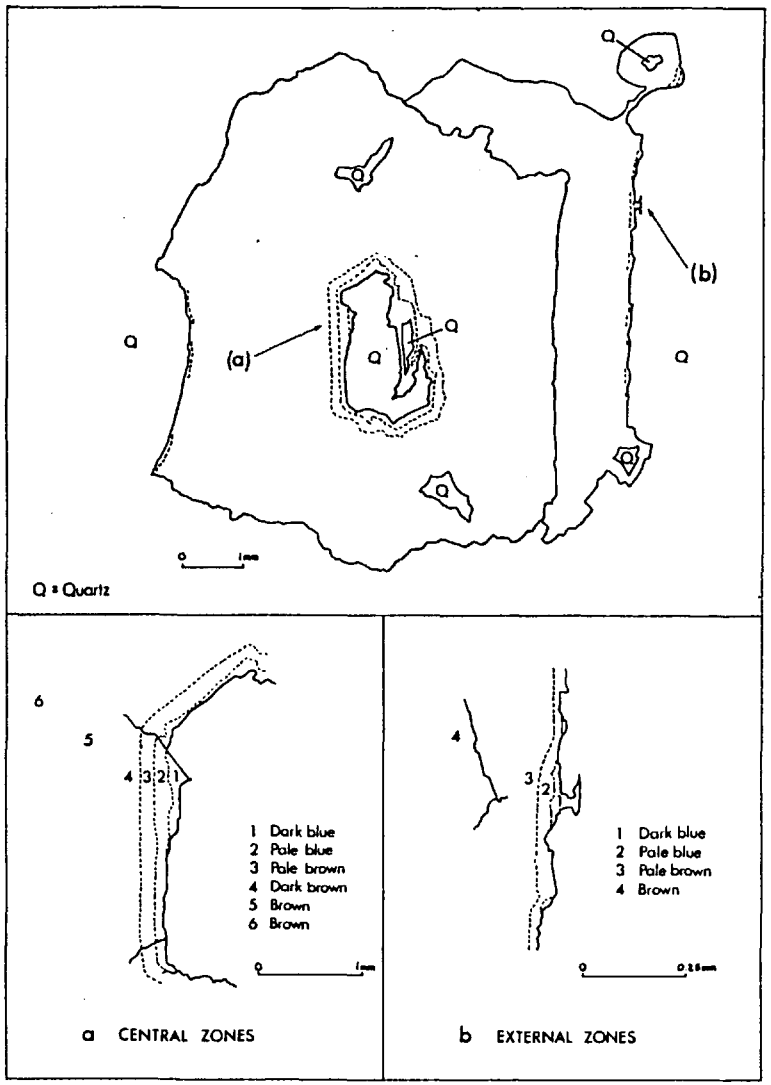

Fig. 6. Quartz-cored tourmaline from Cape Cornwall (Priest's Cove), showing points of analysis.

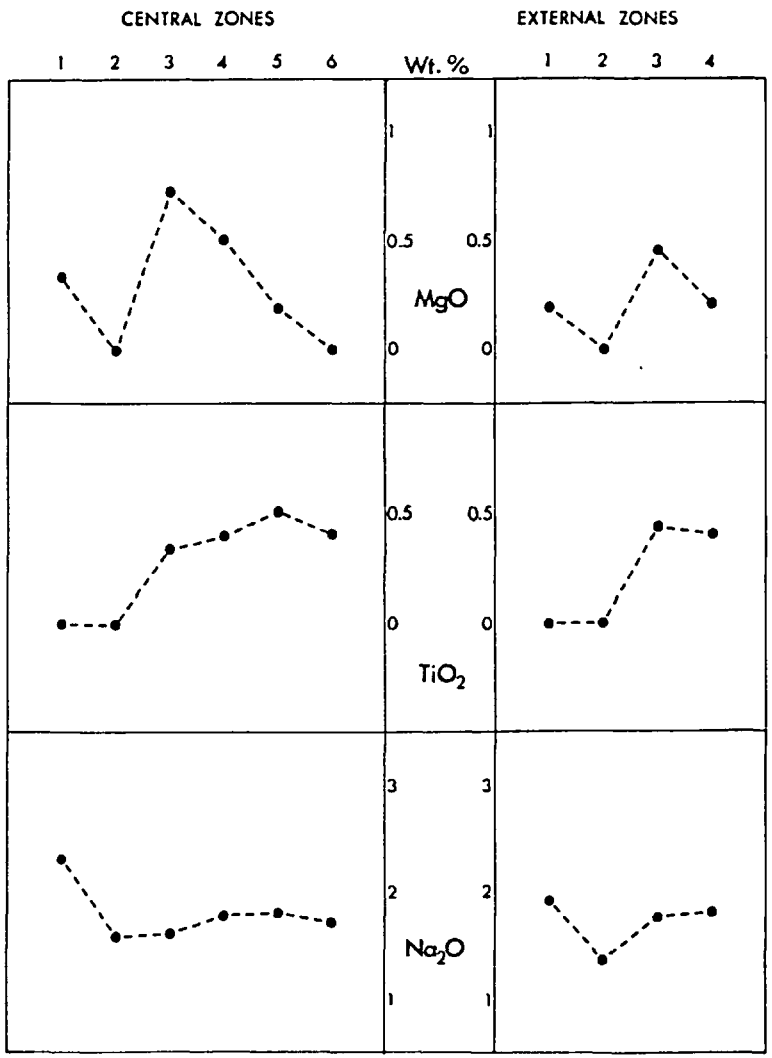

Fig. 7. Local variation in MgO, TiO_2 and Na_2O within a quartz-cored tourmaline from Cape Cornwall (Priest's Cove).

(Numbering of zones as in Fig. 6a and 6b).

Zone	Centre:	1	2	3	4	5	6	Rim:	1	2	3	4
Colour		Dark blue	Pale blue	Pale brown	Dark brown	Brown	Brown		Dark blue	Pale blue	Pale brown	Brown
Na_2O		2.31	1.59	1.61	1.78	1.80	1.72		1.91	1.36	1.76	1.81
MgO		0.29	0.00	0.73	0.51	0.19	0.00		0.19	0.00	0.46	0.21
Al_2O_3		33.79	34.28	33.90	34.91	34.52	34.24		32.37	34.99	34.27	35.29
SiO_2		35.46	34.40	34.44	34.36	34.66	34.48		34.92	35.10	34.53	33.78
K_2O		0.00	0.00	0.00	0.00	0.00	0.00		0.00	0.00	0.00	0.00
CaO		0.19	0.00	0.12	0.12	0.00	0.00		0.00	0.00	0.11	0.00
TiO_2		0.00	0.00	0.34	0.40	0.51	0.41		0.00	0.00	0.44	0.41
MnO		0.00	0.00	0.00	0.00	0.00	0.30		0.00	0.00	0.00	0.26
FeO*		13.06	14.50	13.66	12.96	13.76	13.98		16.88	14.27	14.63	13.79
B_2O_3		10.72	10.72	10.72	10.72	10.72	10.72		10.72	10.72	10.72	10.72
H_2O+		(3.37)	(3.37)	(3.37)	(3.37)	(3.37)	(3.37)		(3.37)	(3.37)	(3.37)	(3.37)
		99.19	98.86	98.89	99.13	99.53	99.22		100.36	99.81	100.29	99.64

*Total iron as FeO.

Table 2. Chemical composition of central and external zones in a quartz-cored tourmaline, Cape Cornwall (Priest's Cove). Numbering of zones as in Fig. 6a and 6b.

Grain	Tregarden	F1'	F2'	F1'	F1'	Megiliggar	F1	F2	F3	F4	F5
Slide No.		LX015b	LX015b	LX051	LX052		MR001	MR001	MR001	MR001	MR001
Na_2O		2.50	1.36	11.49	4.30		11.19	5.01	8.44	0.00	0.23
MgO		0.00	0.00	0.00	0.00		0.00	0.00	0.00	0.00	0.00
Al_2O_3		18.56	18.26	19.59	18.55		19.69	18.82	22.07	18.05	20.39
SiO_2		66.39	66.02	69.44	66.65		69.05	66.82	64.62	65.85	63.46
K_2O		13.07	14.50	0.09	10.53		0.55	9.95	2.76	16.09	15.34
CaO		0.00	0.00	0.13	0.00		0.00	0.00	0.15	0.00	0.00
TiO_2		0.00	0.00	0.00	0.00		0.00	0.00	0.00	0.00	0.00
MnO		0.00	0.00	0.00	0.00		0.00	0.00	0.00	0.00	0.00
FeO		0.00	0.00	0.00	0.00		0.00	0.00	0.27	0.00	0.00
		100.52	100.14	100.74	100.03		100.48	100.60	98.31	99.99	99.42

Legend:

LX015b, F1' & F2' were away from cored tourmalines
LX051 F1' was enclosed within a cored tourmaline
LX052 F1' was partially enclosed in an open-ended tourmaline

MR001 F1 was away from cored tourmalines
MR001 F2 & F3 were adjacent to but outside cored tourmalines
MR001 F4 & F5 were enclosed within cored tourmalines

Table 3. Feldspars associated with cored tourmalines.

Uncored tourmalines from Porthledden Cove, also Cape Cornwall, were found to have pale blue rims of pure schorlite composition, identical to those at Priest's Cove (dark blue outer rims were, however, absent), their brown inner zones also proving similar to their Priest's Cove counterparts. This tends to confirm the view that the pale blue, pure iron and end-member tourmaline formed at a slightly later stage than did the brown variety. (It should be noted that this blue tourmaline is not analogous to the 'hydrothermal' tourmaline of Power (1968), which has yet a different composition).

If the blue tourmaline at Cape Cornwall was indeed the last to form, then that found in the centres of quartz-cored crystals cannot represent residual portions of early-formed tourmaline which has later been replaced.

6. A note on feldspar cores from Tregarden and Megiliggar

Differences between compositions of feldspars within and outside tourmalines indicate that the tourmaline shells may have protected feldspar from alkali changes (Exley and Stone 1964) affecting the granite. The results of electron microprobe analyses shown in Table 3 are consistent with reports of late K-enrichment associated with kaolinisation in the St Austell granite (Exley 1959) and of Na-enrichment with time in the Tregonning-Godolphin complex (Stone 1975).

7. Possible mechanisms for hollow crystal formation

There are many published examples of both natural and experimentally produced cored crystals, for which a few of the modes of origin proposed are listed below. These will be considered as possible mechanisms for the formation of the Cornish cored tourmalines.

1. Removal of the original core in a zoned crystal
(The assumption is made, on morphological grounds, that the original core material belonged to the same mineral species as the remaining rim).

(a) Dissolution of a compositionally discrete core
(McCurry 1971) (natural tourmaline)

(b) Physical separation of a thinner core
(Buckley 1932) (experimental $KClO_3$)

2. Skeletal crystal growth

(a) Replacement of the host mineral
(Brammall and Harwood 1925) (natural tourmaline)

(b) Recrystallisation of the original components
(Wells and Bishop 1955) (natural amphibole)

(c) Direct skeletal growth from a magma or fluid
(Kirkpatrick 1975) (natural olivine and experimental plagioclase)

(1a) Dissolution of a compositionally discrete core
There are two main arguments against this contention. Firstly, in view of the extreme insolubility of tourmaline in most solvents, it is difficult to envisage the kind of post-magmatic fluid that could succeed in dissolving the core of a zoned crystal whilst leaving its rim intact. Secondly, the electron microprobe analyses presented above do not support McCurry's proposition that narrow zones of differing composition within the crystal represent residual patches of a once solid core.

(1b) Physical separation of a thinner core
If tourmaline cores had become mechanically detached, one might expect (as Buckley did) to find such cores elsewhere in the crystallised mass. None has been recognised in these rocks.

(2a) Replacement of the host mineral
Replacement of other minerals is a common role for tourmaline, and one which produces distinctive textures. For example, tourmaline may directly pseudomorph another mineral, or, if replacement is incomplete, may either follow the cleavage planes of its host or form a skeletal network surrounding residual, optically continuous patches of the host mineral. Brammall and Harwood (1925) considered the large irregular masses of Dartmoor tourmaline (mentioned above) to have had a replacement origin; however, they did concede the possibility, on textural grounds, of direct crystallisation of quartz-tourmaline intergrowths from borosilicate segregations within the original magma.
While it is possible that the quartz-cored tourmalines here described are replacement phenomena, there are arguments against such an interpretation. Firstly, most are single, isolated, cored crystals, rather than part of a skeletal network; secondly, the tourmaline shows no tendency preferentially to have formed within one mineral or another, as might be expected if replacement had taken place. Thirdly, polycrystalline and multiphase cores are common, while optical continuity between core and external quartz or feldspar is unusual.

(2b) Recrystallisation
(This relies on similar processes to those of 2c). Tourmaline is exceedingly stable and resistant to chemical attack or remobilisation, existing grains surviving subsequent hydrothermal events, as well as

sedimentary and metamorphic cycles. Other rock-forming silicates are likely to recrystallise more readily than tourmaline, and thus one might expect to find tourmaline recrystallised only in a rock whose entire fabric had been altered. This possibility cannot be ruled out, and indeed, some authors (e.g. Exley and Stone 1964) regard the whole fabric of the southwest England granites as the product of large-scale recrystallisation; however, if feldspars within cored tourmalines have escaped alteration, as suggested above, then the tourmalines themselves must have remained unaffected.

(2c) Skeletal growth from a melt

The phenomenon of skeletal or hollow shell crystallisation has been recorded in apatite (Wyllie and others 1962; Gardner 1972), olivine (Bryan 1972; Donaldson 1974), and plagioclase (Lofgren 1974), as well as various other natural minerals and artificial syntheses.

Kirkpatrick (1975), summarising previous work, described a mechanism for the growth of hollow, skeletal, dendritic and spherulitic crystals from a melt. Increasing 'undercooling' (the degree to which actual temperature falls below liquidus temperature) may result in the following trends:

(i) an increase in crystal growth rate,

(ii) a decrease in diffusion rate through the residual field,

(iii) an increased tendency towards instability at the crystal-fluid interface, favouring the development of regularly spaced outgrowths upon crystals,

(iv) a decrease in the spacing between such outgrowths.

These factors, singly or in combination, determine the habit of crystals. If crystallisation takes place within a temperature range where crystal-fluid interfaces are stable, solid, faceted crystals develop. With an increase in cooling rate (and hence the degree of undercooling), crystallisation takes place at temperatures below those of 'normal' crystallisation, leading, with progressively lower temperatures, to the formation of hollow (or skeletal), dendritic, and finally spherulitic crystals.

During the emplacement of pegmatitic veins and joint infillings, the sudden release of volatiles and/or chilling on contact with cooler host rocks could induce the conditions of moderate but not extreme undercooling necessary for hollow crystal growth. It is therefore quite feasible for hollow tourmalines to have crystallised directly from a melt in the pegmatitic microenvironment of southwest England.

8. Conclusions

On the basis of textural and chemical evidence, and in accordance with crystal growth theory, it is quite possible that the Cape Cornwall

cored tourmalines originally formed as skeletal crystals with hollow cores. By inference, the Tregarden and Megiliggar examples may have originated in the same manner, but the textural evidence from Goonbarrow is less conclusive. The 'dissolved core' hypothesis of McCurry (1971) is considered inapplicable to the southwest England tourmalines here described.

Acknowledgements. I acknowledge analytical facilities afforded me both at Imperial College, London, and at the University of London Reactor Centre, as well as financial support from N.E.R.C. I am grateful to Dr A.C. Bishop and Dr P. Henderson for kindly reading the manuscript; thanks are also due to Dr J.P.N. Badham who gave me two hand specimens from Goonbarrow Pit.

9. References

BADHAM, J.P.N. and STANWORTH, C.W. 1976. The curved crystal pegmatite, Goonbarrow. *Proc. Ussher Soc.*, 3, 441-447.

BLACK, P.M. 1971. Tourmalines from Cuvier Island, New Zealand. *Mineralog. Mag.*, **38**, 374-376.

BRAMMALL, A. and HARWOOD, H.F. 1925. Tourmalinisation in the Dartmoor granite. *Mineralog. Mag.*, **20**, 319-330.

BRYAN, W.B. 1972. Morphology of quench crystals in submarine basalts. *J. Geophys. Res.*, **77**, 5812-5819.

BUCKLEY, H.E. 1932. The growth of $KClO_3$ crystals in the presence of ionic impurities. *Z. Kristallog. Kristallgeom.*, **A82**, 37-46.

DEER, W.A., HOWIE, R.A. and ZUSSMAN, J. 1962. *Rock forming minerals*, Vol. 1. Longman, Green & Co., London, 333pp.

DONALDSON, C.H. 1974. Olivine crystal types in harrisitic rocks of the Rhum pluton and in Archean spinifex rocks. *Bull. Geol. Soc. Am.*, **85**, 1721-1726.

EXLEY, C.S. 1959. Magmatic differentiation and alteration in the St Austell granite. *Q. Jl. Geol. Soc. Lond.*, **114**, 197-230.

EXLEY, C.S. and STONE, M. 1964. The granitic rocks of South-West England. *In* Hosking, K.F.G. and Shrimpton, G.J. (eds.) Present views of some aspects of the Geology of Cornwall and Devon (Royal Geological Society of Cornwall) 131-184.

GARDNER, P.M. 1972. Hollow apatites in a layered basic intrusion, Norway. *Geol. Mag.*, **109**, 385-464.

KIRKPATRICK, R.J. 1975. Crystal growth from the melt: a review. *Am. Miner.*, **60**, 798-814.

LOFGREN, G. 1974. An experimental study of plagioclase morphology. *Am. J. Sci.*, **274**, 243-273.

McCURRY, P. 1971. A pseudomorphic quartz-tourmaline relationship from northern Nigeria. *Am. Miner.*, **56**, 1474-1476.

POWER, G.M. 1968. Chemical variation in tourmalines from south-west England. *Mineralog. Mag.*, **36**, 1078-1089.

STONE, M. 1975. Structure and petrology of the Tregonning-Godolphin granite, Cornwall. *Proc. Geol. Ass.*, **86**, 155-170.

WELLS, A.K. and BISHOP, A.C. 1955. An appinitic facies associated with certain granites in Jersey, Channel Islands. *Q.Jl. Geol. Soc. Lond.*, **111**, 143-166.

WYLLIE, P.J., COX, K.G. and BIGGAR, G.M. 1962. The habit of apatite in synthetic systems and igneous rocks. *J. Petrology.*, **3**, 238-243.

10. Discussion

Dr C Halls suggested that the differentiation relationships which the author had described pointed to the fact that the crystallisation of tourmaline had been comagmatic through at least the later stage of development of the rocks.

The Author agreed, but said that she had examined only a small number of samples and would not like to draw any far-reaching conclusions at that stage.

Dr M. Stone asked whether the micas co-existing with the tourmaline showed increased contents of lithium and fluorine as the iron content of the tourmaline increased.

The Author said that of the samples she had examined, some of the more iron-rich tourmalines were indeed associated with lithian micas (e.g. at Megiliggar).

Dr Stone, continuing, said that biotite became unstable in the presence of minerals containing fluorine, and there was exchange between the octahedral sites in the biotite lattice, LiAl replacing MgFe; thus sites had to be found for the displaced Fe, and it was suggested that tourmaline became the host. This would fit the pattern described by the author.

The Author commented that one had also to assume the availability of boron to accommodate the tourmaline. Her observations had suggested that biotite and tourmaline seemed mutually exclusive, whereas lithium mica and tourmaline commonly occurred together.

Dr Stone reported that biotite and tourmaline did occur together in some cases; for example at Priest's Cove, near St Just.

The Author replied that she had not recorded biotite and tourmaline together in the rocks she had examined.

Dr J.P.N. Badham remarked that biotite and tourmaline occurred together in the middle of the Goonbarrow pegmatite, but not actually in contact.

The Author (in a written reply) noted that thin sections made from the Goonbarrow samples given to her by Dr Badham did not contain biotite and tourmaline together, and in fact Mr R. Barnes, who had worked on these rocks, had remarked upon the inverse relationship between the abundances of the two minerals.

SHORT COMMUNICATIONS

MINERALOGICAL MAGAZINE, SEPTEMBER 1979, VOL. 43, PP. 441-2

Luxullianite *in situ* within the St. Austell granite, Cornwall—a discussion

LISTER (1978) has recently described some exposures of luxullianite—a striking rock consisting predominantly of black tourmaline, pink K-feldspar, and quartz. The relationships between this rock type and the host granite are particularly interesting but need some clarification.

Previous authors have tended to generalize over chemical gains and losses during rock alteration, without being specific as regards the mineralogical changes involved. Such changes are particularly important when discussing the role of alkalis during tourmalinization. If a granite suffers appreciable tourmalinization, a depletion in both Na and K should be seen, as micas and feldspars are replaced. The alkali variations recorded by Lister in the transition from luxullianite to unaltered granite do not show this, so tourmalinization cannot have been the sole alteration process in operation. The Na content does decrease (excepting the modest amount fixed in the tourmaline), which is consistent with breakdown of plagioclase feldspar. However, even allowing for slight changes in density, it is clear that both the luxullianite and the 'transition zone' have experienced extensive addition of K, presumably reflected by the growth of K-feldspar. Thus 'an alkali exchange mechanism' is not sufficient to account for the alkali variations. In fact the content of 13.43% K_2O in LXB4-6 indicates that there would be approximately 80% $KAlSi_3O_8$ by volume in this sample (and more if muscovite or biotite were present). Two alteration processes have therefore occurred: tourmalinization, and the growth of secondary K-feldspar (i.e. K-silicate alteration—Meyer and Hemley, 1967).

The chemical data clearly reveal that the alteration profile is zoned. Such zoning in alteration profiles adjacent to hydrothermal veins is a common feature, both in the south-west England region (Alderton, 1976) and in other metallogenic provinces (Meyer and Hemley, 1967). In the granites of south-west England, the most common type consists of a tourmaline-rich assemblage

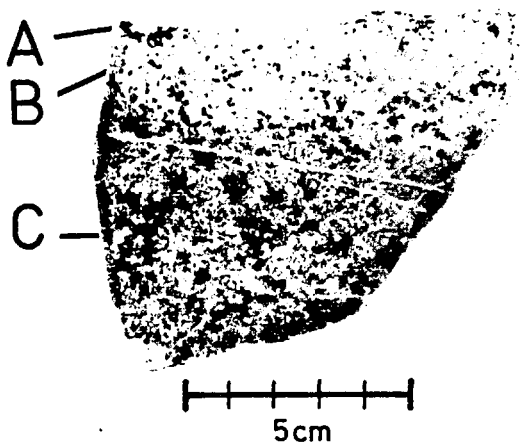

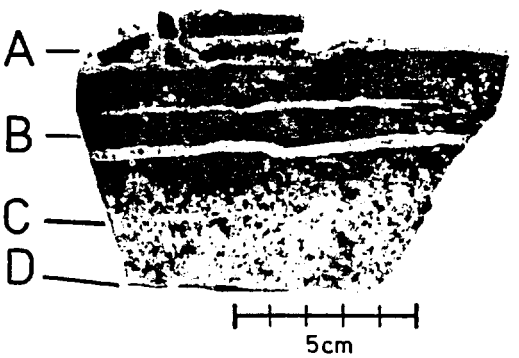

FIGS. 1 and 2: FIG. 1 (*left*). Zoned alteration profile in granite from Carn Gloose, St. Just, Cornwall. A: central fissure containing coatings of orthoclase and wolframite, B: quartz, orthoclase, and minor tourmaline, C: quartz, muscovite, and minor tourmaline (i.e. greisen). FIG. 2 (*right*). Zoned alteration profile in granite from near Hay Tor quarry, Dartmoor, Devon. A: brecciated vein infill of quartz and sphalerite, B: quartz, tourmaline, and apatite, C: quartz, orthoclase, and minor tourmaline, D: Sericitized granite with minor tourmaline.

surrounded by one containing abundant orthoclase, albite, or muscovite. The central portion is often occupied by a vein containing various ore minerals, but similar alteration profiles have been observed around aplite and pegmatite intrusions. Two examples of alteration associated with ore mineralization are shown (figs. 1 and 2).

There seems little doubt that zoned alteration haloes are caused by diffusion of components in the fluid-filled, intergranular pore-spaces of the wall-rocks adjacent to a channelway (Korzhinskii, 1946). Studies by the author suggest that the feldspar and mica-rich zones are often the first to develop and that these zones migrate away from the fissure. The growth of a tourmaline-rich zone is a later phenomenon and results in the superimposition and eventual obliteration of the earlier assemblages.

Rocks which appear identical to luxullianite often form in these alteration environments. In these cases the pink feldspar can be either orthoclase or albite. The example of luxullianite described by Lister must not therefore be regarded as an atypical product of postmagmatic alteration in the region. Furthermore, her chemical analyses demonstrate that luxullianite is not formed by the arrested tourmalinization of a granite (Wells, 1946). The growth of secondary orthoclase also appears to be important and a combination of tourmalinization and K-metasomatism seems likely.

Acknowledgements. I am grateful to Graham Lees for critically reading the manuscript, and the University of Keele for assistance towards feld expenses.

REFERENCES

Alderton (D. H. M.), 1976. Unpublished Ph.D. thesis, University of London.
Korzhinskii (D. S.), 1946. *Zap. vses. miner. Obshch.* **75**, (4), 321-32 (in Russian).
Lister (C. J.), 1978. *Mineral. Mag.* **42**, 295-7.
Meyer (C.) and Hemley (J. J.), 1967. In Barnes (H. L.) (ed.), *Geochemistry of Hydrothermal Ore Deposits*, 166-235.
Wells (M. K.), 1946. *Mineral. Mag.* **27**, 186-94.

[*Manuscript received 28 July 1978; revised 13 November 1978*]

© *Copyright the Mineralogical Society*

Department of Geology, The University, Keele, Staffs. ST5 5BG

D. H. M. ALDERTON

MINERALOGICAL MAGAZINE, SEPTEMBER 1979, VOL. 43, PP. 442-3

Luxullianite *in situ* within the St. Austell granite, Cornwall—a reply

I SHOULD like to thank Dr Alderton for his interesting comments. It is certainly apparent that in the example under consideration, one is observing the combined effects of tourmalinization and K-feldspathization.

Alderton reports alteration profiles in which two separate events may be recognized, namely the development of feldspar- and mica-rich zones followed by the superimposition of a central tourmaline-rich zone. The present example, however, lacks the sharply defined zone boundaries visible in Alderton's illustrations; instead, a strongly megacrystic texture prevails across the transition zone from granite into luxullianite (figs. 1 and 2). Furthermore, the replacement phenomena observed in transitional material indicate direct substitution of tourmaline (and chlorite) for minerals present in the unaltered granite, rather than for those of a K-silicate alteration assemblage.

The partial chemical analysis of LX B4-6 (advanced transition zone) clearly shows an unusually high K concentration; the composition of this sample is consistent with a mineral assemblage containing, for example, about 75% orthoclase, and 7% tourmaline, with the remainder comprising micas, quartz, and accessories. On the basis of field and petrographic evidence, it is suggested that two alteration processes may have been involved, but that these took place simultaneously as manifestations of one and the same event. The K-bearing component of a single hypothetical metasomatic fluid may simply have permeated further from the vein centre than did the tourmalinization agents, thus producing a peripheral zone of K-feldspathization.

The alkali depletion anticipated by Alderton in cases of 'appreciable tourmalinization' (para. 2) has not fully been realized here, since muscovite and alkali feldspar persist into the centre of the luxullianite veins. The influx of K in association with the

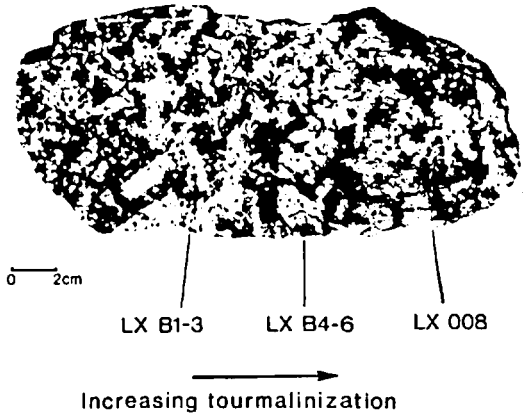

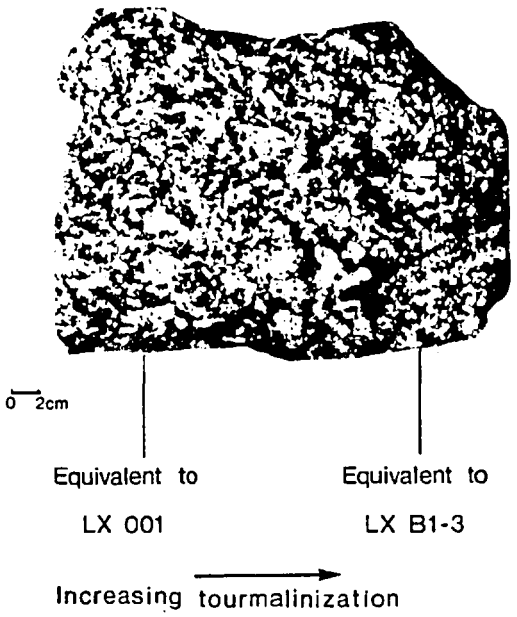

FIGS. 1 and 2: FIG. 1 (*left*). Transition zone from granite into luxullianite, showing megacrystic texture of both transitional material and luxullianite itself. There are no sharply defined zones of alteration such as Alderton illustrates. FIG. 2 (*right*). Transition zone from unaltered granite into the outer portion of a luxullianite vein, showing large K-feldspar megacrysts throughout.

agents of tourmalinization has evidently cancelled out any decrease in alkalis resulting from the replacement of micas (biotites) and feldspars.

It seems clear both from Alderton's remarks and from the present author's observations that luxullianite is not unique, and that a great variety of superficially similar rock types do occur in southwest England. Some examples are directly associated with metalliferous mineralization (e.g. as part of wall-rock assemblages), while others, including the veins at Luxulyan, occur in apparent isolation. Although the development of the characteristic luxullianite textures is relatively rare, the combination of tourmalinization and K-metasomatism would appear to be a fairly common one.

[*Manuscript received 4 September 1978; revised 26 February 1979*]

© *Copyright the Mineralogical Society*

CAROL J. LISTER

Department of Mineralogy
British Museum (Natural History)
Cromwell Road, London SW7